Generation of a 3D city model of Baalbek/Lebanon based on historical photos

Vorgelegt von

Dipl.-Ing.

AHMED ALAMOURI

Von der Fakultät VI-Planen Bauen Umwelt

der Technischen Universität Berlin

Zur Erlangung des akademischen Grades

Doktor der Ingenieurwissenschaft (Dr.-Ing.)

genehmigte Dissertation

Promotionsausschuss:

Vorsitzender: Univ. Prof. Dr. Ing. DOROTHÉE SACK

Berichter: Prof. Dr. Ing. Dr. h. c. LOTHAR GRÜNDIG

Berichter: Prof. Dr. rer. nat. THOMAS H. KOLBE

Berichter: Prof. Dr. Ing. ORHAN ALTAN

Tag der wissenschaftlichen Aussprache: 27.01.2011

Berlin 2011

D83

Generation of a 3D city model of Baalbek/Lebanon based on historical photos

Promotionsausschuss:

Vorsitzender: Univ. Prof. Dr. Ing. DOROTHÉE SACK
Berichter: Prof. Dr. Ing. Dr. h. c. LOTHAR GRÜNDIG
Berichter: Prof. Dr. rer. nat. THOMAS H. KOLBE
Berichter: Prof. Dr. Ing. ORHAN ALTAN

Tag der wissenschaftlichen Aussprache: 27.01.2011

Berlin 2011

D83

ACKNOWLEDGEMENTS

At the outset, I would like to express my profound and gratitude to my supervisor Prof. Dr. Eng. Dr. h. c. Lothar Gründig for his supports and advices during my doctoral research. He has constantly kept me to remain focused on achieving the research aims. His observations and comments helped me to establish the overall direction of the research and to move forward with the investigation in depth. Giving me the opportunities to participate in many workshops, meetings and conferences, he has raised my self-confidence and experience of making presentations at scientific meeting.

As well, I would like to express my great thanks to Prof. Dr. rer. nat. Thomas H. Kolbe who assisted me during the past five years. Very special thanks for his constant interest and encouragement; which helped me complete this thesis.

Furthermore, my deep appreciation also expressed to Dipl. Inform. Gerhard König who was helping to solve and overcome the problems arisen during the research work. In addition, many thanks expressed to all colleagues at the Department of Geodesy and Geoinformation at the Technical University of Berlin, Germany.

I am grateful also to Mr. Dipl.-Eng. Frank Henze (BTU-Cottbus) and to colleagues at Institute of Francais du Proche Orient (IFPO) in Damascus for providing the materials used in this research. In addition, thanks to University of Aleppo, Syria for the finance support during my PhD program in Germany.

Last but not least, I am greatly indebted to my parents who supported me mentally and patiently during my research time in Berlin. Thanks are extended to my family and friends for sharing with me the happy moments and opinions about the life while in Germany.

Ahmed Alamouri

2011, Berlin - Germany

PREFACE

The work presented by this thesis was funded by the coorporation between the University of Aleppo (Syria), Technical University of Berlin (Germany) and Brandenburg Technical University of Cottbus (Germany) in the research area "*the evaluation of digital photogrammetry in the documentation of the cultural heritage*".

The investigation and the implementation of experiments are based on the data of the historical graphical materials of the city Baalbek in Lebanon. This work was presented from October 2005 until September 2010 at the *Berlin Institute of Technology*, *University of Berlin* and has been supervised by Prof. Dr. Eng. Dr. h. c. Lothar Gruendig.

With this thesis, three main problems will be posed and investigated:

- *The first, how can the orientation process of different historical image types be best achieved (with respect to the poor properties of the images used)?*
- *Second, the combination between the different historical image types of Baalbek to achieve an optimal 3D object reconstruction will be discussed.*
- *Finally, it will be investigated: in which Level of Detail (LOD) Baalbek's data set can be modelled with respect to requirements of CityGML (City Geography Markup Language).*

The thesis comprises eight Chapters; the first one includes an introduction about the research motivation and objectives. Some theory and mathematical background of camera calibration will be presented in the 2nd Chapter. In the third one a new approach for relative orientation of non-calibrated historical photos of Baalbek will be described. The fourth and fifth Chapters describe the orientation process based on the combination between different image types. 3D object acquisition, quality assessment of Baalbek's data sets as well as a 3D modelling will be discussed in the 6th and 7th Chapters.

In 8th Chapter, concluding remarks and results are summarized. In addition, perspectives, remaining open questions and problems for future works are addressed.

ZUSAMMENFASSUNG

Diese Arbeit befasst sich mit der Auswertung von historischen Bildern unterschiedlichster Art zur Dokumentation von Objekten des Weltkulturerbes. Beispielhaft wurde verfügbares Bildmaterial (vertikale, terrestrische und Schrägaufnahmen) der Stadt Baalbek in Lebanon verwendet und photogrammetrisch ausgewertet. Bei der Verarbeitung des historischen Bildmaterials tritt eine Vielzahl von Problemen auf, deren Ursache in der Aufnahmesituation (wie zum Beispiel: unterschiedliche Aufnahmezeitpunkte, unterschiedliche Bildmaßstäbe, verschiedene Flughöhen und verschiedene Kameras) bzw. in der Beschaffenheit der Bilder zu sehen ist (unterschiedlicher Kontrast der Grauwerte in den Bildern, Bildrauschen). In der Regel sind keine Daten über die verwendeten Kameras bekannt, was eine Auswertung wesentlich erschwert.

In dieser Arbeit wird eine Strategie entwickelt, die einen Beitrag zur kombinierten Auswertung von historischen Bildern liefert. Der Lösungsansatz sieht drei Stufen vor:

- Unter diesen Bedingungen von den verwendeten Bildern wird in dieser Arbeit eine entsprechende Strategie basiert auf verschiedenen Klassen von historischen Bildern zur Kamerakalibrierung und Bildorientierung entwickelt. Diese Strategie liefert einen effektiven Beitrag für den relativen Orientierungsprozess, da diese kombinierte Auswertung von den historischen Bildern bisher nur unzureichend untersucht wurde. Sie bildet daher einen Schwerpunkt dieser Arbeit.

Zunächst müssen die verfügbaren Bilder im Koordinatensystem Baalbeks gemeinsam orientiert werden, um die unbekannten Parameter der inneren sowie der äußeren Orientierung zu bestimmen. Diese Parameter werden durch einen speziellen Algorithmus auf Basis der Bündelblockausgleichung berechnet und somit die Verzerrungsparameter (radial und dezentral) ermittelt. In der Arbeit wird untersucht, wie die Näherungswerte der Unbekannten optimal geschätzt werden und wie weit sie die erforderliche Genauigkeit und Zuverlässigkeit beeinflussen.

- Zur relativen Orientierung der historischen Bilder von Baalbek wurde ebenfalls die Methode der Bündelblockausgleichung angewendet, da sie den Zusammenhang zwischen den Bildkoordinaten (als Beobachtungen) und den Objektkoordinaten direkt, d.h. ohne Umweg über Modellkoordinaten, herstellen kann. Dieser Zusammenhang lässt sich durch die

mathematische Beziehung zwischen den Beobachtungen $\tilde{L}_i$ (z. B. Bildkoordinaten, Passpunkten, usw.) und den Unbekannten $\tilde{X}_i$ (wie z. B. die Parameter der inneren und äußeren Orientierung) präsentieren. Diese Beziehung kann mathematisch als funktionales Modell dargestellt werden, welches als die im Ausgleichungsprozess angewendete Hauptform gilt. Generell ist der funktionale Ansatz nichtlinear, deshalb wird im Rahmen der Arbeit der Lösung dieses Problems spezielle Aufmerksamkeit gewidmet. Unter der Annahme, dass die Ausgleichung generell mit linearen Funktionen gelöst werden kann, wird ein Linearisierungs-prozess eingeführt.

- In den jetzt orientierten Bildern können räumliche Objektkoordinaten gemessen werden, um 3D-Objekte zu rekonstruieren. In dieser Arbeit wird untersucht, in wie weit durch die Kombination der verschiedenen historischen Bilder eine beste 3D-Objektrekonstruktion möglich ist.

Die 3D-Daten Baalbeks liefern den Input zu einer 3D-Modellierung basierend auf CityGML (City Geography Markup Language). Daher beleuchtet die Arbeit, welcher Detaillierungsgrad (Level of Detail-LOD) bei der Modellierung erreicht werden kann.

Darüber hinaus werden, soweit möglich, CityGML-Objekte (CityGML-Entitäten) der Stadt Baalbek durch semantische Informationen angereichert (z. B. Kategorie, Name und Adresse des Objekts), da sie einen wesentlichen Mehrwert für die Analyse der historischen Entwicklung der Stadt liefern.

Mit der vorliegenden Arbeit wurde erreicht, dass die interne geometrische Konfiguration der unterschiedlichen verwendeten Kameras unter Berücksichtigung der Linsenverzerrung bestimmt werden konnte, und somit eine integrierte dreidimensionale Vermessung auf der Basis historischer Bilder möglich ist. Als weiteres anwendungsbezogenes Ergebnis wurde ein 3D-Stadtmodell von der historischen Stadt auf der Basis von CityGML in zwei verschiedenen LODs generiert.

ABSTRACT

Within this research the combined evaluation of different types of historical photos for the documentation of cultural heritage sites is discussed. For this purpose the historical photos of Baalbek in Lebanon have been used which can be classified into three types: vertical, oblique and terrestrial photos. Due to the poor properties of these photos (such as: different cameras used and no primary data of cameras' parameters, different image scales, different altitudes of the flight, the contrast of the gray values and the image noise are relative high, in addition the images had been taken in different dates, etc.), *it is not a priori clear by which combination of the image orientation process the best results (namely, the accurate determination of camera parameters) could be achieved.* Therefore, an approach for the relative orientation process will be discussed. Since the relative orientation is the position recovery and orientation of one image system relative to another, the potential of the mentioned approach is to reveal (from a mathematical point of view) the direct and indirect impact between the historical images of Baalbek to each other. It can be considered as a new contribution for the image orientation process based on the combination of different image types. This approach consists of three steps; the first one is the orientation of each image type in a separated block with its special properties (e.g. for each type a special camera was assumed). Second, the orientation process only for the vertical and oblique photos together has been achieved. Finally, all types of historic Baalbek's photos have been assembled into the same block and then oriented.

The abovementioned orientation steps were carried out using the bundle block adjustment method. This way has been selected because it enables to model the direct relation between the photo's reference system and object space optimally. The mentioned relation between both systems describes the relationship between the input data which are called observations $\tilde{L}_i$ (e.g. the coordinates of image points, control points, etc.) and unknown parameters $\tilde{X}_i$ (e.g. the parameters of interior and exterior orientation). The requested relationship can be mathematically presented through a model (called *a functional model*) which will be the main form applied in the adjustment problem. In general, the functional model is highly non-linear; therefore a special emphasis has to be respected when solving this problem. Due to the assumption that the adjustment method is generally achieved with linear functions, a linearization process should be enforced.

Based on the oriented model of the historical photos, *the combination between the different historical images of Baalbek - in order to achieve a best possible 3D object reconstruction will be evaluated by independent controls*. Moreover, Baalbek's 3D data extracted from oriented historical photos will be considered the main input data used for a 3D CityGML modelling (City Geography Markup Language). CityGML modelling supports different Levels of Detail (LODs); by them different data collections can be represented and modelled. In this context, it will be investigated: in which LOD Baalbek data acquired can be modelled! In other words: *based on the quality check of Baalbek data we want to know in which LOD Baalbek data available could be modelled*.

In addition, the semantic modelling of this city should be taken into account, because the geometric model does not support all information needed (e.g. classification of objects, building function, building class, names, etc.). Thus, the objects' geometry isn't the only quality concern. This will guarantee the creation of a geometric and semantic 3D city model of Baalbek which on the one hand provides an important document for this city and on the other hand allows to understand and to enable the analysis of the historical developments of Baalbek's building remains from the prehistoric date until 20th century.

Work results are: the internal geometric configuration of the different cameras used and the lens systems were determined; so that the measurement of the applicable 3D object points is possible. Moreover, the quality of Baalbek's data extracted based on the oriented model of the photos has been checked. Depending on the quality assessment of Baalbek's data a 3D city model of this historic city was created in two different LODs. The results will be also considered a data base for other applications and projects in Baalbek's space (for e.g. the Geoinformation System GIS, archaeology, architecture, etc.).

Content

1. Introduction

1.1. Motivations of the research

- **The historical importance of Baalbek**

Baalbek is situated on the northern of the Beqaa-Plain/Lebanon which was settled in the beginning of 3rd millennium B. C. and the old preserved dwellings validate the historical importance of this city. The existing of the Roman Colonia Iulia Augusta Felix Berytus (15 B. C.) was the reason that Baalbek had a settlement of the Roman veteran. Additionally, the constructions such as the temples: Jupiter, Bacchus and Venus are witnesses of Baalbek's wonderful constructions. The sanctuary has been designed in a new form and built in a monumentality which was not known before. Through the (4th - 7th centuries) Baalbek had gotten more Christain churches which could displace but slowly in the old cults. In the Islamic era (in 635 A.D.[1]) and in the (12th - 14th centuries) the site of temples had been converted into a great fort. Since 1984 Baalbek is inscribed through the UNESCO as an important site of the urban heritages (Figure 1.1).

"The sanctuary of ***Jupiter*** Heliopolitan is often referred to as the Acropolis of Baalbek. The Arabs however call it the *Kala'a*, which means fortress. The compound of the temple of Jupiter covers an area of about 27000 square meters, of which 10000 square meters were open courtyards and stairways. The remaining 17000 square meters were covered with peristyles, exedras and interior spaces" (Ragette, 1980, pp. 27-39).

"The temple of Jupiter and its courtyards were planned as a whole. During the Augustan era it became customary in Rome also to place the temple inside a court, although usually at the far end of it. In Baalbek; this would have resulted in an area of about 300 by 130 m, comparable to the great court schemes of Jerusalem, Damascus or Palmyra. The Romans planned to build a courtyard centrally placed in relation to the altar of sacrifice" (Kalayan, 1969).

However, in the first half of the first century A.D. the courtyard was stopped in line with the temple façade, although foundations had already been placed for a further stretch along the North side of the temple. This suspension of construction was probably the result of the

[1] A.D.: date used in reckoning dates after the supposed year Christ was born.

excessive effort required to achieve a rather questionable architectural result. The Figure (1.2) shows the six remaining columns of the temple of Jupiter resting upon the pre-Roman podium wall. The huge stones in the front of it belong to the base course of the intended Roman podium extension.

The second temple in Baalbek is ***Bacchus***. This temple is particularly well preserved. It is, in the fact, the best preserved Roman temple of this size anywhere. We should refer to it as the temple of Bacchus, because the dedication of the building to this Joyous God is far from certain. The temple stands in a curious relationship to the great complex of the temple of Jupiter. The first person to suggest the attribution of the temple of Bacchus was the German archaeologist Otto Puchstein. His theory was based on the carvings around the door of the temple and particularly those belonging to the adytum or inner shrine. "However, the temple of Bacchus represents the remarkable moment of classical architecture where exterior and interior are of equal importance, a condition achieved neither by the exquisite exterior of Pericles nor the great interiors of antiquity" (Ragette, 1980, pp. 40-51). Some parts of the temple Bacchus are represented in the Figure (1.3).

Until the early seventeenth century there was not a specific reference to the round temple of ***Venus***, but an indication was found, that the small temple had already in the year 1630 been turned into a church dedicated to Saint Barbara. "Henry Maubdrell in his journey from Aleppo to Jerusalem in the year 1697 confirmed that the circular temple was used as a church by the Greek Orthodox in the town. He wrote: Coming near the ruins, the first thing you meet with is a little round pile of building, all of marble. It is encircled with columns of the Corinthain order, very beautiful, which support a Cornish that runs all round the structure, of no ordinary state and beauty. This part of the remains is at present in very tottering condition, but yet the Greeks use it for church" (Ragette, 1980, pp. 52-62).

The important reference to the temple of Venus is the following comment by Leon Delaborde in the year 1837: "At the beginning of our investigations we were led to a small temple built near a brook which later passes along the wall of the castle and turns a mill. I refer to the drawing by my father which shows the general layout of this small round temple, the search for elegance which distinguishes it, the slightly heavy coquetry which characterizes it. The whole righthand part of the monument, the one which we can not see on the drawing, has fallen, and the rest will not keep standing for long; the walls are cracking and the columns are out of the plump". The temple of Venus is shown in the Figure (1.4).

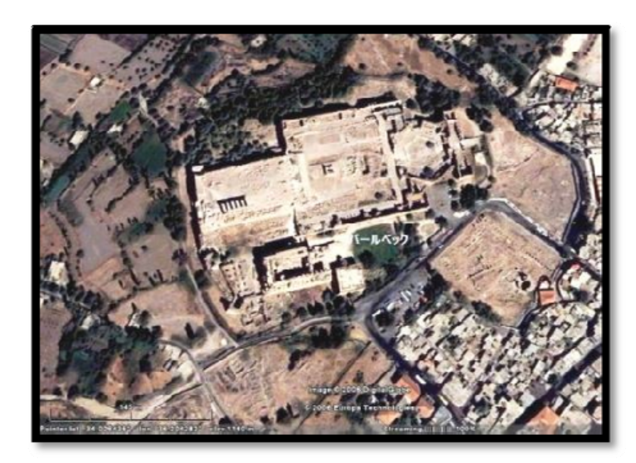

Figure (1.1): City of historic Baalbek (image © 2006 Digital Globe)

Figure (1.2): Rest columns of the Temple Jupiter

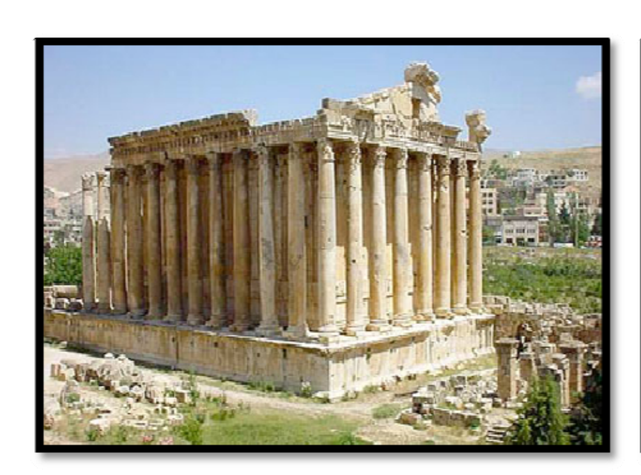

Fig. (1.3): The Temple of Bacchus

Fig. (1.4): The Temple of Venus

- **Modelling with spatial data quality**

The spatial data are in high demand for many applications, projects, researches, etc. Therefore the quality and reliability of the acquired data are essential for any further processing or use (Ragia, 2000). In other words, it should be investigated how best to present the real world using spatial data and depending on the view of the user's requirements.

In this research, 3D modelling using the spatial data extracted from the oriented model of Baalbek's photos will be created. By this modelling the quality measurements of the spatial data will be investigated with respect to the input data (the historical images of Baalbek and their properties). The quality criterions could be categorized into four aspects: geometry, topology, semantic and appearance. The geometric quality will be discussed in detail because it is a main step for 3D object reconstruction and 3D modelling. In addition, the semantic check also takes an important role through the modelling because it enables to understand and to recognize the objects to be modelled.

The intended 3D model of historic Baalbek should be applicable for next evaluations by historians, archaeologists, architects, etc. This will make the data available and therefore it allows for easy measurements requested from other users (e.g. photogrammetrists, architects, etc.) for further projects and applications (like: renovation process, GIS tasks).

- **Graphical material**

The main graphical materials of Baalbek include the historical aerial photos (vertical and oblique photos; taken in the years 1933, 1937 and 1940) as well as terrestrial images which have been taken in the year 1904 and stored in the Brandenburg state office for the archaeology (cf. the Figures 1.5.a, 1.5.b and 1.5.c). Baalbek's photos have poor properties due to following:

- different cameras used and different image scales
- great contrast and high image noise
- different altitudes of the flight
- the images have been taken in different dates

In addition, there are no primary data about the cameras used, therefore in this study a mathematical method will be developed in order to orient these images as well as to use the extracted data optimally.

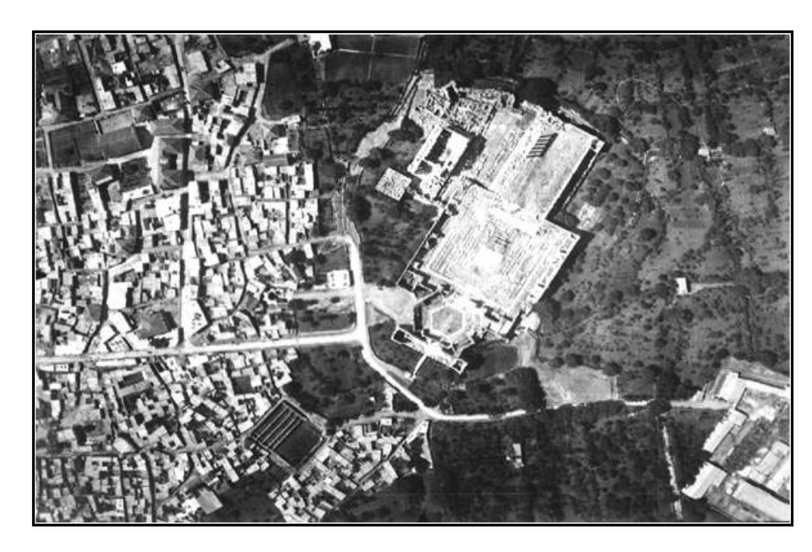

Figure (1.5.a): An aerial vertical image of Baalbek including the temples area

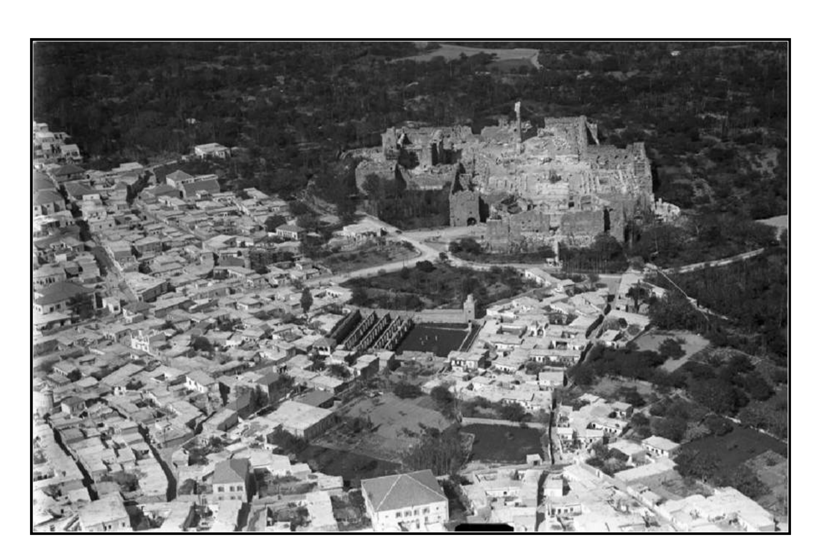

Figure (1.5.b): An oblique photo of Baalbek

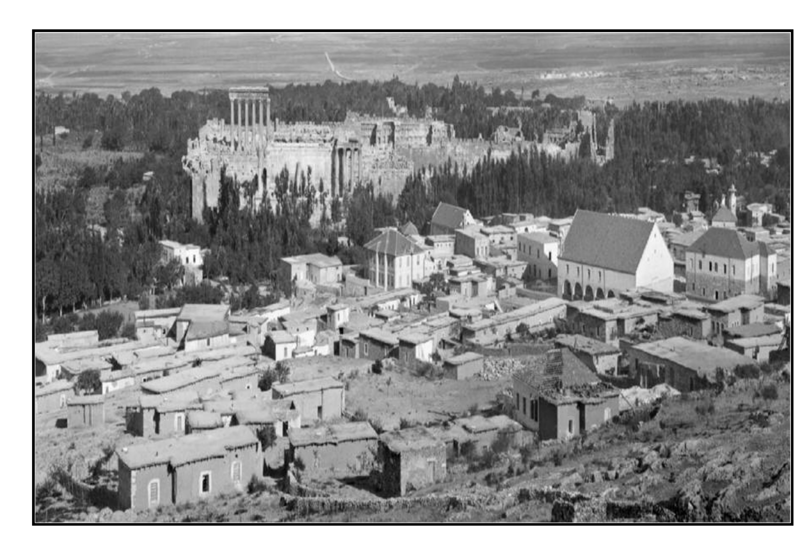

Figure (1.5.c): A section of a terrestrial image of Baalbek taken in 1904 by Meydenbauer

- **Demand of photogrammetric methodology**

In photogrammetry two scenarios could be distinguished. The first one, which is more likely, deals with different image types separately. Moreover, most of the images implemented in this scenario are taken with high resolution cameras and therefore these photos have a high quality. In addition, photogrammetric processes can be accessibly performed due to the availability of different specific software.

In the second scenario, which is less likely, there are other photogrammetric cases such as: if we have to deal with different image types together; in these cases a combination between image types should be taken in account. Other point can be posed that if the images are taken with old cameras (like: Baalbek's photos); this means the photos may have poor properties (e.g. high image noise and contrast). Furthermore, "image matching process is an important problem in this scenario, because with this unusual arrangement and different image types no automatic block adjustment is possible with standard software for automatic image matching" (Jacobsen, 2008).

Within this research, a contribution for a photogrammetric methodology dealing with a combination of different types of historical images will be introduced. It should characterise the potential of combination of image different types. The characteristics of this methodology rely on the following aspects:

- Overcoming challenges arisen through the bundle block adjustment (e.g. formulation of the mathematical model applied in adjustment computations).
- Image sequence that is applied in the orientation process.
- Accuracy analysis (e.g. accuracy parameters would be higher in the combined evaluation than separate one, less or satisfied the required purpose).
- Gross error detection (blunders).
- Image matching (measurement of tie points).
- The relation between cameras to each other, as well as the lens system and determination of distortion parameters.
- How to do if there is no data available for cameras used.

In this thesis, the investigations and implementations of the suggested methodology are based on Baalbek's historical images, but the mechanism should be applicable for further historical photo types of different sites.

1.2. Research objectives

According to the above mentioned motives of the research, the main objectives of this work could be expressed as following:

- ***Image orientation***: the available graphical materials have to be oriented in Baalbek's local coordinates system in order to estimate the unknown parameters of the interior and exterior orientation. These unknowns will be calculated based on the observations (e.g. coordinates of image points associated with ground points known) using the bundle block adjustment method. This method was selected because it gives a best modelling of the direct relation between the photo system and the object space.

  The mentioned relationship can be mathematically presented through a model (a functional model) presenting the main form applied into the adjustment problem. In general, the functional model is a highly non-linear form; therefore a special emphasis has to be put on the solving this problem.

- ***Combination of vertical, oblique and terrestrial images***:

  The combined evaluation of the different types of historical images is an important aim of this work due to the following:

  - Up to now minor investigations about this combination have been achieved. In this context, a contribution for geometry of vertical and oblique image combination has been discussed by (Jacobsen, 2008). In addition, (Tournaire, et al., 2006) have introduced an image-based strategy for a sub-decimetre quality georeferencing of Mobile Mapping System in urban areas using ground and aerial-based images.
  - It is a good aider for image understanding and interpretation. For e.g. vertical images need experience to read! Other types like oblique and terrestrial are easier to interpret.
  - By using the combination between different data sources hidden parts of objects in photos can be detected, this enables a good geometrical data extraction.
  - It is essential to know: by which combination and order of the images the orientation process can be best achieved to get best results (e.g. orientation parameters); where

this enables to know which image sequences would be reasonable and practicable for the orientation process.

- ***Orthophoto creation***: The photos of Baalbek are in the form of a focused perspective. The image's information has to be changed into an orthogonal projection to create orthophotos. For this aim a Digital Terrain Model is essential to reduce and even to eliminate the radial distortions in the images.

- ***3D Reconstruction***: based on the oriented model of the photos the space object points could be measured in order to reconstruct 3D objects. In this step, the possibility of the 3D object reconstruction depending on the graphical materials of Baalbek will be verified.

- ***3D Modelling***: the modelling of 3D data extracted from the oriented historical images of Baalbek is regarded an important aim in this thesis because it enables to represent Baalbek data as well as to document the historic city and its ruins. For this purpose, *CityGML modelling will be implemented. In this context, it will be proved to what extent CityGML can be considered as an accessible standard used for cultural heritage sites documentation.*

- ***Result visualisation***: the work results will be presented in a web-based environment, facilitating the Internet-based graphical characterisation of the GIS contents. Moreover, the 3D model can be offered in Google Earth and as 2D maps.

1.3. Related work[1]

The first excavations and studies of Baalbek as well as an initial documentation of the preserved material remains have been carried out by the first German researchers between 1900 and 1904. In the next decades, French colleagues undertook conservation measurements and an intensified research on the theological problems of the *Heliopolitaean trias* round of the three temples. The French revealed that there was a stairway leading up *Sheikh Abdullah* area. In the 1920s the Department of the Antiquities of the French mandatory government continued the researches and restorative work. Since 1945 the *Lebanese Direction Generale des Antiquites* (LDGA) has continued this work.

[1] Main data sources are: (Van Ess, 1998), (Van Ess et. al., 2003) and (Wiegand, 1921-25)

Current fieldworks are being conducted in different areas of the Roman town of Baalbek. An important aim of the processes concentrates the further documentation, drawing and stratigraphic analysis of the areas and the buildings. The fieldwork projects are as following:

- Bustan el Khan (in the 1960s, 1970s and 2001-2004)
- Area of the so-called Venus temple (in 2002)
- Qala'a in 1960s and Sheikh Abdullah since 2002

The results of these aforementioned works of the town history and geodesy led to a new assumption concerning the chronological sequences of the wonderful constructions of the temples and their interrelationships. These chronological sequences could be summarized in the following points[1]:

- In the Hellenistic period the former comparatively small tell (on which there was probably already a temple building) was converted by the construction of the first large sanctuary.
- The town might have had to move to the foot of tell.
- At this early stage a road axis might have been created, which led across the settlement to another important religious building in the quarter of Haret Beit Sulh.
- The temple of Jupiter and the so-called temple of the Muses were axially oriented towards this hypothetical temple. This held true for the later monumental temple of Jupiter in Roman times.
- In the early Christian period the area of the so-called temple of Venus was transformed into a Christian church complex, and in the 5th century A.D. the large basilica was built in the Great Courtyard of the sanctuary of Jupiter.

Important to note that two photogrammetric efforts were achieved by A. Klotz and M. Gessner in 2005 and 2006 using Baalbek's historical vertical images. Input data used in the mentioned efforts are presented in the Table (1.1).

[1] The points summarizing the chronological sequences are quoted from: www.dainst.org

		Klotz (2005)	Geßner (2006)
Input	Number of images used	14	16
	Camera constant	20 cm	31.86 cm
	Pixel size	0.25 mm	0.042 mm
	σ (image points)	±0.5 pixel	±5 pixel
	σ (object points)	±5 cm (XY), ±10 cm (Z)	±20 cm (XY), ±30 cm (Z)

Table (1.1): Input data used by Klotz and Geßner in the orientation process of Baalbek's vertical images (σ is the standard deviation)

Although the scientific works and researches in Baalbek started in 18th century, there are unexplained issues which could be posed such as:

- The parameters of the cameras used and lens system.
- Building location, design and construction.
- The temples and their interrelationships (geometry and topology).
- Road axes and their changes.
- Thematic and semantic data, etc.

These issues are considered additional motivations for this thesis; especially with using the oblique and terrestrial photos of Baalbek, which could be given more information about the historic city of Baalbek.

1.4. Available materials

1.4.1. Vertical aerial photos

These photos have been taken in the year 1937 through the French mandate and are located in the Institute of Francais du Proche Orient (IFPO) in Damascus as celluloid photographic film. They were performed on glass sheets with the size 18×13 cm and have four fiducial points.

These images were scanned and sent to the Technical University of Cottbus. Unfortunately the resolution of the scanner used is unknown, but by using of the image processing softwares

(e.g. Adobe Photoshop CS2) it can be displayed that the average size of the digital aerial vertical images 6272×4789 pixel.

Consequently, the pixel size can be computed with respect to the following ratio:

$$P_s = \frac{image\ size\ on\ the\ glass\ sheet}{image\ size\ of\ scanned\ digital\ image} \tag{1.1}$$

Hence, the pixel size would be $\sim 29\ \mu m$ and the image resolution about (880) dpi. The camera used for this type was considered as a metric camera, because there are four fiducial points associated with the photos (Luhmann, 2003, pp. 130-134).

The following information can be observed on the photos borders:

Mission vertical 29 12/4/37 3 cmc experience,
GB’39/2 ES M30 CL66 F.O. 26 C-C,
CL85, ALT 2100

The interpretation of this information may reveal that the focal length of the camera used was $260\ mm$ (F.O. 26 C-C). ALT2100 could be the absolute altitude above the sea level. The mean altitude of Baalbek’s ground is approximately $1156\ m$ (in this case: the mean value of Z-coordinates of the control points which were measured in Baalbek’s coordinates system); this leads to the flying altitude of approximately $945\ m$.

Eventually, in the study case of Baalbek the following assumption has been accepted: “the aerial vertical photos have been taken through the same metric camera; moreover they cover a maximal area of Baalbek”. The properties of this type of images are summarized in the Table (1.2). First of all the assumed flying direction over Baalbek was South-West to North-East.

Although the information addressed on the photos borders indicate that the camera focal length may be $260\ mm$, but this value was not taken in the orientation process. This is due to information (presented by Carlier, 1942) referred to the cameras produced in the exposure date of Baalbek’s vertical photos (see Chapter 3.2.1.1). The camera constant applied therefore is $200\ mm$.

Flying year	1937
Number of the images[1]	14
Image size	$(6272 \times 4789)\ Pixel$
Scan resolution	880 dpi
Flying direction	SW-NE
Focal length	$200\ mm$
Flying altitude	$945\ m$

Table (1.2): The properties of the vertical images

1.4.2. Oblique aerial images

The oblique images have been taken in the year 1933. They were scanned using the photo scanner (Epson 4870) with the resolution 600 dpi that means the pixel size is round $42\ \mu m$. Through the scan process two problems have arisen: the first is that the fiducial points on the images are not complete (in standard case there are four fiducial marks), where the area of the transmitted light of the scanner was around 6×9 inch, so the negative film was not completely collected, thus some of these photos have just only one or two fiducial marks. The other one refers to the image resolution; due to the poor quality of the images the high resolution doesn't take an important role in order to get more details from the images. Since that the information source about the camera focal length - for this type of the images - is only the data recorded on the image borders; it was considered that the value of $260\ mm$ is an approximate value of the camera focal length. Other properties of the oblique images are given in the (Table 1.3).

Photograph year	1933
Number of selected images	8
Image size	$(4087 \times 2959)\ Pixel$
Scan resolution	600 dpi
Focal length	$260\ mm$

Table (1.3): The properties of the oblique photos

[1] This number presents only the number of the selected images

1.4.3. Terrestrial photographs

The third part of Baalbek's graphical materials is the terrestrial images which refer to the first German researches in the beginning of the 20th century in Baalbek. These photos are stored in the regional authority of Brandenburg/Germany (Meydenbauer's archive). There are 23 terrestrial images of Baalbek which have been taken in the year 1904. Probable camera - to - subject distance was assumed between $300\ m$ to $500\ m$. The terrestrial photos were scanned using the scan resolution 1000 dpi, which leads to the pixel size $\sim 25\ \mu m$ (Table 1.4).

Photograph year	Beginning of 20th century
Number of selected images	3
Image size	$(11882 \times 7968)\ Pixel$
Scan resolution	1000 dpi
Focal length	$350\ mm$

Table (1.4): The properties of the terrestrial images

According to the Meyer's classification of the cameras which were produced by Albrecht Meydenbauer, the camera focal length was regarded $350\ mm$ as initial value applied into the adjustment computations (Meyer, 1985).

The cameras used for the oblique and terrestrial photos were considered as a non-metric camera, because of no existing of a special referenced frame of the image area that means the coordinates of fiducial points are missed (according to Luhmann, 2003, pp. 130-134).

1.4.4. Additional information

- *Control points*: in the years 2003 and 2004 the coordinates of control points have been measured, in the local system of Baalbek, using tachymeter and reflectorless pointing. The accuracy of the measurements is between $\pm 10\ cm$. The control points were drawn in 27 sketches in the form A4 (selected sketches are presented in the App. A).
- *Tachymeter Leica* (TCRM 1102) was used to measure the above mentioned coordinates of the control points.

- *Topographic maps*: there are two digital topographic maps of Baalbek which had been produced in the year 1962. They have the map scale 1: 20 000 and cover the whole area of historic Baalbek Figure (1.6).

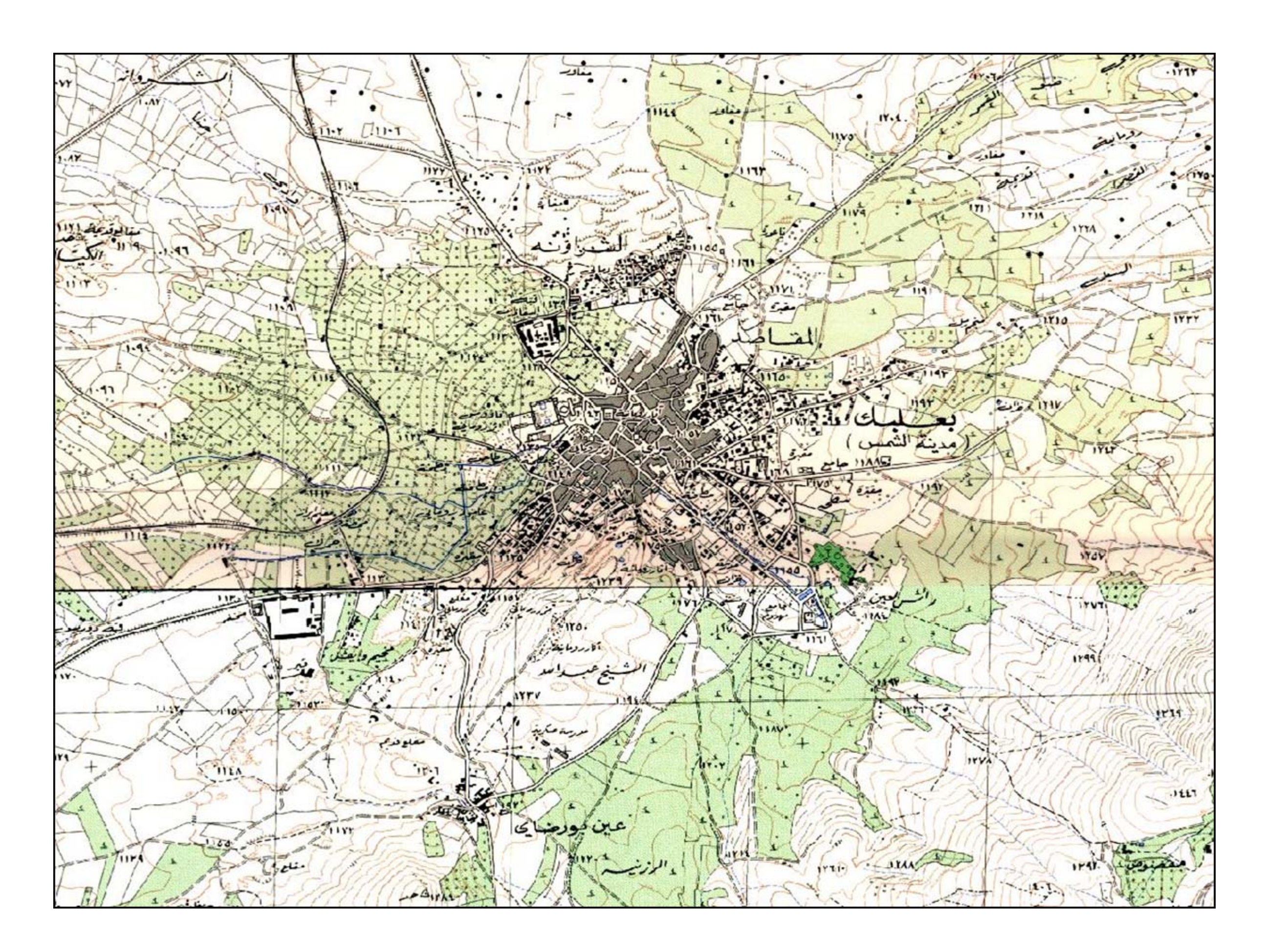

Figure (1.6): A section of Baalbek’s topographical maps
(Source: Institute of Francais du Proche Orient IFPO in Damascus)

A close view of the studied area included in the vertical and oblique images (also the overlapping areas) is depicted in the Figure (1.7).

Figure (1.7): The studied area of historic Baalbek included in the vertical images (red polygon) and oblique photos (orange polygon)

2. Theory of a camera calibration

The term *“camera calibration”* describes the internal geometric status of a camera and lens system. It can be expressed, in general, by the determination of the following elements:

- the calibrated principle distance (c_k) associated with specific focal settings
- the coordinates (x'_0 , y'_0) of the principle point
- lens distortion parameters

On one hand the abovementioned elements are called “*interior orientation parameters”* (see Chapter 2.1) which can be estimated based on different calibration methods (e.g. the method of self-calibration, on the job calibration, etc.).

On the other hand the determination of the spatial position of a camera in the object coordinate system should be taken into the account. In this context, the identification of the spatial location of the respected camera can be carried out based on specific parameters called “*exterior orientation parameters”* (Chapter 2.2).

2.1. Interior orientation

Interior orientation is the term implemented in photogrammetry to describe the internal geometric configuration of a camera and lens system; in other words: the position of the camera projection center should be described according to image coordinate system.

It would be meaningful for the photogrammetrists to know: what occurs to the bundle of the rays coming from the object and passing through the lens of their imaging device. The above mentioned configuration of the passage of a bundle of the light rays through the lens to the image plane can be presented mathematically by set of parameters which are defined as interior orientation parameters. These parameters can be expressed as following (Fryer, 2001, pp. 156-159):

- **Principal distance**

The perpendicular distance from the perspective center of the lens system (projection center) to image plane is termed the *principal distance*. In the aerial photogrammetry where the camera lens is fixed at infinity focus, the terms focal length and principal distance may be used synonymously. Particularly, at close range photogrammetry the cameras used are often focusable; therefore the focal length is the principal distance which should be determined.

- **Principal point**

The principal point of the autocollimation is presented as the perpendicular foot of the center of the lens system (projection center) on the plane of the focus. In standard case the principle point and the ideal origin for a coordinate system on the image plane should be in the same image location. In practice, they locate approximately each to other (Figure 2.1).

- **Fiducial origin**

The fiducial center can be defined through the intersection of the imaginary lines drawn from opposite pairs of fiducial marks in the sides or corners of the image plane (cf. Figure 2.1). In an ideal camera this point would coincide with the physically important principal point of autocollimation. The relationship between the principal point and fiducial center will usually remain constant during the photogrammetric processes, but sometimes with the use of non-metric cameras and/or zoom lenses when re-focusing has occurred between exposures, the interior orientation elements will change.

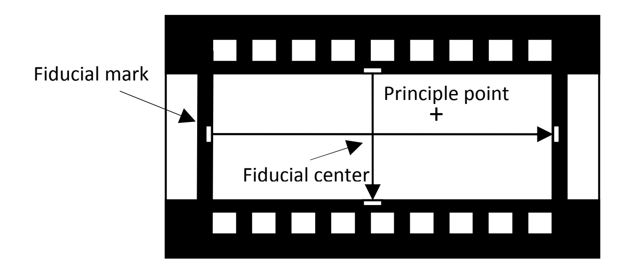

Figure (2.1): The geometry of an image plane (source: Fryer, 2001)

- **Radial distortions**

If an image point is displaced radially either closer to or farther from the principal point then it has been radially distorted. Based on the Gaussian radial distortion, the relationship between the radial distortion and the radial distance can be described (Fig. 2.2). In this case, the relation is presented with respect to different image scales (1:40, 1:80 and 1:60). At small radial distance values, the radial distortion is approximately small that the distortion curve is relative linear. In contrast, an increasing of the radial distance leads to an increasing of the radial distortion values. The equation of the radial distortion is expressed by polynomial (according to Dörstel et al., 2003 & Luhmann, 2003, pp. 118-129):

$$\Delta r = K_1 r^3 + K_2 r^5 + K_3 r^7 - r(K_1 r_0^2 + K_2 r_0^4 + K_3 r_0^6) \quad (2.1)$$

where: K_i … radial distortion parameters

r … radial distance to the principle point

r_0 … constant value; where it has to be selected with respect that a balanced radial distortion should be guaranteed. In practice, it can be assumed of ca. 2/3 from maximal image radius.

Thus, the corrections of the coordinates of an image point could be given as following:

$$\Delta x' = x' \cdot \frac{\Delta r}{r} \quad (2.2.a)$$

$$\Delta y' = y' \cdot \frac{\Delta r}{r} \quad (2.2.b)$$

where: x' and y' … the coordinates of an image point

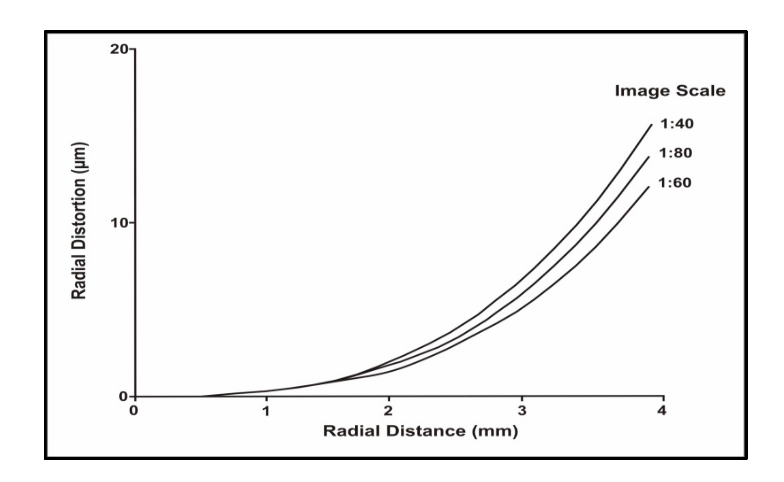

Figure (2.2): Gaussian radial distortion at various image scales for a $25\ mm$ lens fitted to a Pulnix CCD camera (source: Fryer, 2001)

- **Decentring distortion**

In standard case, the elements in a lens system ideally should be aligned to be collinear to the optical axis of the entire lens system. In practice, it is difficult to align these elements strictly collinear (Figure 2.3). This defect leads to decentring distortion in the lens system (Dörstel et al., 2003). The decentring distortion components could be described by the expression (Temiz & Külür, 2008):

$$\Delta x_d = (r^2 + 2\bar{x}^2)P_1 + 2\bar{x}\bar{y}P_2 \quad (2.3)$$

$$\Delta y_d = 2\bar{x}\bar{y}P_1 + (r^2 + 2\bar{y}^2)P_2 \quad (2.4)$$

where:

$\bar{x} = x' - x'_0$ and $\bar{y} = y' - y'_0$; $r^2 = \bar{x}^2 + \bar{y}^2$

P_1 and P_1: are the coefficients of the decentring distortion

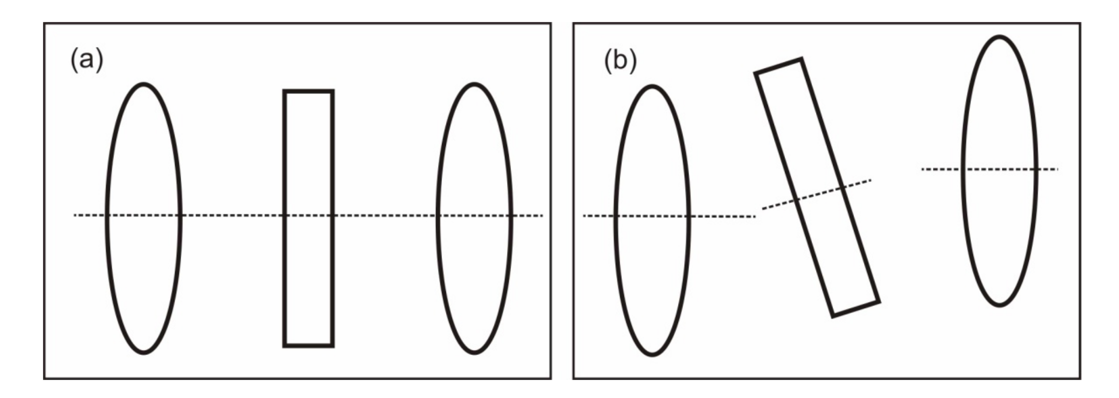

Figure (2.3): Misalignment of the lens elements; (a): lenses are centred perfectly, (b): the lenses are decentred (source: Fryer, 2001)

Based on the coefficients of the decentring distortion the -so called- “profile function” can be derived as following (Fryer, 2001, pp. 162-164):

$$P_r = (P_1^2 + P_2^2)^{1/2} \cdot r^2 \quad (2.5)$$

A graphical representation of the mentioned function is shown in the Figure (2.4). It reveals that the values of the decentring distortion are smaller than the radial distortions. Unless an image scale is large, the decentring distortion will be approximately one or two micrometers.

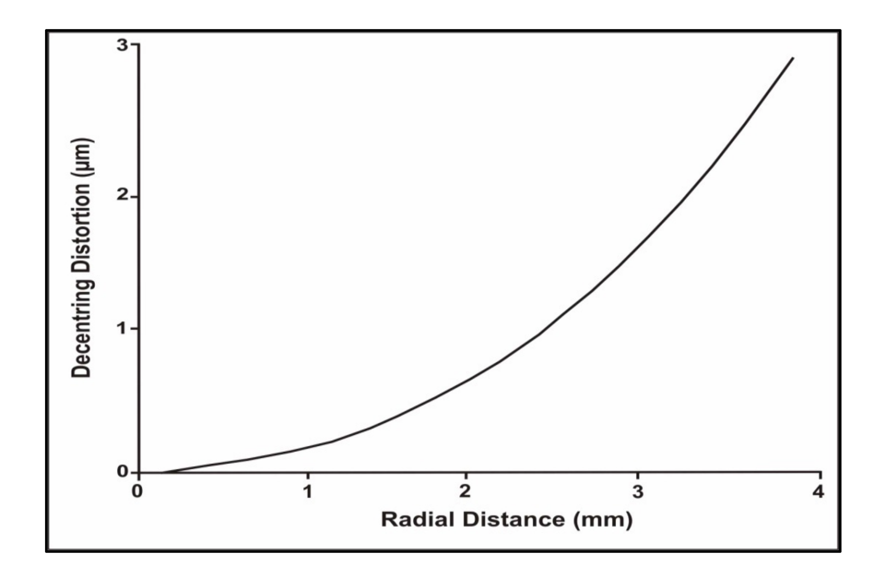

Figure (2.4): A Graphical representation of the decentring distortion for Fujinon 25 mm lens fitted to a Pulnix CCD camera (source: Fryer, 2001)

Consequently, if the interior orientation parameters are known, then the image vector $\boldsymbol{X'}$ can be defined as following (cf. Figure 2.5):

$$\boldsymbol{X'} = \begin{bmatrix} x' \\ y' \\ z' \end{bmatrix} = \begin{bmatrix} x'_p - y'_0 - \Delta x' \\ y'_p - y'_0 - \Delta y' \\ -c_k \end{bmatrix} \tag{2.6}$$

where: x'_p , y'_p measured coordinates of the image point p'
x'_0 , y'_0 coordinates of the principle point H´
$\Delta x'$, $\Delta y'$ correction values
c_k focal length

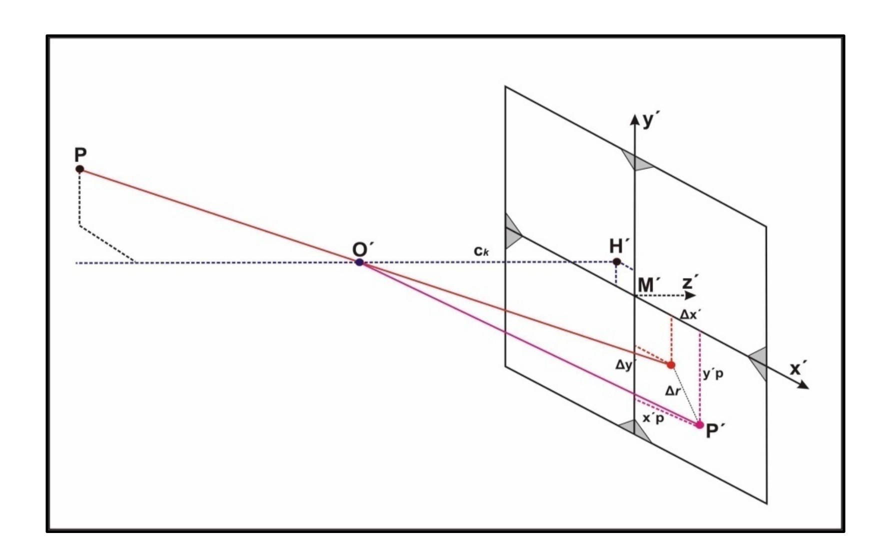

Figure (2.5): Interior orientation parameters (source: Luhmann, 2003)

Previously mentioned, that the determination of the spatial position of a camera should be respected. The camera position is determined based on the exterior orientation parameters. More details about exterior orientation parameters will be described in the next chapter.

2.2. Exterior orientation

2.2.1. Standard case

The term “exterior orientation” describes the spatial position of a camera to the object coordinate system. It can be defined through six parameters representing the relationship between the image coordinates system and the superposed object coordinates system. The vertical and perpendicular exposure of an image is known as the standard case; the optical

axis in this case is Z. The coordinates of the projection center are defined with the vector $\mathbf{X_0}$ to the object coordinate system XYZ (Figure 2.6).

$$\mathbf{X_0} = \begin{bmatrix} X_0 \\ Y_0 \\ Z_0 \end{bmatrix} \quad \text{coordinates of the projection center to the object system XYZ} \tag{2.7}$$

In the context of the spatial orientation, the perspective center can be described through the rotation matrix R which is defined based on the three rotation angles ω, φ and κ around the axes' coordinates XYZ, respectively.

$$R = R_\omega \cdot R_\varphi \cdot R_\kappa$$

$$R = \begin{bmatrix} r_{11} & r_{12} & r_{13} \\ r_{21} & r_{22} & r_{23} \\ r_{31} & r_{32} & r_{33} \end{bmatrix} \tag{2.8.a}$$

The parameters r_{ij} are the rotation matrices which can be calculated from the trigonometric function of the three rotation angles (Luhmann, 2003, pp. 35-40).

$$R = \begin{bmatrix} cos\varphi cos\kappa & -cos\varphi sin\kappa & sin\varphi \\ cos\omega sin\kappa + sin\omega sin\varphi cos\kappa & cos\omega cos\kappa - sin\omega sin\varphi sin\kappa & -sin\omega cos\varphi \\ sin\omega sin\kappa - cos\omega sin\varphi cos\kappa & sin\omega cos\kappa + cos\omega sin\varphi sin\kappa & cos\omega cos\varphi \end{bmatrix} \tag{2.8.b}$$

The rotation angles are given by the expressions:

$$\left\{ \sin\varphi = r_{13}, \tan\omega = -\frac{r_{23}}{r_{33}} \text{ and } \tan\kappa = -\frac{r_{12}}{r_{11}} \right\} \tag{2.9}$$

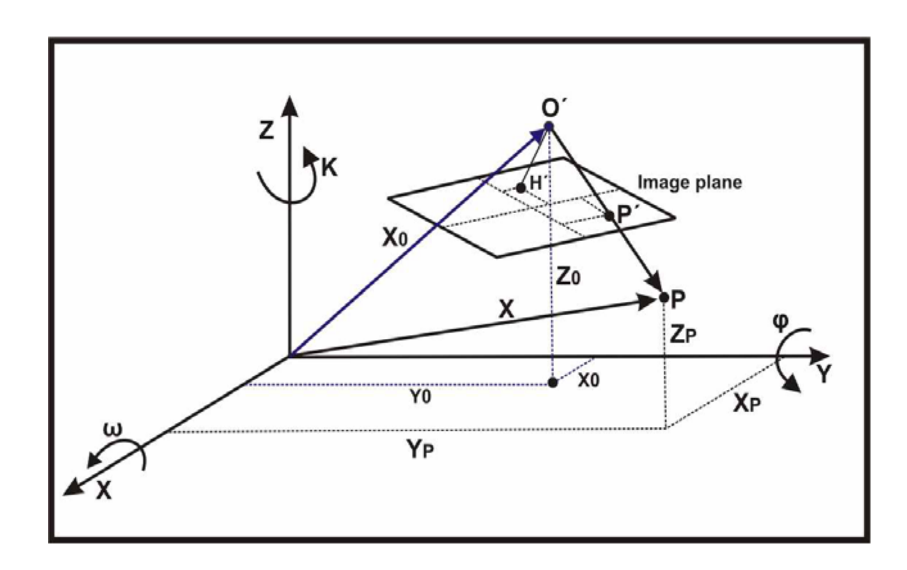

Figure (2.6): The exterior orientation parameters (source Luhmann, 2003)

2.2.2. Special terrestrial photogrammetry

In the special case of the classic terrestrial photogrammetry the optic axis is horizontal. In this case the rotation angels are: $\omega = 0^\circ$, $\varphi = 90^\circ$ and $\kappa = 90^\circ$ (Fig. 2.7). In order to avoid the singularity in the computation process either the rotation sequence must be changed in the trigonometric functions of the rotation angles or the image system must be defined through the axes $x'$and z' instead of $x'$and y'. The new rotation matrix is given (Luhmann, 2003, pp. 37-38 & pp. 235-236):

$$R = R_{\varphi\omega\kappa} = R_\varphi \cdot R_\omega \cdot R_\kappa$$

$$R = \begin{bmatrix} cos\varphi cos\kappa + sin\varphi sin\omega sin\kappa & -cos\varphi sin\kappa + sin\varphi sin\omega cos\kappa & sin\varphi cos\omega \\ cos\omega sin\kappa & cos\omega cos\kappa & -sin\omega \\ -sin\varphi cos\kappa + cos\varphi sin\omega sin\kappa & sin\varphi sin\kappa + cos\varphi sin\omega cos\kappa & cos\varphi cos\omega \end{bmatrix} \quad (2.10)$$

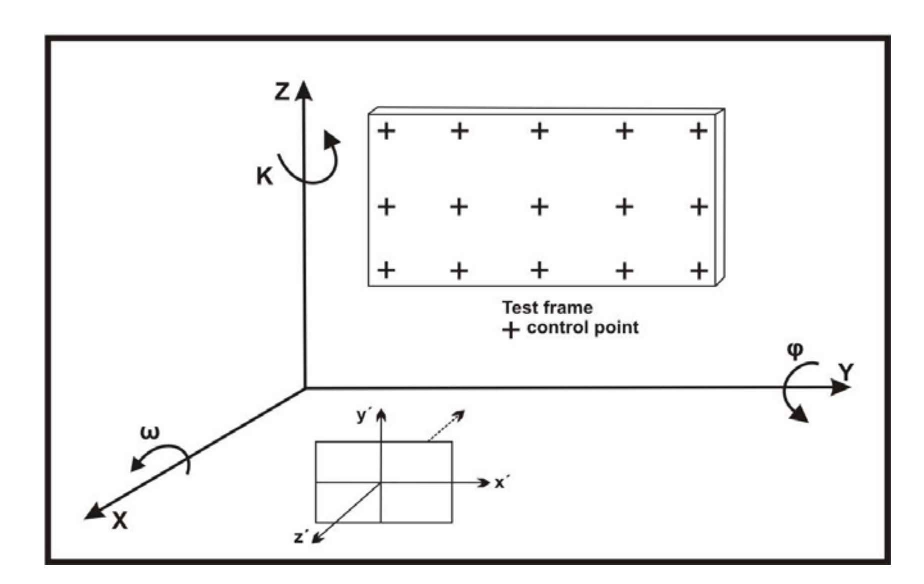

Figure (2.7): Classic case of terrestrial photogrammetry (source: Luhmann, 2003)

Consequently, to determine the internal geometric configuration of a camera, a calibration process of this camera should be enforced. In this context, the methods used for the calibration of close range cameras have developed over the last few decades from those used for aerial cameras. According to (Luhmann, 2003, pp. 502-507 & Fryer, 2001, pp. 164-170) these methods could be classified as following:

- ***Laboratory calibration***: this way was used in the foretime to calibrate the metric-cameras. The goniometer and collimator were the powerful tools used to estimate the parameters of the interior orientation; whereas the direction and the angle of the bundle rays passing

through the lens are known. The laboratory calibration takes in the practice no important role because the users themselves may not normally use it.

- ***Test panel calibration***: the test panel includes control points which are known. In order to perform a significant calibration of a camera eight photos (or more) taken from different directions of the tested panel should be available. The interior and exterior parameters can be calculated based on the method of the bundle block adjustment with respect to the coordinates of image points, approximate values of the unknowns, measured distances, etc.

- ***Analytical plumb-line calibration***: the plumb-line technique was validated by (Brown, 1971). It is based on the assumption that a straight line in the object space will project as a straight line in image plane (with respect that the distortions are absent). Non-straight lines appearing in the image system are attributed to lens distortions. In the practice, the straight lines can be presented with digitized points. These measured points describe the lines and their distortion parameters. An empirical example: if 100 points were recorded in each of 10 horizontal and 10 vertical lines, i.e. on one hand, 2000 items of the data would be available to describe those 20 lines and on the other hand they give information about the parameters of the camera used.

- ***On-the-job calibration***: the term on-the-job calibration is used to identify the parameters of the lens and the camera calibration in the situ at the same time as the photography for the actual measurement of the object. This way is useful if the exposed object is not too large and not complex, in addition the control information (e.g. control points) is available in each exposure. The test panel used in this method can be made as frame from, for example, lightweight aluminium and exposed simultaneously with the object.

- ***Self-calibration***: the self calibration is an extension of the calibration method "*On-the-job calibration*". The main advantage of this method is that the parameters of the interior orientation could be calculated at the same time of the object exposure. In this case the discrete targeted marks on the object (test panel) are implemented as input data required for the determination of the object points and for the estimation of the camera parameters. If the objects measured do not have a special exposure system allowing to self-calibration or if there is *more-camera-online-system*, it would be better to use the *test panel* or *on-the-job calibration*.

2.3. Bundle Block Adjustment (BBA)

The Bundle Block Adjustment (BBA) - and also called: bundle triangulation, multiple images triangulation or multiple images orientation - is an important approach which enables to a simultaneous and a mathematical adjustment of photos together. This adjustment should be achieved in the images' space with respect to: the photogrammetric measurements (e.g. coordinates of the image points), geodetic observations (like: object point coordinates, distances, etc.) and a superordinated coordinates system (Luhmann, 2003, pp. 266).

Basically, the BBA can be defined as "the process of evaluating coordinates of targets and exterior orientation parameters of cameras using the Least Squares Theory (LST) based on the collinearity equations" (Cooper & Robson, 2001, pp. 35-38). Development of the principle of Least Squares Theory is described in the App. (LST).

In addition, it had been pointed (Hell, 1979; Wester-Ebbinghaus, 1978; Krauss, 1982 and Fuchs, 1984), that the BBA is used for point determination accurately, where it is considered as an accurate analytical process (especially in the close range photogrammetry) implemented for photogrammetric or mixed geodetic-photogrammetric determination of points.

The Figure (2.8) shows the principle of BBA, where the coordinates of image points (corresponding to measured object points) are the main input data applied in the calculation process of the BBA. Information about objects (e.g. coordinates of control points, measured distances, angles, etc.) can be also considered as additional input data.

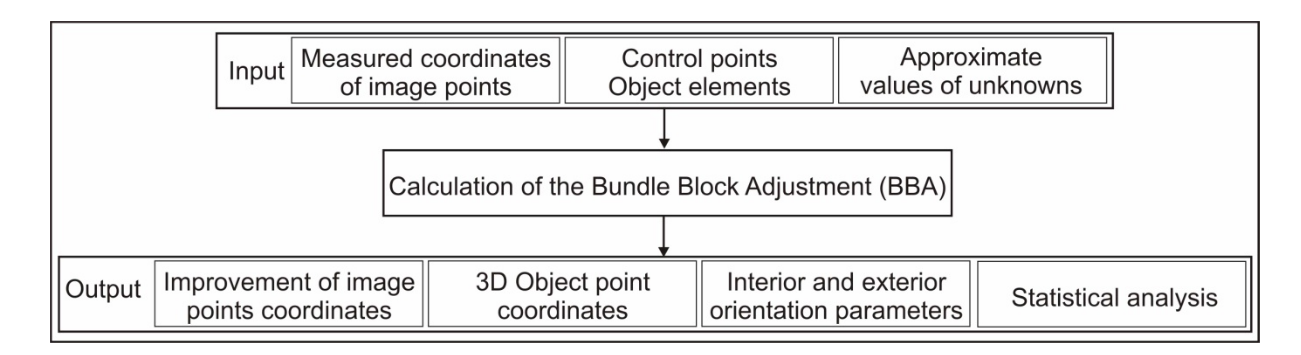

Figure (2.8): The principle of the bundle block adjustment

In general, the constraint equations involved in an adjustment problem can be non-linear. Particularly, the adjustment method is generally performed with linear functions, since it is rather difficult and often impractical to seek a least squares solution of non-linear equations. Therefore, a linearization process has to be enforced to get a linear form (Mikhail &

Ackermann, 1976, pp. 108-110). In the linearization context, approximate values of the unknowns should be determined and then applied into the BBA calculation. BBA results are: adjusted coordinates of object points, the interior and exterior orientation parameters, and finally a statistical process to check the results calculated.

In the BBA, the determination of approximate values of the unknown parameters (orientation parameters, object point coordinates, etc.) is still a main question which could be always posed, because - up to now - the algorithms used for an automatic determination of the approximate values may not give the solution optimally.

Within this thesis, an algorithm for the BBA of convergent exposures (namely: Baalbek's photos) will be used. It determines approximate values for non-linear adjustment. In this algorithm, calculations of approximate values and the BBA are converted by the same mathematical approach and only differ in the choice of free parameters. The algorithm[1] called "Pictran" (see Chapter 3.2.2) and had been developed by Gründig & Bühler (1985).

Pictran's work flow can be structured in two main stages. The first one is the determination of approximate values of unknown parameters (Figure 2.9). Input data entered in this step are: the coordinates of image points, the approximate orientation of images (provided as additional information) and any further geometric information about the object studied. The solution of the normal equation will be attained through a linearization process of the non-linear functional model applied in the adjustment problem. The solution result is approximate values of unknown parameters.

Second stage is the BBA, which will be achieved using the approximate values calculated in the 1st stage. In BBA, the solution of the normal equation is obtained through an iterative process. This process will be terminated at a certain threshold applied (so called: convergence value[2]). Through the iterative process of determination of unknown parameters, the amount of change between successive iterations is determined and compared to the convergence value. If the amount of change between successive iterations is greater than the convergence value, the iterative process continues. If that amount is less than critical convergence value, the iterative process ends (Figure 2.10).

[1] This algorithm has been called in 1985 (BITRI) and nowadays is called Pictran

[2] A convergence value determination depends on: observations, approximate values and camera configuration

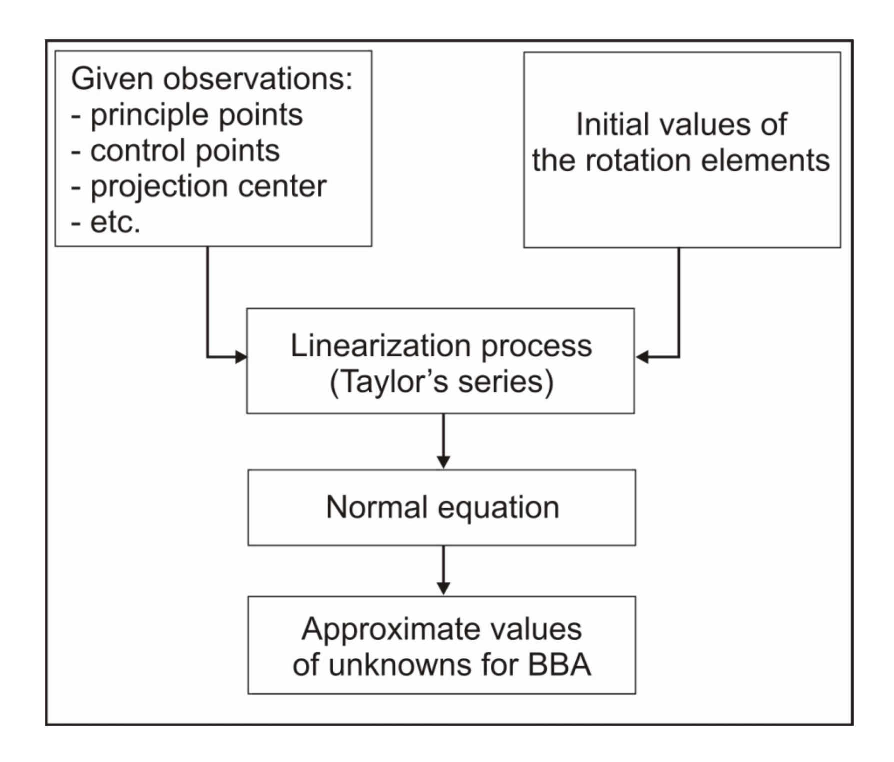

Figure (2.9): The determination of the approximate values of the unknown parameters in the algorithm “Pictran” (source: Gründig & Bühler, 1985)

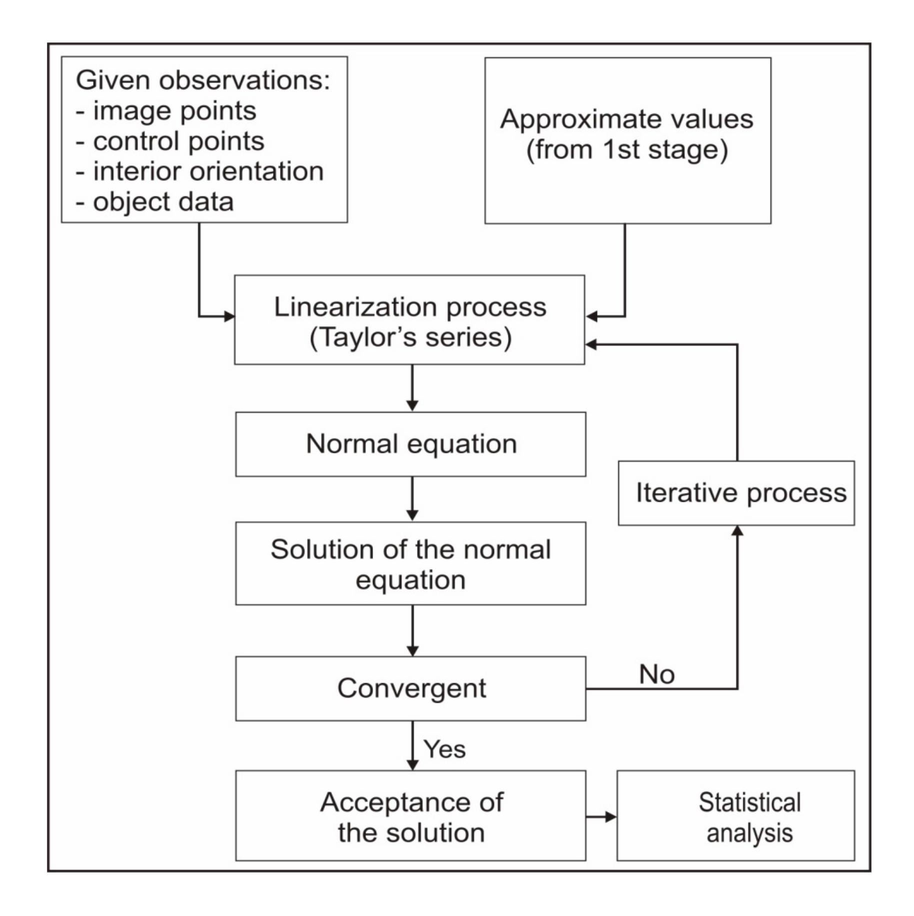

Figure (2.10): The principle of the bundle block adjustment in Pictran using the approximate values calculated (source: Gründig & Bühler, 1985)

3. A new approach for relative orientation of non-calibrated historical photos

3.1. Overview of the orientation process

The orientation process of Baalbek's historical images is an important aim of this research in order to perform an optimal estimation of parameters of cameras used (interior and exterior orientation parameters). This estimation will be enforced based on the method of the bundle block adjustment (Chapter 2.3). Baalbek's historical images, in addition to other data (e.g. control points), are the main input data applied into the orientation process. This process was carried out through three steps which are depicted in the Figure (3.1: a, b and c).

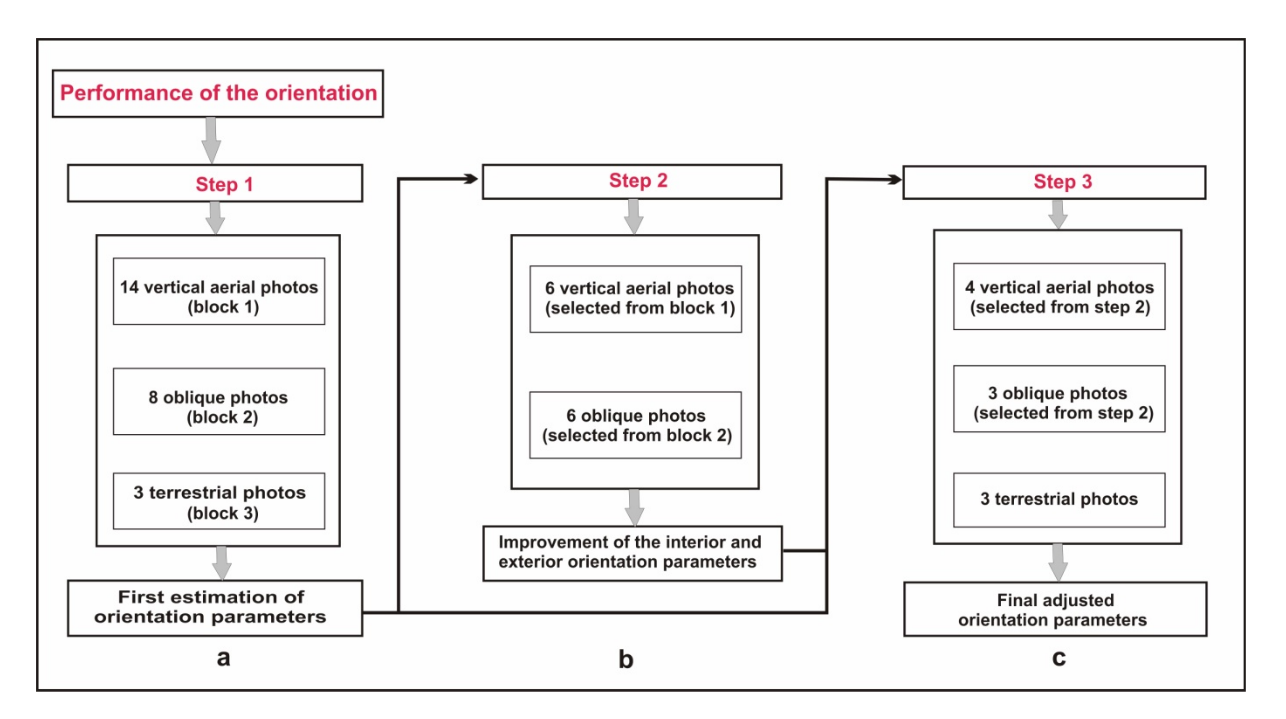

Figure (3.1: a, b and c): Orientation process of Baalbek's historical photos. This process was achieved based on a stepwise refinement of approximate values of orientation parameters

In the first orientation step each image type was separately oriented, where fourteen vertical, eight oblique and three terrestrial images were imported to the block (1), block (2) and block (3), respectively (cf. Figure 3.1, a). Results of this orientation step are rough estimations of interior and exterior orientation parameters as well as determination of the radial and decentring distortions.

The Figure (3.1, b) illustrates the image orientation process based on the combination between the vertical and oblique photos (Chapter 4), where six vertical images from the fourteen images (step1-block 1) were selected depending on image properties (for e.g. low image noise). In addition six oblique photos (from the eight images used in the step1-block 2)

were implemented. This step has been performed with respect to orientation results obtained from the first step of the orientation process. Result of the 2^{nd} step is refinement of the rough results calculated in the first orientation step.

Depending on orientation results computed through the first and second orientation steps, the third one was carried out (Fig. 3.1, c). The results of the 1^{st} and 2^{nd} steps were considered as approximate values for the interior and exterior orientation parameters in the last one. The results of the last step are the final adjusted orientation parameters.

3.2. Orientation of Baalbek's historical vertical aerial images

Basically, the orientation process started with Baalbek's vertical photos due to the existing of a special reference system on the images; with the assumption that the photos have been taken using the same metric camera. This system is presented by fiducial points on the images (Chapter 2.1). It leads to a stable model of the oriented images, which may offer good results (e.g. measurements of applicable object points). In addition, "the photogrammetric evaluation of the vertical photos is more accessible than oblique or terrestrial images, where the Nadir distance (or so called: Nadir angle) is smaller than or equals 3°" (Hildebrandt, 1996).

3.2.1. A primary preparation of vertical photos

3.2.1.1. Camera's focal length

The cameras used in the 1940s (exposure date of Baalbek's vertical images) could be categorized as following (Carlier, 1942):

- Camera "Gallus G20": this camera has the picture size $13 \times 18\ cm$ and it is fitted with the focal length $\mathrm{f} = 20\ cm$. It has been produced for stereo-photogrammetry and in this case is provided with an automatic magazine of 24 Plates.
- Poivilliers precision camera with an image size $13 \times 18\ cm$; This camera has been developed with focal lengths: $\mathrm{f} = 20\ cm$, $15\ cm$ or $12\ cm$; magazine is for 12 Plates.
- Aviophote (Richard make): camera of picture size $13 \times 18\ cm$; $\mathrm{f} = 20\ cm$ or $30\ cm$; and the magazine for 12 Plates.
- Altiphote (Richard make): $13 \times 18\ cm$ for image size and $\mathrm{f} = 20\ cm$ or $26\ cm$.

- Toporex Krauss (made by Barbier Benard and Turenne): this camera uses film and gives a picture with size $18 \times 24\ cm$; f $= 30\ cm$, $50\ cm$ or $70\ cm$.

The vertical photos were formed on glass sheets with the size $13 \times 18\ cm$ (Chapter 1.4.1). Therefore, it could be assumed that the focal length of the camera used for vertical images of Baalbek is $200\ mm$. This value will be used through the calculation of the bundle block adjustment as approximate value of the camera focal length.

3.2.1.2. Image scale determination

An image scale plays an important role in the orientation process because it impacts mainly on the functional model of the adjustment problem posed. In addition, it has direct effect on the computation of the flying altitude and image resolution.

The graphical materials of Baalbek have different image scales (Chapter 1.1). In order to determine the vertical image scales, the distances (d'_{0i}) - in the images - between different object points were measured[1]. Depending on 3D coordinates (X_i, Y_i and Z_i) of the abovementioned object points, distances (D_i) associated with can also be calculated (Table 3.1). Image scale number is given by the ratio:

$$m_{bq} = D_i / d'_i \tag{3.1}$$

where $i = 1, \dots, n; n$ the number of object points selected

$q = 1, \dots, g; g$ the number of images used

$d'_i = d'_{0i} \cdot P_s$

Thus, the image scale can be given (Luhmann, 2003, pp. 105-110):

$$m_q = 1/m_{bq} \tag{3.2}$$

The Table (3.1) shows that there are different image scales due to the different altitudes of the flight. The minimum image scale number is approx. (3141) for the image “scan 1984”. In contrast, the maximum one is (4342) for the image “scan 1989”. Through the calculations of the bundle block adjustment the mean value of the image scale numbers was applied; which is considered in this case ($\overline{m}_b = 4000$).

[1] The main tool used to achieve these measurements is the software *Adobe Photoshop CS2*

With respect to the mean image scale number as well as the camera focal length, the flight altitude is expressed as following:

$$\bar{h}_g = c_k \cdot \bar{m}_b \tag{3.3}$$

Based on the last equation the mean flight altitude is $\sim 800\ m$.

Image	Point	$X_i\ (m)$	$Y_i\ (m)$	$Z_i\ (m)$	$D_i\ (m)$	d'_{0i} (pixel)	$d'_i\ (cm)$	m_{bq}
scan 1980	4009	9520.162	10035.543	1150.262	107.887	877.79	2.55	4238
	4010	9563.068	10134.444	1146.110				
scan 1981	1003	9922.737	10629.434	1158.164	171.425	1582.26	4.59	3736
	1077	9759.969	10575.893	1163.317				
scan 1982	1077	9759.969	10575.893	1163.317	163.692	1356.02	3.93	4163
	1110	9730.840	10414.949	1156.706				
scan 1983	1110	9730.840	10414.949	1156.706	106.296	880.30	2.55	4164
	4020	9814.598	10350.906	1170.192				
scan 1984	1003	9922.737	10629.434	1158.164	171.425	1882.10	5.46	**3141**
	1077	9759.969	10575.893	1163.317				
scan 1985	4009	9520.162	10035.543	1150.262	107.887	887.53	2.57	4192
	4010	9563.068	10134.444	1146.110				
scan 1986	4028	10101.945	10645.258	1163.374	37.758	332.10	0.96	3921
	4029	10109.009	10608.189	1162.079				
scan 1989	4009	9520.162	10035.543	1150.262	107.887	856.78	2.48	**4342**
	4010	9563.068	10134.444	1146.110				
scan 1991	1116	9699.321	10496.582	1158.154	99.975	922.96	2.68	3735
	1077	9759.969	10575.893	1163.317				
scan 1993	1116	9699.321	10496.582	1158.154	99.975	953.79	2.77	3614
	1077	9759.969	10575.893	1163.317				
scan 2025	1116	9699.321	10496.582	1158.154	99.975	868.58	2.52	3969
	1077	9759.969	10575.893	1163.317				
scan 2026	1116	9699.321	10496.582	1158.154	99.975	1038.47	3.01	3320
	1077	9759.969	10575.893	1163.317				
Average								**~ 3878**

Table (3.1): Image scale numbers determination of Baalbek’s vertical photos

3.2.1.3. Scan and ground resolution

Geometrically, the image resolution describes the ability of a sensor to present set of given black and white lines separately, whereas they have the same properties such as: the length, the thickness, contrast, etc. (Luhmann, 2003, pp. 135-136).

The resolution of the vertical aerial photos of Baalbek is ca. 880 dpi which leads to the pixel size $P_s = 0.029\ mm$ (Chapter 1.4.1). The ground resolution R_g can be expressed as following:

$$R_g = P_s \cdot m_b \tag{3.4}$$

Based on the last equation, the ground resolution associated with Baalbek's vertical historical images is $\sim 12\ cm$.

3.2.1.4. Determination of fiducial points

The fiducial marks are necessary to realize a stable model of the images through the image orientation (Chapter 3.2). In our case, Baalbek's vertical images have fiducial marks but their coordinates are unknown. To determine the fiducial point coordinates, it was assumed that the fiducial origin (Chapter 2.1) has the coordinates ($x'_0 = y'_0 = 0$). The fiducial coordinates can be computed based on the measurement of the distances between the opposite pairs of fiducial points in the sides of each image plane.

Thus, each image has a special referenced system based on the fiducial marks associated with. In practice, through the orientation process of aerial images one referenced image system should be applied, which is already known and associated with the camera used. Therefore, it is essential in the study case of Baalbek to define a pattern of the fiducial system for all vertical images of Baalbek. The coordinates of the intended pattern of the fiducial points are presented in the Table (3.2).

Fiducial ID	$x_f\ (mm)$	$y_f\ (mm)$
1	0.00	55.00
2	80.00	0.00
3	0.00	-55.00
4	-80.00	0.00

Table (3.2): The coordinates of the fiducial pattern

The image coordinate system (pixel system) was changed into the camera coordinate system (ideal system) based on the 2D *affine transformation*. The six parameters of the 2D *affine transformation* and the $Sigma_0$ (estimated standard deviation of the unit weight is presented in the App. B).

3.2.2. Orientation process

In close range photogrammetry there are different methods used to perform the camera calibration and to obtain an optimal image orientation. In this context, there are many types of softwares which could be implemented in the photogrammetric applications in order to determine the camera parameters (with respect to the bundle block adjustment). A powerful algorithm, used in this thesis, is the software "Pictran". It enables to determine approximate values of the unknowns and to achieve the bundle block adjustment (Pictran's user Guide - Technet GmbH, 2000).

3.2.2.1. Pictran's basic principle and capabilities

Pictran is a software package developed by Technet GmbH for photogrammetric analysis. Basically, the whole process applying in Pictran is based on the following principle: *starting from a robust simplified mathematical model working with a stepwise refinement to end at the exact, however highly non-linear, mathematically, stochastically and physically correct modelling*.

It was selected to achieve the orientation process of Baalbek's graphical materials due to the following reasons:

- It is possible to enforce the process of images orientation without approximate values of the unknowns; that means a system of coordinates' model will be created through a relative orientation of the photos (this corresponds to the study case of Baalbek).
- Due to the relative orientation, this software has the advantage, that incorrect images could be detected; i.e. errors associated with images can be detected. In other words: it enables to eliminate huge failures shown through the orientation process.
- The program Pictran provides fast operation of the image data due to the special image format: *BT-format*. This fast operation is necessary in this research, because the graphical materials of Baalbek have approximately high memory sizes.

Pictran consists of the modules: **Pictran-D**, **Pictran-E**, **Pictran-O** and **Pictran-B**. The modules of Pictran D, E and O are used for 3D evaluations of the digital photos, the rectification and orthophoto creation, respectively. The module Pictran-B is considered the main module including the bundle block adjustment and therefore it is used for the following applications:

- 3D orientation process
- 3D object features acquisition through the spatial point determination
- Optimal calibration of analogous or digital photos

To create a new project in Pictran, a new camera must be defined (through *option/camera data*). It was assumed that the vertical images of Baalbek have been taken from the same metric camera (Chapter 1.4.1). In this context, the camera "**Baalbek-G1"** was considered for the aerial vertical photos. In addition, the focal length applied is $(c_k = 200)\, mm$ and the coordinates of the principal point $x'_0 = y'_0 = 0$ were assumed as approximate values (with the observation status[1]).

The vertical images were scanned and saved in the TIFF-format[2]. To guarantee fast access to image details, Pictran provides a special image format using BT-format which manages image data favourably (Pictran's user Guide - Technet GmbH, 2000). Images are tiled and saved in a BT-file to realize a faster access to image parts later.

In BT-file the image is divided into tiles which have consecutive numbers. The Figure (3.2) shows an example of an image divided into 20 tiles (dotted line). The tiles will be saved completely, but only the entirely useful parts of the original photo will be respected by further evaluations.

[1] The status can have the values 0, 1 or 2; that means: fixed, unknown or observation, respectively

[2] TIFF: Tagged Image File Format

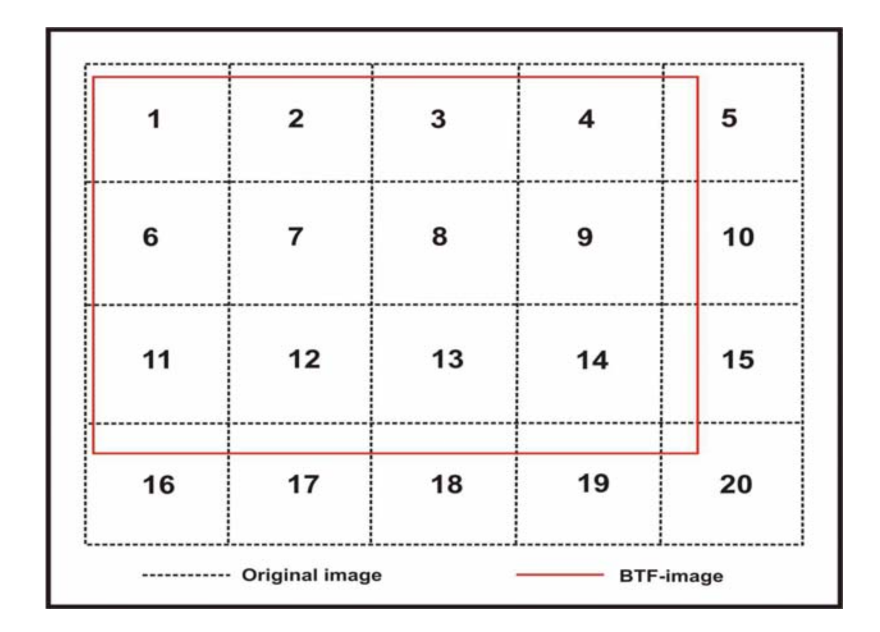

Figure (3.2): An original image and its BT-format

On one hand Pictran allows the user to add the control points using the menu "*exterior orientation*". The control points can be imported and saved in form of a three dimensional right-hand coordinate system. Each control point has 2D image coordinates (x' and y'). To ensure that each control point used should be participated in the calculation of the bundle block adjustment optimally, it will be essential that each one should be shown in two photos at the least.

On the other hand, the creation of a stable model for the bundle triangulation requests the collection of tie points between the images. Tie points are points whose ground coordinates are not known, but visually recognizable in the overlap area between two or more images. The number of tie points requested depends on the overlap area between the images.

Pictran-B offers two different solution modes for the estimation of the approximate values of the unknowns in the bundle block adjustment: *Compact Mode and Advanced Mode*. Both methods use efficient procedures of adjustment calculations (Gauss-algorithm, Hyper-Sparse-technique). If one of these modes does not succeed in the calculation, the second method will find a solution. The compact mode is the standard Pictran-B mode. This mode is especially characterised by its easily and clearly arranged usability. The calculation of approximate values for the unknowns of bundle block adjustment equations is processed by a modification of the functional model (quasilinear replacement problem). The calculation steps in the compact mode are:

1. Check of the consistency (*Bunkon*)
2. First calculation of approximate values (*Bunnae*)
3. Second calculation of approximate values (*Bunob*)
4. Bundle adjustment in object space (*Bunbil*)

In general, there are no approximate values available for the evaluation of the image blocks. The calculation of approximate values by modules *Bunnae* and *Bunob* is necessary before the strict bundle adjustment *Bunbil* because they enable to deal with linear form of the functional model applied in the adjustment calculation. If there are already approximate values available, it can be possible to start directly with the module *Bunob* or even *Bunbil*.

Basically, the reasons to use the advanced mode of Pictran-B can be summarized as following (Pictran's user Guide - Technet GmbH, 2000):

1. This mode enables to recognize large errors shown associated with the observations and control points separately and to eliminate them automatically.

2. The exterior orientation parameters and new additional 3D points are available in the space of the reference model after the pre-calculation by the module *Bunbil*.

3. In some particular cases (for example: extreme oblique photographs), it is possible that the approximate value calculations fail in the compact mode. The advanced mode guarantees a reliable determination of approximate values by combined intersection and resection also for problematic cases.

The advanced mode in Pictran-B includes two main calculation steps. They could be classified into *Pre-analysis* and *In-depth analysis*:

➢ *Pre- analysis*: it consists of the following calculation stages:

1. Check of consistency (*Bunkon*)
2. Check of images linkages (*Bunchk*)
3. Relative orientation (*Bunrel*)
4. Fitting scales (*Bunmas*)
5. Model points in superordinated system (*Bunnae*)
6. Exterior orientation in superordinated system (*Bunbac*)
7. Bundle adjustment in model space (*Bunbil*)

➢ *In-depth-analysis*:

1. Transformation to object space (*Bunhorn*)
2. Bundle adjustment in model space (*Bunbil*)

3.2.2.2. Bunnae's mathematic fundaments and data flow

The compact mode and the advanced mode of Pictran-B approximately have the same calculation sequence. In the study case of Baalbek the standard Pictran-B mode (the compact mode) will be used to enforce the orientation process of vertical images of Baalbek. The first calculation of approximate values for the unknowns[1] will be achieved through the module *Bunnae*; therefore it will be meaningful to describe the mathematic background used in this module. To express the mathematic characteristic (the functional model) of the *Bunnae*, the relationship between the image system and object space system should be respected. This relationship can be given as following (Luhmann, 2003, pp. 237-238):

$$(\mathbf{X} - \mathbf{X_0}) = m_b \cdot R \cdot \boldsymbol{X}' \tag{3.5}$$

where: $\boldsymbol{X}'$: image vector (equation 2.6)

$\mathbf{X_0}$: the projection center vector (equation 2.7)

$\mathbf{X}$: the coordinates vector of an object point P

m_b : image scale number (one scale number will be applied for each image)

R : rotation matrix

Based on the equation (3.5), *Bunnae* residual equations for the observations can be derived and classified into different types:

- **Type 1: basic equations**

$$0 + v_{X_P} = \overline{r_{11}}(x'_p - x'_0) + \overline{r_{12}}(y'_p - y'_0) + \overline{r_{13}}(z'_p - z'_0) + X_0 - X_p \tag{3.6.a}$$

$$0 + v_{Y_P} = \overline{r_{21}}(x'_p - x'_0) + \overline{r_{22}}(y'_p - y'_0) + \overline{r_{23}}(z'_p - z'_0) + Y_0 - Y_p \tag{3.6.b}$$

$$0 + v_{Z_P} = \overline{r_{31}}(x'_p - x'_0) + \overline{r_{32}}(y'_p - y'_0) + \overline{r_{33}}(z'_p - z'_0) + Z_0 - Z_p \tag{3.6.c}$$

The abovementioned equations are expressed in a linear form $l_i + v_i = f(\hat{x})$ where:

[1] All unknowns were applied in *Bunnae* with status (1) - as unknown – in the first iteration. By the further iterations they applied as observations (status 2).

$\bar{r}_{ij} = m_b \cdot r_{ij}$ (rotation matrices)

$x_p^{'}, y_p^{'}, z_p^{'}, X_p, Y_p$ and Z_p are observations

$x_0^{\prime}, y_0^{\prime}, z_0^{\prime}$ are constant values

- **Type 2: orthogonality creation**

The rotation matrix R can be re-formed through algebraic functions (quaternions). The usage of this mathematical form has following advantages:

- The mathematic processes will be easier with algebraic elements than trigonometric one
- The singularity case will be avoided
- It realizes faster access in the bundle block adjustment

Thus, the quaternions-based rotation matrix is given as following (Albertz & Wiggenhagen, 2008; Jun et al., 2008):

$$R = \begin{bmatrix} a & b & c \\ d & e & f \\ g & h & i \end{bmatrix} = \begin{bmatrix} q_0^2 + q_1^2 - q_2^2 - q_3^2 & 2(q_1 q_2 - q_0 q_3) & 2(q_1 q_3 + q_0 q_2) \\ 2(q_1 q_2 + q_0 q_3) & q_0^2 - q_1^2 + q_2^2 - q_3^2 & 2(q_2 q_3 - q_0 q_1) \\ 2(q_1 q_3 - q_0 q_2) & 2(q_2 q_3 + q_0 q_1) & q_0^2 - q_1^2 - q_2^2 + q_3^2 \end{bmatrix} \quad (3.7.a)$$

The new form is bilinear function and valid only if: $q_0^2 + q_1^2 + q_2^2 + q_3^2 = 1$

The rotation matrix R is orthogonal ($R^t \cdot R = I$), therefore 21 orthogonality relationships could be carried out where only 6 relations are bilinear and independent (see Schwidefsky & Ackermann, 1976). The mentioned orthogonality relationships lead to 21 residual equations.

The following equations present only 3 of 21 residual equations:

- the inner product of each line resp. column with itself is 1

$$0 + v_1 = a^2 + b^2 + c^2 - 1 \quad (3.7.b)$$

- the inner product of different lines resp. different columns is 0

$$0 + v_7 = a \cdot d + b \cdot e + c \cdot f \quad (3.7.c)$$

- each element is the same as its sub-determinant

$$0 + v_{13} = e \cdot i - f \cdot h - a \quad (3.7.d)$$

- **Type 3: additional distance observations**

Additional measured distances are essential to realize a stable image scale. Those distances could be computed between object points or between centers of projection observed. They will lead to distance residual equations, which are given:

$$d_i + v_{d_i} = sqr[(X_{i+1} - X_i)^2 + (Y_{i+1} - Y_i)^2 + (Z_{i+1} - Z_i)^2] \quad (3.8)$$

$i = 1, \ldots, n$; n number of object points observed

- **Type 4: additional observations of the coordinate differences**

$$\Delta X_i + v_{\Delta_{X_i}} = X_{i+1} - X_i \quad (3.9.a)$$

$$\Delta Y_i + v_{\Delta_{Y_i}} = Y_{i+1} - Y_i \quad (3.9.b)$$

$$\Delta Z_i + v_{\Delta_{Z_i}} = Z_{i+1} - Z_i \quad (3.9.c)$$

- **Type 5: additional observations of the plane points**

At least three points observed per plane are essential. If the normal vector of the observed plane is denoted by the components *A*, *B* and *C*, the residual equations associated with are:

$$0 + v_{X_{P1}} = A \cdot X_{P1} + B \cdot Y_{P1} + C \cdot Z_{P1} + D \quad (3.10.a)$$

$$0 + v_{X_{P2}} = A \cdot X_{P2} + B \cdot Y_{P2} + C \cdot Z_{P2} + D \quad (3.10.b)$$

$$0 + v_{X_{P3}} = A \cdot X_{P3} + B \cdot Y_{P3} + C \cdot Z_{P3} + D \quad (3.10.c)$$

In addition, the components of the normal vector lead to the following equation:

$$0 + v_4 = A^2 + B^2 + C^2 - 1 \quad (3.11)$$

- **Type 6: unknowns as observations (perspective centers as observations)**

In this case the coordinates of the perspective center should be available. The equations of the residual are expressed:

$$0 + v_{X_0} = X_0 - X_{0.observed} \quad (3.12.a)$$

$$0 + v_{Y_0} = Y_0 - Y_{0.observed} \quad (3.12.b)$$

$$0 + v_{Z_0} = Z_0 - Z_{0.observed} \quad (3.12.c)$$

- **Type 7: constants as observations (control points as observations)**

In the case that the control points are observed and not fixed, they can be taken also into the account. The residuals equations resulted are:

$$0 + v_{X_i} = X_i - X_{i.observed} \tag{3.13.a}$$

$$0 + v_{Y_i} = Y_i - Y_{i.observed} \tag{3.13.b}$$

$$0 + v_{Z_i} = Z_i - Z_{i.observed} \tag{3.13.c}$$

- **Type 8: rotation matrix as observation**

In comparison between the equations (2.9) and (3.7.a), the relationship between the rotation angles can be expressed (with respect to residuals):

$$\sin\varphi + v_\varphi = r_{13} + v_\varphi = 2(q_1 q_3 + q_0 q_2) \tag{3.15.a}$$

$$\tan\omega + v_\omega = -\frac{r_{23}}{r_{33}} + v_\omega = -\frac{2(q_2 q_3 - q_0 q_1)}{q_0^2 - q_1^2 - q_2^2 + q_3^2} \tag{3.15.b}$$

$$\tan\kappa + v_\kappa = -\frac{r_{12}}{r_{11}} + v_\kappa = -\frac{2(q_1 q_2 - q_0 q_3)}{q_0^2 + q_1^2 - q_2^2 - q_3^2} \tag{3.15.c}$$

Basically, the equations of the type 1 and type 2 present the prerequisites for the computation of the pre-values of the unknowns. In the case study of Baalbek (namely: vertical images), the approximate values of interior orientation parameters presented in the type 1 entered through the calculations as following: $c_k = 200\ mm$ and $x'_0 = y'_0 = 0$. On the other hand the control points were considered fixed values; therefore the equations of the type 7 were neglected.

The results of the module *Bunnae* will be used as input data in the module *Bunob* in the compact mode. In addition, in the module *Bunnae* there is one scale per image i.e., the mathematical model applied is robust. To improve this model, a new constraint will be respected that one image scale per image point is applied in the module *Bunob* as well as one conditional equation for orthogonality enforcement. This mentioned constraint is considered as the main difference between both modules (*Bunnae* and *Bunob*) and leads to changes in the residual equations of the type 1 and type 2 (these changes will be described in detail in the next chapter).

The approximate values of the interior and exterior orientation parameters estimated in *Bunnae*, moreover, unknown object points should be geometrically improved in the module *Bunob*. The improved results (namely: *Bunob's* results) will be applied into the final module *Bunbil* which presents the main and final calculation of the bundle block adjustment.

3.2.2.3. Calculation sequence and data flow in Bunbil

The functional model in the module *Bunbil* includes the residual equations which could be categorized in the following types (with respect that one scale per image point is applied):

- **Type 1: Basic equations**

Based on the equation (3.5) the coordinates of an image point observed can be computed:

$$\boldsymbol{X'} = \frac{1}{m_{bi}} \cdot R^{-1} \cdot (\mathbf{X} - \mathbf{X_0}) \tag{3.16}$$

where m_{bi} : the image scale number associated with an image point p_i'; $i = 1, \ldots n; n$ (the number of image points determined). Based on the formula (2.8.a), R^T is given:

$$R^T = \begin{bmatrix} r_{11} & r_{21} & r_{31} \\ r_{12} & r_{22} & r_{32} \\ r_{13} & r_{23} & r_{33} \end{bmatrix} \tag{3.17.a}$$

$$R^{-1} = R^T = \begin{bmatrix} q_0^2 + q_1^2 - q_2^2 - q_3^2 & 2(q_1q_2 - q_0q_3) & 2(q_1q_3 + q_0q_2) \\ 2(q_1q_2 + q_0q_3) & q_0^2 - q_1^2 + q_2^2 - q_3^2 & 2(q_2q_3 - q_0q_1) \\ 2(q_1q_3 - q_0q_2) & 2(q_2q_3 + q_0q_1) & q_0^2 - q_1^2 - q_2^2 + q_3^2 \end{bmatrix}^T \tag{3.17.b}$$

with respect to the condition: $q_0^2 + q_1^2 + q_2^2 + q_3^2 = 1$

Consequently, the vector $\boldsymbol{X'}$ is expressed as following:

$$x'_{pi} - x'_0 = \tilde{r}_{11}(X_P - X_0) + \tilde{r}_{21}(Y_P - Y_0) + \tilde{r}_{31}(Z_P - Z_0) \tag{3.18.a}$$

$$y'_{pi} - y'_0 = \tilde{r}_{12}(X_P - X_0) + \tilde{r}_{22}(Y_P - Y_0) + \tilde{r}_{32}(Z_P - Z_0) \tag{3.18.b}$$

$$z'_{pi} - z'_0 = \tilde{r}_{13}(X_P - X_0) + \tilde{r}_{23}(Y_P - Y_0) + \tilde{r}_{33}(Z_P - Z_0) \tag{3.18.c}$$

where: $\tilde{r}_{uw} = \frac{r_{uw}}{m_{bi}}$; *u, w* =1,…,3

On one hand, since to that an image is 2D coordinates, the value z'_{pi} can be neglected. In practice, it can be assumed in the module *Bunbil* that the value (z'_{pi}) is ca. $(0{,}01 \cdot x'_{pi})$ or

$(0{,}01 \cdot y'_{pi})$. On other hand the lens errors (radial and decentring distortions, displacement of the principle point, etc.) have an impact on the determination of image point coordinates. Therefore, those coordinates (expressed in the equations 3.18 a, b and c) should be radially and decentring corrected.

- **radial distortion**

The radial corrected coordinates of an image point $p'_i(x'_{pi}, y'_{pi})$ are given:

$$x'_{rad.} = x'_{pi} + x'_{pi} \cdot A_1(r^2 - r_0^2) + x'_{pi} \cdot A_2(r^4 - r_0^4) \quad (3.19.a)$$

$$y'_{rad.} = y'_{pi} + y'_{pi} \cdot A_1(r^2 - r_0^2) + y'_{pi} \cdot A_2(r^4 - r_0^4) \quad (3.19.b)$$

where: A_1 and A_2 are radial distortion parameters
r … radial distance to the principle point
$r_0 = \text{const}$

- **decentring distortion**

Going from that the coordinates of an image point were already radial corrected, the other decentring corrected one are expressed:

$$x'_{dec.} = x'_{rad.} + 2A_5 \cdot x'_{pi} \cdot y'_{pi} + A_6(r^2 + 2x'^2_{pi}) \quad (3.20.a)$$

$$y'_{dec.} = y'_{rad.} + 2A_6 \cdot x'_{pi} \cdot y'_{pi} + A_5(r^2 + 2y'^2_{pi}) \quad (3.20.b)$$

where: $A_5$and A_6 are decentring distortion parameters

- **principle point displacement**

The coordinates calculated will be corrected based on the principle point displacement error; with respect that the radial and decentring distortions were achieved. Thus the coordinates will be denoted:

$$x'_{ppd.} = x'_{dec.} + x'_0 \quad (3.21.a)$$

$$x'_{ppd.} = y'_{dec.} + y'_0 \quad (3.21.b)$$

- **affinity and shear errors**

Generally, the shear and affinity errors display the deviation of the image coordinate system from the standard case of orthogonality. Therefore, the coordinates to be corrected based on the mentioned errors can be calculated:

$$x'_{aff.} = x'_{ppd.} + A_3 \cdot x'_{ppd.} + A_4 \cdot y'_{ppd.} \quad (3.22.a)$$

$$y'_{aff.} = y'_{ppd.} - A_3 \cdot y'_{ppd.} + A_4 \cdot x'_{ppd.} \quad (3.22.b)$$

A_3 and A_4: are scale and shear distortion parameters, respectively.

Consequently, the residual equations will be:

$$v_{xp'} = x'_{p\,obs.} - x'_{aff.} \quad (3.23.a)$$

$$v_{yp'} = y'_{p\,obs.} - y'_{aff.} \quad (3.23.b)$$

$$v_{zp'} = z'_{p\,obs.} - z'_{pi} \quad (3.23.c)$$

- **Type 2 - 8 (orthogonality creation… etc.)**

The residual equations of types 2-8 in the module *Bunbil* are the same in the module *Bunnae*.

- **Type 9: principle point and principle distance as observations**

The module *Bunbil* allows applying the principle point and principle distance as observations into the computations. The residual equations are given:

$$v_{x'_0} = x'_{0\,cal.} - x'_{0\,obs.} \quad (3.24.a)$$

$$v_{y'_0} = y'_{0\,cal.} - y'_{0\,obs.} \quad (3.24.b)$$

$$v_{ck} = c_{k\,cal.} - c_{k\,obs.} \quad (3.24.c)$$

To enforce the final calculations of approximate values in the module *Bunbil*, some control parameters (before starting of the adjustment process) should be considered such as: the distance between the camera and the recorded object, object expansions, standard deviation of observations, etc. These parameters have an important role to achieve a stable process of the bundle block adjustment. In this context, the standard deviation of image points coordinates (observations) was applied of ca. 0.1 unit of image system. In contrast, the standard deviation

of object points (control points measured by tachymeter) entered into the adjustment calculation of ca. $\pm 10\ cm$ (see Table 3.3).

Mean camera-to subject distance	$800\ m$
Object expansion	$1500\ m$
Standard deviation of image point coordinates	MFV of image points is 0.1 (image unit)
Standard deviation of object coordinates	$\mathrm{MFV}_X = \mathrm{MFV}_Y = \mathrm{MFV}_Z = \pm 10\ cm$

Table (3.3): Control parameters applied into module *Bunbil*

A useful adjustment result can be created by Pictran-B, if the majority of the input data is convergent. An important indicator of the correctness of the input data majority is that *the values of redundancy and the sum of the redundancy numbers should be identical* (Pictran's user Guide - Technet GmbH, 2000). The determination of the redundancy depends on the number of observations, unknowns and constraint conditions. It is given (see App. C):

$$n_{red.} = n_{obs.} - n_{unk.} + n_{con.} \tag{3.25}$$

$n_{obs.} = 549$ number of observations (image and object points' coordinates)

$n_{unk.} = 305$ number of unknowns (orientation parameters)

$n_{con.} = 14$ number of constraint equations

Based on the equation (3.25) the redundancy will be $n_{red.} = 258$, which equals to the sum of the redundancy numbers (see App. C), i.e. the majority of input data is correct.

3.2.3. Results of orientation process

3.2.3.1. Interior orientation parameters

The Table (3.4) shows the adjusted interior orientation parameters of the camera used (in this case: Baalbek-G1) and their accuracy (estimated standard deviations M_i).

Camera name	$x'_{o\ obs.}\ (mm)$	adjusted $x'_o\ (mm)$	$\mathrm{M}_{x'_0}\ (mm)$
	$y'_{o\ obs.}\ (mm)$	adjusted $y'_o\ (mm)$	$\mathrm{M}_{y'_0}\ (mm)$
	$c_{k\ obs.}\ (mm)$	adjusted $c_k\ (mm)$	$\mathrm{M}_{c_k}\ (mm)$
Baalbek-G1	0.00000	-0.069894	0.4050
	0.00000	-0.049059	0.4057
	200.000	200.253031	0.3151

Table (3.4): Estimated interior orientation parameters - vertical photos (App. C)

3.2.3.2. Exterior orientation parameters

Exterior orientation parameters of the vertical images (namely: coordinates of the perspective centers, rotation elements) calculated based on the module *Bunbil* are the final results refined in the bundle adjustment process.

Results of exterior orientation parameters are expressed in the (Table 3.5). 2D as well as 3D views of the projection centers associated with the images applied in the orientation process are depicted in the Figure (3.3) and the Figure (3.4), respectively.

Image type	Image ID	$X_0\ (m)$	$Y_0\ (m)$	$Z_0\ (m)$	$\omega\ (gon)$	$\varphi\ (gon)$	$\kappa\ (gon)$
Vertical	Scan 2033	9620.087	10658.342	1574.306	-10.99049	-10.81684	23.385370
	Scan 2026	9658.840	10821.765	1766.475	-11.93183	-1.092040	30.618480
	Scan 1984	9699.413	10684.414	1769.116	-11.24757	-5.798905	30.526316
	Scan 1993	9859.140	10748.370	1863.944	-4.181080	9.898223	-70.965947
	Scan 2032	10337.054	10870.662	1909.953	-1.664087	12.28818	-69.235504
	Scan 1981	9970.141	10673.541	1940.080	4.425129	4.625882	131.135824
	Scan 1986	10198.810	10754.433	1942.009	-0.562396	9.735222	-69.011182
	Scan 1991	9837.954	10583.680	1948.053	4.047548	8.247321	-69.417227
	Scan 1980	9235.127	10206.9756	1984.222	0.756046	-12.42311	-53.007673
	Scan 1985	9420.691	10322.495	2019.253	0.498483	-5.372811	147.900302
	Scan 1989	9242.084	10158.075	2026.240	-5.084343	-6.723128	147.272736
	Scan 2025	9791.510	10558.579	2028.774	9.571998	-3.034766	148.071746
	Scan 1983	9608.955	10431.609	2037.015	4.005227	-2.657865	147.853681
	Scan 1982	9743.176	10470.342	2040.897	8.312270	0.882125	146.711345

Table (3.5): Exterior orientation parameters - vertical photos

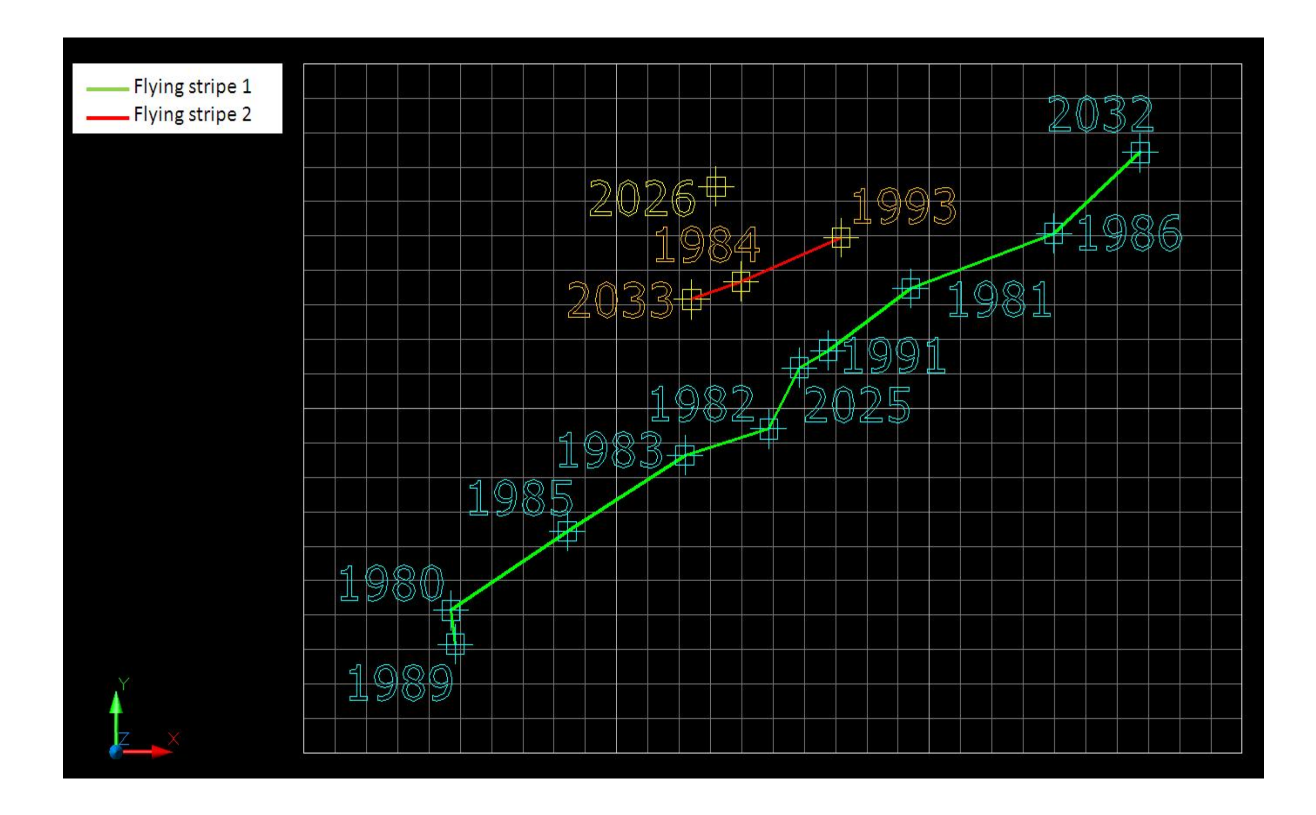

Figure (3.3): 2D position of the projection centers associated with the vertical images; where it can be accepted that there are two flying lines: flying line1 (green) and flying line2 (red), moreover, it can be also assumed that the image 2026 was taken during another flying stripe.

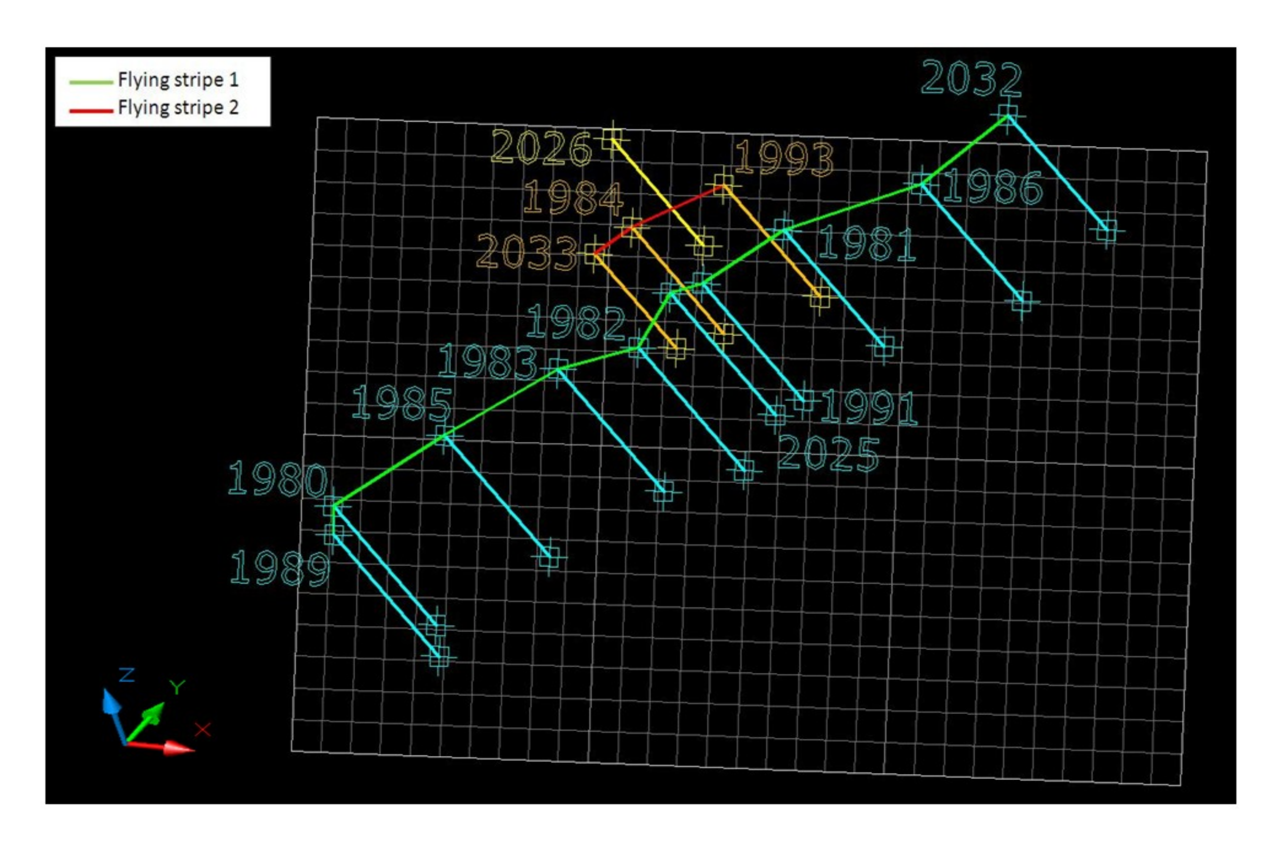

Figure (3.4): 3D view presenting the projection centers associated with the vertical images

3.2.4. Parameter quality assessment

To achieve a significant photogrammetric evaluation of the calculated results, quality assessment measurements should be taken into the account. These measures should reveal to which extent the orientation results calculated are well and fit to further requirements and purposes (e.g. GIS applications, archaeology, etc.). Quality characteristics assessment could be realized using the basic quality criterions: *accuracy* and *reliability*.

3.2.4.1. The term “accuracy”

The accuracy of a quantity reflects how much this quantity is accurately determined, if and only if the functional relationships between observations and to be estimated parameters are correct and pre-assumptions are applied through adjustment calculations (Niemeier, 2008, pp. 270-271). The accuracy measurements are described quantitatively by statistical parameters, which could be denoted as following:

- **Interior accuracy (MFV):** it is defined as the standard deviation of observations before the adjustment. This value is specified by the user before the adjustment. If this assumed value is not confirmed after the adjustment calculation; that means a balanced stochastical model applied into the adjustment process is not guaranteed.
- **Exterior accuracy (M):** exterior accuracy measurements are derived based on the cofactor matrix of unknowns ($Q_{\hat{x}\hat{x}}$). It represents estimated standard deviations of unknowns after the adjustment. These values reveal if those unknowns were determined geometrically well or bad. They do not display observation errors and can not be used for assessment before all large observation errors shown are eliminated.

3.2.4.2. The term “reliability”

The term reliability relates to the controllability of observations applied into the adjustment. It depends on the number of observations participated into calculations and on the exposure configuration. Reliability criterions can be extracted based on the cofactor matrix of residuals Q_{vv} which is given as following (Luhmann, 2003, pp. 64-68 & Niemeier, 2008, pp. 141-142):

$$Q_{vv} = Q_{ll} - \mathrm{A} \cdot Q_{\hat{x}\hat{x}} \cdot \mathrm{A}^T \tag{3.26}$$

The total redundancy (the degree of freedom in the adjustment) is expressed based on the equation (3.26) as following:

$$r = n - u = trace(Q_{vv} \cdot W) = \sum r_i \tag{3.27}$$

where r_i the observational redundancy numbers (partial redundancies)

If the equation system has a unique solution, this means r will equal zero. In addition, if the observation is fully constrained i.e., r_i would equal 1. As explained by (Ghilani & Wolf 2006, pp. 414-416) that the observational redundancy numbers provide insight into the geometric strength of the adjustment. An adjustment that in general has a low redundancy number will have observations that lack sufficient checks to isolate blunders, and thus the chance for undetected blunders to exist in the observations is high. In contrast, a high overall redundancy number enables a high level of internal checking of the observations and thus there is a lower chance of accepting observations that contain large errors.

The participative part r_u of an observation (l_i) to determine an unknown u_j in the adjustment could be computed based on the observational redundancy numbers ($r_u = 1 - r_i$). In addition, the relative influence of an observation error on the residuals is defined through a percentage (EV_i) of observational redundancy numbers r_i that means:

$$\mathrm{EV}_i = r_i \cdot 100\% \tag{3.28}$$

In the case that $\mathrm{EV}_i = 0$, that could mean:

- a large mistake associated with the observation (l_i) is not detectable
- this observation can not be controlled by other observations
- by determination of unknowns this observation will be full participated ($r_u = 1$)

In contrast, if $r_i = 1$ ($\mathrm{EV}_i = 100\%$), that means the observation (l_i) is full controlled, but it doesn't take any role in determination of unknowns (in this case $r_u = 0$). In adjustment calculations it is important that each observation should be well controlled, moreover, it should take a role in determination of unknowns in order to balance the reliability and efficiency of the calculations. This could be met if EV_i values are between 30% to 80%.

3.2.4.3. Outlier detection in observations (normalized residual NV)

An important quality criterion is the normalized residual, which used to detect outliers in observations. It is defined through the following formula (Gruber & Joeckel, 2005; Luhmann, 2006, pp. 64-66):

$$\mathrm{NV}_i = \frac{v_i}{\hat{s}_{v_i}} \tag{3.29}$$

where v_i : a residual associated with an observation (l_i)

$\hat{s}_{v_i}$: the standard deviation of a residual (v_i)

Using the appropriate diagonal elements of the matrix Q_{vv} and a priori standard deviation of unit weight (in general, it is set 1) the standard deviation of a residual is given (Baarda, 1968; Gruber & Joeckel, 2005, pp. 156-157; Ghilani & Wolf, 2006, pp. 416-418; Luhmann, 2006):

$$\hat{s}_{v_i} = \hat{s}_0\sqrt{q_{v_i v_i}} = \hat{s}_{l_i}\sqrt{r_i} \tag{3.30}$$

where $\hat{s}_{l_i}$: the standard deviation of the observation l_i

According to (Baarda, 1968), the normalized residuals follow the standard normal distribution N (0, 1). Therefore, normalized residuals could be used to detect outliers associated with observations. In this context, if an observation has (NV_i) larger than a threshold (k), which depends on the significance level (α), then that observation may have a large error.

Baarda (1968) had computed rejection criteria for various significant levels as following:

- for $\alpha = 0.001 \Rightarrow 1 - \alpha = 0.999 \Rightarrow k = 3.29$
- for $\alpha = 0.01 \Rightarrow 1 - \alpha = 0.99 \Rightarrow k = 2.58$
- for $\alpha = 0.05 \Rightarrow 1 - \alpha = 0.99 \Rightarrow k = 1.96$

However, empirical assumptions are considered to prove if there is an error associated with an observation:

$\mathrm{NV}_i < 2.5 \Leftrightarrow$ there is no large error visible (with probability 80%)

$2.5 < \mathrm{NV}_i < 4.0 \Leftrightarrow$ there is large error visible

$4.0 < \mathrm{NV}_i \Leftrightarrow$ there is large error very likely (with probability 95%)

The interpretation of the abovementioned assumptions can be expressed as following:

- when NV_i is larger than 4, this means that the corresponding residual is, very likely, four times larger than it should be due to the stochastic guide line. In addition, *the observation associated with is incorrect (with the probability 95%)*.
- when NV_i is less than 2.5 that means: *with probability 80% there is no large error shown related to the tested observation.*

3.2.4.4. Estimated standard deviation of unit weight (global accuracy of the adjustment)

In general, the bundle adjustment method gives an estimated value of the standard deviation of unit weight $\hat{s}_0$ (a posteriori). This value should be sufficiently conformed to the a priori standard deviation of unit weight s_0 (in general, s_0 is set 1) in order to preserve a stable stochastical model. The comparison between $\hat{s}_0$ and s_0 can be carried out through a statistic test (model test). Within this test, the square ratio of $\hat{s}_0$ and s_0 will be compared with a certain value - which depends on a significance level α - as following (Matthias et al., 1983):

$$\left(\frac{\hat{s}_0}{s_0}\right)^2 < \frac{\mathrm{CHI}^2\,(\mathrm{F};1-\alpha)}{\mathrm{F}} \qquad (3.31)$$

where:
F: degree of freedom
$1-\alpha$: confidence interval
CHI^2 (F; $1-\alpha$): fractile of the CHI^2-distribution

Based on (3.31) it could be:

- $\hat{s}_0$ (a posteriori) $\gg s_0$ (a priori): i.e., that MVF of observations were too small applied!
- $\hat{s}_0$ (a posteriori) $\ll s_0$ (a priori): i.e., that MVF of observations were too large applied!

In practice, the plausible interval of $\hat{s}_0$ is [0.7 – 1.3]. If $\hat{s}_0$ is in this interval, it could be accepted that bundle adjustment results do not have large errors visible. In this case, also expectations of accuracy and reliability are met sufficiently, but it does not issue a guarantee for quality of each observation separately. In contrast, if $\hat{s}_0$ is not in the plausible interval, it could mean that:

- The stochastic model (Chapter 2.3.2.3) is incorrect; which means either observations are roughly incorrect or their mean errors (MFV) are incorrectly assumed.
- Roughly incorrect observations, which have large normalized residuals, should be checked.

3.2.5. Results check

In this chapter, the results presented in Chapters (3.2.3.1 & 3.2.3.2) will be interpreted and discussed based on qualiy parameters given in the Chapter (3.2.4).

- *Global quality of the adjustment calculations*

Previously mentioned (Chapter 3.2.4.4) that bundle block adjustment computations give an estimated value of the standard deviation of unit weight (a posteriori value). This value should be checked (with respect to s_0 and MFV of observations) to know to what extent the adjustment calculations are accepted and if the stochastical model applied is plausible.

Variances of ($\hat{s}_0$) based on different values of a priori standard deviation of image points (namely: MFV of observations) are shown in the Figure (3.5). An increasing of MFV values of image points leads to a decreasing of ($\hat{s}_0$). This increasing is constrained by the accuracy required of output data used for further applications (in this case: up to two pixels; ca. 25 cm in the vertical image type). To keep $\hat{s}_0$ in the plausible interval, MFV of image points should be between ca. 0.22 to 0.45 (image system unit).

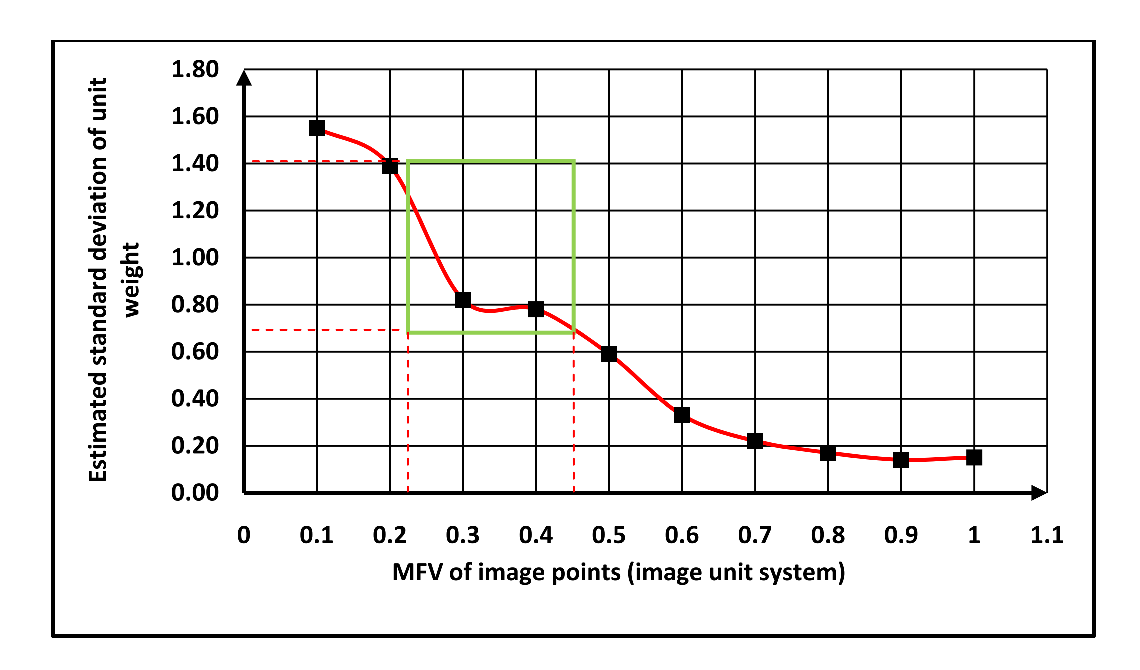

Figure (3.5): Variances of $\hat{s}_0$ based on different initial errors of image points (with respect that there is no large errors associated with observations)

- *Outliers detection*

In adjustment calculations each observation was well controlled, moreover, it took a role in the determination of unknowns, because the observational redundancy numbers r_i are in the range [0.1 - 0.8]. This means that values of (NV_i) are certain and therefore, it was possible to detect errors shown associated with observations. In this context, the most of values (NV_i) are smaller than the critic value (see Chapter 3.2.4.3); i.e. that there is no large error probable through the adjustment process (with probability 80%). The Table (3.6) presents maximum five values of NV_i and their corresponding observations (image points). $\mathrm{NV}_{i\,max}$ is $\sim$2.54 associated with the vertical coordinate of the image point (4019) in the photo "scan -1982".

Image ID	Image point ID	NV	Coordinate
scan 1982	4019	2.535	y'
scan 1986	4038	2.525	y'
scan 1989	4007	2.334	x'
scan 1982	1142	2.255	y'
scan 1983	1208	2.195	x'

Table (3.6): Maximum five values of NV_i and corresponding image points

- *Accuracy of camera's parameters*

The estimated standard deviations of camera interior parameters are as following: $\mathrm{M}_{x'_0} \approx \mathrm{M}_{y'_0} \approx 0.41\,mm$ and $\mathrm{M}_{c_k} = 0.32\,mm$ (Table 3.4). Those values confirm the initial standard deviations of camera parameters applied into the calculations (ca. $0.5\,mm$), which means a balanced stochastic model was guaranteed.

It can be assumed that the vertical images had been taken through different flying stripes (cf. Figure 3.3). The first one includes the following images: "1989, 1980, 1985, 1983, 1982, 2025, 1991, 1981, 1986 and 2032". In contrast, the images: "2033, 1984 and 1993" had been taken through the second one. Finally, it can be also accepted that the image "2026" had been taken in another flying line. Based on Z_0 values of perspective centers calculated (Table 3.5), it could be evaluated that there were different flying heights h_g of vertical images which could be classified as following:

Phase1: $h_g \approx 1765\,m$, phase2: $h_g \approx 1935\,m$ and phase3: $h_g \approx 2030\,m$

On one hand these different flying heights are the reason that Baalbek's vertical images have different image scales. On the other hand and concerning the flying plane (namely: image plane), the rotation elements ω and φ indicate that the plane was approximately horizontal.

3.3. Orientation of Baalbek's historical oblique images

3.3.1. Preliminary requirements

- The camera used for Baalbek's oblique images was a non-metric camera; because there is no reference system defined on oblique images (fiducial marks are not complete). The camera focal length was considered $260\,mm$ as an approximate value based on information noted on borders of the oblique images (Chapter 1.4.1.). In addition, the coordinates of the principle point are considered as following: ($x'_0 = y'_0 = 0$).
- In an analogue way described in the Chapter (3.2.1.2.), image scale numbers of oblique photos are in the range [3082 - 5341] (see App. D). The mean image scale number ($\overline{m}_b = 4000$) was applied into the orientation process.
- According to the equation (3.3) the mean height (namely: camera - to - the subject distance) is ca. $1040\,m$.
- Image pixel size $P_s \sim 0.042\,mm$ (with respect that the resolution of oblique photos is 600 dpi, see Table 1.3). This leads to the ground resolution $R_g \sim 13\,cm\ to\ 22\,cm$ (with respect to image scale numbers).

3.3.2. Orientation process and results

The orientation process was enforced using eight oblique images. Analysis and the consistency check of input data were served by the module *Bunkon* in the compact mode of Pictran-B. Output data of *Bunkon* will be the input file for next analysis in the module *Bunnae*. Primary control parameters applied into orientation process are presented in the Table (3.7). In this context, the primary mean error for image point coordinates and object points (control points used) are ca. 0.05 image unit, $\pm 10\,cm$, respectively.

Mean camera-to subject distance	$1000\,m$
Object expansion	$1500\,m$
Initial mean error of image points	MFV of image points is 0.05 (image unit)
Standard deviation of object coordinates	$\mathrm{MFV}_X = \mathrm{MFV}_Y = \mathrm{MFV}_Z = \pm 10\,cm$

Table (3.7): Initial control parameters applied into the orientation process

Outgoing from initial project parameters, the first and second calculations of approximate values for the unknowns have been achieved through the modules *Bunnae* and *Bunob*, respectively. Based on the results computed in *Bunob* and on equations included in *Bunbil's* types (Chapter 3.2.2.3.), the final adjustment calculations have been enforced. They present the final results of orientation process which are:

- **Interior orientation parameters**

Interior orientation parameters of the camera assumed - in this case: Oblique Image Camera - and the precisions associated with are presented in the Table (3.8).

Camera name	$x'_{o\,obs.}\ (mm)$	$x'_o\ (mm)$	$\mathrm{M}_{x'_0}\ (mm)$
Oblique	$y'_{o\,obs.}\ (mm)$	$y'_o\ (mm)$	$\mathrm{M}_{y'_0}(mm)$
	$c_{k\,obs.}\ (mm)$	$c_k\ (mm)$	$\mathrm{M}_{c_k}(mm)$
	0.00000	0.09653	0.5201
	0.00000	- 0.35368	0.5059
	260.000000	259.707205	0.2468

Table (3.8): Interior orientation parameters - oblique photos (App. E)

- **Exterior orientation parameters**

The Table (3.9) shows exterior orientation elements of Baalbek's oblique photos computed based on the main module *Bunbil*. These parameters (namely, coordinates of perspective centers) are depicted in 2D and 3D views in the Figure (3.6) and Figure (3.7), respectively.

Image type	Image ID	$X_0\ (m)$	$Y_0\ (m)$	$Z_0\ (m)$	$\omega\ (gon)$	$\varphi\ (gon)$	$\kappa\ (gon)$
Oblique	20891	9859.237	10114.124	1259.390	85.737001	18.662419	3.936344
	20893	9945.809	10187.433	1270.521	77.950359	32.064739	11.007095
	20892	9913.973	10177.051	1272.780	78.784011	31.881270	10.013510
	20886	10378.696	10283.857	1312.589	70.189405	68.681595	26.408128
	20905	9801.124	11048.468	1357.635	-75.925934	14.833811	193.813488
	20878	10448.362	10784.164	1387.663	-39.795513	72.007589	141.144015
	20907	9834.774	9979.556	1406.739	72.547493	14.479292	7.233662
	20899	9931.183	9984.379	1463.139	67.526088	26.008982	12.171635

Table (3.9): Exterior orientation elements - oblique photos

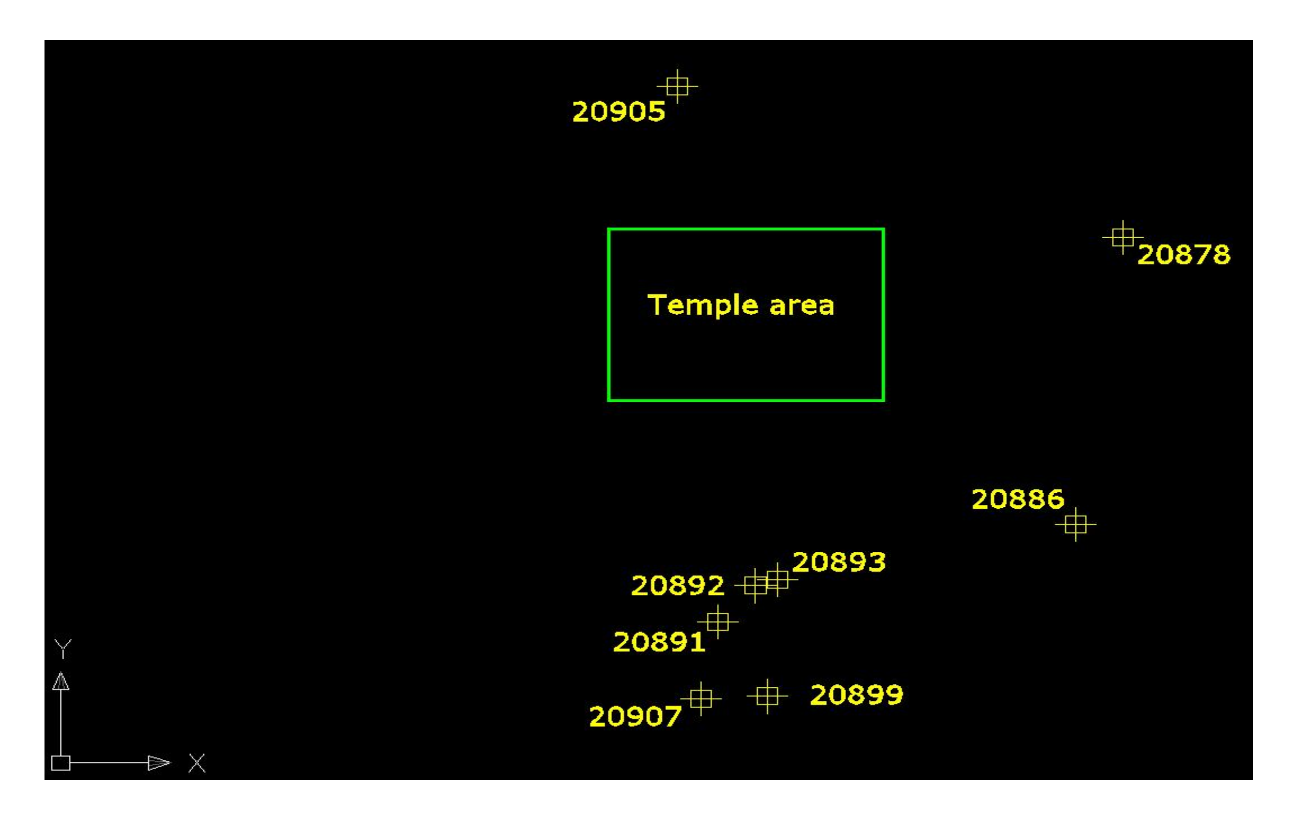

Figure (3.6): 2D position of the perspective centers related to the oblique images

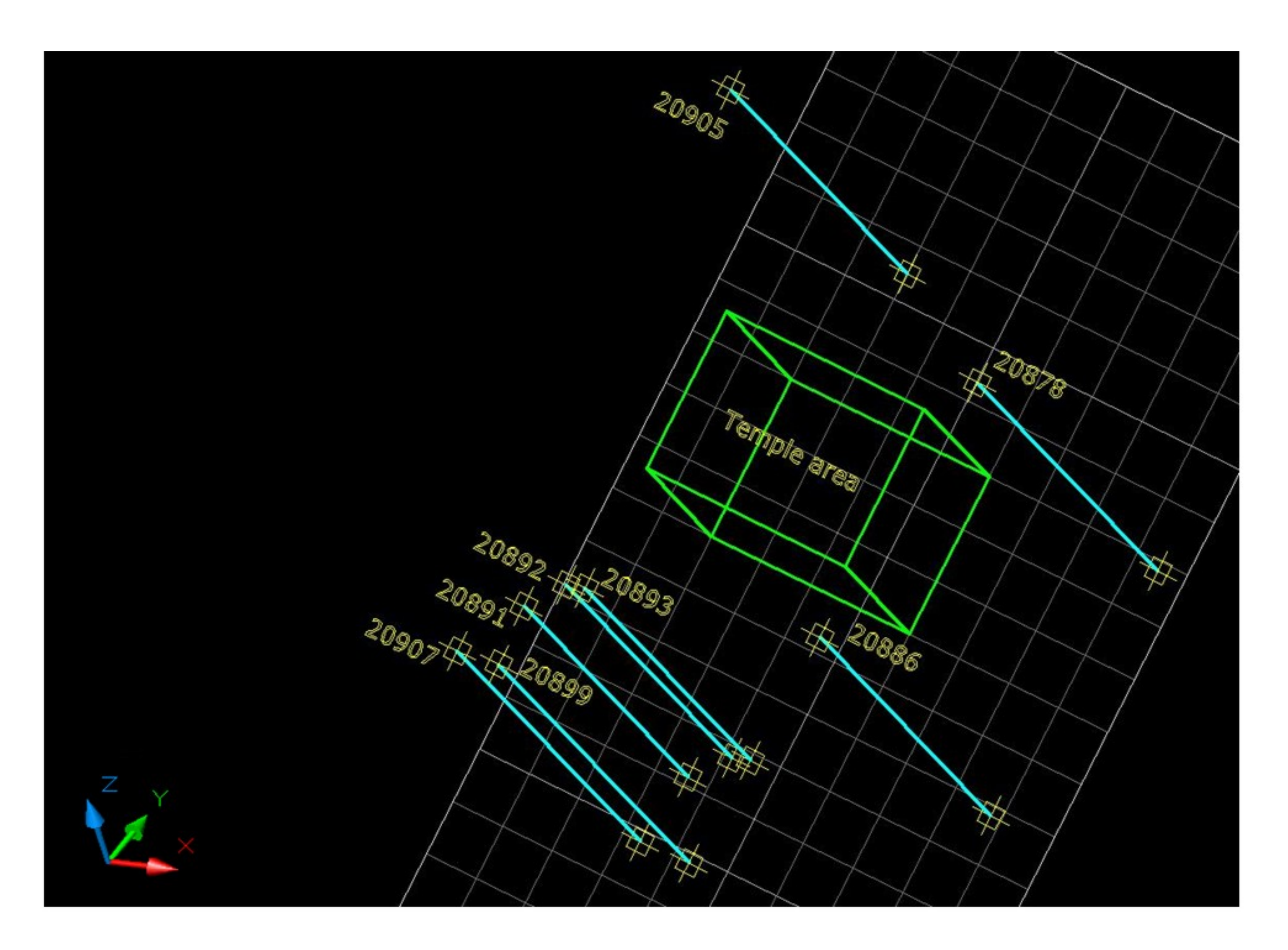

Figure (3.7): 3D view of the perspective centers related to the oblique images implemented in the orientation process

Results of interior and exterior orientation parameters expressed in the Tables (3.8 & 3.9) will be interpreted in the next chapter depending on quality elements discussed in Chapter (3.2.4).

3.3.3. Results interpretation

➢ Final results computed in the module *Bunbil* for oblique images block are in general accepted, where the *estimated standard deviation of the unit weight after the adjustment* is in the interval [0.7-1.3].

The primary MFV of image point coordinates (Table 3.7) led to $\hat{s}_0 \sim 1.43$. An increasing of MFV of image points leads to decreasing of $\hat{s}_0$ (with respect to minimum quantile in the confidence interval of $\hat{s}_0$). Variations of $\hat{s}_0$ based on three applied MFVs of image points were presented in Figure (3.8).

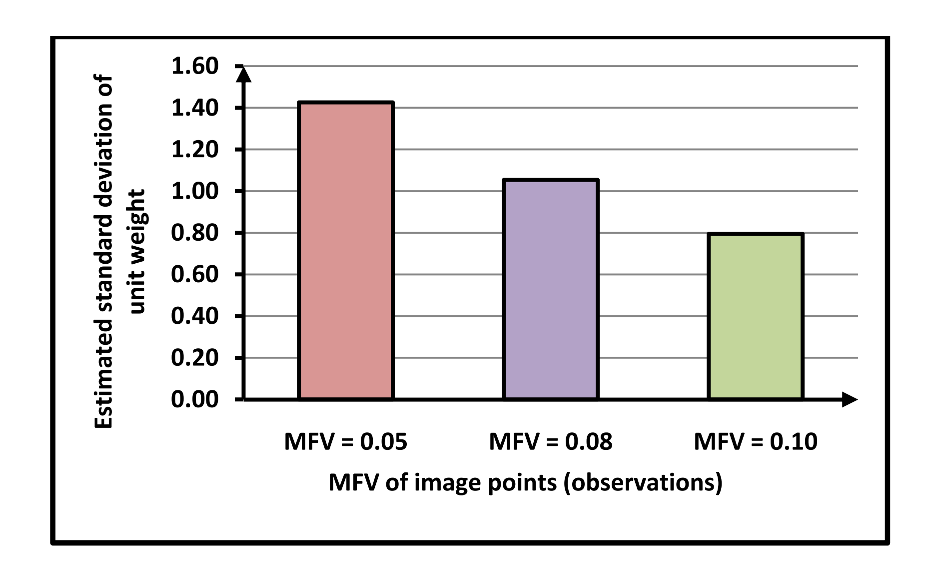

Figure (3.8): $\hat{s}_0$ variances based on three different values of MFV of image points

➢ On one hand to reveal the controllability of observations entered in the adjustment process, the observational redundancy numbers should be proved. On the other hand errors associated with observations can be also detected by analysis of NV_i values.

However, all observations, which have NV_i larger than critical value (2.5), and their partial redundancies are depicted in the Figure (3.9). In this context, the vertical coordinate of image point (4020) -in the image 20982- has the maximum NV_i of ca. (3.7) and EV of ca. (39.5%). It means that the there is *a large error possible* associated with that observation.

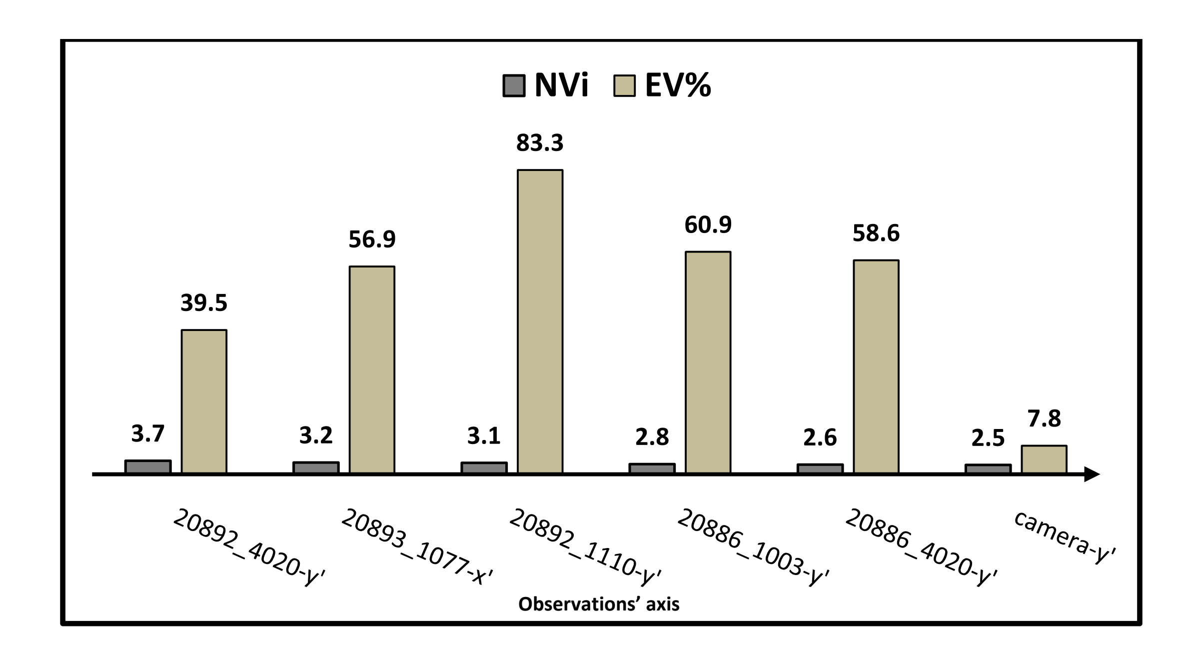

Figure (3.9): The observations which have NV_i values larger than 2.5 and their partial redundancies EV%

➢ The geometrical determination of unknowns (in this case: elements of the exterior orientation) should be checked, because it indicates - geometrically - to what extent the unknowns have been estimated (namely: well, relative well or bad). This geometrical evaluation of unknowns can be achieved based on the *estimated standard deviations of unknowns* **M** (Chapter 3.2.3.2). In this context, coordinates of projection centers have M values between 18 cm to 30 cm. These values confirmed the MFV of unknowns applied into calculations (30 *cm*). It means that a balanced stochastical model was preserved; in addition, exterior orientation parameters were geometrically well determined.

➢ Baalbek's oblique photos can be classified into three groups based on the distance (d) between the camera used and the recorded object (in this case, distances are presented by Z_0, see Table 3.9). These groups are as following:

- Group 1: $d \approx 1265\ m$
- Group 2: $d \approx 1350\ m$
- Group 3: $d \approx 1430\ m$

The above mentioned different distances are the main reason which led to differences in image scales of Baalbek's oblique images.

➢ The rotation elements ω and φ indicate to what extent an image plane is deflected from horizontal plane (cf. Fig. 3.10).

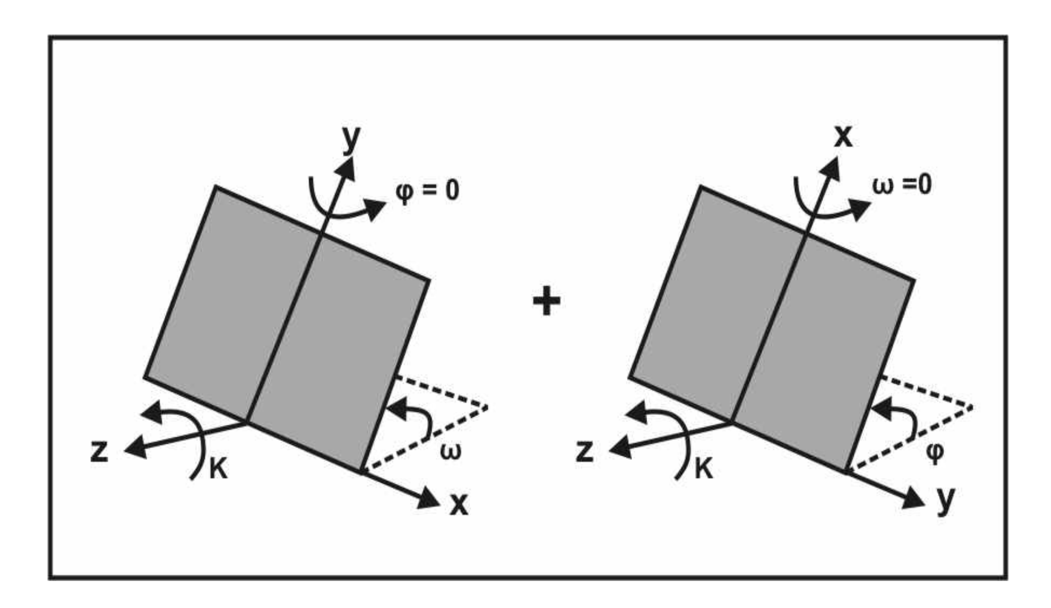

Figure (3.10): An image plane deflection from horizontal based on rotation elements

Rotation of oblique image planes at the x axis is approximately between $67\ gon\ to\ 85\ gon$ (Table 3.9), which reflects that image planes are relatively vertical. Only two images (20905 & 20878) had been taken from the opposite direction because their image planes rotated at $x \sim 325\ gon$ and $\sim 360\ gon$, respectively. In addition, most of Baalbek's oblique images have rotated at y axis with different rotation angles (φ is between $14\ gon$ to $72\ gon$). This means that the exposure model of the images was not stable.

3.4. Orientation of historical terrestrial images of Baalbek

3.4.1. Primary requirements

Based on the image properties (e.g. low image noise, low contrast), only three terrestrial images of Baalbek were selected in order to carry out the orientation process. The photos had been taken by Albrecht Meydenbauer in 1900s (Chapter 1.4.3). The camera used was non-metric camera (no fiducial marks) and saved under the name "*Messbild-camera*" in Pictran project. The focal length was assumed of $350\ mm$ according to the Meyer's classification (Meyer, 1985) of the cameras produced by Albrecht Meydenbauer (Table 3.10).

Camera	Objective	Focal length	Objective adjustment
Nr. I	Pantoskop Nr.5	f = 25 cm	non
Nr. II	Pantoskop Nr.6	f = 35 cm	max 14 cm
Nr. III	Pantoskop Nr.7	f = 53 cm	max 22 cm

Table (3.10): The cameras' types produced by A. Meydenbauer (source: Meyer, 1985)

Image formats associated with camera types were different (between $12 \times 12\ cm^2$ to $40 \times 40\ cm^2$). The mean size of terrestrial images is approximately $12 \times 12\ cm^2$ and correlates the focal length (principle distance) of ca. $35\ cm$. This value was applied into the bundle block adjustment as approximate value of the camera constant. In addition, approximate values of the principle point coordinates were considered ($x'_0 = y'_0 = 0$).

Further parameters respected in the orientation process can be expressed as following:

- The terrestrial image scale is considered of ca. 2500, see App. (F)
- The mean subject distance to camera used is about $875\ m$; according to Formula (3.3)
- Pixel size is $\sim 0.025\ mm$ as well as the ground resolution of images is $\sim 10\ cm$
- MFV of image points is 0.1 (image unit)
- $\mathrm{MFV}_X = \mathrm{MFV}_Y = \mathrm{MFV}_Z = \pm 10\ cm$ (accuracy of object point coordinates)
- Principle point coordinates are considered in the calculation as fixed values[1] (App. G)

3.4.2. Orientation process and results

The process of bundle block adjustment related to Baalbek's terrestrial photos has been enforced successfully using the standard mode of Pictran. The computations of the module *Bunbil* give the final results of the bundle block adjustment. These results include mainly the estimated orientation parameters of the camera used (results are shown in the Table 3.11).

[1] Fixed value has the status 0 in the software Pictran

Camera name		***Messbild-camera***					
Interior parameters		$x'_{o\,obs.}\ (mm)$	$y'_{o\,obs.}\ (mm)$	$c_{k\,obs.}\ (mm)$	$x'_o\ (mm)$	$y'_o\ (mm)$	$c_k\ (mm)$
		0.0000	**0.0000**	**350.000000**	**0.0000**	**0.0000**	**346.629555**
Exterior parameters	**Image**	$X_0\ (m)$	$Y_0\ (m)$	$Z_0\ (m)$	$\omega\ (gon)$	$\varphi\ (gon)$	$\kappa\ (gon)$
	208323	**9945.214**	**9609.729**	**1242.932**	**92.586885**	**21.070925**	**6.023199**
	208325	**9595.373**	**9290.160**	**1204.338**	**103.118737**	**-7.472291**	**5.023643**
	637126	**9650.750**	**9558.398**	**1230.420**	**88.816952**	**1.587573**	**0.113932**

Table (3.11): Messbild-camera parameters - terrestrial photos

Illustrations of the estimated spatial positions of the camera used are depicted in 2D as well as in 3D views in the Figure (3.11) and the Figure (3.12), respectively.

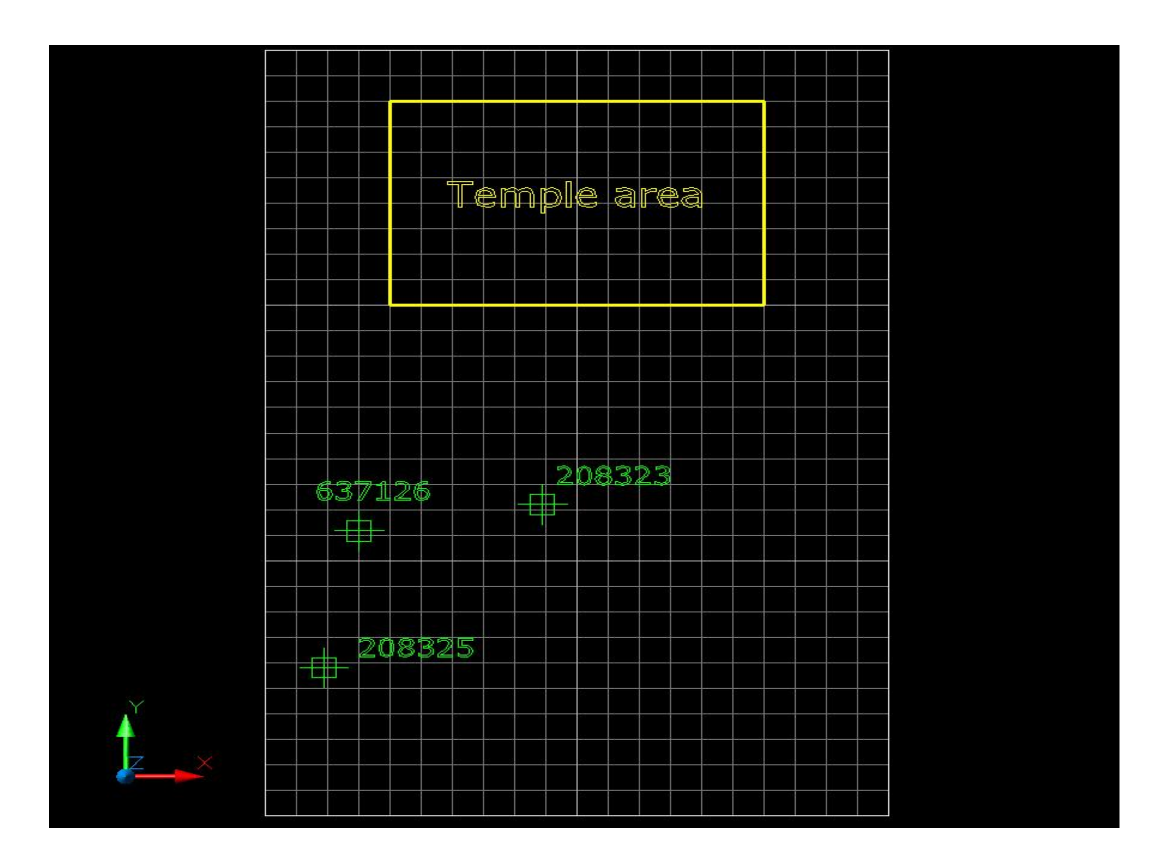

Figure (3.11): 2D view of estimated positions of cameras used in Baalbek's terrestrial photos

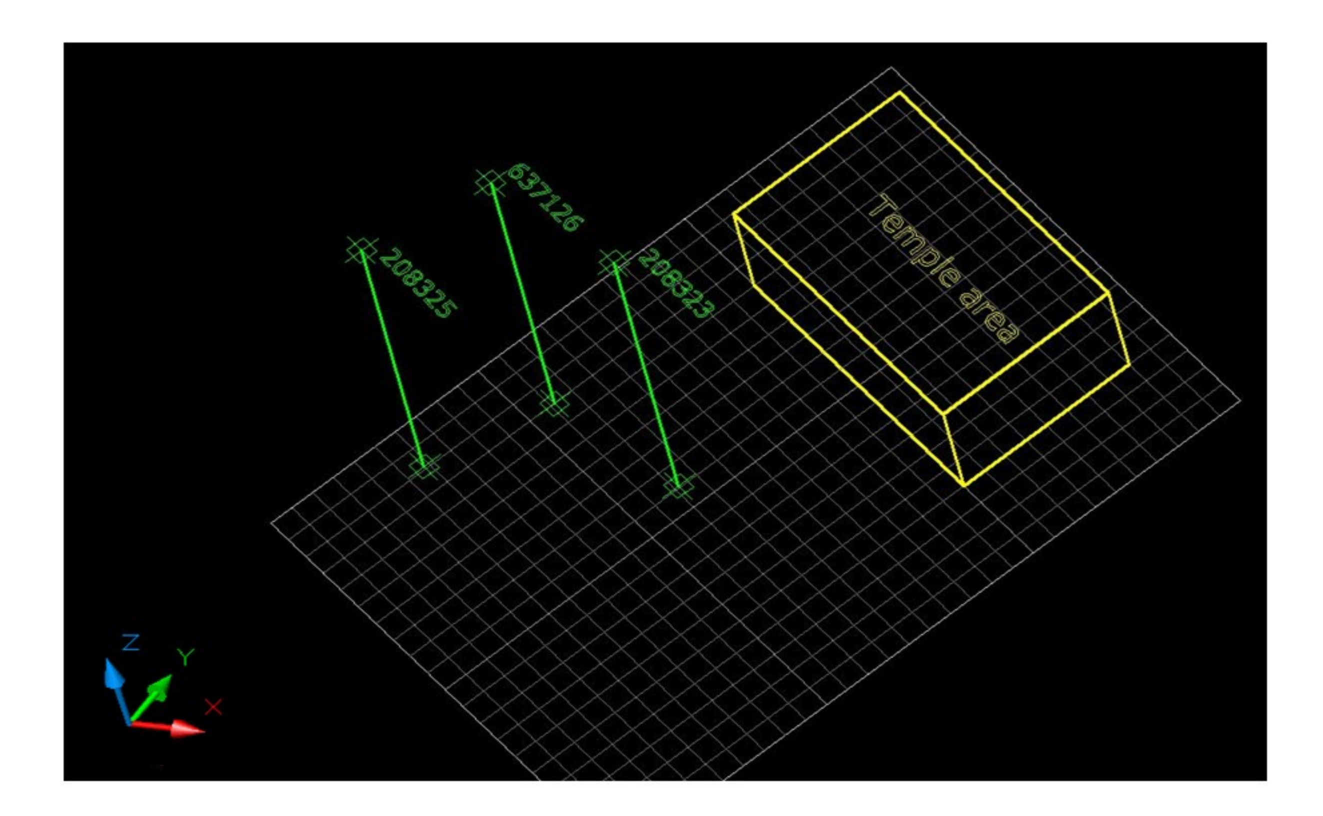

Figure (3.12): 3D view of perspective centers associated with Baalbek's terrestrial photos

3.4.3. Results evaluation

3.4.3.1. Acceptance of terrestrial image block adjusted

Based on the *estimated standard deviation of the unit weight after the adjustment,* it can be revealed: to what extent, in general, the adjustment calculations are accepted as well as the stochastical model well applied. In this context, $\hat{s}_0$ resulted is ~ 1.19 (which belongs to the plausible interval of $\hat{s}_0$). This means that a balanced stochastical model before and after the adjustment process was plausible.

3.4.3.2. Observations' controllability and errors detection (outlier detection)

In the final effort of calculations (in final computations of approximate values in *Bunbil*) there are only two values shown of NV_i larger than the empirical critical value (2.5). The first is the horizontal coordinate of the image point (1228) - in the image 637126; see Figure (3.13) - which has the maximum NV_i of ca. (3.81) as well as EV of ca. (66%). Second one is the x' of the image point (1116), also in the image 637126. This observation has NV_i of ca. (2.93) and EV of ca. (88%).

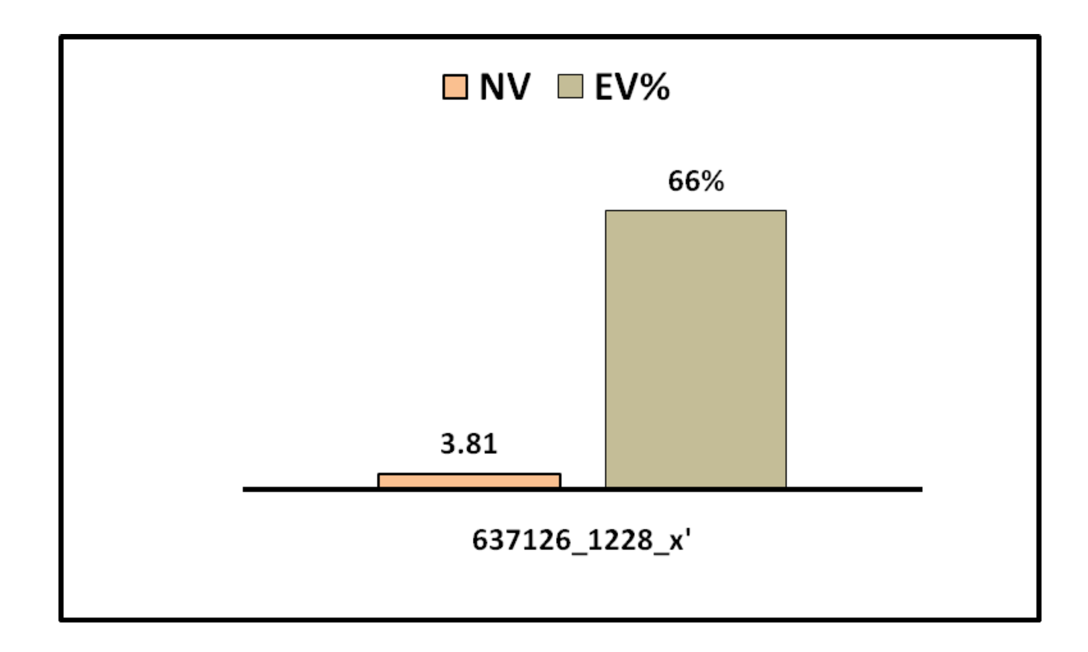

Figure (3.13): Largest (and EV related to) - terrestrial image block

3.4.3.3. Quality of camera parameters estimated

The quality assessment of interior and exterior orientation parameters estimated using bundle block adjustment computations will be proved as following:

3.4.3.3.1. Interior camera parameters

The Table (3.11) shows that the final value adjusted of the camera focal length is with the estimated standard deviation (App. G). Geometrically, it could be accepted that the focal length was well improved and re-determined. In this context, the standard deviation (a posterior) doesn't exceed the assumed one , which means a balanced stochastical model was guaranteed.

3.4.3.3.2. Exterior camera parameters

Projection center coordinates were applied as unknowns (status 1) in the first iteration of adjustment computations; where the a priori mean error was considered . The quality check of the estimated values of center projection coordinates can be described as following

- The first iteration of calculation process - step 1 (Figure 3.14.a):

1. Normalized residuals are greater than (4); this means there are large errors, very likely, associated with observations.

2. The estimated standard deviation (M, after the adjustment) of the coordinates of the center projection is between $3.2\ m$ to $6.18\ m$. It does not confirm the a priori mean error of the unknowns. This means that the stochastical model is not balanced and the a priori standard deviation has to be re-adjusted.

- The last iteration of the calculations (in this case: after five iterations, see Figure 3.14.b):

1. NV_i values are smaller than (2.5); where the most of observations including large errors have been re-checked (e.g. positions of observations were adjusted). In addition, each observation has EV lower than 20% was re-controlled (with respect to MFV).

2. With respect that MFV is $\pm 2/\pm 5m$ (position/height), it could be accepted that the stochastical model applied is balanced.

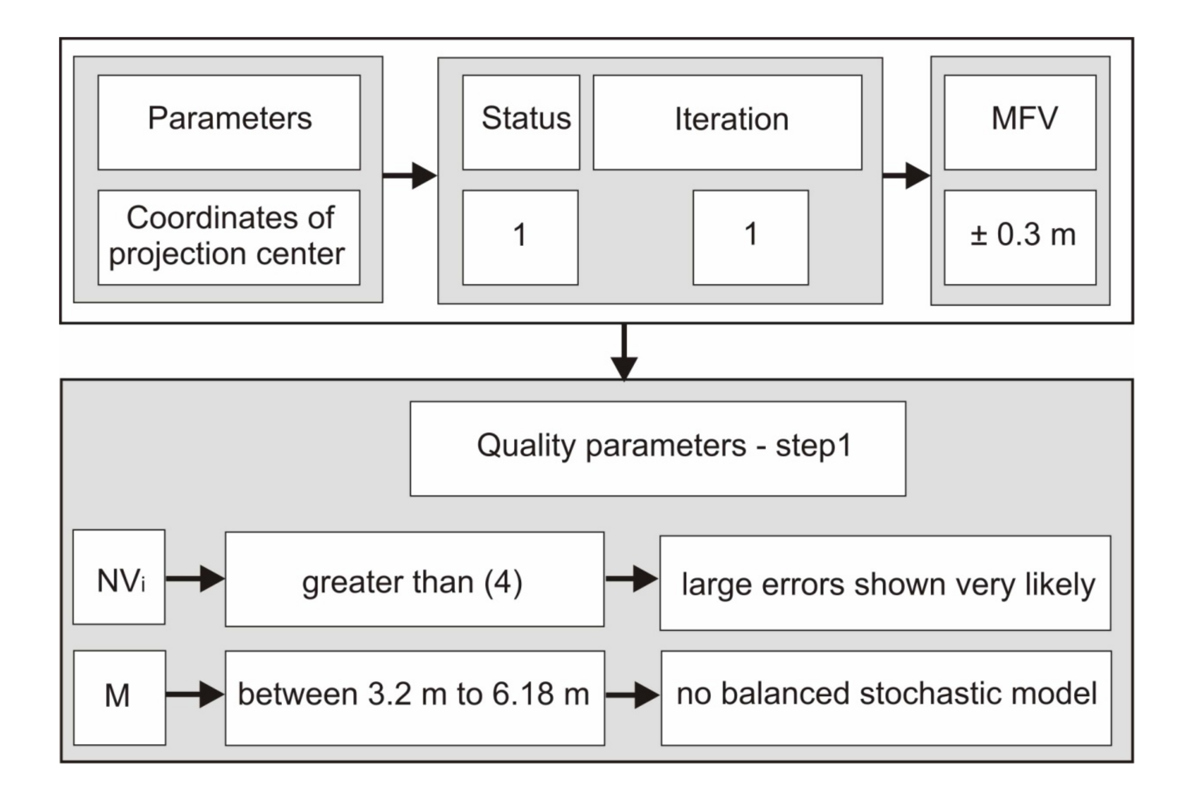

Figure (3.14.a): Quality parameters of projection center coordinates estimated in the 1st iteration of the calculations

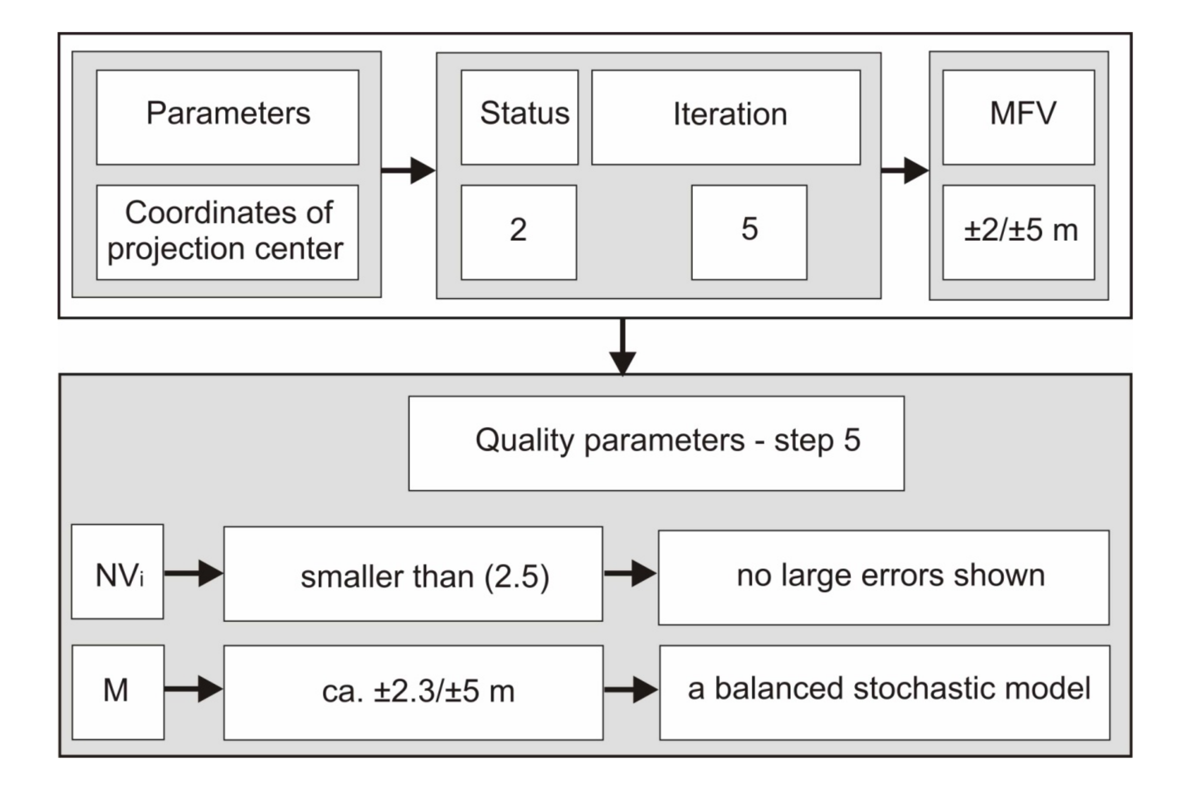

Figure (3.14.b): Quality parameters of projection center coordinates estimated in the final iteration of calculations

3.4.3.3.3. Rotation elements

Theoretically, an image has a horizontal plane, if $\omega = 0\ gon$ and $\varphi = 0\ gon$ (standard case, cf. Figure 3.15, a). In contrast, a vertical plane of an image (a terrestrial image) can be achieved starting from horizontal plane, if the image is rotated:

- either at x with $\omega = 100\ gon$, $\varphi = 0\ gon$ and $\kappa = 0\ gon$; (standard case, cf. Fig 3.15, b)
- or at y with $\varphi = 100\ gon$, $\omega = 0\ gon$ and $\kappa = 0\ gon$; (standard case)
- or $\omega \sim 100\ gon$, $\varphi \sim 0\ gon$ and $\kappa \neq 0\ gon$ (practical case, Fig. 3.15, c)

Baalbek's terrestrial images (used in the orientation process) do not present the standard case of terrestrial image because they have been rotated with $\omega \approx 100\ gon$, moreover, $\varphi \neq 0\ gon$ and $\kappa \neq 0\ gon$ (see Table 3.11).

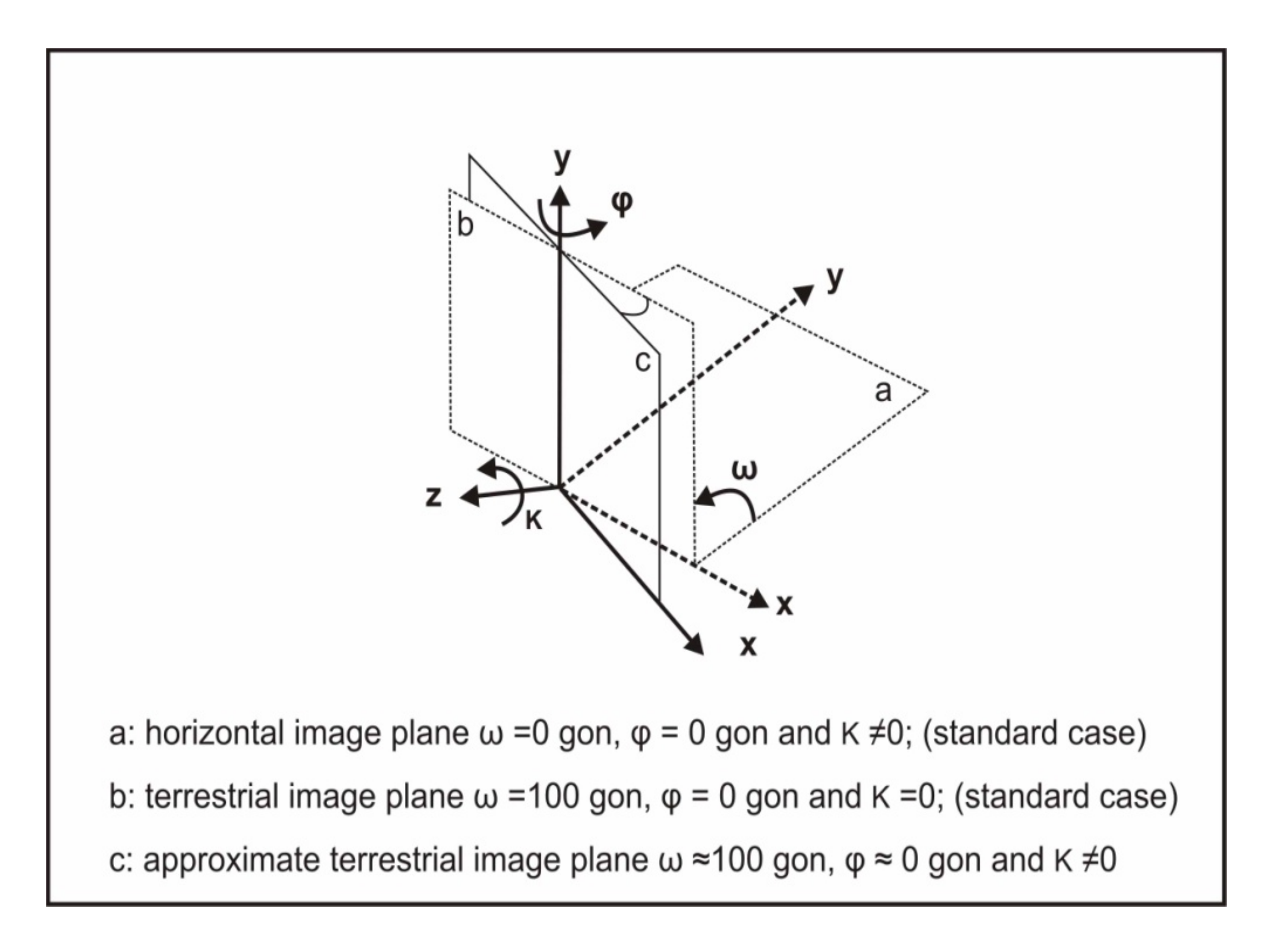

Figure (3.15: a, b and c): Image plane from horizontal to terrestrial plane

3.5. Distortion parameters

It was pointed in (Chapter 2.1), that the aberration of an image point - closer or farther - from the principle point of the image is defined as the radial distortion.

In addition, the alignment of elements of lens system exactly collinear to the optic axis is difficult. This will cause the geometric displacement of images, which is known as decentring distortion.

Due to the assumption that this distortion would have a significant impact on the old cameras used for historic Baalbek, the estimated distortion parameters (referred to all images types of Baalbek) should be discussed to analyse the mentioned impact from geometric point of view.

3.5.1. Vertical image type

- *Radial distortion analysis*

With respect to the radial distortion parameters estimated (in this case A_1 & A_2, see App. H) and based on the formula (2.1), the distortions referred to different image radiuses have been computed and presented in the Table (3.12).

$r\ (mm)$	$\Delta_r\ (mm)$	$r\ (mm)$	$\Delta_r\ (mm)$	$r\ (mm)$	$\Delta_r\ (mm)$
0	0.0000	40	0.0207	80	-0.0061
5	0.0041	45	0.0201	85	-0.0110
10	0.0080	50	0.0185	90	-0.0153
15	0.0117	55	0.0160	95	-0.0185
20	0.0149	60	0.0127	100	-0.0201
25	0.0175	65	0.0086	105	-0.0196
30	0.0194	70	0.0040	110	-0.0162
35	0.0205	75	-0.0010	111	-0.0151

Table (3.12): Distortion values Δ_r related to different image radiuses r (up to maximal image radius which is ca. $11.10\ cm$).

It is clear that the image point referred to the image radius $40\,mm$ has been maximally distorted of ca. $0.021\,mm$. The comparison between the maximal aberration calculated and the absolute value of the minimal one (ca. of $0.020\,mm$ referred to the image radius $100\ mm$) indicates that both values are approximately identical. This means a balanced radial distortion was guaranteed (Brown, 1968; Fryer, 1996).

- *Decentring distortion check*

The decentring distortion values can be discussed through a graphical representation created based on the profile-function of the decentring parameters (equation 2.5). The Figure (3.16) shows the variations of decentring distortion related to the image radiuses presented in the Table (3.12) with respect to the coefficients of the decentring distortion estimated through the orientation process (App. H).

Those variations are in the range $[0 - 0.121]\ mm$; note that the decentring distortion is usually an order of magnitude smaller than the radial distortion and rarely exceeds $30\ \mu m$ at the edge of the image format. Since decentring distortion is basically a quadratic function, its magnitude will only be one-quarter this size in the middle regions of the image (Fryer, 2001).

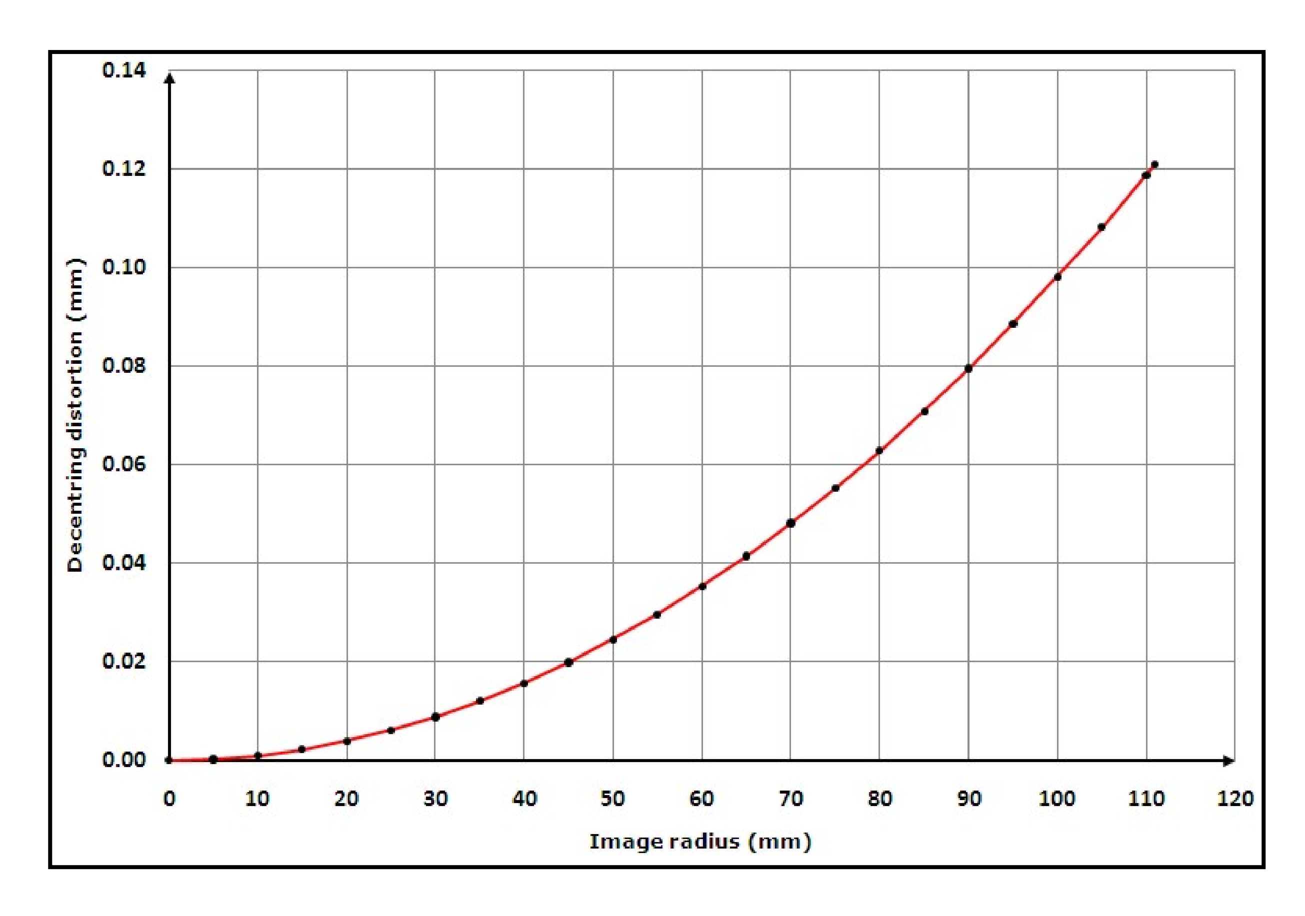

Figure (3.16): Profile function of the decentring distortions related to the camera used for Baalbek's vertical images

3.5.2. Oblique image type

- *Radial distortion evaluation*

In an analogue manner used for calculation of radial distortions of the vertical image type, the other ones referred to the oblique images have been also computed (Table 3.13). Thereby, it can be accepted that for e.g. the image point referred to the radius of $30\ mm$ would be displaced in the reality (with respect to image scale of this image type) of ca. $1.8\ cm$. Moreover, the corrections related to that image point can be calculated based on equations (2.2.a & 2.2.b).

$r\ (mm)$	$\Delta_r\ (mm)$	$r\ (mm)$	$\Delta_r\ (mm)$	$r\ (mm)$	$\Delta_r\ (mm)$
0	0.0000	30	0.0044	60	0.0570
5	-0.0033	35	0.0133	65	0.0501
10	-0.0058	40	0.0241	70	0.0296
15	-0.0068	45	0.0357	75	-0.0096
20	-0.0056	50	0.0466	80	-0.0738
25	-0.0019	55	0.0546	85	-0.1699

Table (3.13): Radial distortions associated with different image radiuses - oblique image type

- *Decentring distortion*

Going from the equation (2.5), the function curves of the decentring distortions (referred to different image radiuses) for vertical and oblique image types are depicted in the Figure (3.17). In this context, parameters of decentring distortion have been estimated through the orientation process carried out based on the bundle block adjustment (App. I).

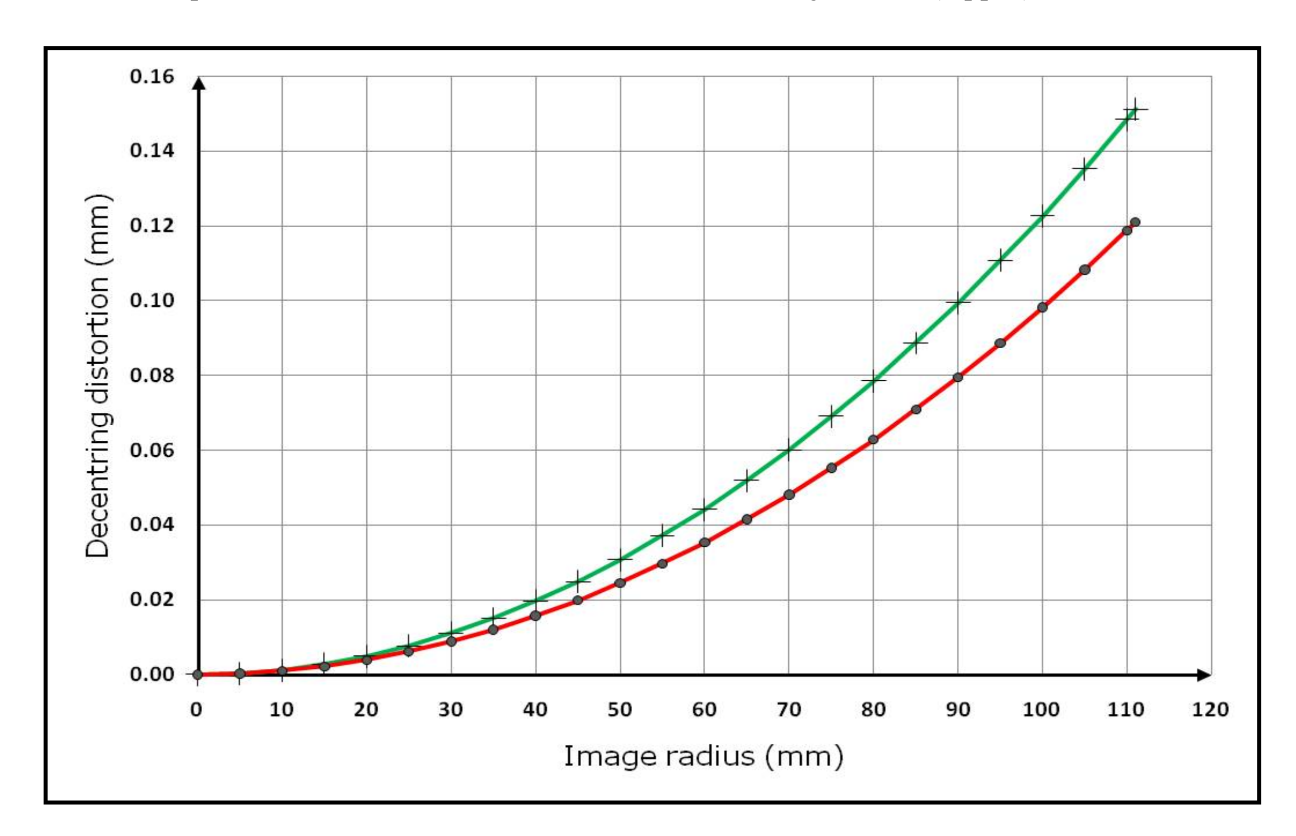

Figure (3.17): Function curves of decentring distortions of vertical image type (red line) and oblique image type (green line).

It is to show that the distortions associated with vertical image type are smaller than the other ones referred to oblique images. The image point that has for e.g. the image radius of $80\ mm$ is distorted in the vertical image type and oblique one of ca. $0.063\ mm$ and $0.079\ mm$, respectively.

3.5.3. Terrestrial image type

In the case of Baalbek's terrestrial images the lens distortion parameters were not taken into the consideration. This is due to the reason that the first effort of the orientation process of this image type has not been successfully achieved and a solution of the adjustment problem was not carried out. Therefore, the impact of lens errors - in this case - has been neglected in order to seek the orientation process with non-strict mathematical model. That means, the image point coordinates calculated using the basic equations expressed in the module *Bunbil* of the software Pictran have not been radially and decentring corrected.

4. Orientation process based on the combination of historical photos

Generally, the most cases of standard photogrammetry deal with a specific image type which can be for e.g. aerial or terrestrial. In some cases of study - like those dealing with cultural heritage assets - the combination between different image types should be taken into the account, because it provides more advanced tools and techniques for the data acquisition and representing the 3D environment.

In this chapter, a methodology for image orientation process based on a combination of different image types will be proposed. This methodology is considered a contribution to suggest a feasible effort of image orientation; with it different types of historical images could be oriented. In addition, the probable combinations of image types (e.g. vertical and oblique types, vertical and terrestrial types, etc.) will be investigated through the orientation process to know by which sequence of image types the orientation parameters will be best geometrically estimated.

To introduce the abovementioned methodology, two strategies will be investigated to orient Baalbek's images based on the combined evaluation of the photos. The first is the orientation process based on the combination between the vertical and oblique image types (step2, cf. Fig. 3.1, b). The other one depends on the combination between all image types available (step3, cf. Fig. 3.1, c).

4.1. Orientation of Baalbek's vertical and oblique images

The orientation process of the vertical and oblique photos together presents the first effort of the combined evaluation of Baalbek's images. Although the two image types have been oriented separately (Chapters 3.2 & 3.3), the orientation process will be also achieved based on one block including the two image types. Here, however, it will be investigated:

- *How does the orientation process work?*
- *What about the mathematical model to be applied in the adjustment problem?*
- *To what extent the primary results calculated (for e.g. the interior and exterior orientation parameters, Chapter 3.2.3 & Chapter 3.3.2) can be geometrically improved?*
- *To which extent the orientation parameters estimated are geometrically accurate with respect to the geometric accuracy of control points applied in the calculation process as well as to the accuracy requested for further applications in Baalbek (for e.g. restoration issues)?*

Basically, the orientation of the two image types (vertical and oblique images) together will be meaningful due to the assumption that the two types have been taken approximately at the same period (end of 1930s); i.e. it could be accepted that they should include approximately same objects (buildings, streets, etc.). This optimizes relatively the object recognition and the matching process between the images. In addition, a sufficient input data (e.g. additional control points, etc.) applied into the bundle block adjustment method will be available.

Going from the first orientation step (Figure 3.1, a) the orientation process based on the combination between the vertical and oblique photos was carried out using the main mode of the software Pictran. With respect to image properties (e.g. low image noise and contrast), six vertical images and also six oblique ones have been selected - from the images used in the first orientation step - to achieve the intended orientation process (Figure 3.1, b).

As previously mentioned in the Chapter (1.4.1) and Chapter (1.4.3) the camera used in the vertical image type was assumed a metric camera and the other one used in oblique image type was non-metric. Camera elements and other parameters (e.g. control parameters) taken into account through the orientation process can be summarized as following:

- *Interior orientation parameters*:

  On one hand it was here assumed that it would be rather unreliable (from geometrical point of view) to seek an orientation process with the first estimation (rough results) of the interior orientation parameters for both image types (see Table 3.4 & Table 3.8). On the other hand it will be investigated how the functional model applied in the adjustment calculations should be formed to obtain a reasonable solution of the adjustment process.

  Therefore, it was suggested to achieve the intended orientation process with non-strict mathematical model using the same initial values of interior orientation parameters entered in the first orientation step, but as constant values as follow:

  - for vertical image type: $x_0' = y_0' = 0$ and $c_k = 200\ mm$ (status 0)
  - in oblique photos: $x_0' = y_0' = 0$ and $c_k = 260\ mm$ (fixed values)

- *Exterior orientation parameters* entered the adjustment calculations as observed values (status 2) based on the approximate values calculated in the 1st orientation step (Table 3.5 and Table 3.9).

- MFV of image point coordinates is 0.1 unit of image system (before the adjustment).

- MFV of object coordinates is $\pm\ 10\ cm$ for X, Y and Z (before the adjustment).

Final results of the bundle adjustment are carried out through computations of the module *Bunbil*. These calculations are mainly based on the mathematical equations expressed in the type (1) and type (2) included in the module *Bunbil* (Chapter 3.2.2.3).

The intended orientation process started directly with the module Bunbil due to that approximate values are already available. Basically, final results include adjusted estimations of approximate values of orientation parameters (in this case, only exterior orientation parameters were geometrically improved, where interior orientation elements were applied as fixed values). Adjusted exterior orientation parameters are presented in the Table (4.1).

Type	Image ID	$X_0\ (m)$	$Y_0\ (m)$	$Z_0\ (m)$	$\omega\ (gon)$	$\varphi\ (gon)$	$\kappa\ (gon)$
Vertical	Scan 1981	9970.199	10673.474	1940.379	4.531503	4.723843	131.313483
	Scan 1980	9235.182	10207.200	1984.189	0.826624	-12.433890	-53.114241
	Scan 1985	9420.748	10323.364	2019.403	0.596787	-5.280830	147.724578
	Scan 2025	9791.513	10558.523	2029.001	9.619294	-2.874932	148.322941
	Scan 1983	9608.965	10431.359	2036.922	4.103334	-2.572921	147.814799
	Scan 1982	9742.978	10470.508	2041.038	8.348914	0.981525	146.765510
Oblique	20891	9860.072	10113.644	1258.483	85.971887	18.761469	3.875808
	20893	9945.856	10187.152	1270.644	78.048073	32.073423	10.998217
	20892	9913.952	10177.201	1272.770	78.870589	31.913799	9.947497
	20886	10378.719	10283.770	1312.715	70.334748	68.725096	26.283109
	20878	10448.289	10784.290	1387.752	-39.981949	72.055536	141.304050
	20899	9930.449	9984.950	1462.984	67. 593067	26.020750	11.957479

Table (4.1): Improved exterior orientation parameters - vertical and oblique images

The calculated coordinates of perspective centers (presented in the Table 4.1) are depicted through 2D and 3D views in the Figure (4.1) and Figure (4.2), respectively.

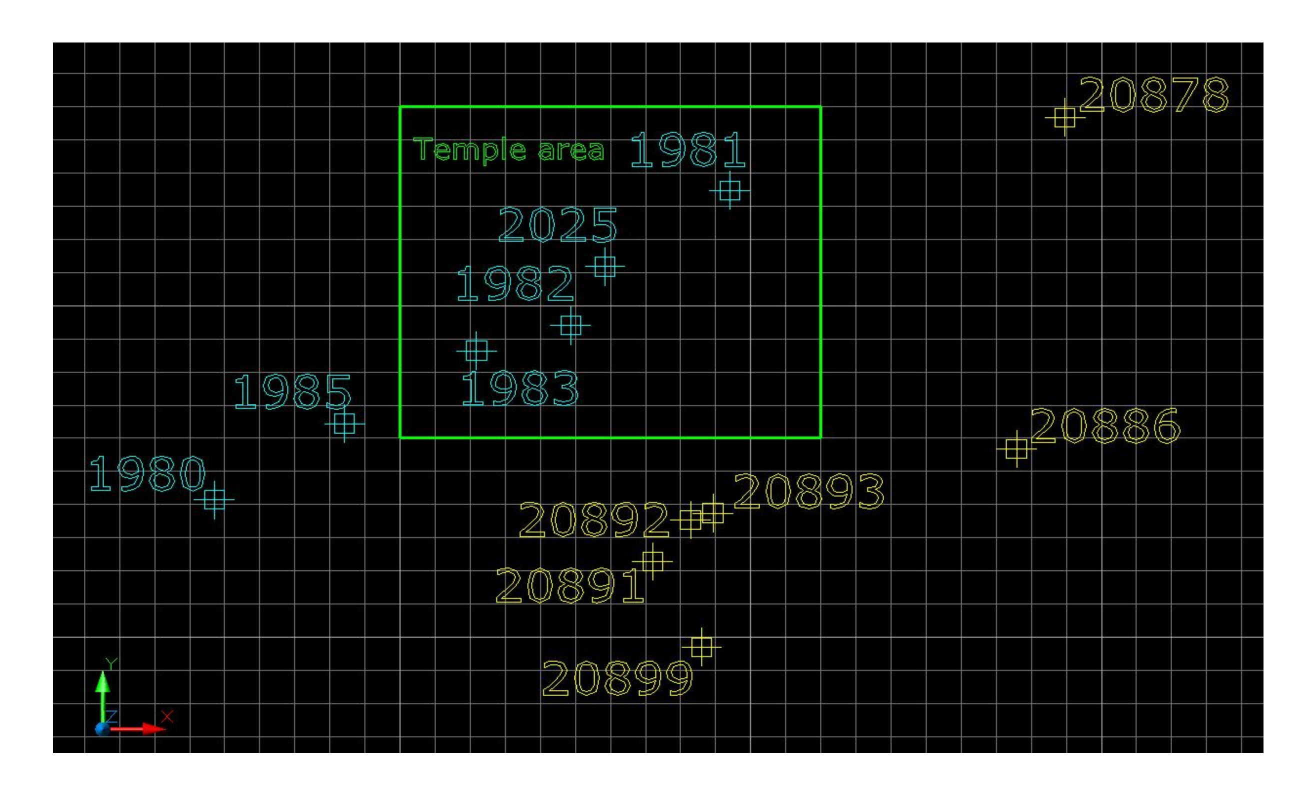

Figure (4.1): 2D view of perspective centers associated with vertical images (cyan color) and oblique ones (yellow color) used in the orientation process (temple area is in green line)

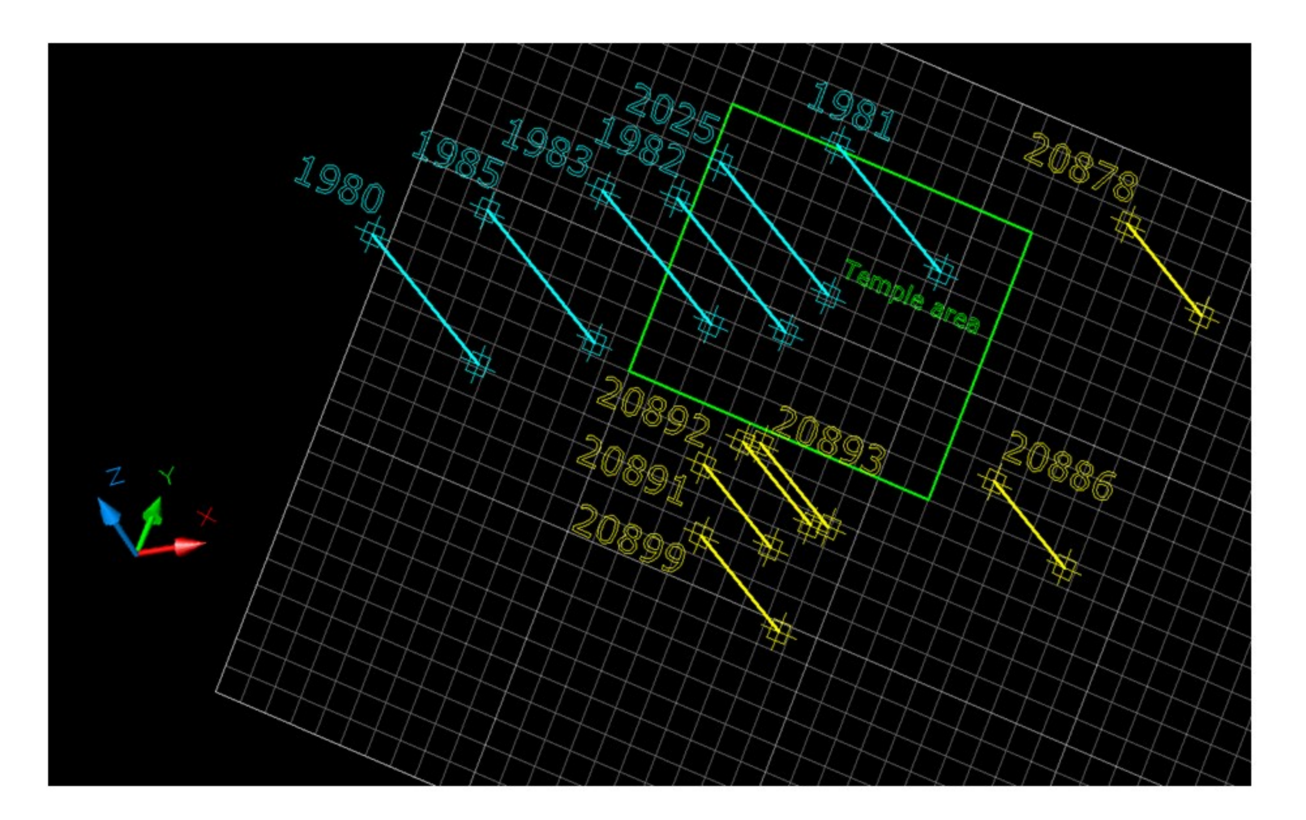

Figure (4.2): Spatial positions of perspective centers associated with vertical and oblique images implemented in the orientation process (heights of vertical images are presented in cyan color and other ones for oblique photos in yellow)

4.2. Results quality

4.2.1. General acceptance of the adjustment calculations

Final results have been attained after six iterations (App. J). In general, the adjustment calculations associated with the block of vertical and oblique images have been accepted; where the *estimated standard deviation of the unit weight after the adjustment* is ca. 1.15 which belongs to the plausible interval [0.7-1.3]. It should be noted that the initial MVF of image points applied into adjustment calculations was increased to 0.25 pixel to guarantee a balanced stochastical model through calculations.

4.2.2. Outliers (normalized residuals and controllability check)

On one hand the maximum value of NV_i is ca. 3.6 associated with the image point (1208) in the vertical image (scan-1983); it can mean that point may have a large error visible.

On the other hand a relative partial redundancy of an observation (Chapter 3.2.4.2) should be respected in order to reveal the role of that observation in determination of unknowns. In this context, the relative partial redundancy associated with the maximum value of normalized residuals is ca. EV=89%. It means the observation, which has the $(NV_{i\,max})$, has been well controlled, in addition, it took a role in determination of unknowns with the percentage 11%.

4.2.3. Quality of exterior orientation parameters

Most of values of the estimated standard deviation M (a posterior) of projection center coordinates are smaller than $1\,m$. In this case, a posterior standard deviation M does not exceed the primary standard deviation assumed i.e., a stochastical model between input and output data has been guaranteed.

Previously mentioned (Chapter 4.1) that the geometrical check of the results calculated in the first step of the orientation process is the main motivation respected to achieve the orientation process based on combined evaluation of Baalbek's images. Therefore, it will be meaningful if the results calculated in 1st orientation step (in this case: exterior orientation parameters presented in the Table 3.5 & Table 3.9) are compared with other one calculated based on the combined evaluation of vertical and oblique photos (Table 4.1.). This comparison gives the differences between both results calculated (differences are presented in the Table 4.2).

Type	Image ID	$\Delta X_0\ (m)$	$\Delta Y_0\ (m)$	$\Delta Z_0\ (m)$	$\Delta\omega\ (gon)$	$\Delta\varphi\ (gon)$	$\Delta\kappa\ (gon)$
Vertical	Scan 1981	0.06	-0.07	0.30	0.106374	0.097961	0.177659
	Scan 1980	0.05	0.22	-0.03	0.070578	-0.010780	-0.106568
	Scan 1985	0.06	0.87	0.15	0.098304	0.091981	-0.175724
	Scan 2025	0.00	-0.06	0.23	0.047296	0.159834	0.251195
	Scan 1983	0.01	-0.25	-0.09	0.098107	0.084944	-0.038882
	Scan 1982	-0.20	0.17	0.14	0.036644	0.099400	0.054165
Oblique	20891	0.84	-0.48	-0.91	0.234886	0.099050	-0.060536
	20893	0.05	-0.28	0.12	0.097714	0.008684	-0.008878
	20892	-0.02	0.15	-0.01	0.086578	0.032529	-0.066013
	20886	0.02	-0.09	0.13	0.145343	0.043501	-0.125019
	20878	-0.07	0.13	0.09	-0.186436	0.047947	0.160035
	20899	-0.73	0.57	-0.15	0.066979	0.011768	-0.214156

Table (4.2): Differences of exterior orientation parameters calculated in the 1st orientation step and the other one estimated based on combined evaluation of images (vertical and oblique)

The Table (4.2) indicates that differences between exterior orientation parameters computed in the 1st orientation step and the other ones based on image combination are not large. This reveals that approximate values (for exterior parameters) applied into the adjustment process are relatively well assumed (from a geometrical view). In addition, the criterion of minimizing input data measurement residuals was sufficiently realized.

Orientation protocols referred to some selected vertical and oblique images[1] have been created. They include the results of the interior and exterior orientation parameters estimated based on the first orientation step (orientation of each image type separately) and the second one based on the vertical and oblique images combination (App. K).

The question that is to pose: how sensitive the results would be, if the interior orientation parameters estimated in the first step would have been used in the step2 as initial values (as observations). In that case, it would be essential - to express the expected impact on results - to start from the basic equations (3.16) and the equations presented in the type 9 in the module *Bunbil* (namely, equations: 3.24.a-c). In that case, additional residual equations would be available and therefore a strict functional model would be applied in the orientation process. This issue will be discussed in the next section.

[1] Due to license issues, only two vertical and two oblique images have been chosen.

4.3. Orientation process based on combination of Baalbek image types

On one hand and outgoing from the assumption that the different image types of Baalbek are main data sources (especially historical data), a new attempt was enforced to orient all image types together to improve the results of the last orientation process described in the Chapter (4.1) and to know to which extent these results have a good geometric quality.

On the other hand it is common, that the generation of 3D models depends on the input data available (e.g. 3D spatial data, semantic information, etc.). In geometric context, there is a direct impact of geometry on the generation process of a 3D model, i.e., the more geometry the more accurate generation of a 3D model.

Therefore, it is essential to have more details acquired based on Baalbek's images oriented to create a 3D model. This model will support users' requirements in different sectors such as architecture or archaeology. In this context, the main question could be here posed: *how can we obtain more information about objects to be modelled (like data about Baalbek's historical entities*) *to generate a best 3D model of Baalbek*?

Basically, there are different techniques used to extract 3D objects (e.g. photogrammetry, laser scanning, etc.), but most of these techniques have the problem that there are hidden objects which are - in some cases - difficult to detect or recognize. An important solution for this challenge is a combination between different techniques supporting the data requested. Therefore, in Baalbek's modelling, hidden objects can be well detected using the combination between different image types of Baalbek. This will support good data collections of the historic city; where these data sets will relatively enhance the intended 3D modelling of the historic Baalbek.

4.3.1. Orientation flow and results

The intended effort of orientation process based on combining of Baalbek's historical image types was attained using different images selected from image blocks implemented in last orientation stages. In this context, four vertical, three oblique and three terrestrial photos have been chosen[1] (cf. Fig. 3.1, c).

Computations of bundle block adjustment started - in this step - directly with the module *Bunbil* in the compact mode of software Pictran because there are approximate values of

[1]Image selection depends on different parameters like: image appearance, image noise, image contrast, etc.

unknowns (orientation parameters). Basically, approximate values applied are the results of the estimated orientation parameters calculated through the first orientation step (orientation of each image type separately, see Chapter 3) as well as the results computed by orientation process based the combined evaluation of vertical and oblique images (Chapter 4.1).

The initial parameters entered through calculations can be concluded as following:

- In the vertical image type (Table 3.4):
  - $c_k = 200.253031\, mm$
  - $x'_0 = -\, 0.069894\, mm$
  - $y'_0 = -\, 0.049059\, mm$
- In the oblique photos (Table 3.8):
  - $c_k = 259.707205\, mm$
  - $x'_0 = 0.09653\, mm$
  - $y'_0 = -\, 0.35368 mm$
- In the terrestrial photos (Table 3.11):
  - $c_k = 346.629555\, mm$
  - $x'_0 = 0.000$
  - $y'_0 = 0.000$
- MFV of image points coordinates is of 0.10 unit of image system (before the adjustment).
- MFV of object coordinates is $\pm\, 10\, cm$ for X, Y and Z (before the adjustment).

Although the computations in *Bunbil* (in the first iteration) was successfully achieved (not terminated), but the *estimated standard deviation of the unit weight after the adjustment* was not in the plausible interval [0.7-1.3] (it was ca. 2.98). This means:

- the stochastical model is incorrect (mean error of observations was applied incorrectly),
- or there are too large errors visible associated with observations,
- incorrect observations should be controlled based on normalized residuals

With respect to abovementioned criterions, a priori standard deviation of image points was hierarchically increased to 0.8 (unit of image system). This led, in general, to a successful orientation process; and calculations of bundle block adjustment were accepted where the *estimated standard deviation of the unit weight after the adjustment* is ca. 0.72 (more detail presented in the App. L). Results of this orientation step are the final adjusted estimations of interior and exterior orientation parameters (Table 4.3).

Parameters	Camera	$x'_{o\,obs.}\,(mm)$	$y'_{o\,obs.}\,(mm)$	$c_{k\,obs.}\,(mm)$	$x'_o\,(mm)$	$y'_o\,(mm)$	$c_k\,(mm)$
Interior parameters	**vertical**	-0.069894	-0.049059	200.253031	0.173740	0.138436	200.354646
	oblique	0.096526	-0.353679	259.707205	0.199348	-0.566046	260.484178
	terrestrial	0.000000	0.000000	346.629555	-0.089678	0.607910	345.845772
Exterior parameters	**Image ID**	$X_0\,(m)$	$Y_0\,(m)$	$Z_0\,(m)$	$\omega\,(gon)$	$\varphi\,(gon)$	$\kappa\,(gon)$
	1981	9970.198	10673.477	1940.415	4.541686	4.783209	131.282676
	1985	9420.803	10323.351	2019.296	0.656547	-5.259832	147.771561
	2025	9791.504	10558.522	2029.064	9.609923	-2.814618	148.325941
	1983	9608.958	10431.354	2036.93	4.116163	-2.510717	147.788284
	20891	9860.130	10113.512	1258.449	85.809626	18.740673	3.819419
	20893	9945.694	10186.942	1270.790	77.858137	31.915680	11.009249
	20892	9913.893	10177.268	1272.665	78.742428	31.879360	10.039255
	208325	9595.383	9290.120	1204.406	103.139401	-5.835934	5.022840
	637126	9650.565	9558.459	1230.297	88.908909	3.269174	0.023612
	208323	9945.255	9609.743	1242.905	92.523778	22.599575	6.174791

Table (4.3): Final improved estimations of interior and exterior orientation parameters calculated based on the combined evaluation of different image types of Baalbek

Illustrations of spatial positions of perspective centers are presented in 2D view (cf. Figure 4.3) as well as in 3D view (cf. Figure 4.4).

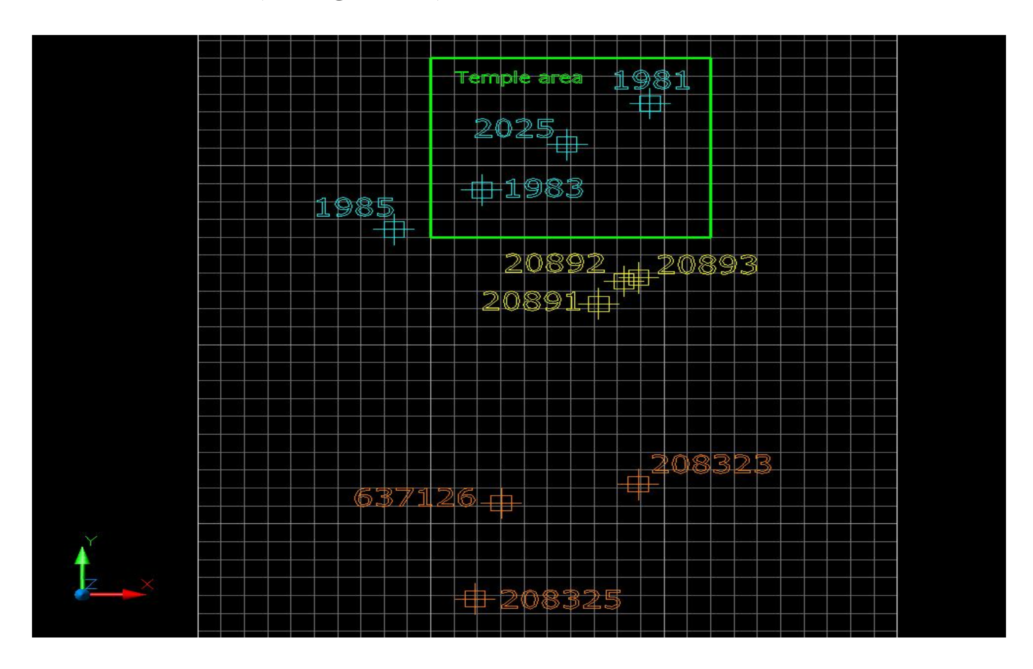

Figure (4.3): 2D positions of perspective centers related to Baalbek’s vertical, oblique and terrestrial images implemented in the orientation process

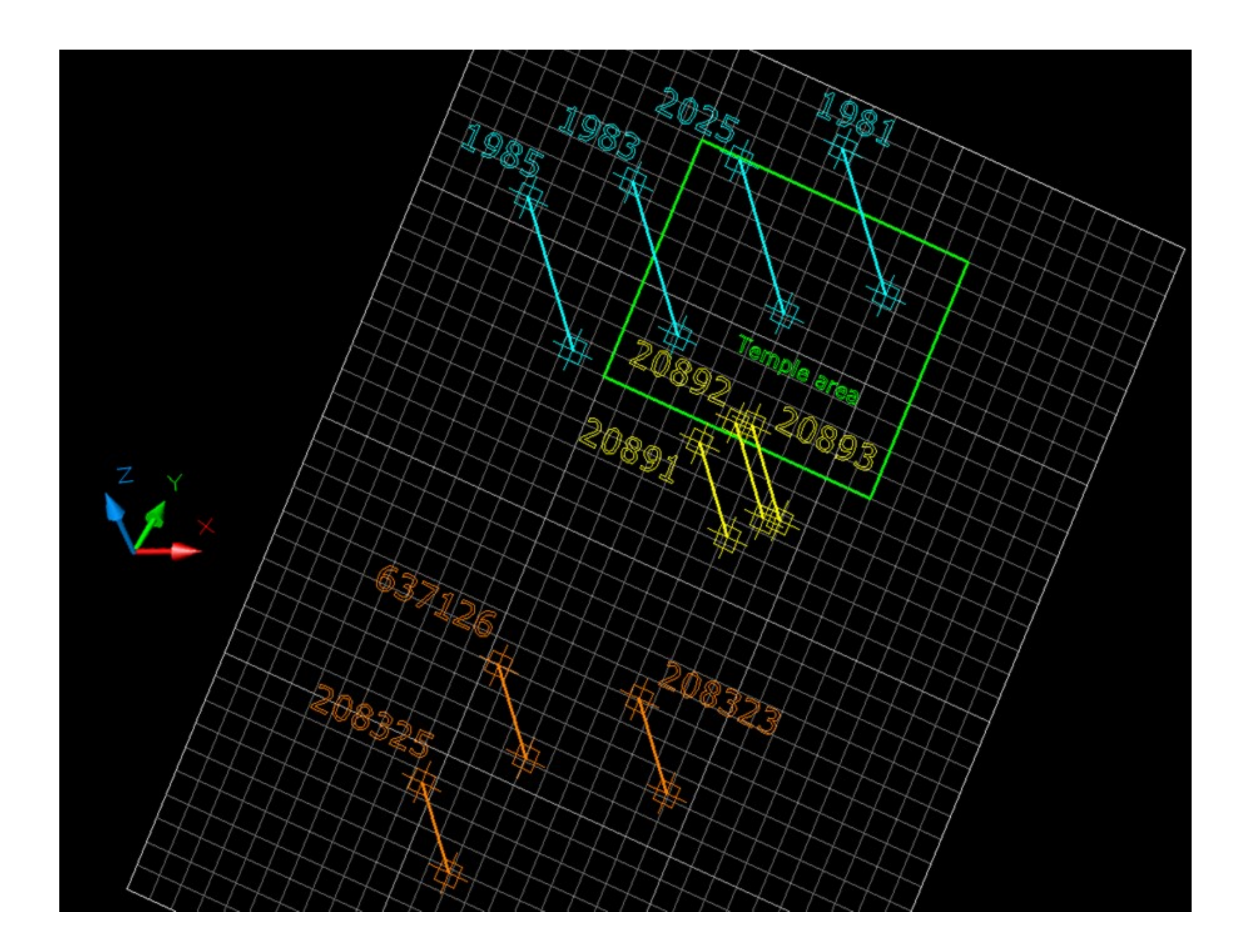

Figure (4.4): 3D view of perspective centers referred to Baalbek's vertical (cyan color), oblique (yellow color) and terrestrial (orange color) images implemented in the orientation process based on combined evaluation of three historical image types

4.3.2. Results interpretation

Results presented in the Table (4.3), which are calculated through orientation process based on the combined evaluation of Baalbek's images types, will be interpreted and checked based on different criteria as following:

4.3.2.1. Acceptance of image block calculations

Previously mentioned (in Chapter 4.3.1), that bundle block adjustment computations were accepted due to that ($\hat{s}_0$) is in the requested range. Variations of ($\hat{s}_0$) according to different values of a priori standard deviation of image points (adjustment observations) are shown in the Figure (4.5).

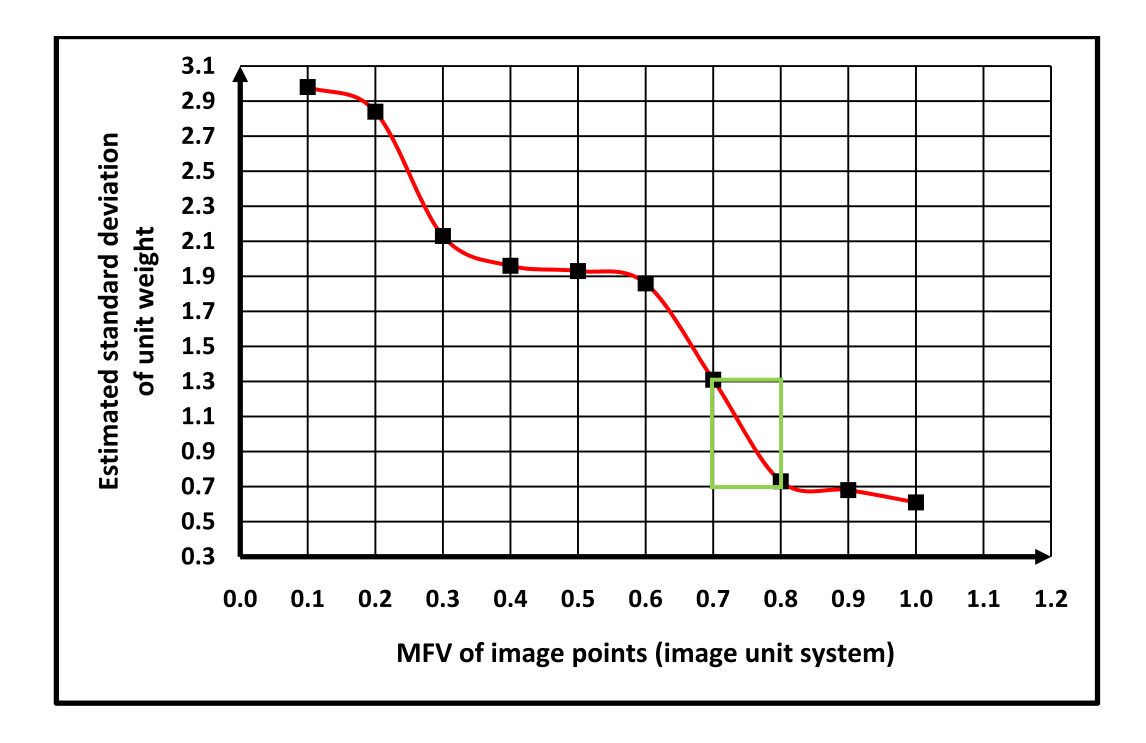

Figure (4.5): Variances of ($\hat{s}_0$) based on different values of the mean error of image points (orientation process based on combined evaluation of Baalbek's images types)

It is obvious (Fig. 4.5) that an increasing of MFV values of image points leads to a decreasing of ($\hat{s}_0$). This increasing is limited by the accuracy required of output data used for further applications (in our case: up to two pixels; ca. 25 cm). A priori standard deviation of image points was applied of (0.1 image unit) and led to ($\hat{s}_0$) of ca. (2.98). In contrast, the mean error of image points (1 image unit) led to ($\hat{s}_0$) of ca. (0.61). The two values of ($\hat{s}_0$) do not belong to the significant range [0.7 - 1.3]. Basically, to keep a balanced stochastical model of the adjustment process i.e., to keep $\hat{s}_0$ in the confidence interval, a prior standard deviation of image points (observations) should be applied between 0.7 to 0.8 (image system unit).

4.3.2.2. Controllability and errors associated with observations

The controllability and observation errors could be checked by normalized residuals analysis. According to NV$_i$ values (see App. L) only one value is larger than the critical value (4) associated with the horizontal coordinate of "image point 1110" in the "terrestrial image 208323". The relative partial redundancy associated with the maximum value of normalized residuals is EV=88%. It can mean that the observation (image point 1110) has been well controlled as well as its ratio for determination of unknowns is 12%. In contrast, most of observations have NV$_i$ values smaller than the threshold 2.5 (which means no large errors

visible). In addition, their partial redundancies are from 60% to 80%; which means most of observations have been well controlled.

4.3.2.3. Quality of interior orientation parameters estimated

By comparison of MFV and M of interior orientation parameters estimated based on the combined evaluation of Baalbek's images types (Table 4.4), it could be accepted that the stochastical model applied into adjustment calculation is balanced, where the MFV values of interior orientation parameters were confirmed after the bundle block adjustment by M values. This means a balanced stochastical model was guaranteed and well applied in the calculation process. In this context, values of the estimated standard deviation of the cameras' interior parameters do not exceed the assumed one i.e. those parameters have been well determined geometrically.

The query may be here noted that the MFV entered the calculations with a relative large value (especially for the camera used for the terrestrial type $\mathrm{MFV}_{x_0'} = 3\ mm$). The reason is that the images used are very old; therefore it was supposed to give - only in this case - more freedom of MFV values (but this freedom is limited with the geometric accuracy of the output data requested for further applications).

Camera	$\mathrm{MFV}(mm)$			$\mathrm{M}(mm)$		
	$\mathrm{MFV}_{x_0'}$	$\mathrm{MFV}_{y_0'}$	MVF_{c_k}	$\mathrm{M}_{x_0'}$	$\mathrm{M}_{y_0'}$	M_{c_k}
vertical	1.0000	1.0000	2.0000	0.7116	0.7057	0.5842
oblique	1.0000	1.0000	2.0000	0.7160	0.7200	0.8123
terrestrial	3.0000	2.0000	2.0000	2.0964	1.4395	0.8863

Table (4.4): A posterior standard deviations (M) of interior orientation parameters estimated based on the combined evaluation of Baalbek's image types; with respect to a priori mean error (MFV) of these parameters applied into computations

4.3.2.4. Quality of exterior orientation parameters

Exterior orientation parameters presented in the Table (4.3) will be evaluated in analogue way implemented to check exterior orientation parameters calculated based on the combining between the two image types: vertical and oblique (Chapter 4.2.3).

The estimated standard deviation M (after the adjustment) of coordinates of projection centers is approximately between $\pm 0.5\ m$ to $\pm 0.7\ m$. This means that the space position of cameras used has an error visible bounded to $\pm 0.7\ m$.

A comparison between last results (in this case only exterior orientation parameters are respected, Table 4.3) and other ones (namely: results of the 1st step given in Tables 3.5, 3.9 and 3.11 and results of the 2nd step presented in the Table 4.1) gives differences arisen between the results computed. These recorded differences are presented in the Tables (4.5) and (4.6).

Type	Image ID	$\Delta X_0\ (m)$	$\Delta Y_0\ (m)$	$\Delta Z_0\ (m)$	$\Delta\omega\ (gon)$	$\Delta\varphi\ (gon)$	$\Delta\kappa\ (gon)$
Vertical	1981	0.06	-0.06	0.33	0.116557	0.157327	0.146852
	1985	0.11	0.86	0.04	0.158064	0.112979	-0.128741
	2025	-0.01	-0.06	0.29	0.037925	0.220148	0.254195
	1983	0.00	-0.26	-0.08	0.110936	0.147148	-0.065397
Oblique	20891	0.89	-0.61	-0.94	0.072625	0.078254	-0.116925
	20893	-0.11	-0.49	0.27	-0.092222	-0.149059	0.002154
	20892	-0.08	0.22	-0.12	-0.041583	-0.00191	0.025745
Terrestrial	208325	0.01	0.04	0.07	0.020664	1.636357	-0.000803
	637126	-0.19	0.06	-0.12	0.091957	1.681601	-0.09032
	208323	0.04	0.01	-0.03	-0.063107	1.52865	0.151592

Table (4.5): Differences between exterior orientation parameters computed based on combined evaluation of three image types (Table 4.3) and other ones calculated based on implementation of each image type separately (Tables 3.5, 3.9 and 3.11)

Type	Image ID	$\Delta X_0\ (m)$	$\Delta Y_0\ (m)$	$\Delta Z_0\ (m)$	$\Delta\omega\ (gon)$	$\Delta\varphi\ (gon)$	$\Delta\kappa\ (gon)$
Vertical	1981	0.00	0.00	0.04	0.010183	0.059366	-0.030807
	1985	0.05	-0.01	-0.11	0.059760	0.020998	0.046983
	2025	-0.01	0.00	0.06	-0.009371	0.060314	0.003000
	1983	-0.01	-0.01	0.01	0.012829	0.062204	-0.026515
Oblique	20891	0.06	-0.13	-0.03	-0.162261	-0.020796	-0.056389
	20893	-0.16	-0.21	0.15	-0.189936	-0.157743	0.011032
	20892	-0.06	0.07	-0.11	-0.128161	-0.034439	0.091758

Table (4.6): Differences between exterior orientation parameters computed based on combined evaluation of three image types (Table 4.3) and other ones calculated in the 2nd orientation step (presented in the Table 4.1)

Most of the differences presented in the Tables (4.5) and (4.6) are not large with respect to the required absolute accuracy for the generation of a 3D model. This reveals that approximate values applied into the bundle block adjustment process are geometrically good assumed. Moreover, the principle of minimizing input data measurement residuals was sufficiently attained. The comparison between the differences referred to vertical and oblique images (Table 4.5) and the other ones (for the same images) given in the Table (4.6) indicates that the last ones are smaller; which means that the inclusion of the terrestrial image type in the 3rd orientation step improved the geometric accuracy of estimated parameters with respect to the combination of just vertical and oblique image types carried out in the 2nd orientation step.

In addition, the achievable accuracy of orientation parameters as well as the precision of 3D applicable object point coordinates (accuracy of position and height) allow to use extracted 3D object points to generate a 3D model of Baalbek in different Levels of Detail (LODs) (Gröger et al., 2008).

4.4. Additional check issues of results

There are still issues - related to quality of orientation process results achieved based on combination of different image types - that request to be investigated sufficiently such: the check of lens system distortions and sequences of image combination applied in the achieved orientation process.

- *Lens system distortion*:

Starting from the assumption that a reasonable photogrammetric methodology dealing with combination of different historical image types would be an important product of this thesis, therefore, the achievement of an orientation process with non-high strict mathematical model applied in the adjustment problem is preferable (at least in the study case of Baalbek due to poor image properties).

Consequently, in the orientation steps based on the combined evaluation of Baalbek’s image types the impact of lens distortions has not been taken into account. This leads, however, to a reduction of the strictness degree associated with the functional model applied in calculations, although this will directly affect on the geometric accuracy of main observations (image point coordinates). In contrast, it is important to mention that the distortion impact had been respected in the 1st orientation step. This means that image points had been radially and decentring corrected and, thus, their impact on the geometric accuracy of the 1st step results

(which were applied as initial values in the 2nd and 3rd orientation steps) was taken in the consideration.

- *Sequences of image combination*

With respect to the available historical images of Baalbek, there are four possibilities of image type combination to achieve the orientation process: (vertical-oblique), (vertical-terrestrial), (oblique-terrestrial) and (vertical-oblique-terrestrial).

In this research, the orientation process based on the combined image evaluation started with the vertical-oblique images (step2). This is mainly due to difficulties (e.g. high image noise led to an inaccurate determination of object and tie points in images) arisen in the flow of the orientation process referred to the terrestrial image type (in the 1st orientation step). In addition, it has been pointed (Chapter 4.1) that both types (vertical and oblique) have been taken approximately in the same period (1930s), which could mean that they include approximately same objects (like: buildings, streets). This could optimize the object recognition and the matching process between the images and may be a feasible support for calculations of the bundle block adjustment.

Therefore, it was firstly avoided to carry out the orientation process based on a combination including the terrestrial image type in order to get reliable results. Once, the orientation process based on the first combination (vertical-oblique) has been successfully attained, it was directly assumed to consider the oriented block based on the mentioned combination as a basic start for Baalbek's terrestrial image type and then the possibility to achieve the 3rd step of the orientation process.

Consequently, it could be accepted that the sequence of image combination: *"**vertical-oblique** then all image types: **vertical-oblique-terrestrial**"* was a reasonable suggestion to orient Baalbek's historical photos (with respect to results achieved). It is important to note that other combination sequences (for e.g. vertical-terrestrial, oblique-terrestrial, etc.) could be achieved and discussed, but this is still limited that new data about the terrestrial images should be provided.

Finally, image orientation protocols related to selected images of historic Baalbek are presented in the App. (K). These protocols include a comparison between results of the interior and exterior orientation parameters estimated based on the last orientation step (combination of all image types) and other ones calculated in the 1st and 2nd orientation steps.

5. Orientation of Baalbek's vertical images using LPS

Baalbek's vertical images are considered an important source of data describing Baalbek's historical status in the 1930s because these photos include many objects (e.g. buildings, part of buildings, streets, etc.) which had been today changed, renovated or even destroyed. Furthermore, these images support a basic data (e.g. geometric and semantic information) which could be used for a generation of 3D model of Baalbek. Therefore, the oriented model of these images should be controlled as possible to guarantee a best orientation results as well as an optimal 3D features acquisition (with respect to the geometrical point of view).

Thus, in this chapter, an effort for image orientation process will be achieved to reveal to what extent the estimated orientation elements (Chapter 4) are geometrically well determined and to what extent they are accurate and correlate the control points applied! This process will be also achieved based on the bundle block adjustment method using approximate values of orientation parameters (estimated orientation parameters associated with the vertical image type of Baalbek, see Chapters 3.2 & 4.1).

Furthermore, another mathematical model can be applied into the orientation process. This model is based on a system of mathematical equations developed - among other things - for the study cases dealing with aerial photogrammetry and generation of orthophotos. In those cases: the optic axis is Z, the image plane is approximately horizontal and the viewing direction is approximately vertical.

The main tool used to enforce the mentioned orientation process is the software LPS[1] (Leica Photogrammetry Suite); more detail about this process, LPS and its mathematical model will be expressed in next section.

5.1. Leica Photogrammetry Suite (LPS)

Leica Photogrammetry Suite is defined as a collection of integrated software tools which offer different photogrammetric processes for geospatial imaging applications. The main primary component of LPS is *LPS-Project Manager* which reduces the cost and time associated with different photogrammetric processes when collecting geographic information. LPS was selected to achieve the intended aim of this work stage because *LPS-Project Manager* addresses issues and problems related to (LPS user's Guide, 2008):

[1] Copy right 2008 ERDAS, Inc.

- Collecting Ground Control Points (GCPs) in field or office.
- Measuring GCPs and tie points on multiple mages; which guarantees a stable model through calculations in the bundle block adjustment.
- Performing quality control in order to verify the overall accuracy of final product. This is essential to verify, in general, the acceptance of images block calculations.
- Integrating data from different techniques e.g. airborne Global Position System (GPS) and other photogrammetric sources; through this integration further works will be available for e.g. if new measurements based on GPS in Baalbek’s space are available, new input data can be applied in the orientation process.
- Capability to use photos scanned from desktop-scanners; this fits Baalbek’s historical vertical images which are particularly photos scanned.
- Extracting of a Digital Terrain Model DTM automatically from images (which is necessary to generate orthophotos of Baalbek).
- Finally, this software was especially developed to deal with vertical aerial images.

In *LPS-Manager* and its triangulation process the self-calibration is respected because it is considered the most common approach used to reduce the influences of the systematic errors related to image process system (Konecny, 1994 & Wang, 1990). In this context, the internal geometry of each image and the relationships between overlap areas of images will be determined. When multiple images are involved in a data block, such as a modelling method can significantly ease the need of acquiring GCPs.

Tie points are common points whose ground coordinates are not known, but they are visually recognizable in the overlap area between two or more images. They connect the images in the same block to each other and they are necessary input data for the triangulation process. *LPS-Project Manager* automates the identification and measurement of tie points.

The triangulation process is establishing of a mathematical relationship between the images contained in a project, the camera or sensor model, and the ground. In this context, it is necessary to form a functional model which presents the mathematical relationship between observations and unknowns associated with the adjustment problem. Basically, in the block of triangulation process, a functional model can be formed based on the collinearity equations (Luhmann, 2003, pp. 238):

$$x'_p = x'_0 + z' \cdot \frac{r_{11} \cdot (X - X_0) + r_{21} \cdot (Y - Y_0) + r_{31} \cdot (Z - Z_0)}{r_{13} \cdot (X - X_0) + r_{23} \cdot (Y - Y_0) + r_{33} \cdot (Z - Z_0)} + \Delta x' \quad (5.1)$$

$$y'_p = y'_0 + z' \cdot \frac{r_{12} \cdot (X - X_0) + r_{22} \cdot (Y - Y_0) + r_{32} \cdot (Z - Z_0)}{r_{13} \cdot (X - X_0) + r_{23} \cdot (Y - Y_0) + r_{33} \cdot (Z - Z_0)} + \Delta y' \quad (5.2)$$

where: x'_p , y'_p measured coordinates of the image point p'

x'_0 , y'_0 coordinates of the principle point H´

$\Delta x'$, $\Delta y'$ correction values

c_k focal length

X_0 , Y_0 and Z_0: coordinates of the projection center

X, Y and Z: object point coordinates

The residuals, which should be minimized, can be expressed through a linear form using the equation (2.26, App. LST). These residuals (corrections) will be added to the initial estimations of unknowns through iterative calculation process which will be terminated until the corrections to the unknown parameters are less than *a user-specified threshold* (*convergence value*). Information resulting from triangulation process (e.g. estimations of interior and exterior orientation parameters, etc.) is regarded as input data for a rectification process of images (orthophotos), 3D features extraction, etc.

The bundle adjustment in *LPS-Project Manager* provides three main functions:

- The ability to determine the position and orientation of each image in a project as they existed at the time of image exposure. The resulting parameters are referred to as exterior orientation parameters.

- Determination of ground coordinates of any tie points measured on the overlapping areas of multiple images. The precise ground point determination of tie points is useful for generating GCPs from images in lieu of ground surveying techniques.

- The good ability to distribute and minimize the errors associated with the images, GCPs and image measurements. The bundle block adjustment processes information from an entire block of images in one simultaneous solution (that is, a bundle) using statistical techniques to automatically identify, distribute and remove errors visible.

5.2. Orientation of Baalbek's vertical images using LPS - process flow and results

Basically, there are different types of geometric models included in *LPS-Project Manager* (e.g. frame camera, digital camera, etc., Fig. 5.1). A geometric model selection is necessary to define the camera applied and it depends on the type of the camera associated with the images that to be oriented. Due to that the vertical images of Baalbek have been taken with a metric camera (see the Chapter 1.4.1) the geometric model was considered "Frame Camera" which corresponds to the camera referred to those images.

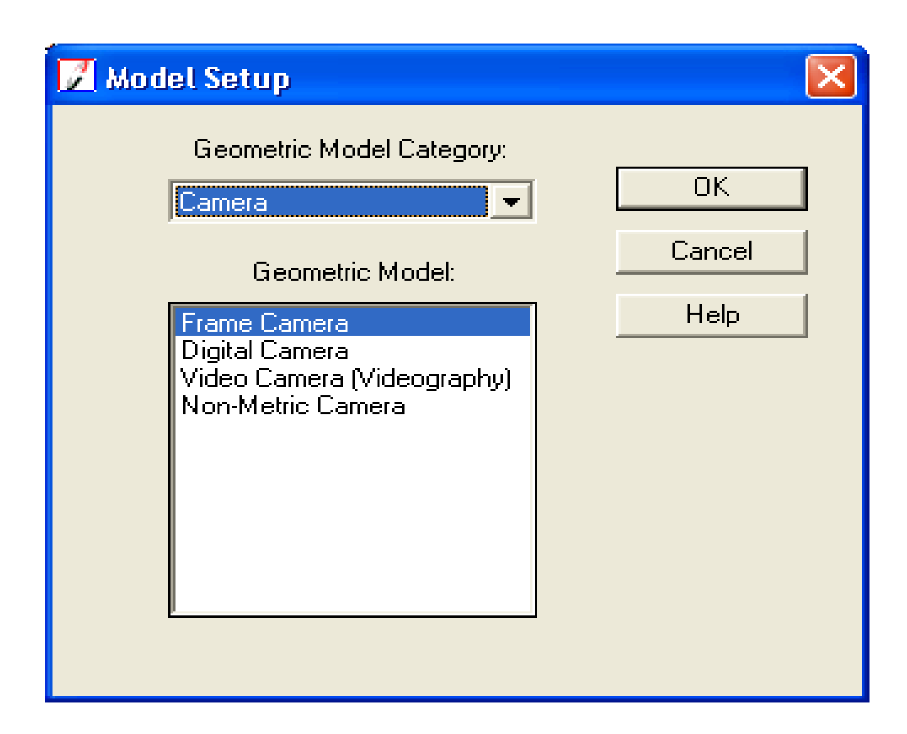

Figure (5.1): Geometric models classification; the frame camera model was selected according to the type of the camera used in the vertical images of Baalbek

Pyramid layers computation[1] of the images used in the orientation process (in this case, seven vertical images were implemented) is an important step in this process. On one hand pyramid layers are computed to optimize an image display and on the other hand to perform an optimal automatic tie point collection. Initial information about fiducial points, interior[2] and exterior

---

[1] Pyramid layers generated by LPS Project Manager are based on a binominal interpolation algorithm and Gaussian filter. Using this filter, image contents are preserved and computation times are reduced (LPS - User's Guide, 2008).

[2] In this step, interior camera parameters were applied as fixed values.

camera parameters is imported based on the orientation results calculated using the compact mode of the software Pictran (Chapter 3.2.3).

During the triangulation process, control points are implemented to establish a mathematical relationship between the camera, images and 3D ground surface. In addition, a generation of tie points between overlapping images should be taken into the account because this process will guarantee a stable model of adjustment calculations. *LPS-Project Manager* performs this process automatically.

The required number of tie points collected depends on the amount of the overlap between the images. In Baalbek's project, the number of tie points per images was typed (10). Tie points recorded should be controlled to validate and ensure the requested accuracy. If a tie point is not determined correctly, it should be adjusted. An overview showing the vertical images used, control points and tie points is depicted in the Figure (5.2).

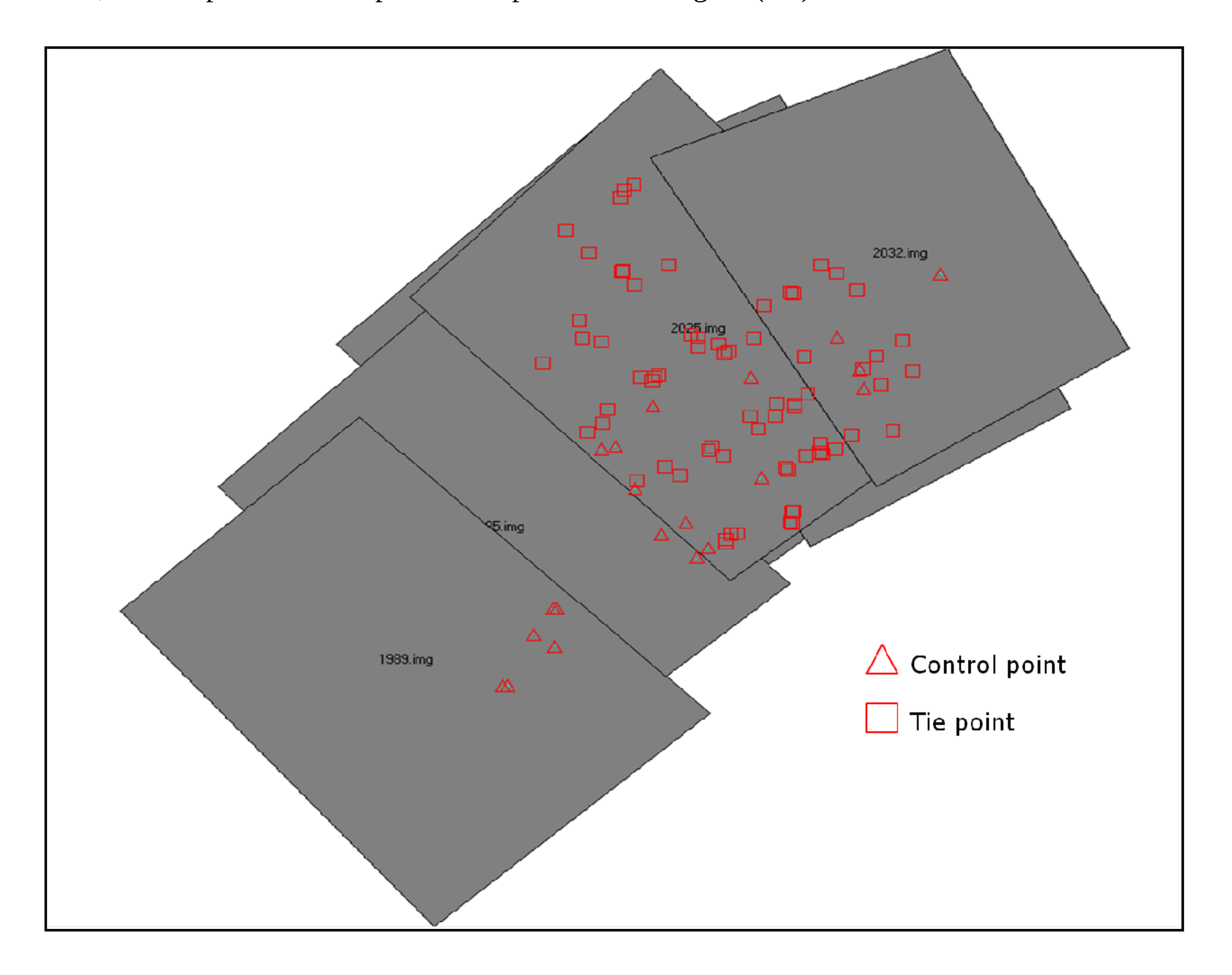

Figure (5.2): Alignment of vertical images used in LPS-based orientation process

LPS-Project Manager provides two error or blunder checking models which identify and remove errors from the photogrammetric network of observations. The input observations including the measured image coordinates are analyzed to determine the erroneous input data contributing to overall instability of output aerial triangulation results.

The first model of error check is "*Time Saving Robust Checking*" which uses a robust iteration with selective weight functions to detect large errors in the input observations (in this model, the individual redundancy of each observation is not computed). The second one is "*Advanced robust checking*". It uses a robust iteration solution with selective weight functions based on the redundancy of each observation. In addition, the weight functions used in this check meet the requirements of a rigorous robust estimation function (LPS user's Guide, 2008, pp. 329-330).

Basically, the model of "*Advanced robust checking*" was applied into LPS-based triangulation process of Baalbek vertical aerial images. With this model the weight of each observation is predicted for the next iteration of processing. The new weight is computed based on weight functions with respect to observation residuals. During successive iterations, the weight for a bad observation decreases until it approaches zero. At this point, observations containing gross errors can be detected.

Once the triangulation process has been achieved, a report will be available including all triangulation results which can be summarized as following:

- Final interior and exterior orientation parameters of each image (Table 5.1).
- 3D coordinates of tie points and their accuracy.
- Adjusted GCPs coordinates.
- Image coordinates residuals.
- Total RMSE (Root Mean Square Error) of the solution: it presents the standard deviation of unit weight after the adjustment. It is an indicator of the global quality of the attained solution. This value is based mainly on the photo coordinate residuals and the ground coordinate residuals.
- RMSE of the GCPs in the object system (GCPs accuracy).
- RMSE of GCPs photo coordinates.

OS	Camera	$x'_{o\ obs.}\ (mm)$	$y'_{o\ obs.}\ (mm)$	$c_{k\ obs.}\ (mm)$	$x'_o\ (mm)$	$y'_o\ (mm)$	$c_k\ (mm)$
LPS	vertical	-0.0690	-0.0490	200.0000	-0.0690	-0.0490	200.0000
	Image ID	$X_0\ (m)$	$Y_0\ (m)$	$Z_0\ (m)$	$\omega\ (gon)$	$\varphi\ (gon)$	$\kappa\ (gon)$
	1981	9970.1732	10673.4904	1940.0917	4.208667	5.071778	131.130556
	1982	9743.2099	10470.4121	2040.6187	8.257222	0.523667	146.688333
	1985	9420.7017	10322.5015	2019.1659	0.941667	-5.183667	147.571000
	1986	10198.7218	10754.3967	1941.1403	-0.587000	9.754778	-68.217000
	1989	9242.0868	10158.0734	2026.2353	-5.132667	-6.839222	147.004667
	2025	9791.5418	10558.6648	2029.0143	9.938222	-2.928778	147.611444
	2032	10337.0624	10870.6683	1910.0828	-1.051000	12.508667	-67.681889

Table (5.1): Results of LPS-based orientation process referred to vertical images (in this case: interior orientation parameters applied as fixed values, OS: Orientation Step). It should be mentioned that coordinates of projection center (Z_0) related to the images: "1981" and "1982" have been controlled with respect to other ones (for the same images) estimated based on the standard mode of Pictran-B.

Adjusted positions of projection centers of each image in the oriented block are depicted in 2D view (cf. Figure 5.3) and in 3D view (cf. Figure 5.4).

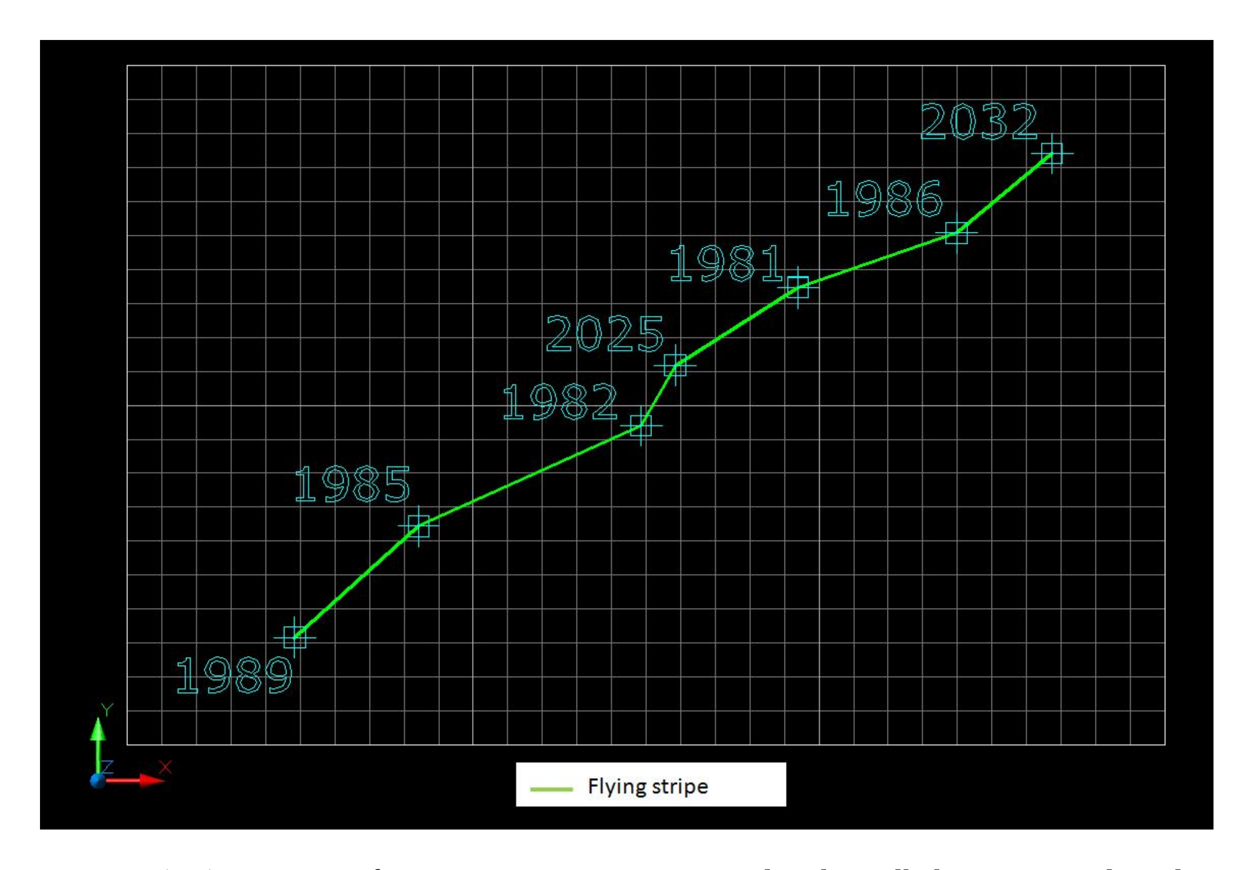

Figure (5.3): 2D view of perspective centers associated with Baalbek's images selected

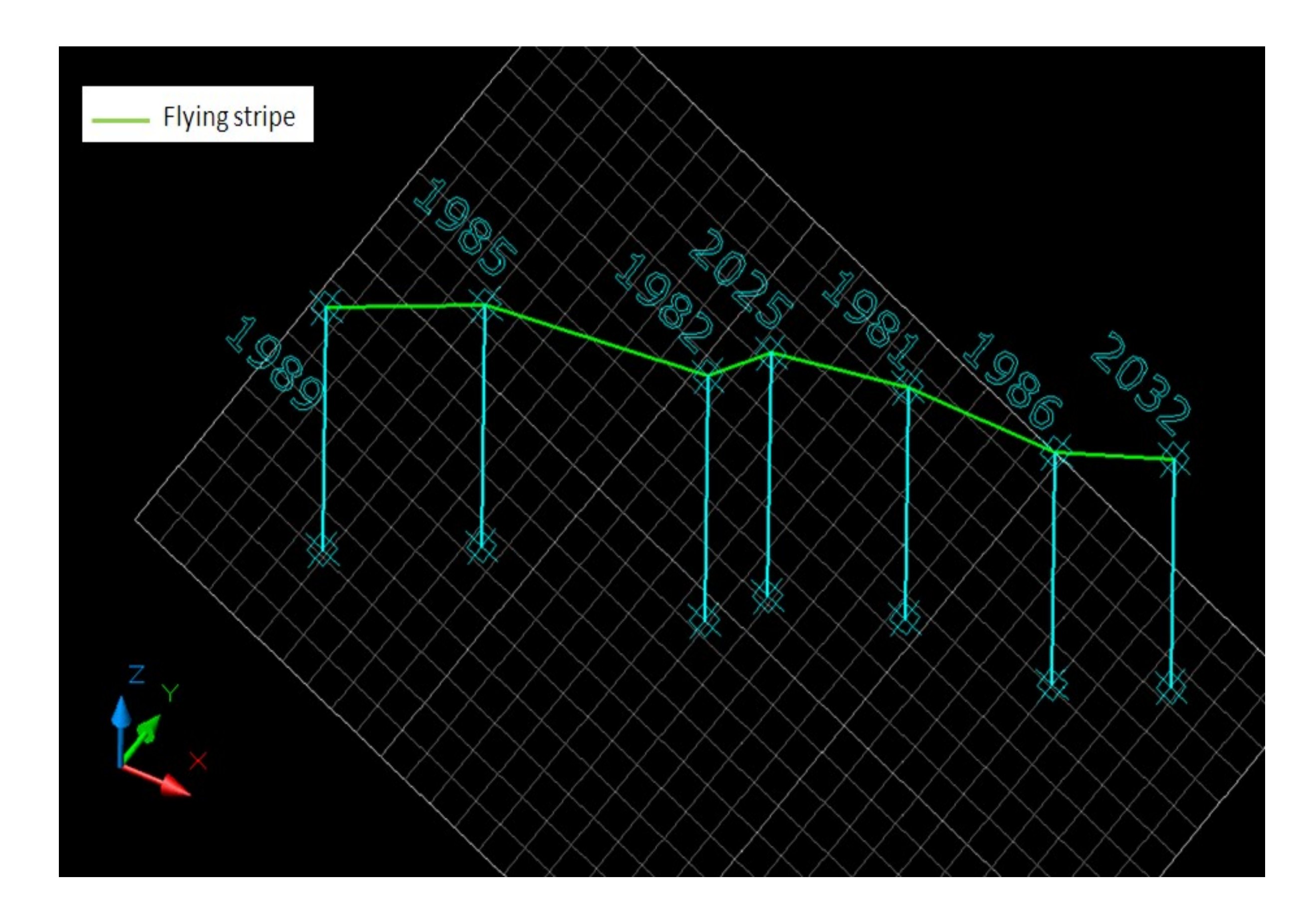

Figure (5.4): 3D view showing spatial positions of perspective centers associated with Baalbek's vertical images oriented based on LPS

5.3. Results check

- *Calculations convergence*

It is known that the way of the bundle block adjustment is an iterative process in order to improve approximate values applied. This process will be terminated at a threshold applied (convergence value, Chapter 2.3).

When the calculations of a bundle block adjustment are not convergent, that means there are large errors visible as well as an insufficient redundancy of measurements associated with an unknown or more one.

In this context, the calculations block related to the vertical images of Baalbek is convergent with respect that the critical value applied into the calculations is $(0.005)\ m$ (see system control, App. M).

- *Total RMSE of the block solution*

The standard deviation of the unit weight of the last iteration related to the calculations of the bundle block adjustment is considered the most important control of the results. It indicates the global quality of that iteration.

It depends on the residuals of the image point coordinates and the ground coordinate residuals. Generally, a smaller value of estimated standard deviation of the unit weight indicates that the residuals of observations have been minimized.

The triangulation summary shows that the standard deviation in the last iteration is ca. 0.43 (see block system control, App. M) i.e., that the adjustment calculations are accepted and the criteria of minimizing input measurement residuals is attained.

- *RMSE of GCPs in object system*

RMSE of GCPs in object system reflects the amount of change between the original GCPs coordinates and newly estimated one computed using the estimated unknown parameters through the adjustment process.

In this context, RMSE values of GCPs coordinates X, Y and Z are in the range $[0.7 - 1.2]m$ (for some points located closely of image borders, RMSE of Z coordinates reached $1.6\ m$). It could be accepted that newly GCPs computed using estimated unknown parameters (exterior orientation elements) conform to the original GCPs applied into calculations with respect to the poor geometric properties of vertical images, and the geometric accuracy requested for the generation of a 3D city model (namely: the absolute accuracy needed for generation of a 3D model concerning standards of CityGML City Geography Markup Language, Gröger et al., 2008).

- *Results comparison*

A comparison between last results of orientation parameters (in this case: just the exterior parameters estimated based on LPS of some selected images; where the interior parameters entered the orientation process as fixed values) and the other ones calculated using the compact mode of Pictran-B is given in the Table (5.2). It could be accepted that both results conform each other relatively (with respect to the geometric accuracy). Differences between both results may have resulted from:

- Involving of different data sets in one system (e.g. new observations)
- Different levels of accuracy
- Different stochastical model was applied in LPS

OS	**Image ID**	$\Delta X_0\ (m)$	$\Delta Y_0\ (m)$	$\Delta Z_0\ (m)$	$\Delta\omega\ (gon)$	$\Delta\varphi\ (gon)$	$\Delta\kappa\ (gon)$
LPS & Step1	1985	0.011	0.006	-0.087	0.443184	0.189144	-0.329302
	1986	-0.088	-0.036	-0.869	-0.024604	0.019556	0.794182
	1989	0.003	-0.002	-0.005	-0.048324	-0.116094	-0.268069
	2025	0.032	0.086	0.241	0.366224	0.105988	-0.460302
	2032	0.008	0.006	0.130	0.613087	0.220487	1.553615
LPS & Step2	1985	-0.047	-0.862	-0.237	0.344880	0.097163	-0.153578
	2025	0.029	0.142	0.013	0.318928	-0.053846	-0.711497
LPS & Step3	1985	-0.101	-0.850	-0.130	0.285120	0.076165	-0.200561
	2025	0.038	0.143	-0.049	0.328299	-0.114160	-0.714497

Table (5.2): Differences between parameters of exterior orientation (referred to selected images) estimated based on LPS and other ones calculated using the compact mode of Pictran-B, where OS: Orientation Step

Consequently, Baalbek's vertical images (also oblique and terrestrial photos) have been sufficiently oriented. Therefore, further work stages such: creation of orthophotos, data extraction, etc. can be started. These steps will be described in detail in next chapter.

6. Spatial data acquisition

As previously mentioned (Chapter 1.2), that the documentation of the historic Baalbek (from 1900s to 1940s) is an important objective of this thesis. For this purpose, historical oriented photos of Baalbek will be implemented, where 3D object points could be measured to reconstruct 3D objects.

Due to that there are different image types of historic Baalbek, one can pose the following question: *by which combination between different oriented images of Baalbek an optimal process of 3D object reconstruction could be achieved? In addition, to what extent the geodetic and geometric accuracy of applicable 3D object points is?*

In this chapter, 3D object reconstruction process (3D data acquisition) based on Baalbek's historical photos oriented using Pictran and LPS will be investigated and discussed to answer the abovementioned question. In addition, a classification of 3D applicable points acquired will be suggested; where it could be determined in which photo/photos an object point is shown as well as from which photo that point could be optimal recorded. This classification is essential for further applications and activities in Baalbek's space (e.g. a creation of a 3D city model concerning the standards of City Geography Markup Language).

The reconstruction process of 3D object points consists of the following stages:

- Creation of Baalbek's orthophotos based on the oriented historical images. In this step it is necessary to create a Digital Terrain Model (DTM) of the studied area.
- Generation of the region mosaic.
- Spatial data acquisition: although 3D data extraction can be carried out directly based on an oriented model of images (an object point can be determined using at least two oriented images including that point), but in this research the process of 3D data acquisition referred to Baalbek's images is achieved separately for planimetry and height, due to the different accuracies that are obtained during photogrammetric 3D point measurements for the XY and Z coordinates.

However, the output of this work stage presents the geometrical reconstruction process of the studied area of Baalbek as well as the 3D feature extraction of Baalbek's historical entities.

6.1. Creation of Digital Terrain Model of Baalbek

In general, there is some confusion about the two terms: Digital Terrain Model (DTM) and Digital Elevation Model (DEM). DTM and DEM describe the continuum of a surface as an infinite amount of three dimensional points (X, Y and Z) in a space. The measured values of the XYZ-triple (using different measurement techniques) are mostly irregular spaced. These irregular spaced points are normally converted in a regular spaced grid (square grid, same spacing in X- and Y- directions) by using different interpolations techniques (for e.g. Kriging technique). One XYZ-triple in the DTM/DEM is therefore representing an area of the square of the grid spacing of the grid; thus called grid cell.

A DEM can be defined as a digital representation of a surface. This digital representation is based on digital stored XYZ-triples of that surface. It is meaningful to mention which surface is meant by using a DEM (e.g. DEM of the vegetation surface, DEM of the ground water surface, etc.). In the case that a DEM refers to the earth surface (namely, digital stored XYZ-triples of the earth surface), it will be called DTM; that means a DTM is a special case of a DEM (Köthe, 04/2000).

Particularly, height differences on the ground lead to radial distortions in usages of digital images. An effective approach used to reduce (or even to eliminate) these distortions is a linking between digital images used and a DTM associated with. This linkage is considered an important step in order to generate orthophotos (rectified images). In this context, a DTM joints each image point (in the image to be rectified) with a special position in a new image (a raster rectified image which called orthophoto) related to. In addition, it enables to integrate Z-values for image points through interpolation process.

Consequently, Baalbek's DTM has to be generated definitively in order to create orthophotos of Baalbek. A generation of such model is possible by using different techniques. In this project, two approaches were implemented. The first one is using of Baalbek's historical images oriented (in this case Baalbek's vertical images). Due to poor properties of these images (Chapter 1.1) it was difficult to generate a DTM of Baalbek with high quality. Therefore, the DTM generated based on Baalbek's images was not applied in further applications (like: image rectification, 3D modelling). The other approach used to create Baalbek's DTM is based on topographical maps covering the whole studied area of Baalbek.

However, two topographical maps of Baalbek are available which were obtained from the institute of *Francais du Proche Orient* (*IFPO*) in Damascus (Chapter 1.4.4). Both maps have been scanned with scan-resolution of 300 dpi. Properties of Baalbek’s maps implemented can be summarized as following:

- Emission date is in the year 1962
- The maps cover the whole area of Baalbek
- Maps’ scale is 1:20 000
- Ground resolution is ca. of 1.7 m (with respect to pixel size)
- Ellipsoid used is Clark 1880
- Both maps have been created with the stereographic projection
- Contour lines interval is 10 m
- Longitude line is 38°
- Latitude line is 40°50´

A new map[1] covering only the area included in the vertical images of Baalbek was derived based on the abovementioned topographic maps. The derived map has been georeferenced onto the local coordinate system of Baalbek associated with vertical images in order to enforce the transformation between the new map and the images.

The intended transformation has been attained using GCPs. In this context, the required number n of GCPs requested depends on the order of this transformation. This number is given as following (Leica Geosystems, 2005, pp. 154-156):

$$n = \frac{(t+1)\cdot(t+2)}{2} \tag{6.1}$$

where t: the order of the transformation

If the required number of GCPs is not satisfied, it will not be possible to resample the input data (namely: Baalbek’s new map); this means the georeference process will not be executed. In the resample process, the interpolation method “Nearest Neighbour” has been applied where it preserves original gray values associated with the input data used (see: resample-parameter, App. N). The resampled map has the output cell size of ca. 0.98 m (more details expressed in the report of resample-parameters, App. N).

[1] The new map is indicated with the name *submap_baalbek*

Going out from the georeferenced map, the digitization process of contour lines included in Baalbek's new map can be carried out. The interval of digitized contour lines was preserved of $10\,m$. Height values associated with digitized contour lines are between $1080\,m$ to $1450\,m$. Using digitized contour lines the surfacing process generating Baalbek's DTM has been successfully executed.

Surface interpolation calculates Z values at spatial locations where no Z samples exist in the input data source. The output is a continuous raster image that contains Z values calculated from the interpolation method. The surface tool (in Erdas Imagine) uses a TIN (Triangulated Irregular Network) interpolation methods. However, two TIN interpolation methods are available: Linear and Nonlinear. The Linear interpolation method results in the TIN triangles being defined as angular planes. The Nonlinear one results in a smooth surface. For Baalbek's DTM generated, the TIN Linear interpolation method was used. Properties of Baalbek's DTM created can be summarized through following points:

- Output file name: *dgm_karte_lokal*
- Cell size for X and Y is 9 m
- Coordinates of the upper left point: X = 76505.35 m and Y = 12298.39 m
- Coordinates of the lower right point: X = 12534.97 m and Y = 8313.97 m

A section of Baalbek's DTM (raster image) and contour lines digitized are shown in the Figure (6.1). In addition, a 3D overview of Baalbek's DTM including the studied area of Baalbek and the mountain *Abdullah* in Baalbek are depicted in the Figure (6.2).

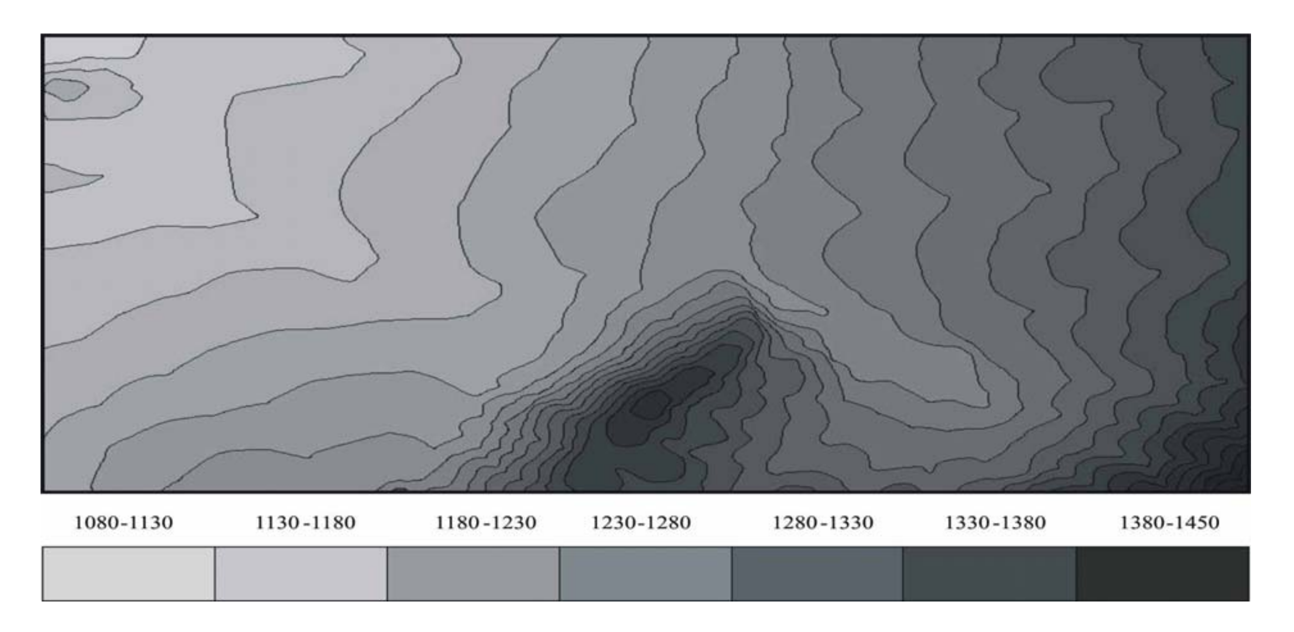

Figure (6.1): A section of Baalbek's DTM created based on topographical maps

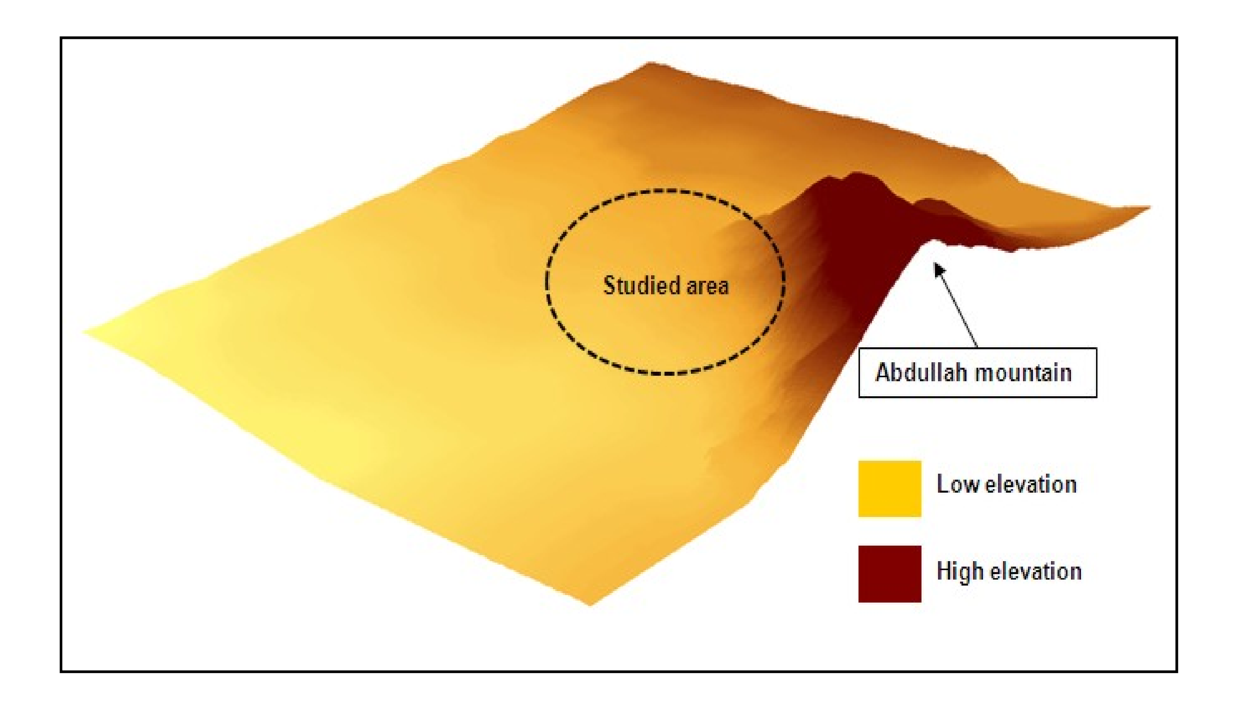

Figures (6.2): A 3D overview of Baalbek's DTM including the studied area of Baalbek (dotted circle) and the mountain *Abdullah*

6.2. Baalbek's DTM quality

"The grid cell size is the most common criterion concerning the quality of a DTM. An increasing of the grid cell size associated with a DTM leads to a decreasing of the DTM resolution that means an increasing of the generalization of the real surface. The DTM precision, with respect to the grid cell size and its altitude, depends on the slope gradient of the real surface and the size of the terrain unit. The DTM will be accurately created, if the real surface is steep and the terrain units are small. Units smaller than the grid cell size will not be visible in the DTM because they just merge through the grid" (Köthe, 04/2000).

The ground resolution of input data (e.g. map/image) takes an important role in calculations of a DTM grid cell size. With respect to the assumption that a grid cell size computation based on a 1 pixel to 10 pixels in the DTM to be created, i.e. the ground resolution of 1 meter leads to cell size for the DTM intended of 10 meters. Thus, the ground resolution of Baalbek's map (ca. 1.7 m) leads to an appropriate critic cell size 17 m (in the DTM). In the context of a decrease of the generalization of the real surface the cell size of Baalbek's DTM should not exceed the mentioned critical cell size. However, Baalbek's DTM cell size resulted is 9 m; which means that the generalization of the real surface throughout the model was relatively decreased.

6.3. Orthophotos generation

6.3.1. Definition

An orthophoto is an image transformed geometrically. This transformation converts the original photo, which is in general distorted, into an orthogonal projection. The orthogonal projection of an image enables displaying object surfaces (e.g. building roofs) included in that image in an orthogonal view.

The aforementioned transformation process is called *"image rectification"*. Depending on the height differences of object points included in an image, a rectification process of that image can be either *planar* or *differential*. Through the first one the whole image (or a selected sector from the image) will be converted into the reference system using the parameters of the projective transformation. It means each image point will be transformed with the same coefficients into the rectified photo. Unlike by the other one (non-plane rectification) each image point will be converted into the orthophoto with respect to its coordinates X, Y and Z (Luhmann, 2003, pp. 314-320).

Due to that height differences related to object points lead to radial distortions in images (see Chapter 6.1), an image rectification type could be specified based on the radial distortions associated with the image to be rectified. In this context, the relation between the height difference Δh - associated with the object points P_1 and P_2 (see Figure 6.3) - and image radial distortion $\Delta r'$ can be given as following (Wiedemann, 2004):

$$\Delta h = \frac{c_k}{r'} \cdot \Delta r \tag{6.2}$$

where:

$\Delta r = \Delta r' \cdot m_b$ (m_b: image scale number)
r': image radius
c_k: camera focal length

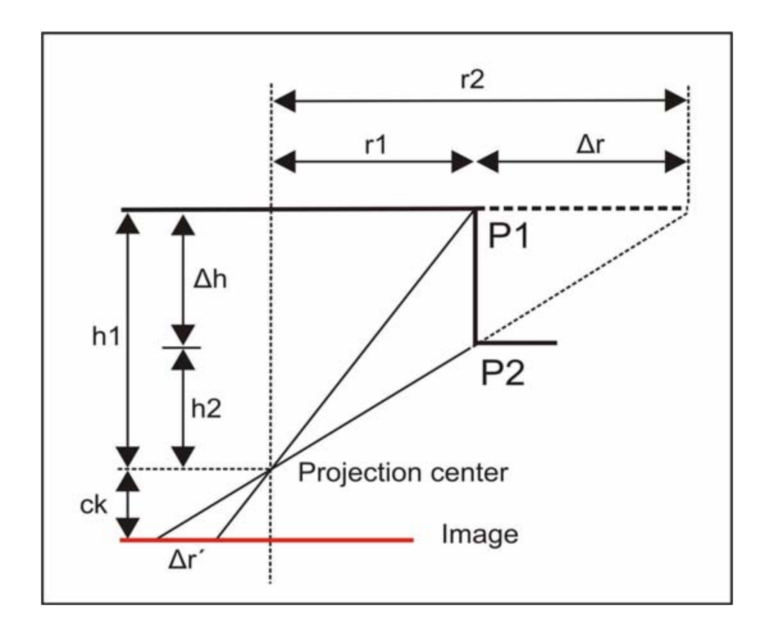

Figure (6.3): An illustration of the relation between the height difference Δh of the points P_1, P_2 and the radial distortion $\Delta r'$associated with

In the case that the maximum image radius r'_{max} is respected, it means the maximum height difference Δh_{max} should be taken into the account. Therefore, the formula (6.2) can be re-formed as following:

$$\Delta h_{max} = \frac{c_k}{r'_{max}} \cdot \Delta r_{max} \tag{6.3}$$

Going from the assumption that:

- the maximal distortion $\Delta r'_{max}$ of an image point - in an orthophoto - is not allowed to exceed $0.05\ mm$; this leads to $\Delta r = 20\ cm$,
- Baalbek's vertical images size is ca. $18 \times 13\ cm$ (Chapter 1.4.1); i.e. the maximum image radius is ca. $11.10\ cm$,

thus, the critical height difference can be calculated by a substitution of mentioned values in the formula (6.3) with respect that camera constant applied is $200\ mm$:

$$\Delta h_{max} = \frac{0.200}{0.111} \cdot 0.20 \approx 0.36\ m$$

Consequently, if height difference of Baalbek object points (namely the control points) is larger than Δh_{max} that means the planar image rectification can not be applied. Basically, the height difference between the maximum and minimum Z-values of Baalbek object points

measured is ca. of 61.60 m; therefore, the differential rectification process of Baalbek's vertical images has to be enforced.

6.3.2. Mathematical principle of differential rectification

The differential rectification of an image is a creation of a new image (orthophoto) based on the original image and its points individually (in this case: a Digital Surface Model DSM, a DEM or a DTM is required, Chapter 6.1). The transformation between original and new image is achieved with respect to the orthogonal projection. It means each object included in the original image should be presented based on a perpendicular view in the other one.

The mathematical process, which has to be respected in order to carry out the differential rectification of an image, could be described as following (Luhmann, 2003, pp. 317-319):

- Determination of the rectangular area of the object to be converted. In this context, the low left point (X_1, Y_1) and the upper right point (X_2, Y_2) of the interested area - local object coordinate system - should be taken into the account (Figure 6.4).

- An image rectification needs a scale number m_r of the orthophoto intended as well as a determination of an interval between rectified image points. This interval is defined as a density of image points resulted and described by two components Δx_r and Δy_r.

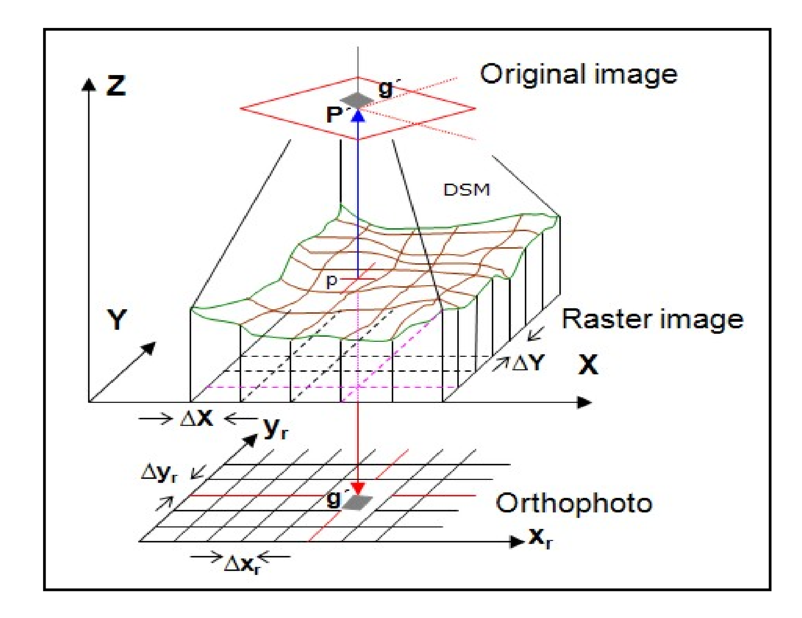

Figure (6.4): Principle of an orthophoto creation (source: Luhmann, 2003)

- Generation of a raster image associated with object coordinate system. In this raster image, the whole object area will be projected with respect to the raster image size. Particularly, the cell size of the raster image is given:

$$\Delta X = m_r \cdot \Delta x_r \tag{6.4.a}$$
$$\Delta Y = m_r \cdot \Delta y_r \tag{6.4.b}$$

- Integration of Z_i - value for each point (X_i, Y_i) of the abovementioned raster image. Height values will be calculated based on a DEM associated with; in this case an interpolation process should be performed.

- In the original image (non - rectified), image point coordinates (x'_i, y'_i) corresponding to the object point (X_i, Y_i, Z_i) can be computed based on the equation (3.16) with respect that the camera parameters (the interior and exterior parameters) are known. They are given as following:

$$x'_i = F(X_0, Y_0, Z_0, x'_0, c_k, \omega, \varphi, \kappa, \Delta x', X_i, Y_i, Z_i) \tag{6.5.a}$$
$$y'_i = F(X_0, Y_0, Z_0, y'_0, c_k, \omega, \varphi, \kappa, \Delta y', X_i, Y_i, Z_i) \tag{6.5.b}$$

- A New gray value related to the image point (x'_i, y'_i) will be calculated. In this context, an interpolation method should be taken into the consideration. In Baalbek’s orthophotos creation the method “*Bilinear Interpolation*” was used because it gives a well qualitative rectification of an image (Luhmann, 2003, pp. 397-398). By this method the requested gray value of a pixel is computed depending on its four nearest neighbours (Figure 6.5). Thus, based on the gray values g_1, g_2, g_3 and g_4 the new one (g') can be expressed as following (Pum, 2003 & Luhmann, 2003, pp. 397-398):

$$g' = g_1 + dx \cdot (g_2 - g_1) + dy \cdot (g_3 - g_1) + dx \cdot dy \cdot (g_4 - g_2 - g_3 + g_1) \tag{6.6}$$

- The resulted gray value will be saved in the position $(x_r, y_r)_i$ - in the orthophoto - which corresponds to the other one, namely the position (x'_i, y'_i), in the original image.

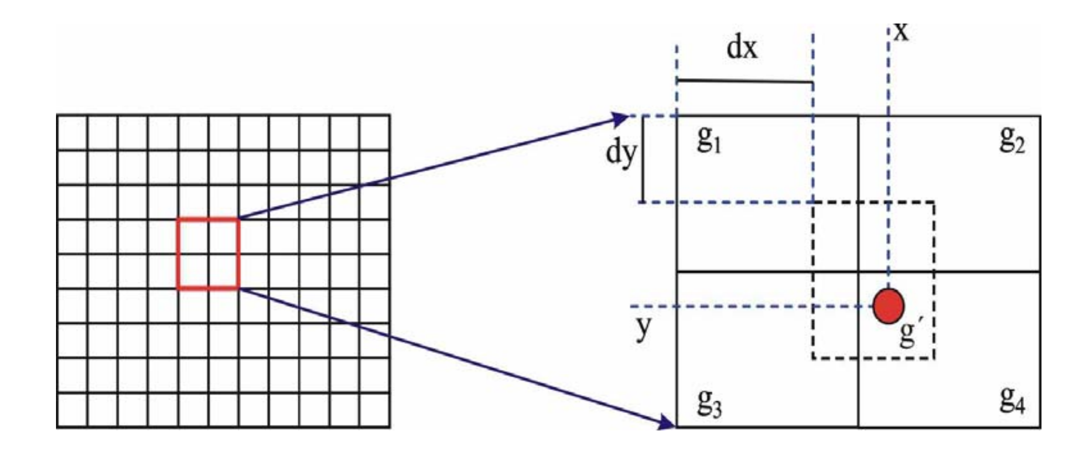

Figure (6.5): Principle of the method “*Bilinear Interpolation*” used in the rectification process of Baalbek’s photos

Appearance of black areas resulted in orthophotos indicate that some object parts are hidden in original images but included in DEM/DTM. In contrast, objects included in original images and not presented in DEM/DTM will be displaced and distorted in orthophotos. To overcome this challenge multiple images related to the same area studied should be implemented. In this way, different sights of objects can be available which enable to detect hidden objects.

6.3.3. Baalbek’s orthophotos

Baalbek data acquired based on intended orthophotos is considered an important data base required for a geometric reconstruction of the historic Baalbek. Although that the object reconstruction using a single rectified image - in some cases - is possible, but it is restricted to the geometric data which should be already available and associated with the object to be reconstructed (Kraus, 2003). In this context, a creation of multiple orthophotos can solve this problem because an existing of multiple rectified images supports more data (e.g. geometric data) requested for the object reconstruction. Therefore, multiple orthophotos of the historic Baalbek should be generated, which enable to perform a best reconstruction of this city.

With respect that interior and exterior orientation parameters of Baalbek’s vertical images are known (Chapter 3.2.3 & 5.2), seven orthophotos of Baalbek have been generated[1]. These images cover the whole studied area of Baalbek and have the cell size of ca. $0.13\,m$ for coordinates X and Y (see: orthophoto-parameters, App. O). Two vertical images of Baalbek and their orthophotos are depicted in the Figure (6.6).

[1] The main tool used is *LPS Project-Manager*

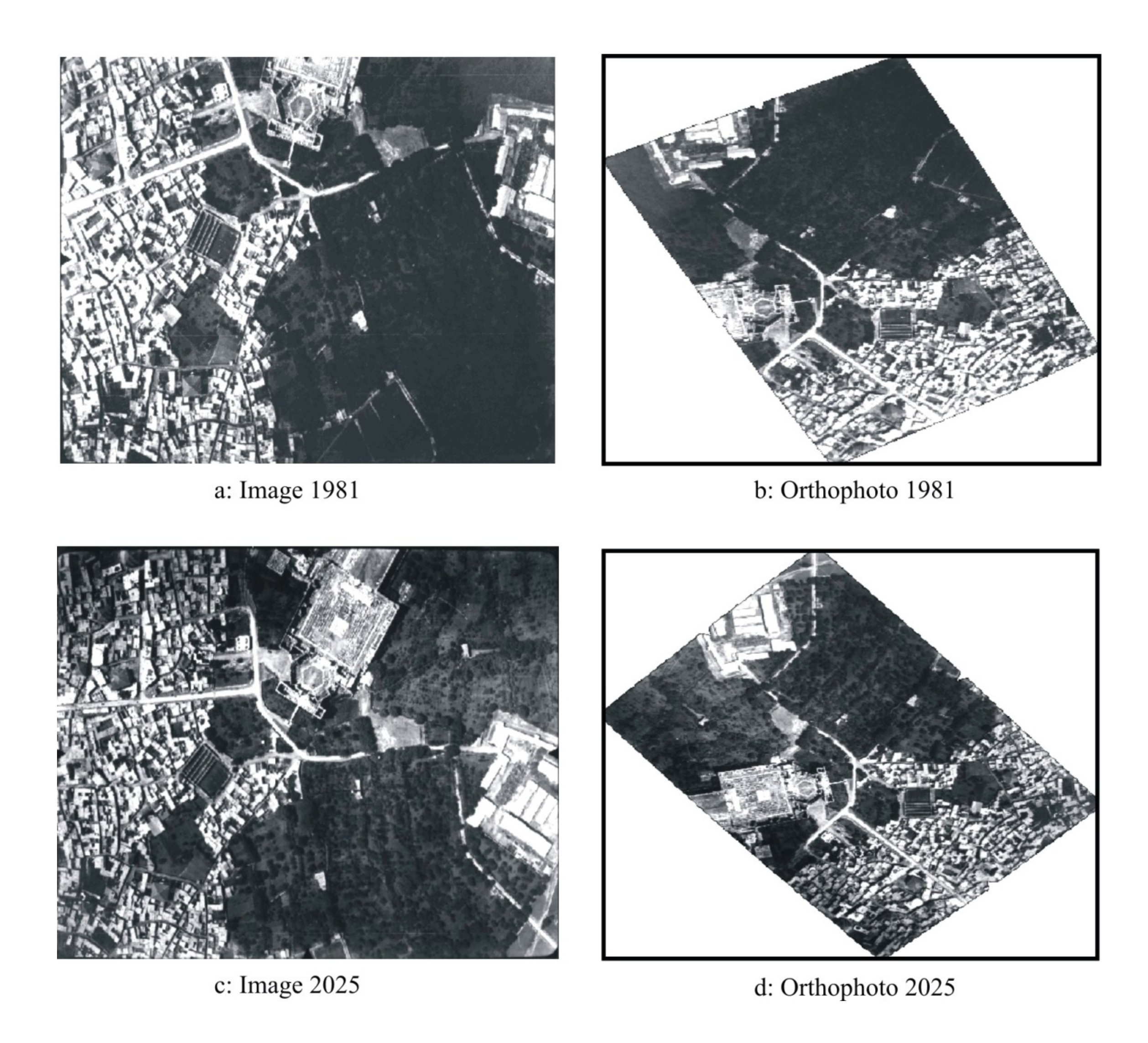

Figure (6.6): An illustration of two original vertical images of Baalbek and the orthophotos associated with; (a: image 1981, b: orthophoto 1981, c: image 2025 and d: orthophoto 2025)

6.4. Quality of Baalbek's orthophotos

According to (Kraus, 2003), the quality of the differential rectification could be discussed based on the following aspects:

- Input data (e.g. image resolution, accuracy of control points applied, etc.).
- Image distortion (radial and decentring distortion parameters).
- The approximation of the surface curvature in the DTM grid.
- Interior and exterior orientation parameters, etc.

Particularly, an important criterion concerning the orthophoto quality is the *position error* Δr in the orthophoto (Figure 6.7), which is given based on the *position error* ΔR in the reality as following:

$$\Delta r = \frac{1}{m_0} \cdot \Delta R = \frac{1}{m_0} \cdot \frac{\Delta Z}{\frac{c_k}{r} + \ tan\alpha \cdot cos\beta} \tag{6.7}$$

where:

m_0…image scale number (in our case, it was applied 4000)
c_k… camera focal length ($\sim 200\ mm$)
r … the distance in orthophoto between the both footprints for object point P_i and nadir point
α … the angle of terrain slope
β … the horizontal angle between the line of largest slope of the optic axis passing through P_i
ΔZ…height error; which is defined as a treble of the precision related to contour lines. It could be expressed as following:

$$\Delta Z = 3(0.00015h) \tag{6.8}$$

Variances of the *position error* Δr based on different image radiuses were calculated; with respect that the flying height $h = 800\ m$ (Chapter 3.2.1.2), the terrain curvature is $tan\ \alpha = 10\%$ as well as $\beta = 50$ gon. The maximum *position error* Δr_{max} is ca. of $(0.041)\ mm$, which leads to the maximum displacement - in the reality - of ca. $17\ cm$ (see Table 6.1).

$\boldsymbol{r}\ (\boldsymbol{mm})$	$\boldsymbol{\Delta R}\ (\boldsymbol{m})$	$\boldsymbol{\Delta r}\ (\boldsymbol{mm})$
55	0.097	0.024
60	0.106	0.026
65	0.114	0.029
70	0.123	0.031
75	0.132	0.033
80	0.140	0.035
85	0.149	0.037
90	0.157	0.039
95 (*max*)	0.165 (*max*)	0.041 (*max*)

Table (6.1): Variances of *position error* Δr in orthophotos based on different image radiuses (with respect to the image size)

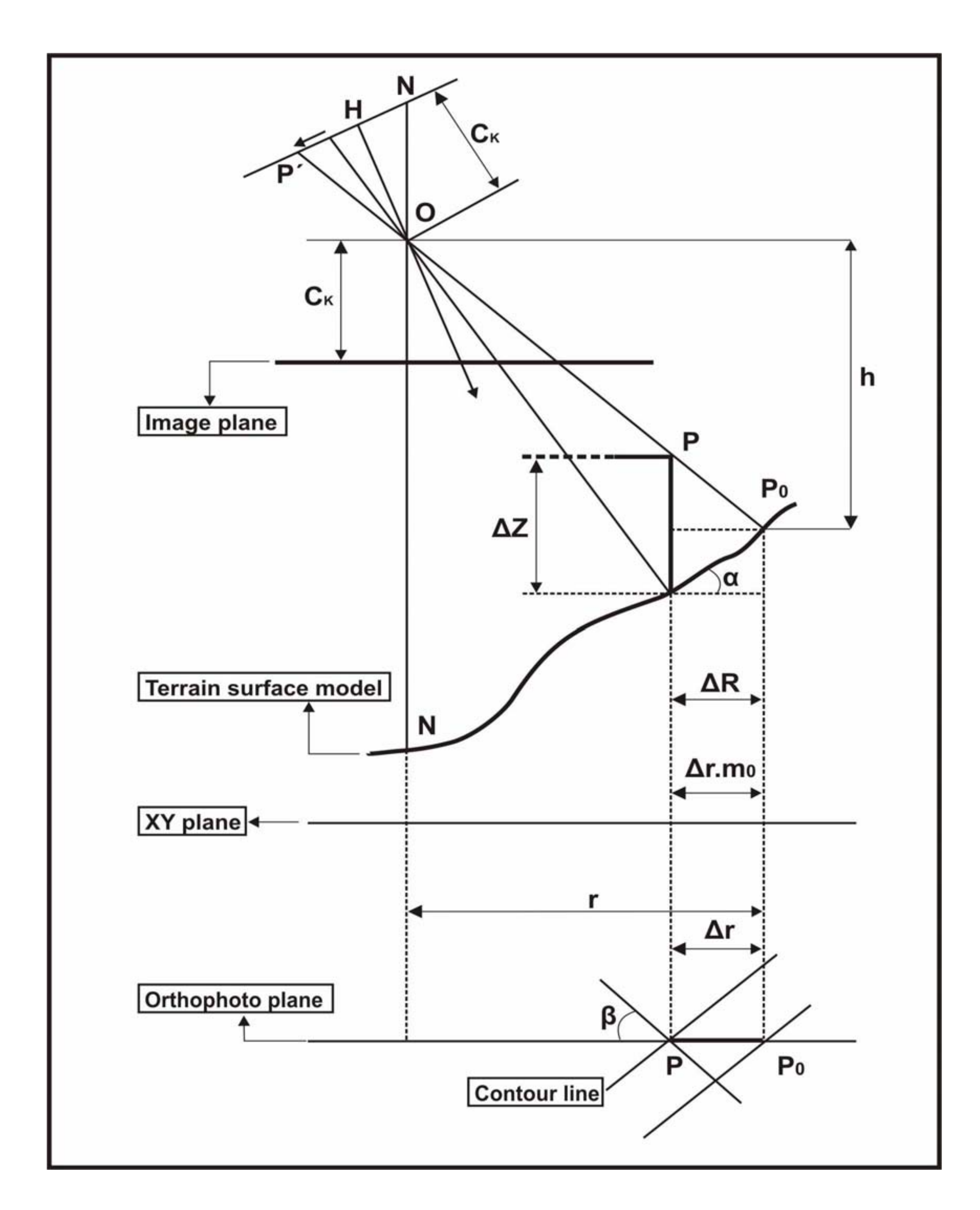

Figure (6.7): Illustration of the *position error* Δr - in the orthophoto - of an object point P with respect to different parameters; for e.g. the terrain model slope, camera focal length, image scale number, etc. (source: Kraus, 2003)

6.5. Region mosaic creation

The term ***mosaic*** can be defined as "the montage process of multiple rectified images (multi-orthophotos) in order to merge them in uniform image" (Wiedemann, 2004). In this context; the geometric and radiometric adjustments of orthophotos have to be taken into the account because they have an impact on the merge process.

The main challenge arising through a generation of the mentioned uniform image (mosaic) of Baalbek's region is the creation of cut lines between the orthophotos used. In general, the performance of cut lines depends on the overlapping between the rectified images. Non-planar objects in orthophotos as well as the image noise lead to challenges through the overlapping between the historical images (e.g. objects matching and recognition will not be an easy task, etc.). A digitizing approach (semi-automatic) has been enforced to define cut lines - as possible - in an optimal way. An illustration of adjusted cut lines is shown in the Fig. (6.8). In addition, radiometric failures such as: noise, contrast, brightness, etc. were adjusted using the histogram matching approach. The principle of this approach is to define an image as a muster which is used to adjust gray values associated with other orthophotos used to generate the mosaic intended. In this context, gray values matching of Baalbek's orthophotos has been achieved with respect that the (orthophoto - 1985) was applied as a muster image.

Consequently, the seven orthophotos of Baalbek (Chapter 6.3.3) have been merged together and a uniform raster image has been generated successfully (Figure 6.9). Baalbek mosaic created will be considered a main source to extract 2D geometry of the historical Baalbek.

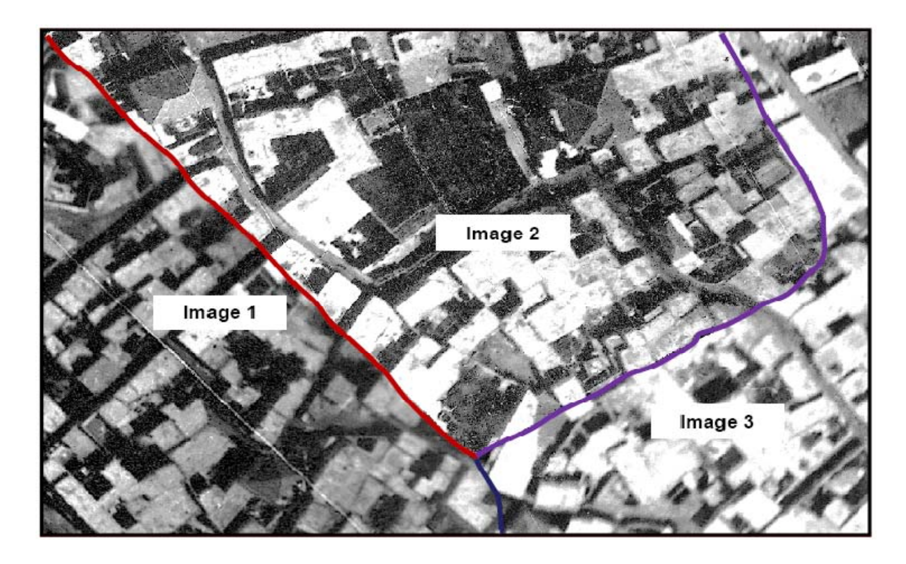

Figure (6.8): A section of three cut lines created between 3 orthophotos of Baalbek

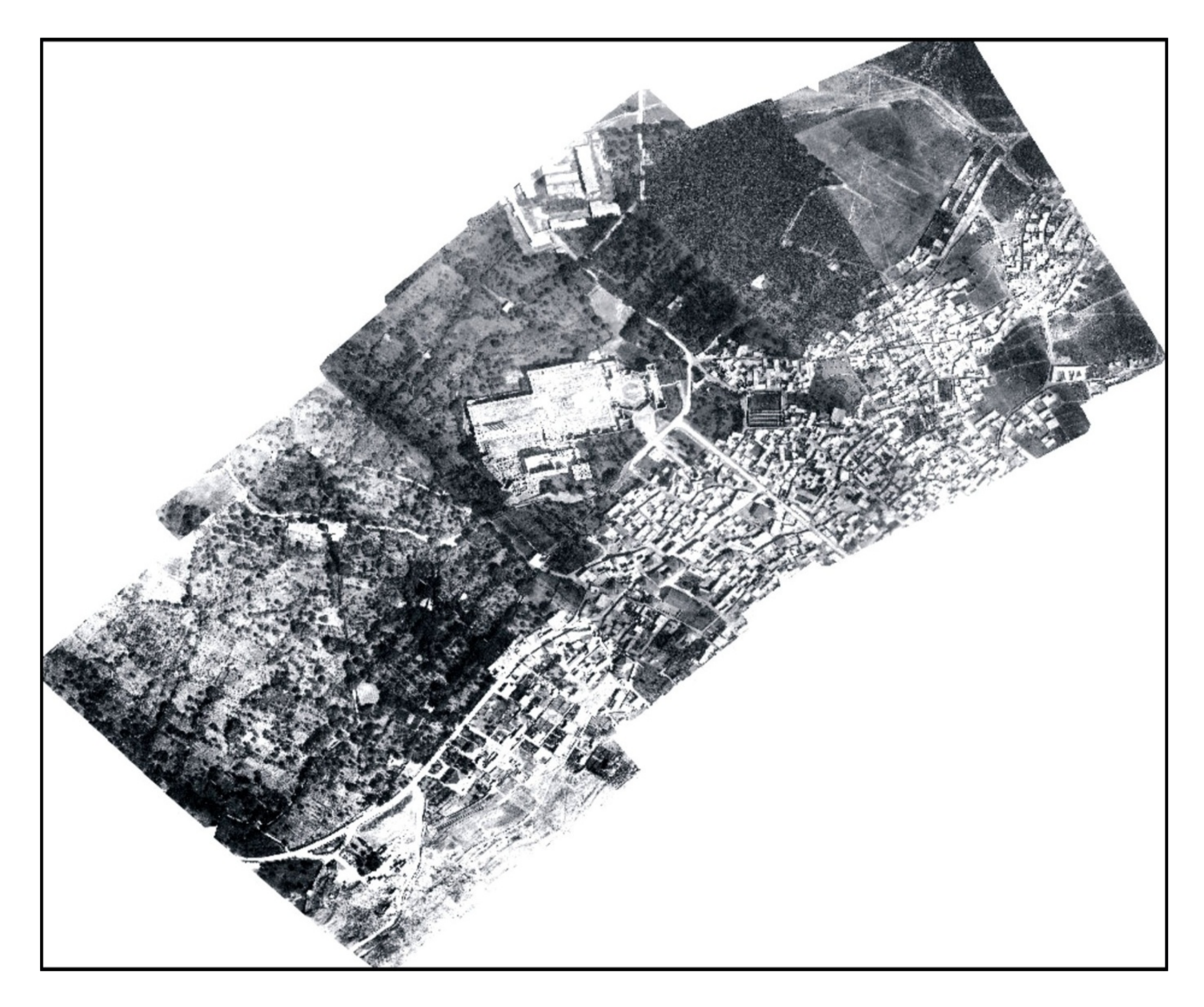

Figure (6.9): Baalbek mosaic created based on the seven orthophotos which covers the whole area of interest; main temples of Baalbek: Jupiter, Bacchus and Venus are included

6.6. Extraction of spatial data

6.6.1. Extraction of 2D objects

Baalbek’s orthophotos are considered the main planimetrical source to extract 2D coordinates of requested objects. Basically, the recognition of objects included in Baalbek’s orthophotos was the main challenge through the feature acquisition process due to the high noise and contrast of Baalbek’s images. Therefore, it was difficult to use a full-automatic process for recognition and detection of objects shown in Baalbek’s mosaic.

In addition, the rectification of an image is partly geometrically inaccurate and/or incomplete (for e.g. buildings or part of buildings are distorted from their true position as they are not modelled in the DTM used). To avoid this problem, it is possible to generate a true orthophoto by using Digital Surface Model (DSM) and considering occluded areas. In this context, it is

difficult to generate true orthophotos of historic Baalbek, because it is difficult to have a DSM describing the entities included in Baalbek's historical images; where most of these entities had been nowadays destroyed. Therefore, only orthophotos have been generated.

Most of the objects included in Baalbek's orthophotos are buildings; therefore it will be more accessible to extract the buildings (also some streets, routes) through polygon or multiple polygons consisting - in this case - at least from four vertices (cf. Figure 6.10). Extracted polygons have been saved as vector data which can be directly used for further applications without conversion into other data-formats. In this context, each vector layer has different attributes such as: area and perimeter of a polygon. Non-building objects (e.g. trees, vegetation, etc.) have been acquired as discrete points.

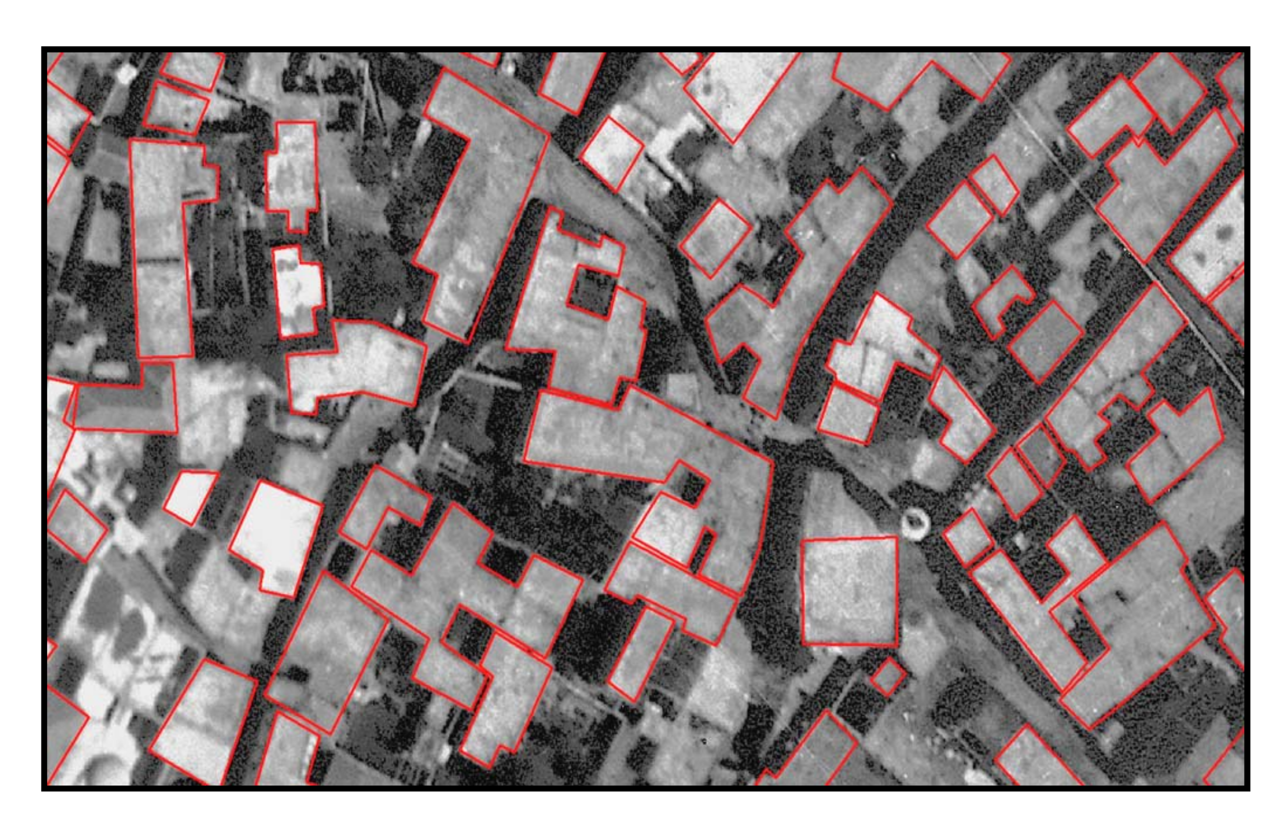

Figure (6.10): 2D building data extracted as polygons (red lines); due to the noise and contrast of Baalbek's images different buildings or parts of buildings were aggregated together

6.6.2. Integration of height values

For each 2D extracted point there is a height value (Z) associated with which is given as a function of the 2D position. Since 2D extracted objects are polygons, it was assumed that each polygon will have the average height value calculated based on height values of polygon vertices:

$$\bar{Z}_i = \frac{\sum Z_k}{n} \quad (6.9)$$

where:

$\bar{Z}_i$: average height

Z_k: height values referred to polygon vertices

$i = 1, 2 \ldots m$ (m: number of created polygons), $k = 1, 2 \ldots, n$ (n: number of polygon vertices)

The calculation of height values of polygon vertices is carried out using two strategies. The first is the method of stereo analysis which enables to obtain the height values using Digital Stereo Model based on different pairs of oriented vertical images. The second one is based on the oriented model of Baalbek's historical oblique and terrestrial photos.

6.6.2.1. Height values determination based on stereo analysis

3D stereo view can be created using at least two overlapping oriented aerial images. In general case, the two images (namely, the two cameras used) are not perpendicular to the stereo basis line. The principle of stereo analysis is based on the correlation of homologous (corresponding) points shown in both left and right images. Stereo analysis method allows for the rotation and scaling of overlapping images for a best creation of Digital Stereo Model which is a useful tool for many applications (e.g. land use, land cover, GIS, etc.).

Once the oriented the Digital Stereo Model has been created, the calculation process of height value of an object point can be expressed as following (Luhmann, 2003, pp. 320-326):

- *with respect to left image:*

  $$\mathrm{Z} = \mathrm{Z}_{left} = Z_{0\,left} + m_b \cdot (Z' - Z_0)_{left} \quad (6.10.a)$$

  where:

  $Z_{0\,left}$: the height value of projection center of left image

  Z'_{left}: Z-coordinate of an image point in object system (left image)

- *in an analogue way for the right image:*

$$Z = Z_{right} = Z_{0\,right} + m_b \cdot (Z' - Z_0)_{right} \tag{6.10.b}$$

$Z_{0\,right}$: the height value of projection center of right image

Z'_{right} : Z-coordinate of an image point in object system (right image)

Based on Baalbek's Digital Stereo Model[1] and on the equations[2] (6.10.a) or (6.10.b) the height values of polygons' vertices can be determined. An illustration of Baalbek's Digital Stereo Model and a polygon generated based on four vertices is shown in the Figure (6.11).

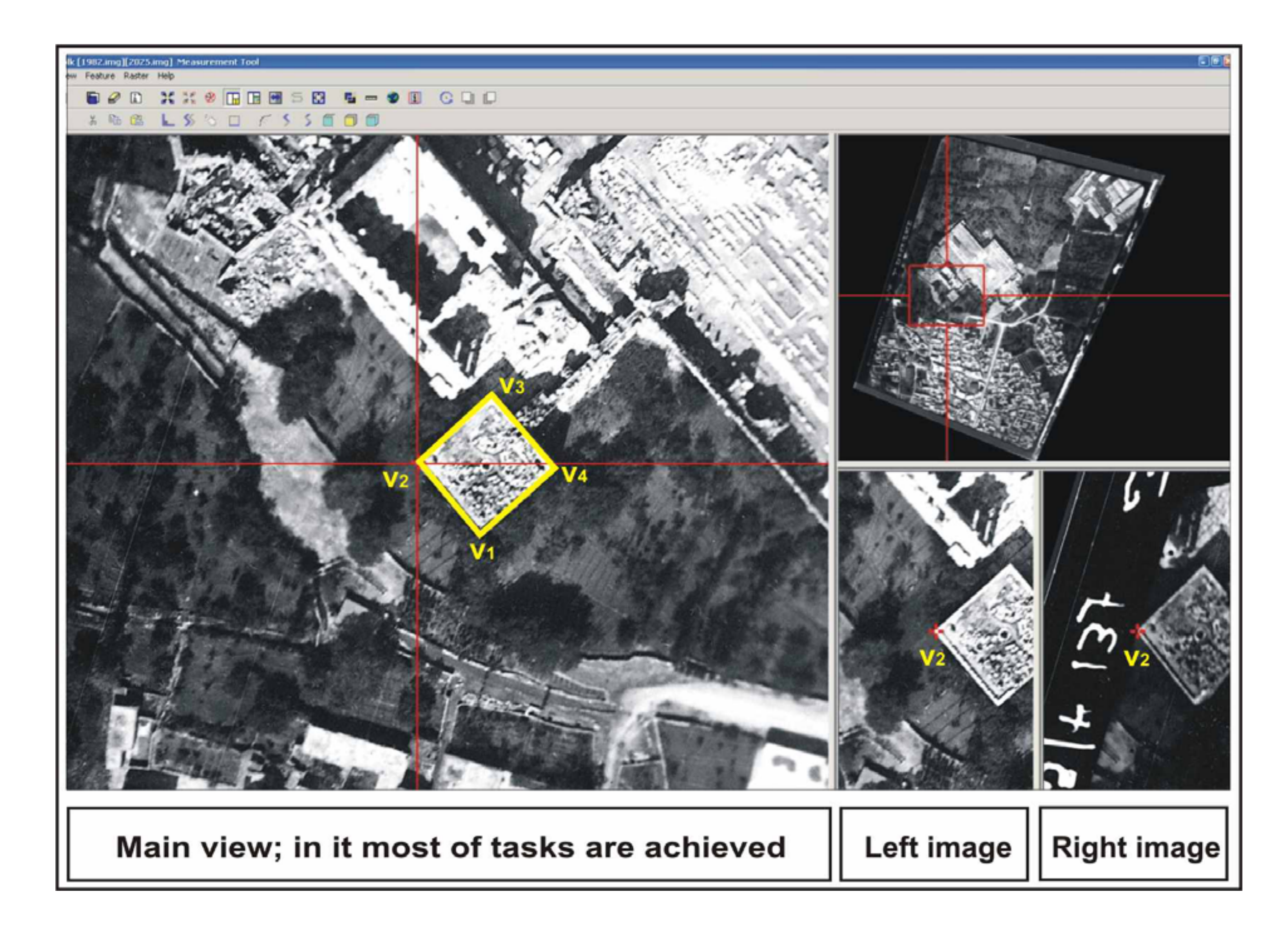

Figure (6.11): Baalbek's Digital Stereo Model including a polygon created in the main view (yellow line) based on the four vertices (v_1, v_2, v_3 and v_4). Both left and right views show the vertex v_2 whose height was in the calculation process. The main tool used, in this step, to create the Digital Stereo Model of Baalbek is "Stereo Analyst - Erdas Imagine, Leica Geosystems, 2005".

[1] Basically, 3D coordinates of object points can be calculated using Digital Stereo Model
[2] Both equations are derived based on the collinearity equations

Due to the poor properties of Baalbek's images it was difficult to determine exactly a point position in the selected image pair. This led approximately to a point displacement which affects the determination of height values where each height value is given as a function of the 2D point position (Chapter 6.6.2).

6.6.2.2. Height determination using oriented oblique and terrestrial images

The main principle in this step is also creation of a stereo model based on Baalbek's oriented oblique and terrestrial photos. The Figure (6.12) shows the geometry of stereo model based on a pair of images which are - in this case - oblique or terrestrial. The Epipolar plane ($PO'O''$) intersects the planes of the left and right images at the Epipolar lines E' and E'', respectively.

With respect that the given location of the object point P at the left image is P', the homologue of P at the right one is P'' which will lie along the Epipolar line E''. "Any search procedure to locate P'' as a probable match of P' can be confined to the Epipolar line E''; in practice, due to none of values used to derive the line equation is exact, the search takes place along a narrow band centred on this line" (Cooper & Robson, 2001).

Starting from the coordinates of the image points P' and P'' and depending on the equations (6.10.a) and (6.10.b), the related height value can be determined.

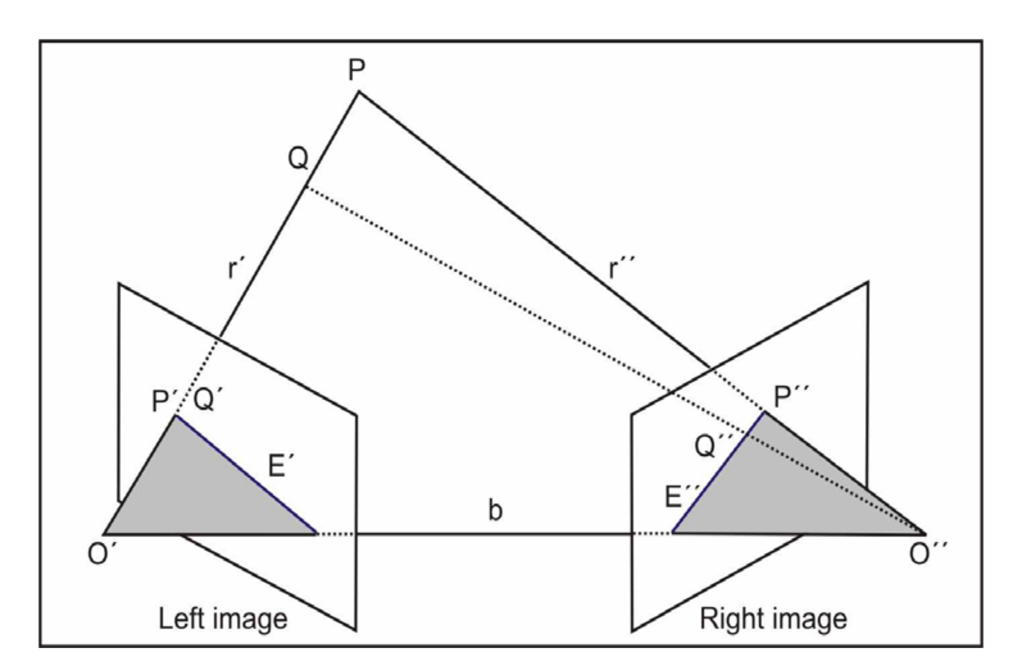

Figure (6.12): A geometry of stereo model based on two images (left and right images), which includes Epipolar lines as well as Epipolar Plane

Basically, height values calculated using the abovementioned strategies are absolute values because they are determined according to the local coordinates system of Baalbek. In this context, these values do not give for e.g. the real height value of a building or wall, etc., therefore it is essential to identify the heights relatively to other landmarks (e.g. the ground).

To explain this identification, let for e.g. two object points (P_1 and P_2) of a wall be regarded, which have the absolute heights H_1 and H_2, respectively (Figure 6.13). However, the real height of the wall determined by both points is given by height difference:

$$\Delta h = H_2 - H_1 \tag{6.11}$$

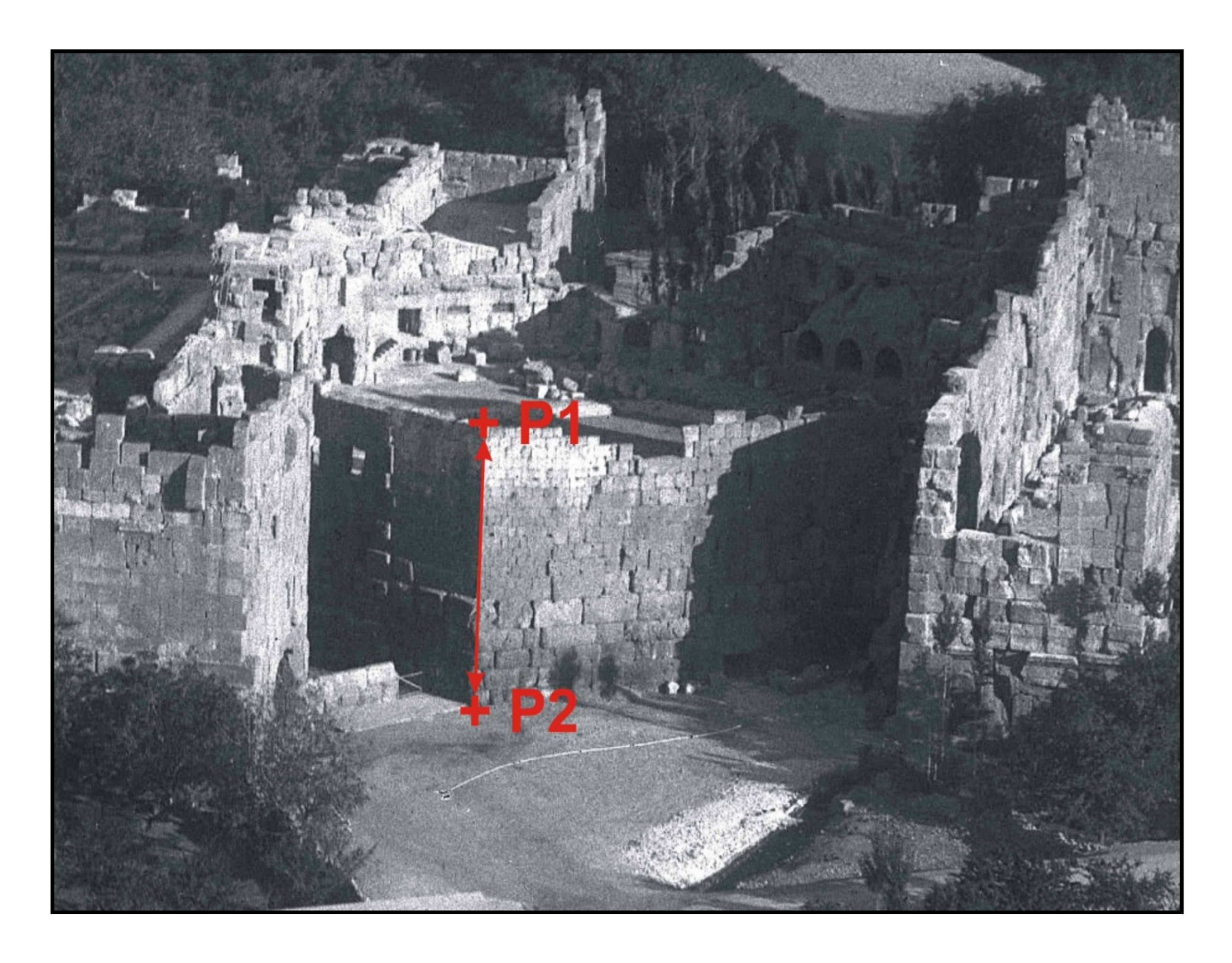

Figure (6.13): A view of the wall of Hexagonal court in Baalbek's sanctuaries; the wall height is determined based on the points $P_1$and P_2

6.7. Classification of applicable 3D object points

3D geometric object reconstruction depends mainly on 3D applicable points associated with. This means the more quality (spatial accuracy) of 3D applicable points the more optimal performance of 3D object reconstruction. Therefore, 3D object points - applied into the object reconstruction process - should be verified and then classified according to certain quality characteristics in order to know to which extent they are accurate!

In that context, 3D applicable object points extracted based on Baalbek's historical images will be classified according to their spatial accuracy in order to know in which photo an object point could be best recorded. This classification enables to create a best process of 3D object reconstruction.

The classification of 3D extracted object points consists of the following steps:

- *In which photo or photos an interested object point is shown?*

This step reveals in which image/images the interested point is shown where the more images including that point lead to more possibilities to observe and measure this point. In addition, existing of different image types of Baalbek (vertical, oblique and terrestrial) including this point enables also to more accessibility in the observation and measurement of object points. This embodies, however, the process of 3D object reconstruction based on the combination of different image types. Probable possibilities of existing of an object point in Baalbek's historical image types are presented in the Figure (6.14).

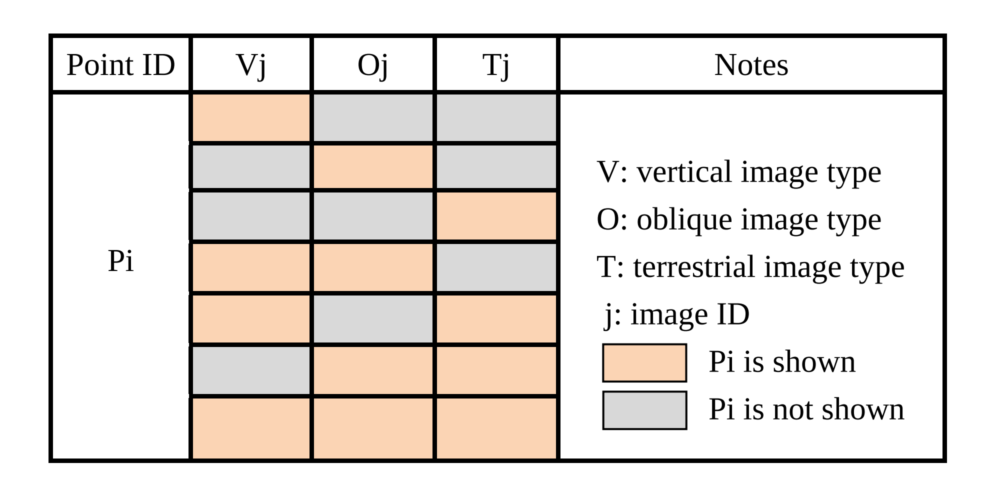

Figure (6.14): Probable possibilities of an object point's existing in Baalbek's historical images. Based on the image types there are 12 possibilities, e.g. in the 1st one: the point P_i is only shown in the vertical image type (in all cases image ID should be respected)

- *General Estimated Standard Deviation* (GESD):

Let be regarded that an object point P_i has the coordinates (X_i, Y_i, Z_i) as well as the estimated standard deviations referred to those coordinates are S_{X_i} , S_{Y_i} and S_{Z_i}, respectively. These standard deviations can be determined based on the cofactormatrix of adjusted observations (Chapter 2.3.4). The term (GESD) can be defined as following:

$$\mathrm{GESD}_i = S_i = \sqrt{S_{X_i}^2 + S_{Y_i}^2 + S_{Z_i}^2} \qquad (6.12)$$

where $i = 1, 2 \ldots n; n$ number of applicable points

The image index (ID) as well as the image type (in this context: V = vertical, O = oblique and T= terrestrial) should be taken into the account. Therefore, the formula (6.12) can be given:

$$S_{i(kj)} = \sqrt{S_{X_i}^2 + S_{Y_i}^2 + S_{Z_i}^2} \qquad (6.13)$$

where (j) the image ID and (k) image type

- *Determination of* $(\mathrm{GESD})_{\mathrm{min}}$

It was above pointed that starting from existing of an object point P_i in an image (cf. Fig. 6.14) the GESD associated with could be determined according to the equation (6.13). Following assumptions therefore could be discussed (Figure 6.15):

- Assumption (I): if the interested object point is shown in the vertical image V_j; that means there is GESD = $S_{i(\mathrm{V}j)}$ associated with.
- Assumption (II): if the interested object point is shown in the oblique image O_j; that means there is GESD = $S_{i(\mathrm{O}j)}$ associated with.
- Assumption (III): if the interested object point is shown in the terrestrial image T_j; that means there is GESD = $S_{i(\mathrm{T}j)}$ associated with.

Based on the comparison between the values $S_{i(\mathrm{V}j)}, S_{i(\mathrm{O}j)}$ and $S_{i(\mathrm{T}j)}$ the minimum one can be determined, and therefore, it could be accepted that the studied point could be optimally shown and recorded in the image which has the ID = j and the type (k).

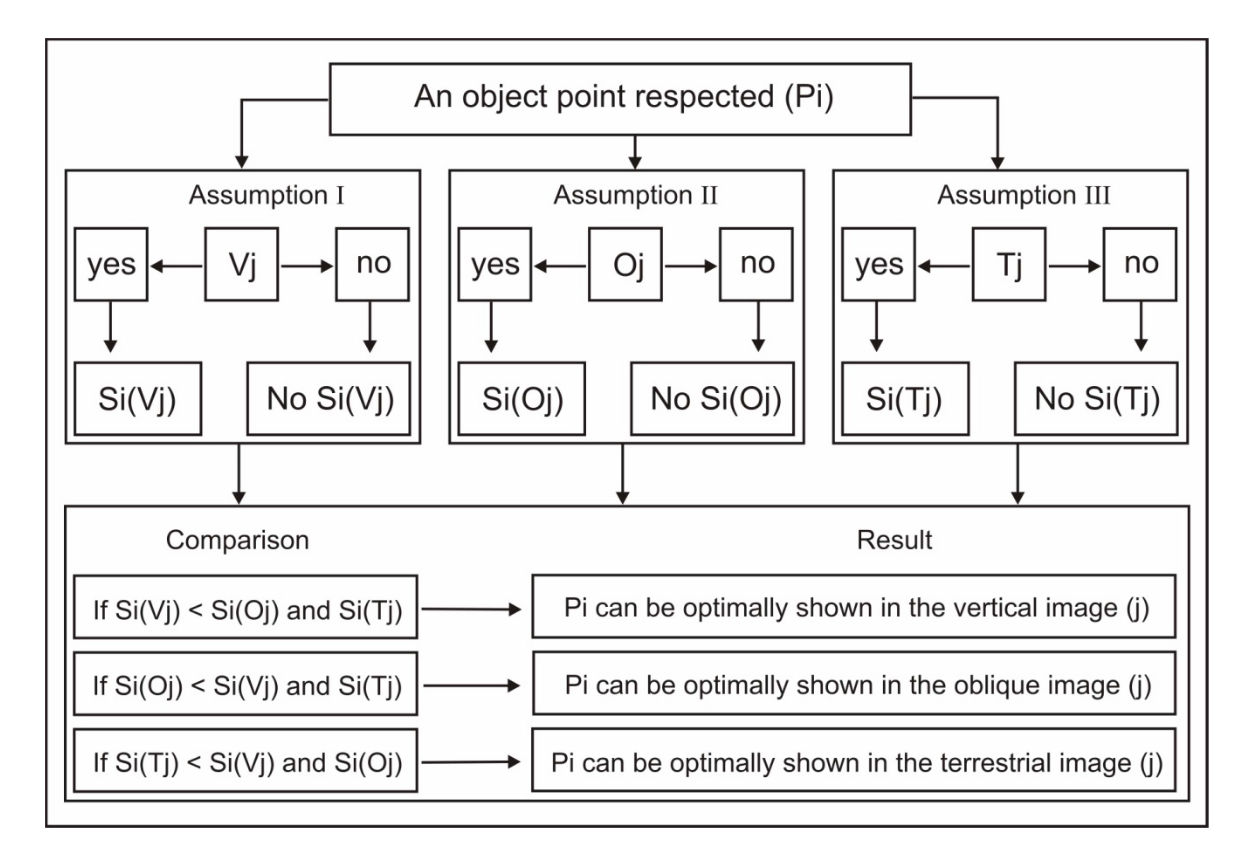

Figure (6.15): The mechanism used to determine the minimum value of GESD associated with an object point. It consists of two levels; the first is calculation of (GESD) related to an interested object point. Second one is the comparison process between the values of GESDs to determine the minimum one which reveals in which image (and type of this image) that point can be visible and recorded optimally.

Baalbek's 3D data extracted based on the oriented historical photos will be considered the main input data for 3D CityGML modelling which supports different Levels of Detail (LODs) by them we can represent different data sets.

The selection of LODs depends mainly on the quality check of the data sets available. This check could be carried out with respect to different quality parameters (e.g. geometry, semantic, etc.). These qualiy characteristics, the quality check (geometric and semantic) of Baalbek's acquired data and finally the LOD selection for Baalbek's 3D city model will be discussed in the following section.

7. Baalbek's 3D data and CityGML modelling

The modelling of 3D data collected based on the oriented historical images of Baalbek is considered an essential task in this research, because it enables to give a digital representation about historic Baalbek and its entities as well as to document the historic city and its remains as they looked like. In the context of a city modelling, standards of *CityGML (City Geography Markup Language) will be implemented. In addition, it will be proved to what extent CityGML-based modelling can be considered as an accessible standard used for cultural heritage sites documentation.*

CityGML is defined as an open data model used for representation and exchange of virtual 3D city models. It is an international standard for the semantic and geometric representation of 3D city and landscape models (Kolbe, 2009). The modelling based on CityGML supports different four aspects of virtual 3D city model: semantic, geometry, topology and appearance. In this context, objects of reality can be represented in up to five well defined Levels of Detail (LODs are from LOD0 to LOD4, see Kolbe, 2009). Those 5 LODs were based on previous work related to different research groups on the usage of levels of detail in the 3D city modelling (Köninger & Bartel, 1998, Coors & Flick, 1998, Schilcher et. al., 1999).

The coarsest level LOD0 is essentially a 2.5D DTM (cf. Fig. 7.1, a). In contrast, the LOD1 is the well-known blocks model of the buildings with flat roofs structures. In this LOD, the geometry of a building is represented a prismatic object with a flat top (Fig. 7.1, b). In other words: geometry of a building can be either represented with *gml:SolidType* as a volumetric object or the exterior surface of the building is represented with *gml:MultiSurfaceType*. Buildings are represented in LOD1 in a simple form i.e., extensions to buildings such as balconies need to be disregarded when creating of the LOD1 model. In order to ensure a broad system support, CityGML is also restricted to non-curved geometries, as these often cannot be handled by GIS or spatial database management systems. Therefore, curved surfaces must be approximated by facetted surfaces of planar patches (Kolbe, 2009).

On one hand LOD2 has more details about the roofs' structures. In addition, exterior surfaces of a building can be represented in higher details (Fig. 7.1, c). In LOD2 outer walls of a building can be represented using multiple faces, but in LOD1 just only a single face for each wall. Furthermore, a building in LOD2 has distinctive roof structures and large building installations like balconies and stairs. In this context, these installations can be represented within the *BuildingInstallations* class as *gml:Geometry*.

On the other hand different parts of the outer façade of the building can be represented starting from LOD2 with different classes of CityGML. These classes are aggregated under *_BoundarySurface* class and therefore can be used to explicitly differentiate Roof Surfaces, Wall Surface, Ground Surface, and Closure Surface.

LOD3 of CityGML includes openings associated with the outer façade of the building such as windows and doors (cf. Fig. 7.1, d). Here, these openings are represented with *Door* and *Window* classes which are defined as sub-classes of the abstract class *Opening*. The class *Window* is used to represent the windows inside and the outer façade of the building. Similarly for the class *Door*, this is used to model the doors that are between the adjacent spaces and located at the outer façade of the building (Isikdag & Zlatanova, 2009).

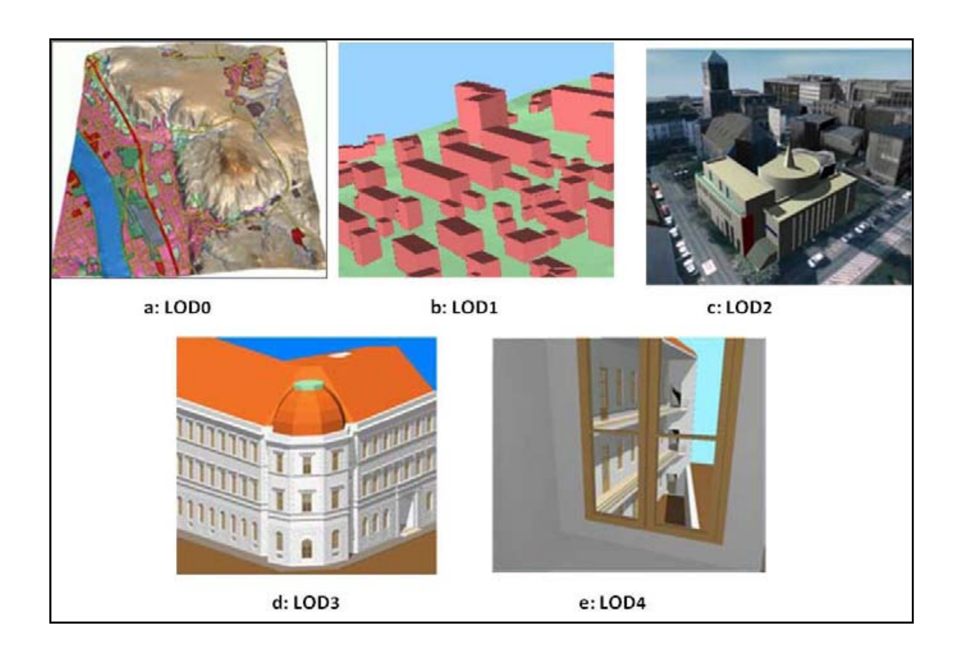

Figure (7.1): The five levels of detail (LODs) defined by CityGML. LODs of CityGML (LOD0 to LOD4) are depicted in a, b, c, d and e, respectively (source: Gröger et al., 2008)

The last LOD of CityGML is LOD4 which represents interior structures of objects. According to (Kolbe, 2009, Isikdag & Zlatanova, 2009) the main classes of CityGML used to realize the interior structure of a building are *Room* and *IntBuildingInstallation*. The class *Room* presents the semantic object for modelling of the space inside the building. It should be closed (using e.g. *ClosureSurface*) and can be represented (from geometrical view) by *gml:Solid*. In addition, semantic data related to the room can be preserved within the classes aggregated under *_BoundarySurface* class. They can be used to semantically differentiate the *CeilingSurface*, *InteriorWallSurface* and finally *FloorSurface* (Fig. 7.1, e).

LOD selection depends on the quality of data sets used. Geometric data quality has an indirect impact on the semantic quality, because the geometry affects the possible achievable CityGML LOD which determines also the semantic resolution. In the case that data to be used for CityGML modelling is based on photogrammetric evaluation, then image resolution (as input data set) will have a direct impact on the achievable semantic quality; where image resolution affects the determination and 3D reconstruction of separate objects like parts of building (e.g. balconies).

Consequently, and in the context of 3D modelling of the historic Baalbek, it will be determined in which LOD Baalbek's data could be modelled! In other words: the quality of Baalbek's data should be taken into account to know in which LOD this data could be represented.

In the CityGML-based modelling context, the data quality check can be carried out based on different parameters. These quality parameters for geodata can be categorized into six criteria as following (Guptill & Morrison, 1995, Joos, 1998 and Int03a, 2003):

- Positional accuracy (geometry check)
- Semantic accuracy
- Completeness
- Correctness
- Temporal conformance
- Logical consistency

In the study case of historic Baalbek, the geometric and semantic modelling in Baalbek's 3D city model is considered an important step for further applications (e.g. in archaeology). Therefore, the quality of Baalbek's data set will be discussed with respect to geometrical and semantic aspects.

However, with respect to CityGML point of view, an approach for the geometrical evaluation of Baalbek's data will be introduced to decide which LOD can be used. In addition, the quality of semantic modelling of Baalbek's data will checked whereas the geometry quality doesn't support and reflect all information requested about the data quality assessment i.e., the object's geometry isn't the only the quality concern.

7.1. Quality model of spatial data

To express the quality parameters in detail, the following terms should be defined:

- *Conceptual Reality* (*CR*): according to (DEU, 1998), the conceptual reality is the user's understanding of the real world (user's idea about the real world). In practice, it may be a part of the real world which is to be modelled. If there are e.g. 30 buildings as well as 20 streets in real world, due to user's requirements only 26 buildings and 15 streets could be presented (Fig. 7.2, a). This means that (*CR*) can be defined as a sub-data set of real world.
- *Digital Data Modelling* (*DDM*): it describes a digital data set of elements included in (*CR*) that means it is the digital presentation of *CR*'s objects. Theoretically, each element in the (*CR*) should be coupled with a corresponding element in (*DDM*); but due to errors (for e.g. object misclassification, object recognition and extraction) during the digital presentation process, there are missing objects in the (*DDM*). The Figure (7.2, b) shows that there are four buildings as well as four streets - in the (*CR*) - which do not have a digital presentation in the (*DDM*).

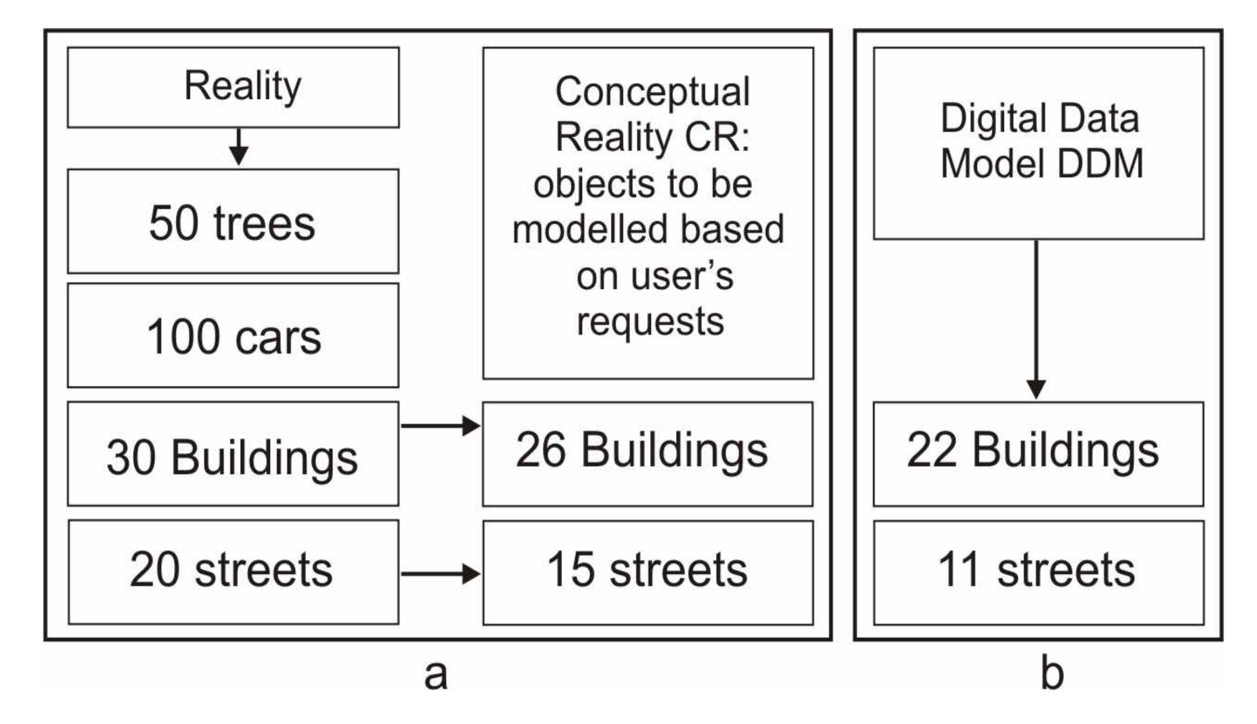

Figure (7.2): Differences between reality, conceptual reality (a) and the digital data model (b)

According to (Guptill & Morrison, 1995, Joos, 1998 and Int03a, 2003) the quality parameters can be categorized into six characteristics:

1. *Positional accuracy (geometry)*:

It is the geometrical check of all objects included in (*CR*) and (*DDM*). In practice, absolute positional accuracy is often separated in two parts: horizontal and vertical. The first one is related to the determination of errors in X/Y directions. In contrast, the vertical accuracy reveals errors of object's height.

2. *Semantic accuracy*:

It means that in both (*CR*) and (*DDM*) all object classifications should be correct and all attributes associated with the objects should have valid values. Thus, an interested object should be geometrically classified in a correct class (e.g. building) which should be identical in the (*CR*) and (*DDM*). Furthermore, in the context of semantic accuracy each attribute related to that building (e.g. the attribute: building type) should have the correct value.

In addition, it is not sufficient to check the geometry and semantic issues of a 3D city model on their own due to the *in between coherence*. "Semantic information can help to reduce the ambiguities for geometric integration, if it is coherently structured with respect to geometry. The 'spatio - semantic' coherence presents the relationships of spatial and semantic entities. This coherence denotes the quality or the state of cohering, namely a logical, orderly and aesthetically consistent relationship of objects" (Stadler & Kolbe, 2007).

However, six categories referred to the abovementioned coherence of 3D city models can be defined with respect to their semantic and spatial complexity (Stadler & Kolbe, 2007):

- Only geometry, no semantics: this class comprises just geometry based on 3D graphics formats like VRML, X3D, or legacy CAD geometry formats and there is no semantic information referred to geometric objects. These 3D models include a more or less structured geometry, often organized in scene graphics (Foley et al., 1995).
- Only semantics, no geometry: this category describes a case in which it is known, that specific geospatial features of known types are included in the 3D city model, but where geometry is unknown or not available. Those types of data may be derived from economic or accounting data where the geometry, in that case, is not essential to be known (see Fischer et al., 1998, Brenner, 2003).
- Simple objects with unstructured geometry: here, objects are represented by geographic features. Each one has a spatial attribute consisting of an unstructured collection of 3D

surfaces and possibly a number of scalar, non-spatial attributes. This model has to be rated highly coherent, if the morphology described by the geometry is simple, and minor coherent if the unstructured geometry describes a complex shape.

- Simple objects with structured geometry: In this case, geometry is not only detailed but also structured with respect to spatial decomposition. When it comes to semantics, no more than existence of a building is indicated. In this context, the relations can not be established between sub-geometries and the missing semantic components resulting in a low degree of coherence (cf. Gülch and Müller, 2001, Marshall et al., 2001).
- Complex objects with unstructured geometry: within this class, semantics are detailed. Since geometry is detailed, yet unstructured, relations between semantics and geometry cannot be established on different aggregation levels. Therefore, coherence is given only to the degree that it is known that the aggregated building object in total is spatially represented by a set of 3D surfaces (Foley et al., 1995).
- Complex objects with structured geometry: this category deals with the case that both geometry and semantics are given as a complex aggregation. Here, however, if all semantic components correlate to geometric ones on the same level of the hierarchy, then full coherence of the structure will be attained (Fischer et al., 1998; Brenner, 2003).

3. *Completeness*:

By the extraction process of objects existing in reality (as start point), different acquisition rules (e.g. text-based explanations for human understanding of the reality) should be taken into consideration, because they allow defining an extraction order, with it users/operators know exactly what and how it should be done to extract an object in a best possible way (cf. Figure 7.3). So, in other words, these rules should be defined and applied for all objects of Conceptual Reality (*CR*). Once, each user/operator can generate a 3D city model in different LODs based on own *CR* extracted.

The question could be posed: to what extent the conceptual reality correlates with the extracted 3D city model associated with; namely: to what extent the dual structure between both domains (*CR* and generated city model) is complete. In this context, the term completeness can be defined as a description of the relations between the virtual data set and 3D city models. These relations describe the abovementioned dual structure (with respect to

geometry and semantics) of features/entities, which are extracted from reality and denoted in a 3D digital representation.

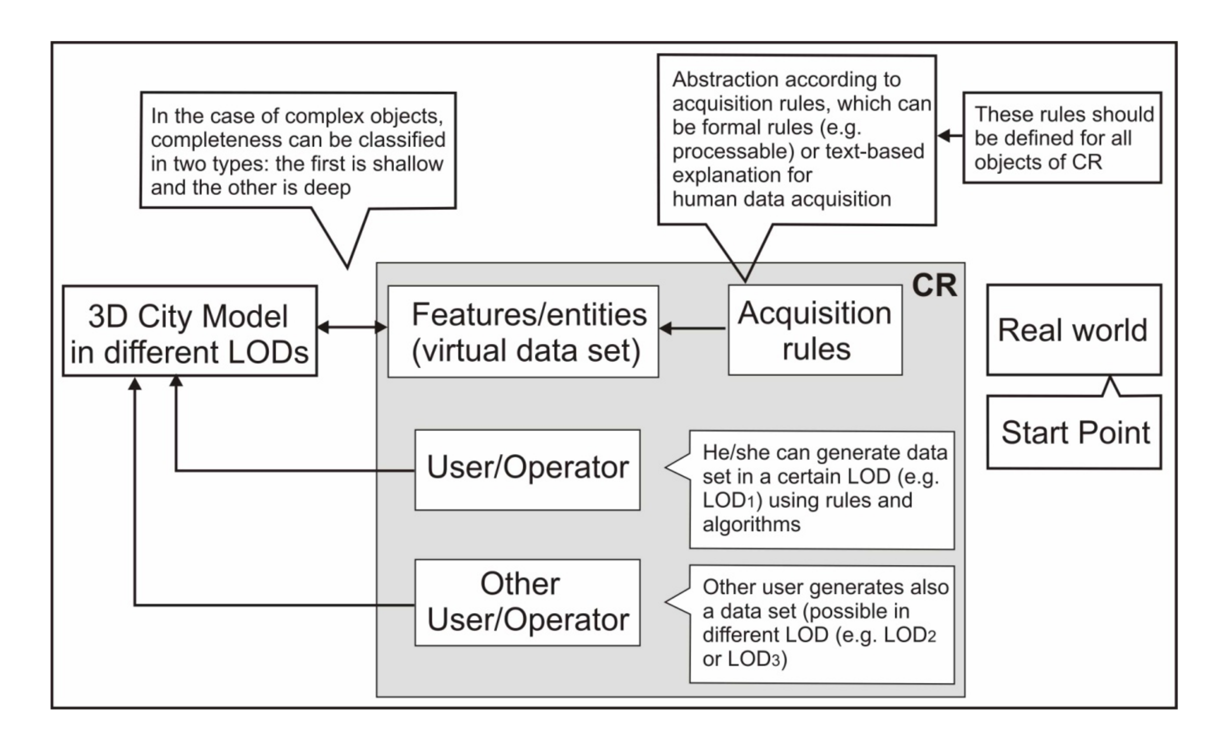

Figure (7.3): The linkage between Conceptual Reality (*CR*) and 3D city model

In general, it is desirable to have a coherent thematic and spatial structuring of the objects. This means, that each complex thematic object is associated with a complex geometry object and each of the thematic components are also assigned to geometric components (being substructures of the original complex geometry). A fully coherent data set has the advantage that each geometry object 'knows' what thematic role it plays and that each thematic feature 'knows' its location and spatial extent (Kolbe, 2009).

In the case of having the abovementioned fully coherent, both semantics and geometry are given as a complex aggregation (Stadler & Kolbe, 2007). In the complexity context, the check of completeness makes sense, because it indicates to what extent the relations between *CR* and extracted city model are complete. Therefore, it will be meaningful to define a feasible model of quality check referred to completeness.

However, in this research, two classes for completeness check (completeness accuracy which is dealing with quality of completeness referred to a complex objects) are suggested: *deep* and *shallow* completeness (Figure 7.4).

- Deep completeness

With it each element (e.g. building) in the domain (*CR*) has exactly one coupled element (in this case: building extracted) in the co-domain (*DDM*) and vice versa; it leads to the assumption that the relation between the domain and co-domain is bijection. In addition, each object in the domain (*CR*) and its digital element in the co-domain (*DDM*) have the same attributes. This means that the relation between (*CR*) and (*DDM*) is (1:1).

Figure (7.4) shows that the object "Building" in (*CR*) has a coupled object in (*DDM*). It comprises two children "Building part1" and "Building part2". Each child has also one coupled element in the co-domain (*DDM*). This linkage depends on the categories of "spatio - semantic" coherence, e.g. the case of complex objects with structured geometry (namely: fully coherence) leads to deep completeness.

- Shallow completeness

In this class, there is at least an element in the conceptual reality that does not have coupled element in the produced digital data set. In this case, the relation between the domain and co-domain is not bijection. To express this class, let start from the components: wall and roof surfaces (which are children from the child "Building part1"). Although they have been presented in (*CR*), there is no coupled elements in (*DDM*) associated with, which means the completeness in this case is shallow.

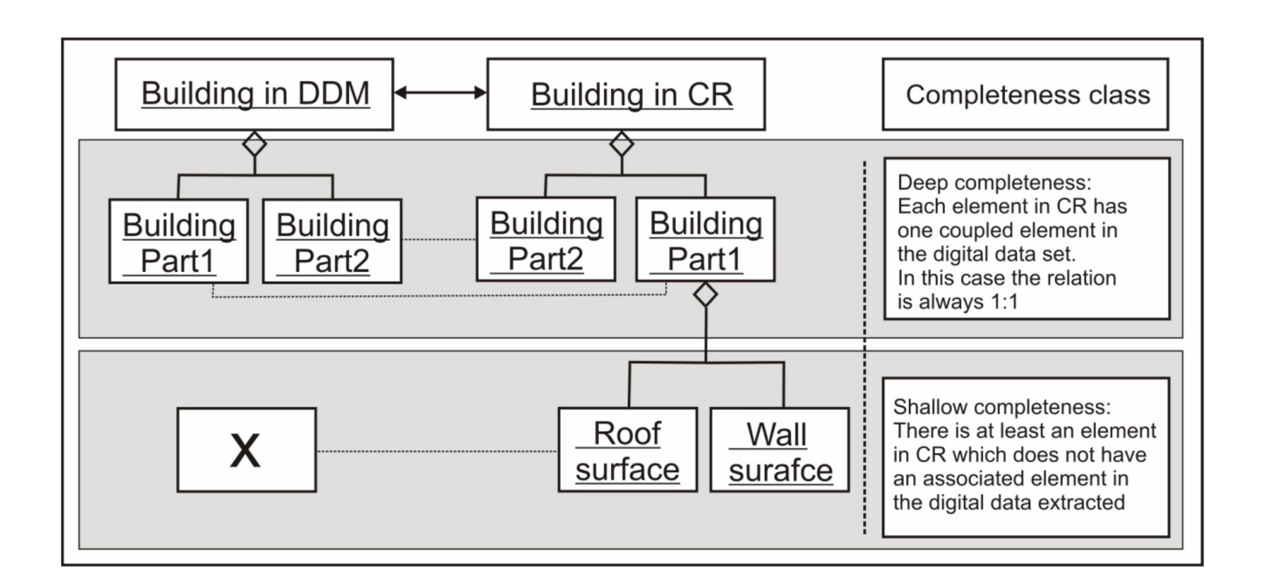

Figure (7.4): The two completeness categories: *deep* and *shallow*; which reveal to what extent aggregated object hierarchies between conceptual reality and digital data set are complete

Basically, the two completeness classes were discussed based on the assumption that the user or operator knows the object in *CR* and he wants to check whether it has an associated object in the generated city model. In contrast, one can ask if the completeness check would start from the digital data set to *CR*. This is still an open issue which depends on the quality of the extracted city model and understanding of the reality.

4. *Correctness*: each feature in (*CR*) and its coupled object in (*DDM*) have attributes which should have the same valid values.

5. *Temporal conformance*: it consists of four items:
   - accuracy of the time measurement
   - date of data update (e.g. the last update of the data set)
   - update frequency
   - temporal validity: it means that the validity expiration of a data set referred to a certain object is associated with a certain time or date.

6. *Logical accuracy*: specific logical rules should be same for specific object types. In this context, all line strings e.g. must be closed, all object points must be 3D, etc. Other rules should be also taken into account are the rules for schema conformance; e.g. an application schema should contain a *name* and a *version* string.

7.2. Quality model of Baalbek's data

Within this section, a geometric and semantic quality evaluation of Baalbek's data set will be discussed with respect to the concept of CityGML modelling. In addition, the geometry impact of Baalbek's data on the semantic modelling as well as the thematic data addition will be assessed.

7.2.1. Geometric quality of Baalbek's data

A new contribution for geometry check of Baalbek's data set will be introduced. It describes a methodology for data quality check dealing not only with the geometry related to selected object points, but also with the whole area of interest. The proposed methodology of geometry check is achieved separately for planimetry (horizontal accuracy) and for height (vertical accuracy). This is due to the different accuracies that are obtained during photogrammetric 3D point measurements for the XY and Z coordinates.

7.2.1.1. Horizontal accuracy

The basic idea of 2D geometry check is that to determine the planar displacement of an arbitrary patch included in the study area (namely: Baalbek's area). This displacement is based on deformations related to arbitrary object points included in the selected patch. So, in other words, we aim to know information about the 2D data quality for the whole area within the selected patch.

Basically, each patch to be checked can be described by a polygon generated based on object points. This means that the quality information will be available for the whole area within the studied polygon.

However, the suggested process of 2D geometry check comprises following steps:

- **Step I**

A section of the oriented model of Baalbek's mosaic has been specified by a polygon (PT[1]) generated based on a few control points (CPs) measured by tachymeter (in this case five CPs were used). Three criteria should be respected in the selection of control points:

- The first is: that the CPs were not used in orientation process to keep statistically independency in the deformation calculation of CPs used.
- Second, CPs should be spread all over the studied area.
- Finally, it is important that the polygon should be created with a convex form which is, in general, more accessible in further mathematical processes (e.g. accessibility for interpolation process).

- **Step II**

The aforementioned CPs were also measured based on the region mosaic of Baalbek; which means a new polygon (PM[2]) was generated. An illustration of the created polygon PM and its attributes (e.g. polygon's area and perimeter) is presented in the Figure (7.5).

- **Step III**

Based on the overlapping between both polygons PT and PM (cf. Figure 7.6), the planimetrical displacements (Δ_i) of CPs selected can be calculated as following:

[1] **PT**: **P**olygon based on five CPs measured using **T**achymeter, the points are: 4011, 4014, 4031, 4039 and 4040

[2] **PM**: **P**olygon based on CPs measured using Baalbek's **M**osaic

$$\Delta_i = \sqrt{(X_t - X_m)^2 + (Y_t - Y_m)^2} \qquad (7.1)$$

where: i: 1, 2 … 5

X_t, Y_t: coordinates of the CPs measured using tachymeter

X_m, Y_m: coordinates of CPs measured using Baalbek's mosaic

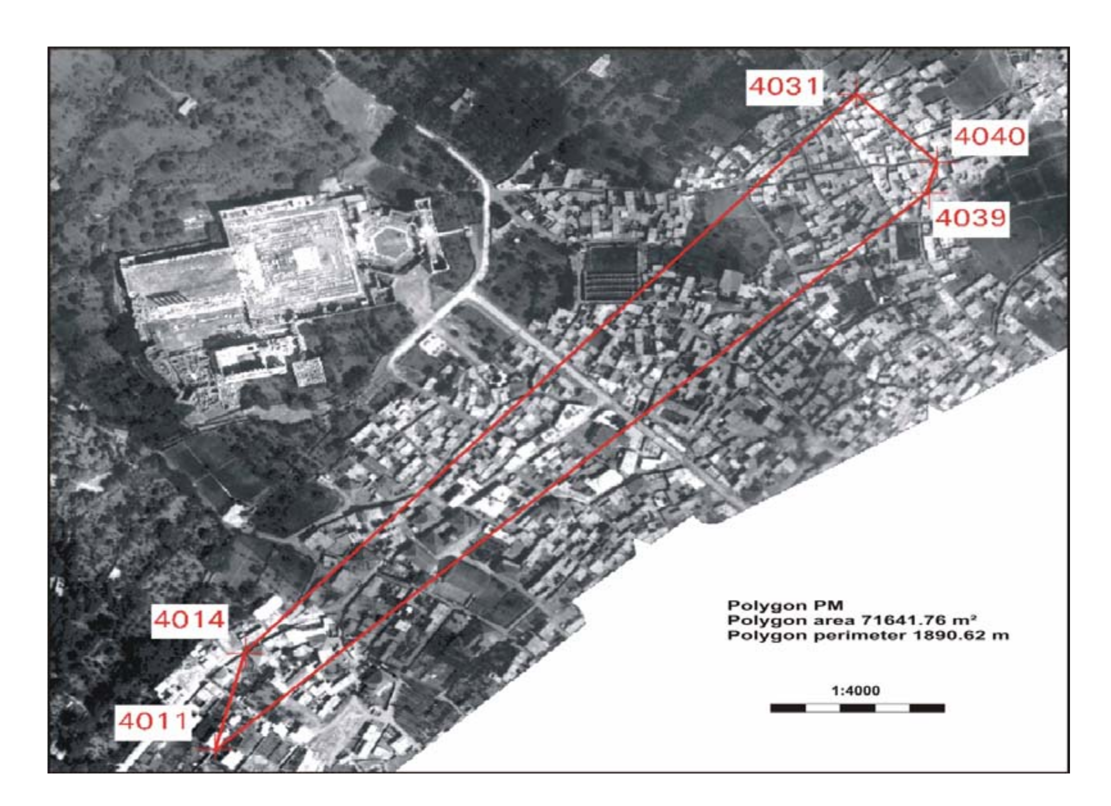

Figure (7.5): An illustration of the polygon PM (red line)

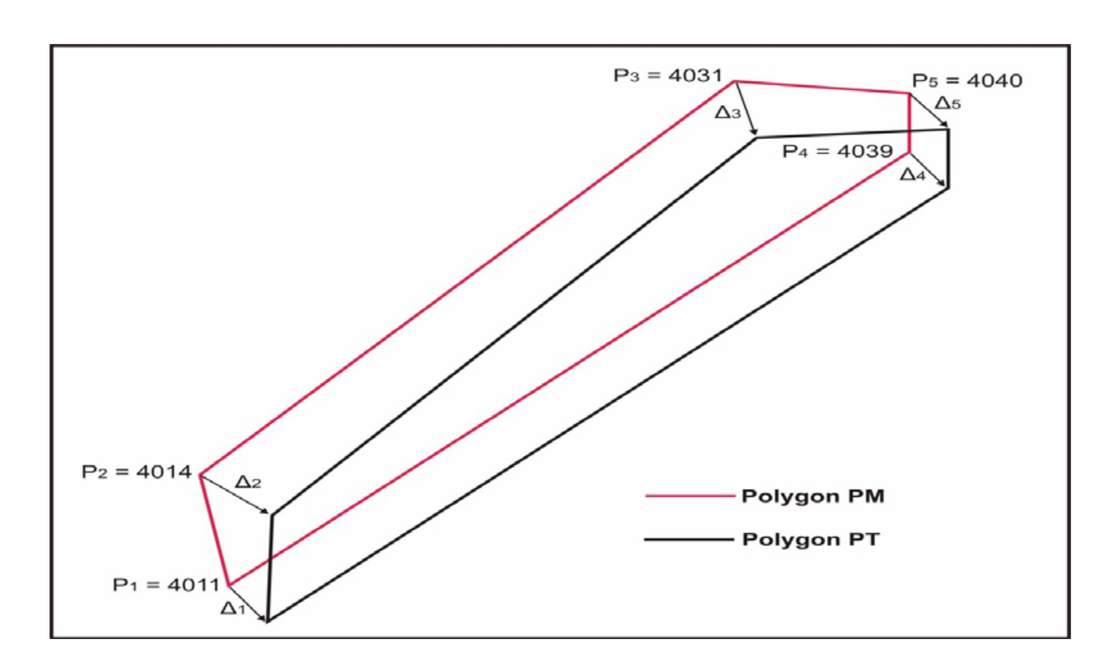

Figure (7.6): The overlapping between the polygons PM and PT

Coordinates of polygon vertices and in between distances (d_t and d_m for distances computed based on tachymetric and photogrammetric measurements, respectively) are given in the Table (7.1). Positional deformations associated with those vertices have been calculated (with respect to the formula 7.1) and they are ~ 12 to $38\ cm$ (Figure 7.7).

Vertex	X_t	Y_t	X_m	Y_m	d_{ID}	d_t	d_m
4011	9598.018	10111.211	9598.276	10111.487	$d_{(4011-4014)}$	104.770	104.394
4014	9624.838	10212.490	9625.057	10212.387	$d_{(4014-4031)}$	794.925	794.999
4031	10164.672	10796.001	10164.701	10796.174	$d_{(4031-4040)}$	100.505	100.700
4040	10236.036	10725.231	10236.153	10725.216	$d_{(4040-4039)}$	33.720	33.852
4039	10227.138	10692.706	10227.259	10692.553	$d_{(4039-4011)}$	856.696	856.304

Table (7.1): Polygon vertices coordinates measured based on tachymeter and photogrammetric evaluation, in addition the distances in between (values in meter)

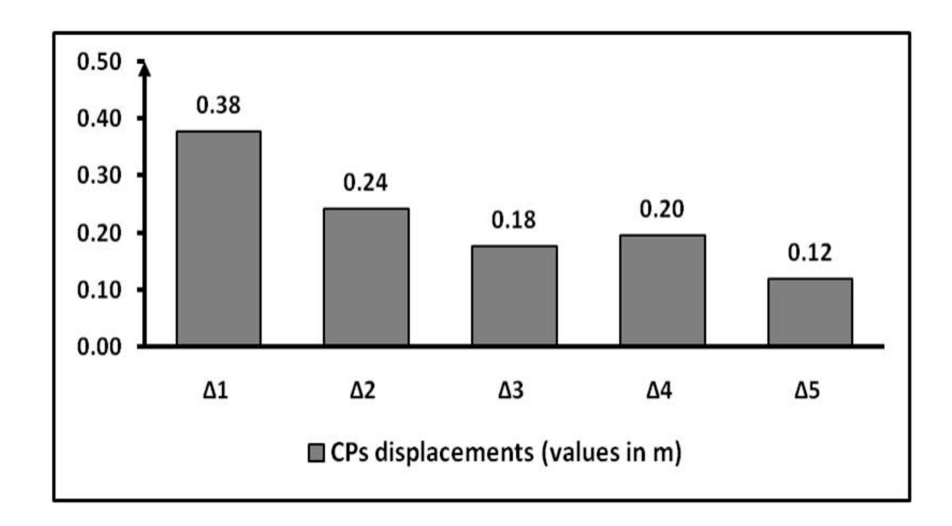

Figure (7.7): Displacement values related to polygon vertices (namely, the five selected control points). The vertex P_1 (4011) has been maximally displaced (ca. $38\ cm$)

- **Step IV**

As it was mentioned previously, we aim to obtain information about the 2D data quality for the whole area within the polygon. It means, the quality assessment of points included in the polygon should be controlled. For this aim, a raster grid has been generated so that the Grid Vertices (GVs) should be spread all over the studied area (namely: studied polygon PM). First of all, 2D coordinates of GVs (Fig. 7.8) can be determined based on Baalbek's mosaic.

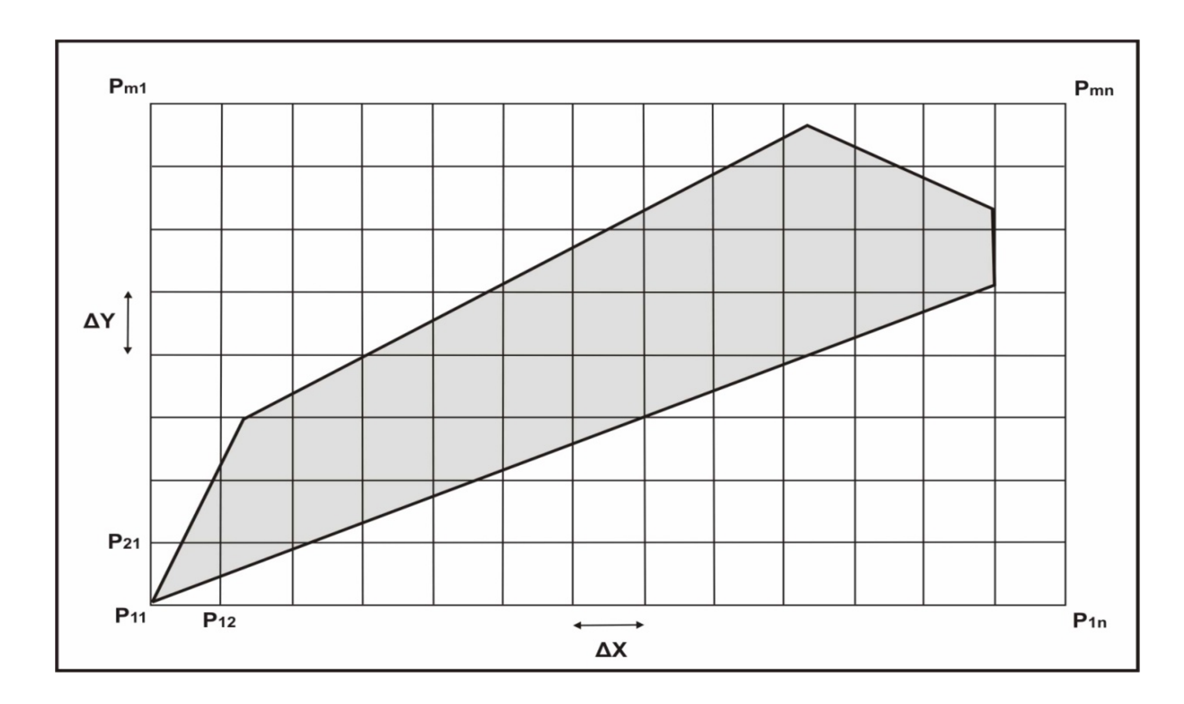

Figure (7.8): Raster grid covering the whole area of the polygon PM (shaded area), where the raster interval is considered $\Delta X = \Delta Y = 50\ m$

Once that the GVs were determined, displacement values associated with can be calculated based on the displacements of the polygon PM vertices. However, it could be therefore investigated: to what extent grid vertices are displaced. In addition, it will be proved whether these displacements are smaller than the largest one Δ_1 related to the polygon vertex (P_1).

In order to reveal the impact of input data (displacements of polygon vertices P_1, P_2 … and P_5) on the output (GVs' displacements), an interpolation process should be carried out. The interpolation method, here used, is Inverse Distance Weighting (IDW). IDW is an interpolation technique, which relies on the value of known sample points to estimate the values at surrounding points using an inverse distance weighting method (Philip & Watson, 1982; Watson & Philip, 1985). The main principle of IDW function is that the value of a variable at a specific location can be inferred from surrounding sampled locations, depending on the distance and the number of surrounding sample points.

A general mathematical form for this method can be expressed as follow (Shepard, 1968; Ware et al., 1991):

$$\Delta = \frac{\sum(\lambda_i \cdot \Delta_i)}{\sum \lambda_i} \tag{7.2}$$

where:

Δ : displacement value (to be estimated) of the interested grid vertex

Δ_i : displacement values of polygon PM vertices

λ_i : the weight that determines the relative importance of individual displacement Δ_i, one option to define this weight is:

$$\lambda_i = \frac{1}{d_i^p} \qquad (7.2.a)$$

i = 1 to n (n … number of polygon vertices) and p is an exponent (power parameter) defined by the user

d_i : distances between the interested grid vertex and the polygon PM vertices

IDW relies mainly on the inverse of the distance raised to mathematical power. The power parameter enables to control the significance of known points on the interpolated values based on their distance from the output point. Greater values of the power parameter assign greater influence to values closest to the interpolated point. In this study case, the power parameter entered in the weight function with the value 1.

IDW does not make assumptions about spatial relationships except the basic assumption that nearby points ought to be more closely related than distant points to the value at the interpolated location. This technique determines cell values using a linearly weighted combination of a set sample points (Tung, 1983; Watson & Philip, 1985; Naoum & Tsanis, 2004).

Consequently, by using of IDW interpolation to estimate displacements related to arbitrary grid points (with respect to other ones referred to displacements of the polygon vertices) the following assumption was taken in account:

The displacements of GVs should be distributed smoothly and unknown displacements of GVs are computed as a linear combination of the given displacement values of polygon vertices with the inverse distance as weights.

Based on this assumption two issues should be respected:

- Smooth distribution of GVs' displacements: by defining a higher power parameter, more emphasis can be put on the nearest points. Thus, nearby data will have the most influence, and the surface will have more detail but less smooth. Basically, this case was avoided,

because it is necessary to perform the interpolation process with respect to distant points. It could mean that nearby data will not have the most impact on the interpolation process and therefore the surface will not have more detail but more smooth.

- Linear combination: the formula (7.2) shows that the output displacement is a function to known displacements entered in the interpolation process, so it can be reformed:

$$\Delta = \frac{\lambda_1 \cdot \Delta_1 + \lambda_2 \cdot \Delta_2 + \cdots + \lambda_5 \cdot \Delta_5}{\sum \lambda_i}$$

$$\Delta = \frac{\lambda_1}{\sum \lambda_i} \cdot \Delta_1 + \frac{\lambda_2}{\sum \lambda_i} \cdot \Delta_2 + \cdots + \frac{\lambda_5}{\sum \lambda_i} \cdot \Delta_5$$

$$\Delta = a_1 \cdot \Delta_1 + a_2 \cdot \Delta_2 + \cdots + a_5 \cdot \Delta_5 \tag{7.2.b}$$

Thus, the equation (7.2.b) indicates that the displacement to be determined is mathematically expressed in a linear function based on displacements of the surrounding sample points.
The question to be posed: *is there a displacement value (referred to an arbitrary grid vertex) that can be greater than the highest or less than the lowest input* (namely: displacements of the polygon vertices)?

Basically, the output value for a cell using IDW is limited to the range of values used to interpolate. Since that IDW is a weighted distance average, the average can not be greater than the largest or less than the lowest input data. Therefore, it can not create ridge or valley if these extremes have not already been sampled (Watson & Philip 1985).

The mentioned declaration was met through the determination process (based on the equation 7.2.c) of displacements referred to 30 grid points selected. Calculated displacements are in the range $[16 - 28]cm$.

7.2.1.2. Height accuracy

The geometrical analysis of heights was done in an analogous way described in the evaluation of positional quality of Baalbek data. In this case, height displacement values Δ_{hi} associated with different object points are given:

$$\Delta_{hi} = H_t - H_m \tag{7.3}$$

where:

H_t : Height values referred to object points selected measured using tachymeter
H_m : Height values referred to object points selected using Baalbek's oriented photos

Based on the equation (7.3), height displacement values related to sample object points have been calculated using measurements based on tachymeter and oriented photos. For further height displacements referred to arbitrary object points, the IDW interpolation method was implemented. Here, the assumption of smooth distribution and linear combination were also preserved. The output values are in the range $[15 - 70]\ cm$.

7.2.2. Quality of semantic data

7.2.2.1. Definition

According to (Krämer et al., 2007), the quality of a semantic data set is expressed by the term "semantic accuracy" which can be given when: all objects included in this data set are correctly classified and all attributes associated with have correct values. The classification of objects will be correct if each object (O) in (*CR*) and its corresponding O' in (*DDM*) belong to the same class (in this case: the relation 1:1 is respected, see Chapter 7.1). This can be explained with an example:

Let (CB) and $(CB)'$ be the "Class-Building" in (*CR*) and (*DDM*) respectively. Therefore, classification of objects is correct if the following formula is true:

$$\forall\ O \in CR \quad \exists\ O' \in DDM \ \rightarrow \ (f(O) = O'\ and\ (CB) = (CB)') \tag{7.4}$$

This means: for each object *O* there is a digital representation O' which has to belong to the same class of the object *O*.

In contrast, validation of objects attributes in (*DDM*) can be defined as following:

$$\forall\ O' \in DDM \quad \forall P' \in E_{DDM} \ \rightarrow val(P') \in \ V_{P'} \tag{7.5}$$

where:

P' … an attribute of an object in *DDM*
E_{DDM} … set of all digital attributes of objects in *DDM*
$val(P')$ … value of the attribute P'

$V_{P'}$ … set of all valid values for the attribute P'

In an analogous way, all attributes of objects in (CR) are valid if:

$$\forall\, O \in CR \quad \forall P \in E_{CR} \rightarrow val(P) \in V_P \tag{7.6}$$

where:

P … an attribute of an object in CR
E_{CR} … set of all attributes of objects in CR
$val(P)$ … value of the attribute P
V_P … set of all valid values for the attribute P

7.2.2.2. Semantic accuracy and geometry

Basically, geometric quality has an indirect impact on semantic quality (semantic resolution and thematic addition), because it affects directly the possible achievable CityGML-LOD which determines also the semantic resolution and vice versa (Figure 7.9). In this context, the resolution of Baalbek's historical photos has an impact on the achievable semantic quality due to the resolution of the images affects the determination and 3D reconstruction of separate objects like parts of buildings (e.g. balconies, etc.).

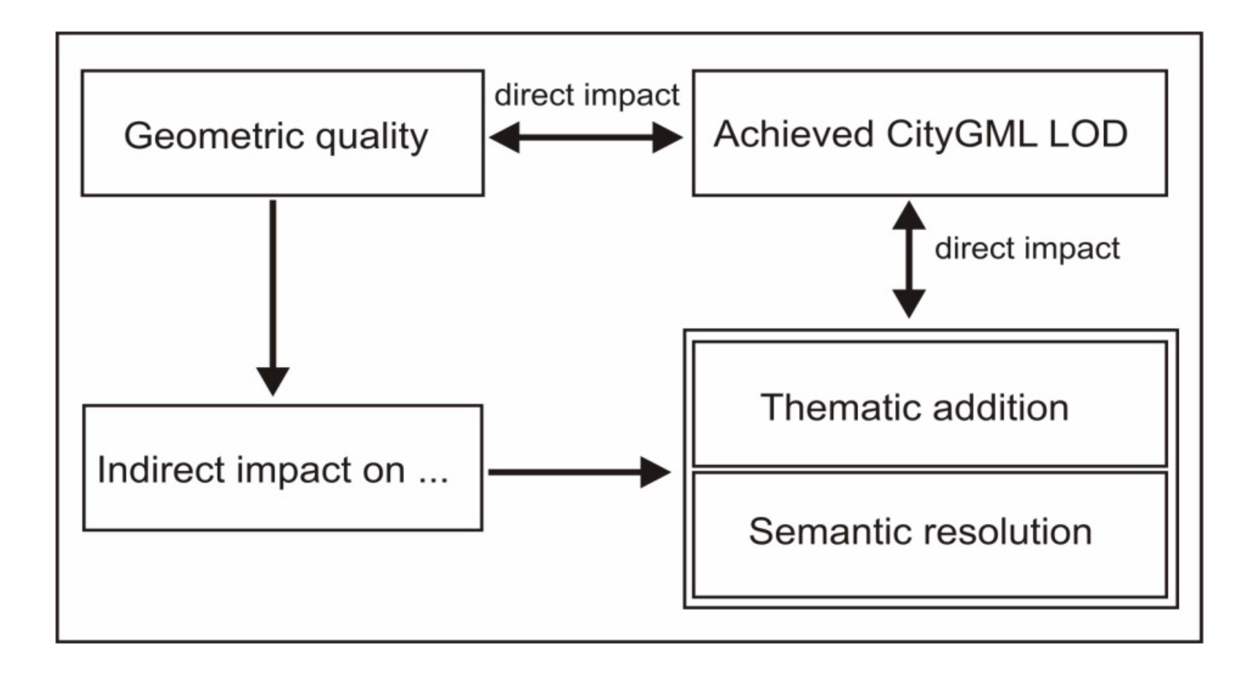

Figure (7.9): The relation between semantic and geometric quality

7.3. Interpretation of quality check of Baalbek's data

7.3.1. Geometry

According to (Gröger et al., 2008), the accuracy requirements for CityGML modelling are given in an implementation specification referred to CityGML. They are debatable and should be considered as discussion proposal. The accuracy is described as the standard deviation of the absolute 3D point coordinates (Table 7.2). Relative 3D point accuracy will be added in a future version of CityGML as it is much higher than the absolute accuracy.

In LOD1 the positional and height accuracy of 3D points must be 5 m or less. In contrast, by LOD2 the positional and height precision of object points must be 2 m or better. In this LOD, all objects with a footprint of at least $4m \times 4m$ have to be considered. Both types of accuracies in LOD3 are 0.5 m and the minimal footprint is $2m \times 2m$. Finally, in the last LOD, the accuracy must be 0.2 m or less.

	LOD0	LOD1	LOD2	LOD3	LOD4
Model scale description	Regional, landscape	City, region	City districts	Architectural models	Architectural models, interior
Class of accuracy	Lowest	Low	Middle	High	Very high
Absolute 3d point accuracy	Lower than LOD1	5/5 m	2/2 m	0.5/0.5 m	0.2/0.2 m
Generalisation	Maximal generalisation	Object blocks as generalised features;> 6*6m/3m	Objects as generalised features >4*4m/2m	Objects as real features; >2*2m/1m	Constructive elements and openings are represented
Building installations	-	-	-	Representative exterior effects	Real object form
Roof form/structure	no	Flat	Roof type and orientation	Real object form	Real object form
Roof overhanging	-	-	Yes	Yes	Yes
City Furniture	-	Important objects	Prototypes	Real object form	Real object form
SolitaryVegetation objects	-	Important objects	Prototypes higher than 6 m	Prototypes higher than 2 m	Prototypes, real form
Plant Cover	-	> 50*50 m	>5*5 m	< LOD2	< LOD2
To be continued for the other feature thems					

Table (7.2): LOD 0-4 of City GML with its accuracy requirements – these accuracies are not normative, but just proposal (source: Gröger et al., 2008)

In Baalbek project, the achievable accuracy of applicable 3D object points is smaller than 1 m for the position/height. Therefore, it will be geometrically possible to use Baalbek's 3D features extracted based on historical images to create a 3D city model of Baalbek in LOD1 and LOD2.

An overview of Baalbek's 3D model (in LOD1) is presented in the Figure (7.10) as well as a close illustration of parts of the temples Jupiter and Bacchus - in LOD2 - is also presented in the Figure (7.11).

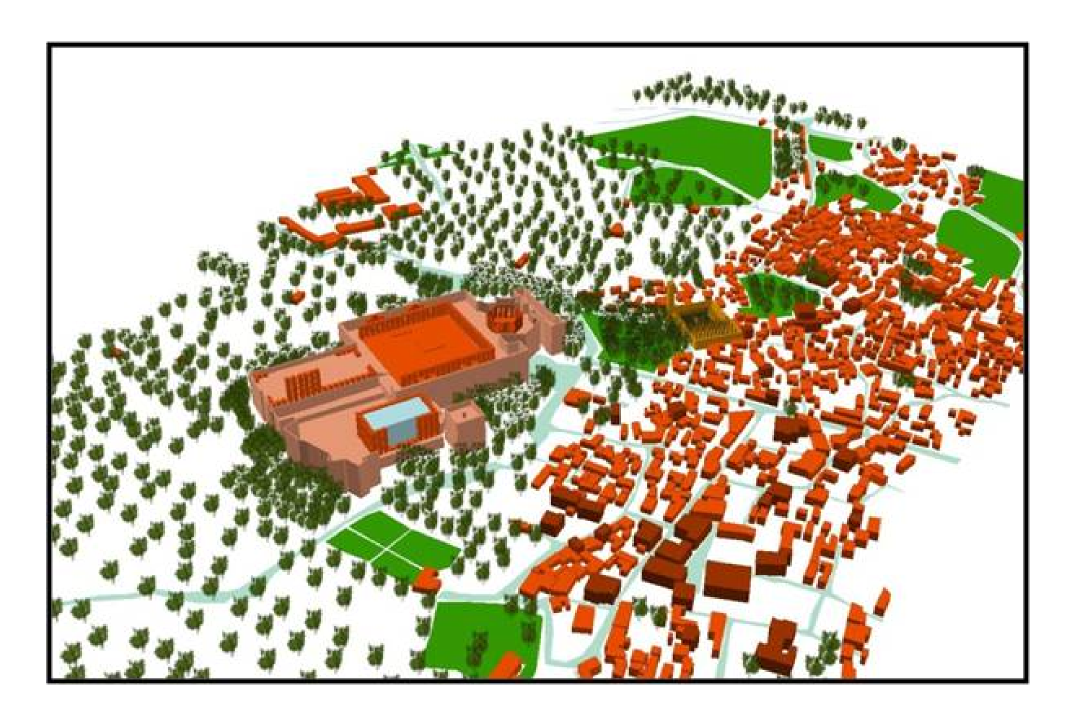

Figure (7.10): 3D city model in LOD1 of historic Baalbek. Buildings are represented as solids; streets are reconstructed by polygons. These entities are modelled using different tools like: "ArcMap and ArcScene"

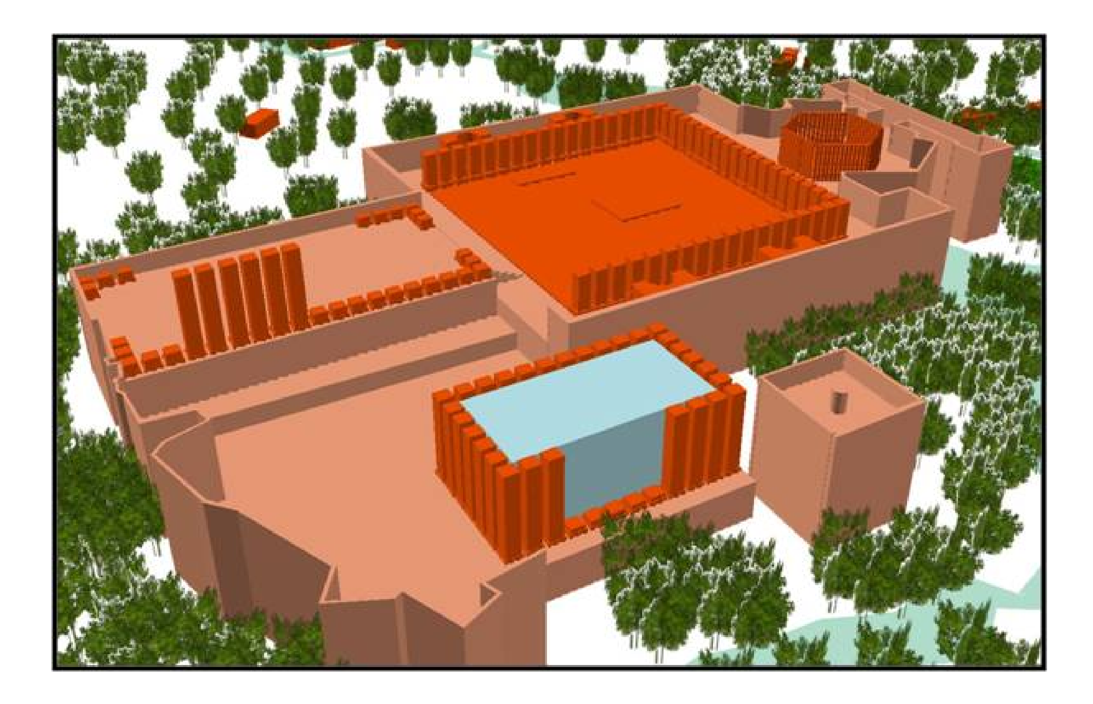

Figure (7.11): A close view of 3D model of the both temples: Jupiter and Bacchus in LOD2

A summary about the number of different extracted objects like: buildings, trees, roads, etc. is presented in the Table (7.3).

Objects	Building	Road	Solitary vegetation objects like: trees	Vegetation area	Temple
Number	737	42	1645	24	2

Table (7.3): Number of objects extracted using Baalbek’s historical photos

7.3.2. Semantics

Basically, the geometric model of Baalbek presented in the Figures (7.10) & (7.11) includes complex buildings (like the temple of Jupiter) which were digitized as several roof polygons (Chapter 6.6.1). After that all roof polygons were extruded by providing a Z-value. Furthermore, in Baalbek’s 3D model each building is represented by one or more roof polygons and also with corresponding solids, which complies with the cell decomposition representation scheme of 3D computer graphics. All elements have been stored as 3D Shapefile which was converted to CityGML file format[1].

Baalbek’s CityGML file represents a photogrammetric reconstruction of the temple of Jupiter. It contains one *CityModel* including a number of so called: *GenericCityObjects*. Each *GenericCityObject* has four *GenericAttributes*: AREA, PERIMETER, ID and Z. Basically each digitized roof polygon is represented two times: one time as roof-polygon and other one as a *surfaceMember* of its corresponding Solid (Figure 7.12).

[1] The tools used for this conversion is the software: Feature Manipulation Engine FME

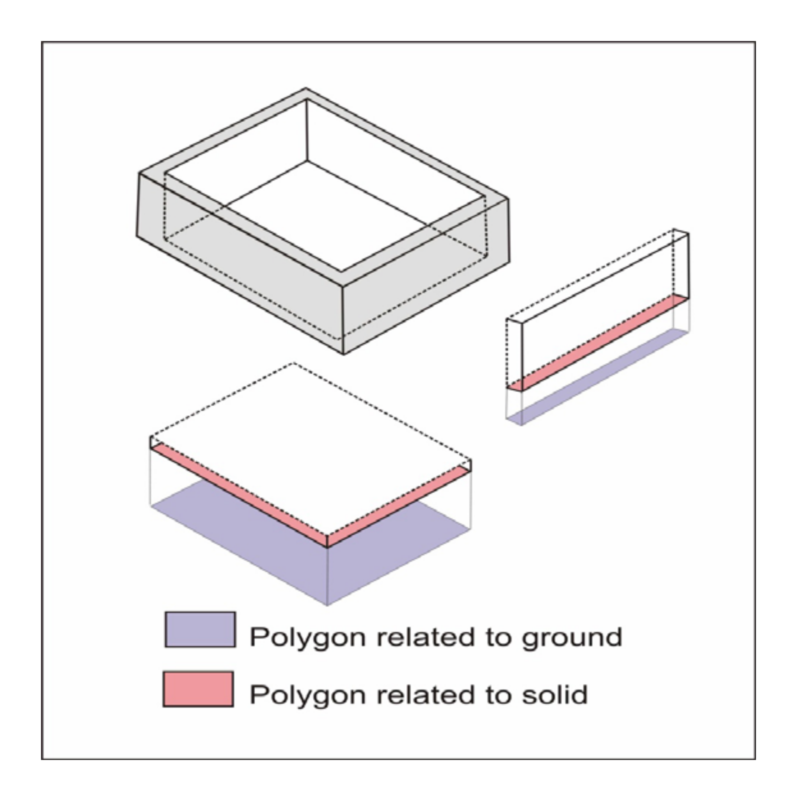

Figure (7.12): An illustration of the coupled representations of each digitized polygon; one time related to the ground and other one to the volume associated with

In addition, different geometric and semantic challenges are met in the above mentioned file such as:

- It contains only *GenericCityObjects* and for e.g. no Buildings or other semantic information (like building name, function, etc.)
- A real world building may be represented by several *GenericCityObjects* which depend on the numbers of digitized roof polygons. In this context, each building is described in the cell decomposition representation scheme and not in the boundary representation scheme as explained in ISO 19107 GI-Spatial scheme
- Finally, each polygon is provided two times (App. P)

That is to say that the above mentioned file can be validated correctly according to XML Schema. Nevertheless, it has been modelled as intended by the Specification of the CityGML Encoding. Therefore, this file has been converted to a new CityGML file (here it is called CityGML-file$_2$) in order to overcome the above mentioned posed challenges.

The conversion process of the file$_1$ to the file$_2$ is carried out by an algorithm developed in Java that uses the citygml4j API. The citygml4j API (CityGML for Java-Application

Programming Interface) is a Java class library that facilitates the work with the OpenGIS® CityGML Encoding Standard.

In the following, the algorithm will be explained in five steps:

1. *Read file*: in this step the original file (CityGML-file$_1$) is read using the citygml4j API. Hence, the citygml4j tree of content objects is traversed from the root (*CityModel*) to its leaves (geometry).

2. *Extraction of polygons*: each polygon, that is found, is stored only one time in a list.

3. *Graph (adjacency list)*: in order to build a graph, first for every polygon an axis-aligned minimum bounding box is computed (Figure 7.13, a). The minimum bounding boxes are defined by the minimum and maximum X, Y and Z coordinates within the *posList* of a polygon. This will provide two points at the lower left and the upper right corner of a cuboid. Once, it will be proved, whether the bounding boxes of each two polygons are meeting or not! In this context, two bounding boxes are meeting if their boundary sets are intersecting (in all three dimensions). If a meeting is being detected, it is assumed that the two corresponding polygons are neighbored. The adjacency list stores the neighborhoods between all polygons in the form of nested lists. The main list stores all polygons. Additionally, every polygon in this list stores its neighboring polygons. Due to that the usage of minimum bounding boxes for the determination of neighborhoods is an approximation process; the detected neighborhoods so far must not project exactly the real solution. Two cases of polygons adjacencies are depicted in the Figures (7.13, b) and (7.13, c).

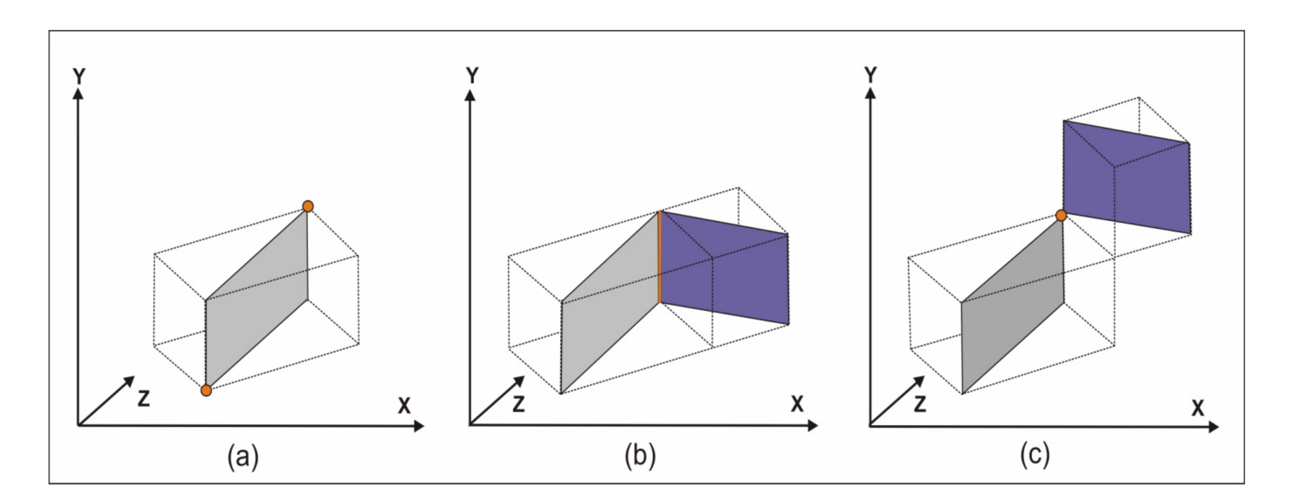

Figure (7.13): An axis-aligned minimum bounding box defined by the lower left point and the upper right point (a), two cases of polygons meeting: with a line (b) and with a point (c)

4. *Extraction of connected components*:

Based on the graph structure, the connected components can be extracted. In this case, a connected component comprises all polygons that are directly or indirectly neighbored with each other. Polygons that are part of different connected components are always disjoint. The connected components are extracted by traversing the graph structure in a breadth-first search. That is to say, a first polygon is extracted, and then the neighbors of this first polygon, next the neighbors of each neighbor of the first polygon and so on.

To express the principle of the breadth-first search process, suppose that there is a cubic solid available and represented by several surfaces (Figure 7.14). The process of breadth-first search, used to extract the connected components related to the abovementioned solid, can be described by a tree including each polygon extracted and its neighbors (Figure 7.15).

Consequently, it can be assumed that polygons of each connected component are somehow neighbored and the polygons of two connected components are always disjoint. Further on, it is supposed that every connected component within this graph represents one real-world building.

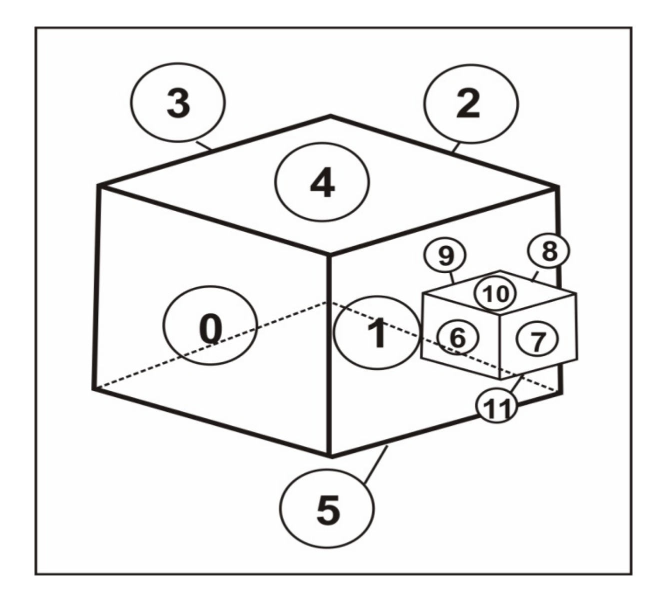

Figure (7.14): A solid represented by multi-surfaces; (in this illustration: 12 polygons with ID from 0 to 11)

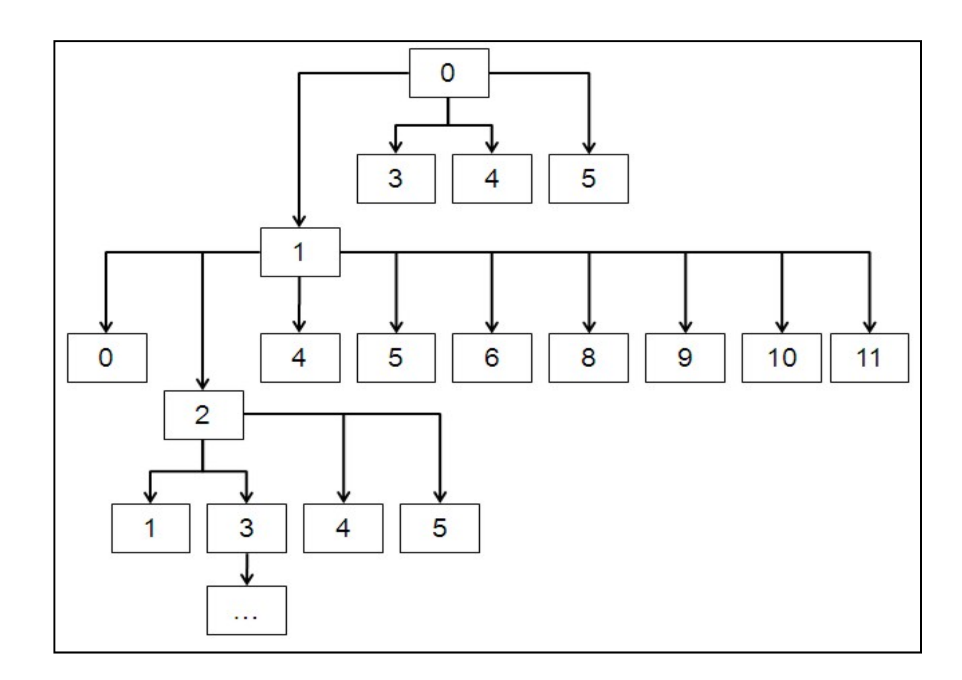

Figure (7.15): The tree of the breadth search process applied to detect the polygons and their neighbors related to the solid depicted in the Figure (7.14). In this case, it can be noted that the polygon 0 (namely the surface 0) has four neighbors (1, 3, 4 and 5); furthermore, the first neighbor (1) of the polygon (0) has also 9 neighbors.

5. *Generating of the new file (write file)*: finally, an intermediate file is written by means of citygml4j library. Therefore, for each connected component a new *Building* element is generated and the new attributes: *yearOfConstruction* and *function* as well as the *GenericAttributes* NAME, EPOCH and RESTORATION plus one *lod2MultiSurface* property are added. The *lod2MultiSurface* contains all polygons of the corresponding connected component. The structure of the new CityGML file is presented in the App. (Q).

However, a comparison between the original CityGML file and the new one from geometric and semantic views can be achieved. In this context, it can be found that the new CityGML file includes one *Building* element. In addition, five attributes are available where three of them are *GenericAttributes* (Table 7.4).

Point of view	Original file	Output file
Semantic	CityGML file	New CityGML file
	1 CityModel	1 CityModel
	66 *GenericCityObject* elements	1 Building
	AREA	StringAttribute NAME
	PERIMETER	StringAttribute EPOCH
	ID	dateAttribute RESTORATION
	Z	function
		yearOfConstruction
Geometry	33 GenericCityObject elements have a lod4Geometry property with: - a polygon inline (related to floor polygons) - a solid inline (related to extrusion solids)	1 lod2MultiSurface property with one MultiSurface and 420 Polygon elements inline

Table (7.4): A comparison between Baalbek's original and new CityGML files

Furthermore, different views (screenshots) showing the semantic structure referred to the CityGML file resulted are presented in the Figures (7.16.a-c).

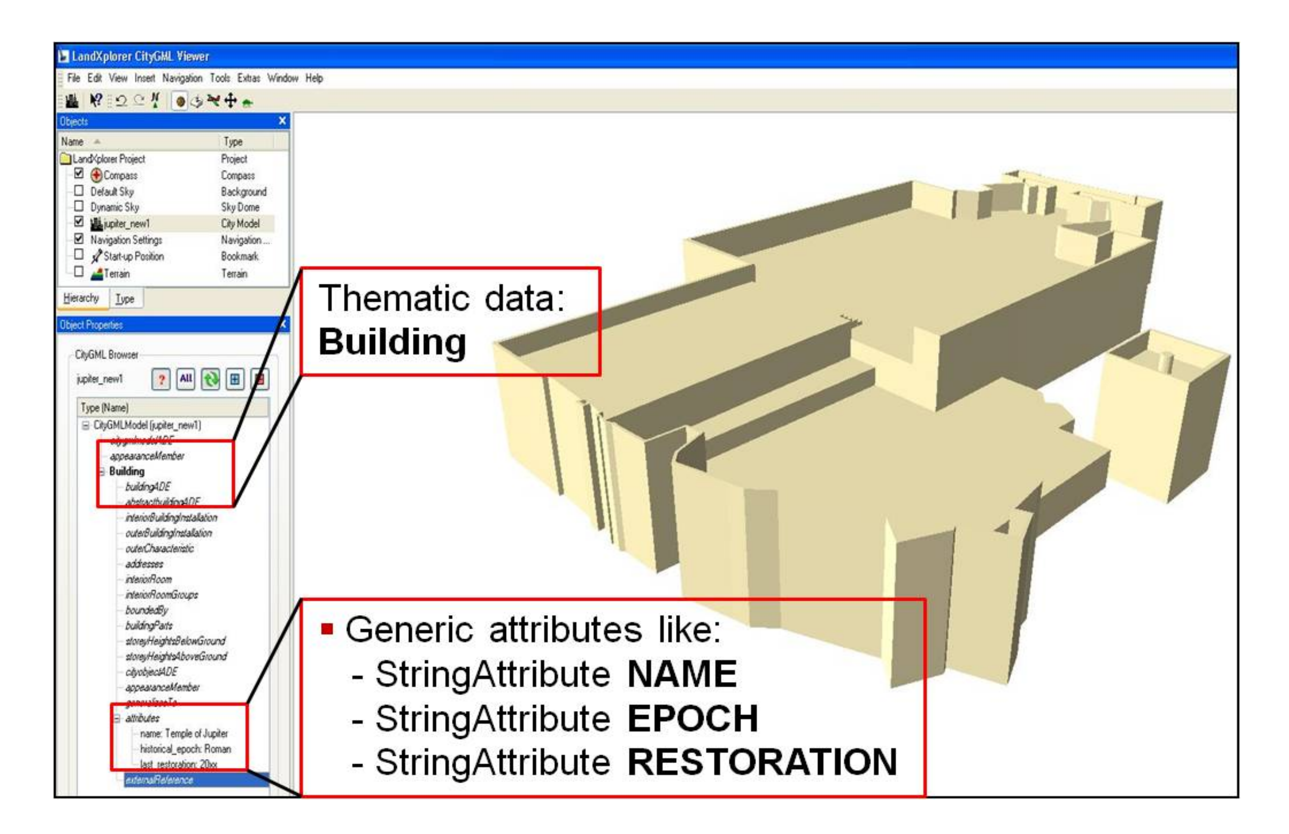

Figure (7.16.a): A 3D view of the temple Jupiter using LandXplorer CityGML Viewer. Thematic data like: name of the building, historical epoch, etc. are addressed under the class "attributes", where it is possible to add new information

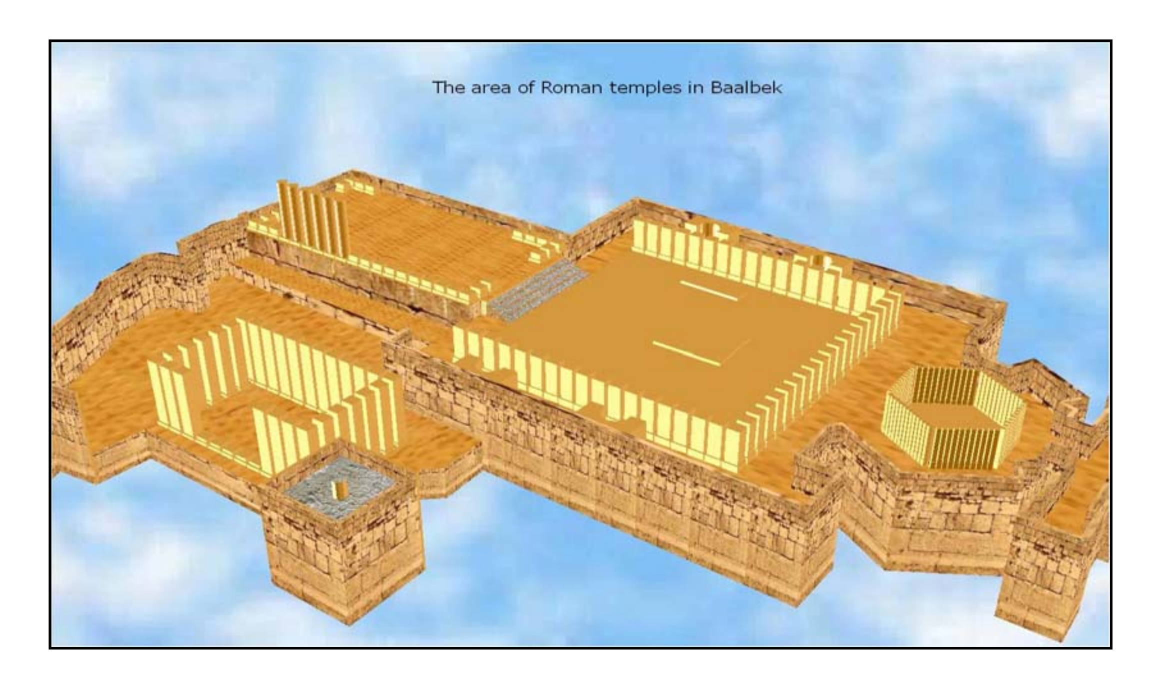

Figure (7.16.b): An illustration of 3D geometric and semantic model (in LOD2) of some parts (with texture) of the temples: Jupiter and Bacchus. The main tools used in this case are: FME Universal Translator and the software Aristoteles[1]

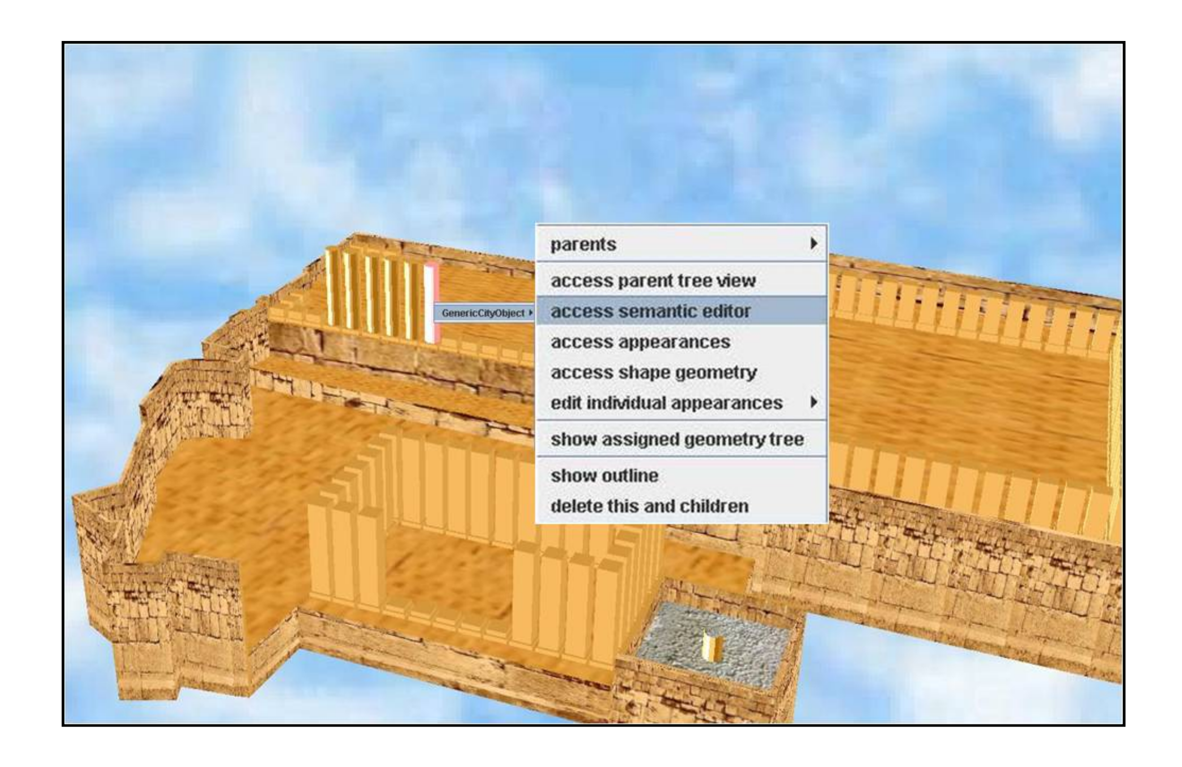

Figure (7.16.c): The possibility to add thematic information using a semantic editor

It is important to mention that the terrain is an essential part of a city model. In CityGML, the terrain is represented by the class *ReliefFeature* in LOD 0-4. A *ReliefFeature* consists of one

[1] Aristoteles viewer project is developed for different applications that need to develop or evaluate new features and attributes for 3D models. (Source: http://www.ikg.uni-bonn.de/aristoteles/index.php/Aristoteles).

or more entities of the class *ReliefComponent.* Its validity may be restricted to a certain area defined by an optional *validity extent polygon* (Gröger et al., 2008). Basically, CityGML representation of Baalbek's DTM is not achieved in this research (also other issues such: vegetation objects[1] like: tree, transportation objects[2] like: roads). These issues are considered as future tasks which should be achieved to improve the generated 3D model of historic Baalbek.

7.4. Baalbek's data visualisation

Today the 3D visualization has a variety of applications and technologies which enables us to render a detailed simulation of urban systems also of antique settlements. 3D visualization simulates spatial reality, allows the viewers to recognize what they see in the real world, but the transition between different realities is not easy and does not always satisfy expectations. In addition, an integrated and high level management of information is also missing. When dealing with cultural heritage assets, the acquisition of information in a three-dimensional form is still not always an easy task. A huge number of applications requires more advanced tools for representing and analyzing the 3D environment.

In this section, we aim to access and manage the available data of Baalbek's 3D model using an innovative method called "ISEE". This method allows the user to access the information in real time navigating in a 3D environment.

7.4.1. Accessing information through ISEE method

To access the historical information using Baalbek's 3D model produced, a method called ISEE will be used. The idea of the method is based on the using the simple action of "seeing" (and thus the name of the method, "I see"), as a mean to investigate and add information. The system can be used with modern web browsers, allowing access to a wider audience without any special requirements (Pecchioli, 2010).

The principle of ISEE is to find the relevant information using only the perspective of the user, what he/she is looking at. In the ISEE method, the term "Information Zones" (IZs) defines the information associated with regions of the 3D space. In addition, "View Zone" (VZ) is the portion of the 3D model which is being looked at in the interactive 3D Viewer.

[1] Single vegetation objects are modelled by the class *SolitaryVegetationObject*, while for areas filled with specific vegetation the class *PlantCover* is used.

[2] The main class *TransportationComplex* is used for representation of transportation objects.

Information Zones do not necessarily coincide with a 3D object represented in the model, they might be just a part of it, or even they may include many objects at the same time. An illustration of (IZs) and (VZs) is depicted in the Figure (7.17). The perceived dimension of the VZ on the screen is also constant, but its real size is depending on the distance from the object. The angle of the view cone is constant (cf. Fig. 7.17), and the closer the object is, the smaller the width, so that the perceived dimension of the VZ on the screen is constant, but its real size depends on the distance from the object.

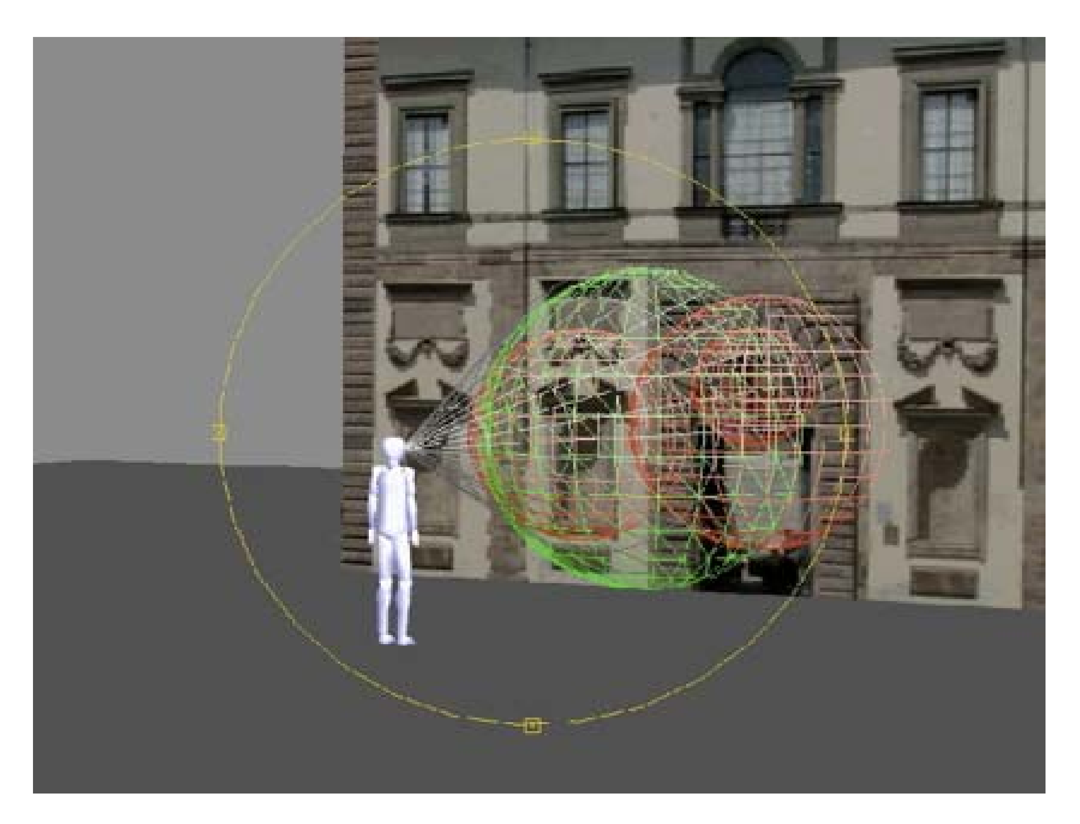

Figure (7.17): An illustration of: Information Zones (IZs: red spheres), View Zone (VZ: green sphere) and View Cone (VC presented in gray cone) - source (Pecchioli, 2008)

Defining 3D zones interactively is not so intuitive, where one has many degrees of freedom. On one hand the first choice is a "sphere", easy to define (radius and center), but the zone does not coincide exactly with the sphere, as the sphere is just meant to represent an approximation of it. Thus especially at the boundary this will be inexact. So defining of a "smooth transition" at the zone boundaries would be preferable. This can be achieved by associating a quantity (which is called the concentration of information) to each point of the space, representing "*how much*" information is contained at that point in the zone.

On other hand the choice to use the 3D Gaussian function allows providing intuitive and efficient means of filtering information and defining the mentioned concentration. This is a

function which assigns a value to each point of the space (it can be seen as a fog, denser in the center, and less dense on the periphery). In addition, it describes the concentration of information adequately.

One can also implement other smoothly decreasing functions (functions that are not strictly decreasing would have an unpredictable behaviour for the user); the difference between them would likely be minor. The real difference would be arisen if discontinuous functions were used. Furthermore the Gaussian function has several interesting advantages such as:

- It has a mathematically simple definition
- It has few parameters, and these parameters can be identified with the position and the dimension of the Gaussian function
- It can be handled in a computationally efficient way

It is important to note that the Gaussian function is not used to define the exact location of the information, but rather an approximated zone which can be subsequently used to search and retrieve the information. The amount of information is not connected with the size of the Gaussian function, but it depends just on the size of the object.

The Gaussian function that represents the VZs is structured as following (Figure 7.18):

- The ***center*** of the Gaussian is chosen on the point, representing the first intersection between a 3D scene and a ray cast, passing though the current point of view and the center of view plane. Basically you can shoot in the direction you are looking and the point (P) is the point where your ray encounters an object.
- The ***width*** of the Gaussian: it is proportional amount and is defined through the distance between the center and the current view point. In other words, it is similar to the size of the viewed area.

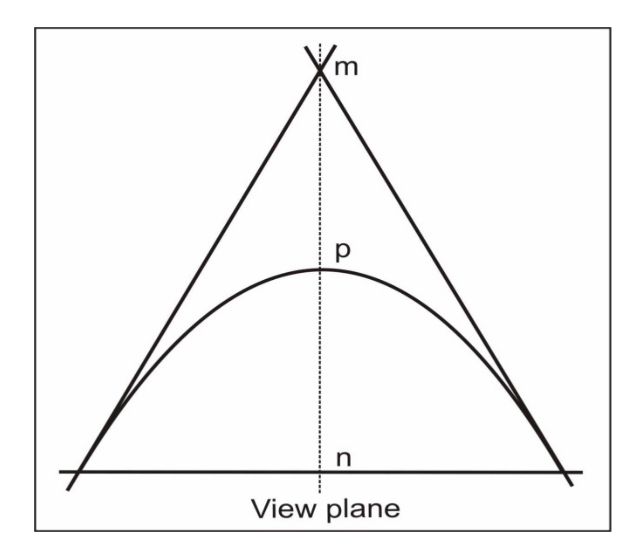

Figure (7.18): An illustration of the Gaussian center (P); where the point (m) is the point of view and the point (n) is the center of view plane

The information is ranked with a new measurement of "spatial relevance of the information". The spatial relevance depends on the position/orientation in the 3D space and allows representing the data in an intuitive interface. In addition, the new measurement is based on the relation between the (IZ) and the (VZ). Intuitively, the relevance of information should be maximal when its (IZ) coincides with the (VZ), decreasing when they are far apart. Moreover, the information is always associated with extended zones rather than with points, therefore it can also use the size of a zone to decide if it is relevant.

The usage of extended zones gives to the proposed ranking algorithm a superior performance than rankings based only on the distance. Selection methods (like: ray casting) work with points or discrete objects and do not cope well with overlapping objects. The proposed ranking algorithm matches the intuitive expectation of the users, as was verified with a formal usability test that was performed at completion of the work.

This ranking method has several advantages over previously used methods, due to:

- High densities of data and partially overlapping regions.
- It uses also the size of regions (level of detail[1]) to filter the information, it has a better performance than purely distance based methods.

[1] Here with level of detail we mean the size of the region where the information is related to, for e.g. if it relates to a detail of a painting of the whole painting. This isn't related to the level of geometrical detail of 3D model.

- Unlike selection methods like for e.g. ray casting, it copes well with overlapping and partially hidden regions and avoids users needing to be extremely precise to find information they are interested in.
- A user can interactively refine his/her search either by carefully focusing on the parts of the model he/she is looking at.

7.4.2. Baalbek Web Application (BWA)

Through Baalbek Web Application, the interactive visualization makes information more accessible and improves user experience. The idea of using the simple action of "seeing" can represent an easy instrument for the users to access the information of the context of historic Baalbek. Thus, a web application using ISEE was developed, within the user can:

- visualize and navigate in Baalbek's model (in LOD1)
- access the information in its context
- read in detail window the meta-data
- use one or more filter keys for a local search
- manage many data in different formats (UTF-8, XML, etc.)
- transfer and share of data to other users (i.e. by sending only the URL)

BWA[1] is expressed through a "*homepage*" giving access to following topics (Figure 7.19):

- the location of the city
- the temples of Baalbek
- historical and archeological information about the city
- Baalbek model in LOD1 and LOD2

In the web application only the LOD1 model can be explored interactively (Figure 7.20). The LOD2 model has been visualized using another viewer called *Aristoteles*[2], which can not be used in the browser. Therefore the user can also access a movie of the LOD2.

[1] Baalbek's Web Application is available under: http://isee.kitabi.eu/.

[2] Aristoteles viewer project is developed for different applications that need to develop or evaluate new features and attributes for 3D models. (Source: http://www.ikg.uni-bonn.de/aristoteles/index.php/Aristoteles).

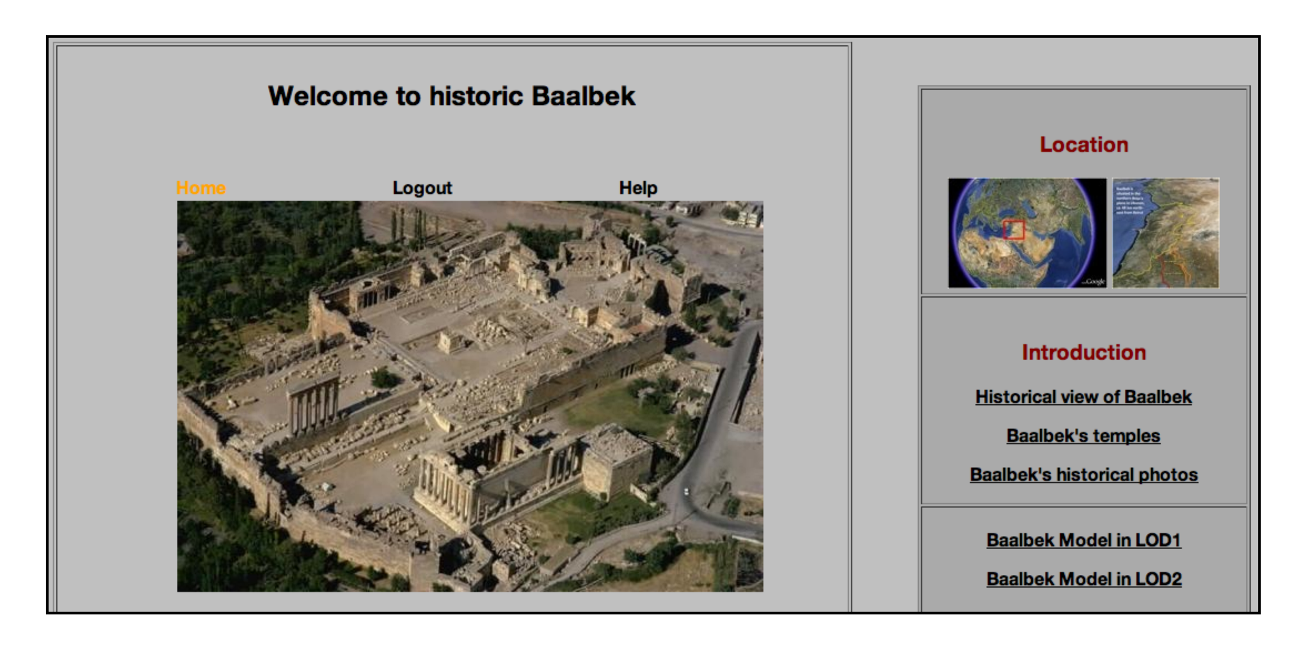

Figure (7.19): Baalbek's home page

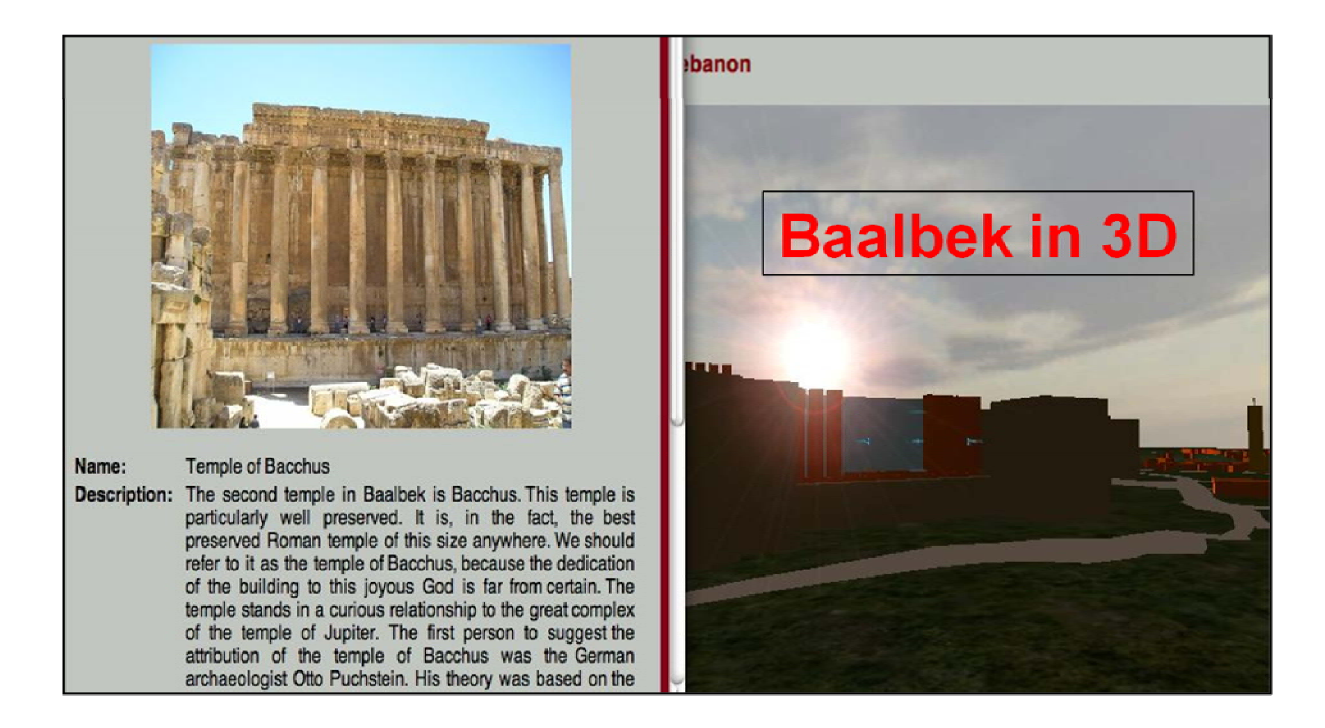

Figure (7.20): Baalbek's model (LOD1) in ISEE

8. Summary and outlook

Within this research the combined evaluation of different image types (vertical, oblique and terrestrial) for the documentation of cultural heritage sites was posed and discussed. This combination is considered an important topic which should be taken in account. This is due to that up to now minor investigations (related to the combined evaluation of different types of historical images) were achieved.

Furthermore, a suggestion of a photogrammetric methodology dealing with different types of photos (especially, historical photos) is in a high demand, because it would provide a scientific mechanism, with it, photogrammetric processes (like: image orientation, image matching, etc.) could be carried out in a best way (with respect to geometry point of view).

To achieve the abovementioned evaluation, Baalbek’s historical images were used. Baalbek’s photos can be classified into three types: the first is vertical aerial images (taken in the year 1937 through the French mandate and located in the Institute of Francais du Proche Orient IFPO in Damascus). Second one is oblique photos (taken in the 1939). The last type is terrestrial photos which are stored in the regional authority of Brandenburg/Germany (Meydenbauer’s archive) and had been taken in the year 1904.

Due to the poor properties of Baalbek’s graphical materials (such as: different cameras used, no primary data of camera parameters, different image scales, different altitudes of flight, high contrast and image noise; in addition the images had been taken in different dates, etc.), an approach for relative orientation process was discussed (with respect to the bundle block adjustment method). This approach consists of three steps: the first one is the orientation of each image type separately. Second, the orientation process only for the vertical and oblique photos together has been achieved. Finally, all types of historic Baalbek’s photos have been assembled into the same block and then oriented.

3D object reconstruction has been attained by using the oriented photos. Baalbek’s extracted data was considered the main input data which was implemented to generate a 3D city model of the historic city according to CityGML. In the created model, not only the geometry of Baalbek’s historical entities (e.g. buildings) was represented, but the semantic and thematic modelling of this city has been also taken into account, because the geometric model does not support all information needed (e.g. classification of objects, building function, names, etc.).

8.1. Retrospection and review

In this section it will be reviewed to what extent the goals posed in this research have been carried out. Basically, the six research aims were as follow: (1) Image orientation, (2) Combination of different image types, (3) Orthophoto creation, (4) The process of 3D object reconstruction, (5) 3D modelling, and (6) Result visualisation. However, concepts and issues (referred to each aim) improved and developed in this thesis will be here described.

- **Image orientation:**

It was not a priori clear by which combination of image orientation process best results (interior and exterior orientation parameters) could be attained. This ambiguity is due to the poor properties of Baalbek's images. Therefore, a feasible approach for the relative orientation of Baalbek's photos available was investigated.

First of all, each image type was separately oriented. So, in other words, each type of Baalbek's photos was imported to a separated block with its special properties (e.g. for each type a special camera was assumed). In this stage, the orientation process was successfully performed, but the geometric impact of image types to each other was not taken into consideration. This means, the estimation of orientation parameters for each image type was independent. In that case, the impact (from geometrical point of view) between different image types through the orientation process was not presented.

Furthermore, the orientation process for vertical and oblique images of Baalbek was attained. This step is the first effort, in this research, of combined evaluation of different image types referred to Baalbek. Here, the mathematical function applied in the adjustment calculations was based on input data (e.g. observations like: image points) from both image types, and therefore, unknown parameters (orientation parameters) related to vertical images were estimated with respect to other ones referred to oblique photos and vice versa.

In the last step of this suggested approach, all types were assembled to one block and then oriented together. In this orientation case, an additional geometric impact referred to the terrestrial image type of Baalbek was respected. This led to additional input data, and therefore to strict functional model. It is important to mention that this additional type used in the orientation process guaranteed a stable model of the estimation process of unknown parameters.

- **Combination of different image types**

In the context of orientation process based on image combination of Baalbek's photos, there are four possibilities of image type combination: vertical with oblique images, vertical with terrestrial image types, oblique with terrestrial and finally vertical-oblique-terrestrial.

In this work, the orientation process started with the combination between vertical and oblique images. This was mainly due to challenges (e.g. image properties) arisen in the flow of the orientation process referred to Baalbek's terrestrial image type. In addition, the vertical and oblique images have been taken approximately in the same period (1930s), it could mean that they include same objects (like: buildings, streets, etc.). This could optimize the object recognition and the matching process between images and may be a feasible support for calculations of the bundle block adjustment.

Therefore, it was firstly avoided to carry out the orientation process based on a combination including the terrestrial image type in order to get reliable results. Once, the orientation process based on the first combination (vertical-oblique) has been successfully attained, it was directly assumed to consider the oriented block of vertical and oblique images as basic start for Baalbek's terrestrial image type and then the possibility to achieve the orientation process based on three types.

Consequently, it could be accepted that the sequence of image combination (namely: vertical-oblique then all image types: vertical-oblique-terrestrial) was a reasonable suggestion to orient Baalbek's historical photos. It is important to note that other combination sequences (for e.g. vertical-terrestrial, oblique-terrestrial, etc.) could be verified, but this is still limited that new data about the terrestrial images should be provided.

However, it could be accepted (regarding to results of orientation process) that the internal geometric configuration of the different cameras used and the lens systems were determined, whereas the interior and exterior orientation parameters were well geometrically estimated, so that the measurement of the applicable 3D object points is possible.

- **Orthophoto creation**

Baalbek's orthophotos were generated with respect to the estimated orientation parameters. By the generation of orthophotos, it was necessary to create a DTM of the studied area. In this context, a DTM was created using two topographical maps covering the studied area. The cell

size of orthophotos was computed automatically based on the scale and resolution of the images. The cell size is approximately bounded to $0.13\ m$ for X and Y. The resample method “Bilinear Interpolation” was implemented due to the well quality of the gray values calculation.

- **3D object reconstruction process**

Depending on the oriented model of historical photos, the combination between the different historical images of Baalbek to create a best 3D object reconstruction (with respect to geometric accuracy) was investigated. Baalbek’s 3D data acquired based on the oriented model of photos has been considered a main data source for 3D CityGML modelling (City Geography Markup Language) which supports different Levels of Detail (LODs), by them we can represent and model different data collections.

- **3D modelling and result visualisation**

The modelling of 3D data extracted based on the oriented images of Baalbek was regarded an essential task in this work, because it enables to give a digital representation about historic Baalbek and its entities as well as to document the historic city and its remains as they looked like. In the context of city modelling, standards of CityGML were implemented. In addition, it was investigated to what extent CityGML-based modelling can be considered as an accessible and reasonable standard used for cultural heritage sites documentation.

It was also investigated in which LOD Baalbek data can be modelled with respect to quality aspects such: the geometry and the semantic data quality. The result was the generation of a 3D city model of Baalbek in two different LODs (namely, LOD1 and LOD2) with respect to quality assessment of Baalbek’s data available.

Finally, a visualization of results of investigations and experiments of historical Baalbek in Lebanon was introduced. The visualization process has been carried out using a method called ISEE. The method allows the user to access the information in real time navigation in a 3D environment. We chose to link the information to 3D zones in the space. These 3D zones have to be defined interactively, and with minimal user interaction (just by looking), therefore we have chosen to keep them geometrically very simple (like spheres).

We thought that the interactive visualization makes information more accessible and improves user experience. The idea of using the simple action of “seeing” can represent an easy

instrument for the users to access the information of the context of Baalbek. Thus, we developed a web application using ISEE, where the user can visualize and navigate in the model in LOD1 and also access a movie of the LOD2.

8.2. Thesis contributions

After the review and retrospection referred to aims of this research; intended contributions of this thesis for other scientific researches should be extracted and discussed. It deals mainly with conceptual and methodic developments and issues achieved in this work and their benefits and the applicability for further researches and projects related to. In this context, contributions will be discussed with respect to - among other things - two main research areas: photogrammetry and documentation of heritage sites.

- **Contribution for photogrammetry**

It is common that photogrammetry is a science that allows obtaining information of objects in reality based on different processes applied on images. The traditional and largest application of photogrammetry is to extract object information from aerial images. In last decades, many strategies had been introduced to carry out the abovementioned application. In addition, different efforts dealing with terrestrial images had been also achieved to acquire object data from terrestrial views.

In contrast, minor strategies referred to the combined evaluation of different image types e.g. vertical and oblique images, oblique and terrestrial ones, etc. have been achieved. Therefore, the suggestion of a methodology to deal with combination of image types is still not easy task, because there is no clear specification or protocol with them, we can carry out the mentioned combination in a best way. In other words, there is no clear methodology with it, the orientation process based on combined evaluation of different image types could be best performed with respect to the geometry point of view (e.g. geometric quality of orientation parameters).

In this thesis, a contribution for a photogrammetric methodology dealing with different types of historical images and their combination has been investigated. It was presented how photogrammetric processes such: camera calibration, image orientation, orthophoto creation, error detection, etc. can be best attained.

The suggested methodology was applied on Baalbek’s historical images, but the mechanism proposed can be also applied as a start point for study cases dealing not only with a specific

image type (e.g. just aerial image type) but also with combination of image types. Thus, users or operators (like: photogrammetrists) can depend on the issues referred to the mathematical model (functional model) and its variations applied in adjustment calculations.

- **Contribution for heritage site documentation**

Archaeological heritage sites receive the attention from most of the world governments for preserving them in a best way, because they are considered an important linkage between past and present. Moreover, these governments are looking forward to find suitable solutions to preserve historical assets and also to restore heritage parts which have been damaged.

In addition, some of historical sites had been destroyed (or maybe some parts). This leads to challenges to generate a best documentation, due to a data missing about objects related to those sites. Therefore, a feasible emphasis should be achieved to overcome the problem of non optimal modelling process. A solution can be suggested is to use available data sources like: historical images which can provide sufficient data needed. Definitively, those images require a lot of photogrammetric evaluation, analysis and different processes (e.g. orientation, rectification, etc.) in order to use them in a feasible form for further application (like: 3D model).

However, in this work, a contribution dealing with historical images (namely: Baalbek's historical images) for heritage site documentation was proposed. It was described how to achieve a reasonable orientation process based on different historical images which have poor properties like: low image resolution, noise, different brightness, etc.

Furthermore, it was revealed how to overcome different challenges related to recognition and detection process of objects included in the images. This led to reduce the misinterpretation of the data extracted from historical images and therefore to create a reasonable 3D city model which enables to give a digital representation about historic Baalbek and its entities as well as to document the historic city and its remains as they looked like.

- **Contribution for documentation of historic Baalbek**

The historic Baalbek is an important one of main standards of Arab heritages. This is due to the 5000 years of history in the city and the ancient building remains. As such historic city cannot be ignored in any serious effort toward the documentation of cultural heritages. Therefore, in this work, the documentation of historic Baalbek was achieved. This

documentation relied on different aspects such as the usage of historical photos, the generation of a 3D city model, etc.

However, the abovementioned documentation provides varied supports required for further applications (e.g. restoration). These supports could be summarized in the following points:

- Historical images
- Camera parameters and lens distortions
- Extracted data (Shapefile)
- Baalbek’s DTM
- 3D model in LOD1 and LOD2 (geometry and semantics)

• **Contribution for CityGML modelling**

The basic idea of CityGML is to reach a common definition and understanding of the basic entities, attributes and relations included in a 3D city model. This common definition includes not only the geometry of objects, but also the semantics. Geometry and semantics can be realized through standards defined by the ISO 19100 family framework for the modelling of geographic features.

So, a contribution was - in this research - introduced related to the issue: to what extent CityGML standards can be a feasible solution which can be used for - and among other -the documentation of cultural heritage sites.

Depending on results of Baalbek’s CityGML Modelling, it is so clear that CityGML provide huge supports for 3D digital representation of details to be modelled. Furthermore, it allows the semantic modelling which requires the appropriate qualification of 3D data. It gives the possibility for users (e.g. archaeologist, architects) to know what each geometric object in Baalbek model means (e.g. name, address, historic data, etc.). In that case, it enables to analyse and interpret all data available based on for e.g. the archaeology point of view.

8.3. Outlook

In the broader concept of the documentation and creation of high realistic 3D modelling of the archeological sites and historical buildings, there are still issues that request to be investigated and studied sufficiently in order to have further progress and improvements. In the context of historic Baalbek, these issues could be summarized as following:

- Further accurate measurements (e.g. GPS measurements) in Baalbek's local coordinate system can be achieved, which can be also applied in the orientation process in order to improve and verify the results of adjustment problem.
- Integration between the photogrammetric data set resulted based on Baalbek's historical images and a new data set acquired using advanced technologies like laser scanning. This integration is an essential task, due to that the 3D documentation of historical sites is interdisciplinary, therefore it should be discussed and analysed from different points of view. In addition, the usage of laser scanning in documenting of cultural heritage sites is considered an effective technique due to different advances for e.g. it allows for the fast and reliable generation of millions of 3D points representing an object scanned.
- Developing of Baalbek Web Application - generated in this research - using the innovative techniques related to. This will allow an interactive representation of a context that can be easily understood by all users.

REFERENCES

Albertz, J. & Wiggenhagen, M., (2008): Guide for Photogrammetry and Remote Sensing. Berlin/Hannover, Wichmann. Heidelberg.

Albert, J., Bachmann, M., Hellmeier, A., (2003): Zielgruppen und Anwendungen für Digitale Stadtmodelle und Digitale Geländemodelle. Erhebung im Rahmen der SIG 3D der GDI NRW (in German only); available at the following website: *http://www.ikg.uni-bonn.de/sig3d/pdf/Tabelle_Anwendung_Zielgruppen.pdf*.

Baarda, W., (1968): A Testing Procedure for Use in Geodetic Networks, Netherlands Geodetic Commission. Band 2, Nr. 5.

Brenner, C., (2003): Building Reconstruction from Laser Scanning and Images. In: Proc. ITC Workshop on Data Quality in Earth Observation Techniques. Enschede, The Netherlands, November 2003.

Brown, D. C., (1971): Close range camera calibration. Photogrammetric Engineering, 37(8), pp. 855-866.

Calier, A. H., (1942): Cameras and Equipment, Single Lens Cameras for Reconnaissance. International archives of photogrammetry and Remote Sensing, Band 9.1: pp.125-126.

Cooper, M. A. R., Robson, S., (2001): Theory of close range photogrammetry. In: Close Range Photogrammetry and Machine Vision. K. B. Atkinson. London, Whittles Publishing, Caithness, KW5 6DW, Scotland, UK.

Coors, V., Flick, S., (1998): Integrating Levels of Detail in a Web-based 3D-GIS. Proc. of ACM GIS'98 in Washington D.C., USA, ACM Press.

DEU (1998), Deutsches Institute für Normung, E. V.: Geoinformation-Datenbeschreibung-Qualität, DIN V ENV 12656, 1998.

Dörstel, C., Jacobsen, K., Stallmann, D., (2003): DMC - Photogrammetric accuracy - calibration aspects and generation of synthetic DMC images. Zürich: In: Grün, A.; Kahmen, H. (Hrsg.) Band I, pp. 74-82.

Fischer, A., Kolbe, T. H., Lang, F., Cremers, A. B., Förstner, W., Plümer, L., Steinhage, V., (1998): Extracting Buildings from Aerial Images using Hierarchical Aggregation in 2D and 3D. Computer Vision & Image Understanding, Vol. 72, No. 2, Academic Press.

Foley, J., van Dam, A., Feiner, S., Hughes, J., (1995): Computer Graphics. Principles and Practice. Addison Wesley, 2nd Ed.

Fryer, J. G., (2001): Camera calibration. In: Close Range Photogrammetry and Machine Vision. K. B. Atkinson. London, Whittles Publishing, Caithness, KW5 6DW, Scotland, UK.

Fuchs, H. (1984): Interactive Bundle Adjustment with Metric and non-Metric Images Including Terrestrial Observations and Conditions. Commission III, ISP Congress, Rio de Janeiro.

Ghilani, C. D., Wolf, P. R., (2006): Adjustment Computations Spatial Data Analysis, John Wiley & sons, Inc., Hoboken, New Jersey.

Gröger, G., Kolbe, T. H., Czerwinski, A., Nagel, C., (2008): OpenGIS City Geography Markup Language (CityGML) Implementation Specification. Version 1.0.0, OGC Doc. No. 08 - 007, Open Geospatial Consortium.

Gruber, F. J., Joeckel, R., (2005): Formelsammlung für das Vermessungswesen, B. G. Teubner Verlag / GWV Fachverlage GmbH, Wiesbaden.

Gründig, L., Bühler, W. (1985): Zur Näherungswertbestimmung und Bündelausgleichung von Konvergentaufnahmen. In: Bildmessung und Luftbildwesen 53, Heft 6, pp. 199-208.

Gründig, L., (2003a): Grundlagen der Ausgleichungsrechnung. Lecture Notes. Berlin.

Gründig, L., (2003b): Statistische Testverfahren. Lecture Notes. Berlin.

Guptill, S. C., Morrison, J. L., (1995): Elements of Spatial Quality, Elsevier Science, Kidlington, Tarrytown, Tokyo.

Gülch, E., Müller, H., (2001): New applications of semiautomatic building acquisition. In: Automatic Extraction of man-made objects from aerial and space images (III), Baltsavias, E., Grün, A., Van Gool, L. (Eds.), Balkema, Lisse.

Hell, G. (1979): Terrestrische Bildtriangulation mit Berücksichtigung zusätzlicher Beobachtungen. DKG, Reihe C, Nr. 252.

Hildebrandt, G., (1996): Fernerkundung und Luftbildmessung für Forstwirtschaft,Vegetation-skartierung und Landschaftsökologie. pp: 74-75. Karlsruhe, Wichmann Verlag.

Int03a, (2003): International Organization for Standardization: Geographic information-metadata, ISO 19115.

Isikdag, U., Zlatanova, S., (2009): Towards Defining a Framework for Automatic Generation of Buildings in CityGML Using Building Information Models. 3D Geo-Information Sciences. Seoul, Korea, Springer: Chapter 6, pp. 79-96.

Jacobsen, K. (2008): Geometry of vertical and oblique image combinations. EARSeL Symposium Istanbul.

Joos, G., (1998): Zur Qualität von objektstrukturierten Geodata. PhD-Thesis, Universität der Bundeswehr München.

Jun, L., Donghong, W., Yongsheng, Z., (2008): Triangulation of airborne three-line images using unit quaternion. The International Archives of Photogrammetry, Remote Sensing and Spatial Information Sciences. Beijing. Vol. XXXVII, Part B1: pp. 573-578.

Kalayan, H., (1969): Notes on the Heritage of Baalbek and the Beqa'a. Beirut.

Kolbe, T. H., (2009): Representing and Exchanging 3D City Models with CityGML. In: 3D Geo-Information Sciences. Seoul, Korea, Springer: chapter 2, pp.15-31.

Konecny, G., (1994): New Trends in Technology, and their Application: Photogrammetry and Remote Sensing-From Analog to Digital. Paper presented at the Thirteen United Nations Regional Cartographic Conference for Asia and the Pacific, Beijing, China.

Köninger, A., Bartel, S., (1998): 3D-GIS for Urban Purposes. Geoinformatica, 2(1), March 1998.

Köthe, R., (04/2000): http://www.scilands.de/e_index.htm. Göttingen, scilands GmbH - Gesellschaft zur Bearbeitung digitaler Landschaften.

Krämer, M., Haist, J., Reitz, T., (2007): Methods for Spatial Data Quality of 3D City Models. Europgraphics Italian Chapter Conference. Raffaele De Amicis and Giuseppe Conti (Editors).

Krauss, H., (1982): Das Bild-n-Tupel; Ein Verfahren für photogrammetrische Ingenieurvermessungen hoher Präzision im Nahbereich. DKG, Reihe C, Nr. 276.

Kraus, K., (2003): Photogrammetrie. Wien, Walter de Gruyter, Berlin·New York. Band 1, pp. 431-440.

LPS user’s Guide, Leica Geosystems, (2008): Leica Photogrammetry Suite (LPS) - User's Guide, Georgia.

Leica Geosystems Geospatial Imaging, (2005): Erdas Imagine - User's Guide. Norcross, Georgia, pp. 145-175.

Luhmann, T., (2003): Nahbereichsphotogrammetrie. Oldenburg, Wichmann.

Marshall, D., Lukacs, G., Martin, R., (2001): Robust Segmentation of Primitives from Range Data in the Presence of Geometric Degeneracy. IEEE Transactions on Pattern Analysis and Machine Intelligence, Vol. 23, no. 3, pp. 304-314.

Matthias, H. J., Kasper, P., Schneider, D., (1983): Amtliche Vermessungswerke Band 2, Triangulation 4. Ordnung, Verlag Sauerländer, Aarau, Schweiz.

Meyer, R., (1985): Albrecht Meydenbauer - Baukunst in historischen Fotografien. Leipzig, Fotokinoverlag.

Mikhail E. M. & Ackermann, F., (1976): Observations and Least Squares, IEP-Dun-Donnelley Harper & Row, Publishers, New York Hagerstown San Francisco London.

Naoum, S. & Tsanis, I. K., (2004): Ranking spatial interpolation techniques using a GIS-based DSS. Global Nest: the int. J. Vol. 6, No. 1, pp. 1-20, Printed in Greece.

Niemeier, W., (2008): Ausgleichungsrechnung. Braunschweig, de Gruyter.

Pecchioli, L., (2010): ISEE: advanced open e-learning authoring environments, Electronic Imaging & the Visual Arts - EVA 2010 Florence, Italy, V. Cappellini Pitagora Editrice Bologna (eds), pp.96-101.

Pecchioli, L., (2008): Accessing Information navigating in a 3D interactive environment. European Doctorate in Technology and Management of Cultural Heritage, XX Cycle, IMT Institute for Advanced Studies, Lucca, Italy.

Philip, G. M., Watson, D. F., (1982): A Precise Method for Determining Contoured Surfaces. In: Australian Petroleum Exploration Association Journal 22, pp. 205-212.

Pictran, Technet GmbH (2000): Pictran- User's Guide. Berlin.

Pum, D., (2003): Digitale Bildverarbeitung in der Lebensmittel und Biotechnologie. Wien. pp: 4-7.

Ragette, F., (1980): Baalbek; published by Chatto & Windus Ltd, London.

Ragia, L., (2000): A quality model for spatial objects. International Archives of Photogrammetry and Remote Sensing. Amsterdam. Vol. XXXIII. B4: pp. 855-862.

Schilcher, M., Guo, Z., Klaus, M., Roschlaub, R., (1999): Aufbau von 3D Stadtmodellen auf der Basis von 2D-GIS. Zeitschrift für Photogrammetrie und Fernerkundung (ZPF) Vol. 67, No. 3.

Schwidefsky, K., Ackermann, F., (1976): Photogrammetrie, B. G. Teubner Stuttgart, 7., neubearbeitete und erweiterte Auflage des Grundriss der Photogrammetrie.

Shepard, D., (1968): A two-dimensional interpolation function for irregularly-spaced data. In: Proceedings-1968 ACM National Conference, pp. 517-527.

Stadler, A., Kolbe, T. H., (2007): Spatio - Semantic coherence in the integration of 3D city models. In: the 5th international Symposium on Spatial Data Quality - Modelling qualities in space and time.

Temiz, M. S., Külür, S., (2008): Rectification of digital close range images: sensor models, geometric image transformations and resampling. The international Archives of Photogrammetry and Remote Sensing. Beijing, China. Vol. XXXVII, Part B5: pp. 89-94.

Tournaire, O., Soheilian, B. and Paparoditis, N. (2006). Towards a sub-decimetric georeferencing of ground-based mobile mapping systems in urban areas: matching ground-based and areai based imagery using road marks. The International Archives of

Photogrammetry, Remote Sensing and Spatial Information Sciences. Commission I symposium. Paris.

Tung, Y. K., (1983): Point Rainfall Estimation for a Mountainous Region. In: Journal of Hydraulic Engineering, 109, 1386-1393.

Van Ess, M., (1998): Heliopolis - Baalbek, Forschen in Ruinen 1898 - 1998. Berlin, Schiler Berlin.

Van Ess, M., Bunk, T., Daiber, V., Fischer-Genz, B., Henze, F., Hitzl, K., Hoebel, F., Ritter, B., Wienholz, H., (2003): Archaeological Research in Baalbek. A preliminary report on the 2001-2003 seasons, Bulletin d'Archeologie et d'Architecture Libanaise (BAAL) 7: 109-144.

Wang, Z., (1990): Principles of photogrammetry (with Remote Sensing), Press of Wuhan Technical University of Surveying and Mapping, and Publishing House of Surveying and Mapping, Beijing, China.

Ware, C., Knight, W., Wells, D., (1991): Memory Intensive Statistical Algorithms for Multi-beam Bathymetric Data. Computers & Geosciences Vol. 17, No. 7, pp. 985-993.

Watson, D. F., Philip, G. M., (1985): A Refinement of Inverse Distance Weighted Interpolation. In: Geoprocessing 2, pp. 315-327.

Wester-Ebbinghaus, W., (1978): Photogrammetrische Punktbestimmung durch Bündelausgleichung zur allseitigen Erfassung eines räumlichen Objektes. BuL46, pp. 198-204.

Wiedemann, A., (2004): Handbuch Bauwerksvermessung. Geodäsie-Photogrammetrie-Laserscanning. Berlin, Birkhäuser.

Wiegand, T., (1921-25): Baalbek. Ergebnisse der Ausgrabungen und Untersuchungen in den Jahren 1898 bis 1905. Band I-III. Berlin/Leipzig.

APPENDIX

Appendix A

Sketches referred to different control points measured by Tachymeter

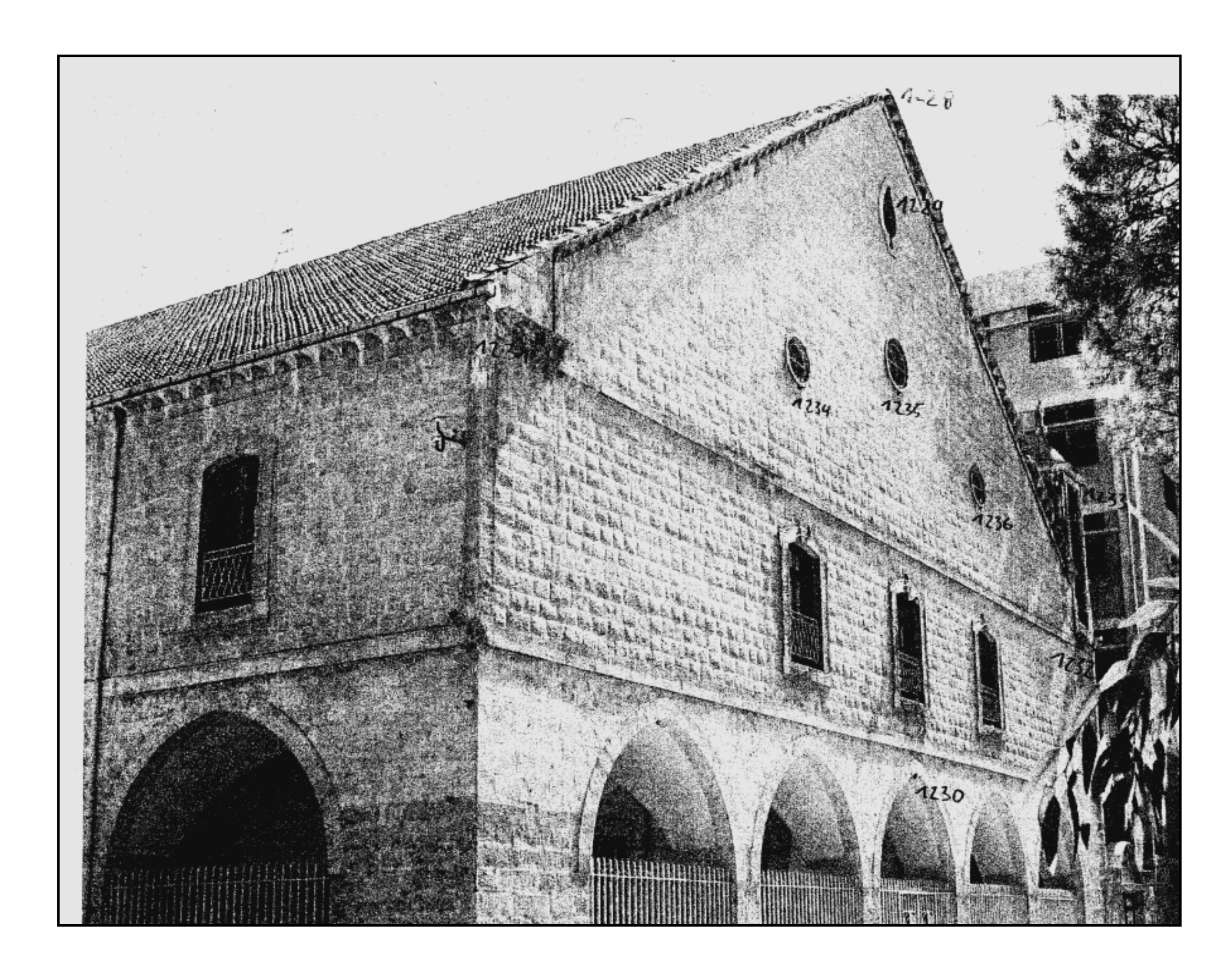

Figure (A.1): Sketch_1 showing control points like: 1230, 1236. 1234 etc. which were measured using Tachymeter in the local coordinate system in Baalbek (source: Department for Surveying BTU-Cottbus)

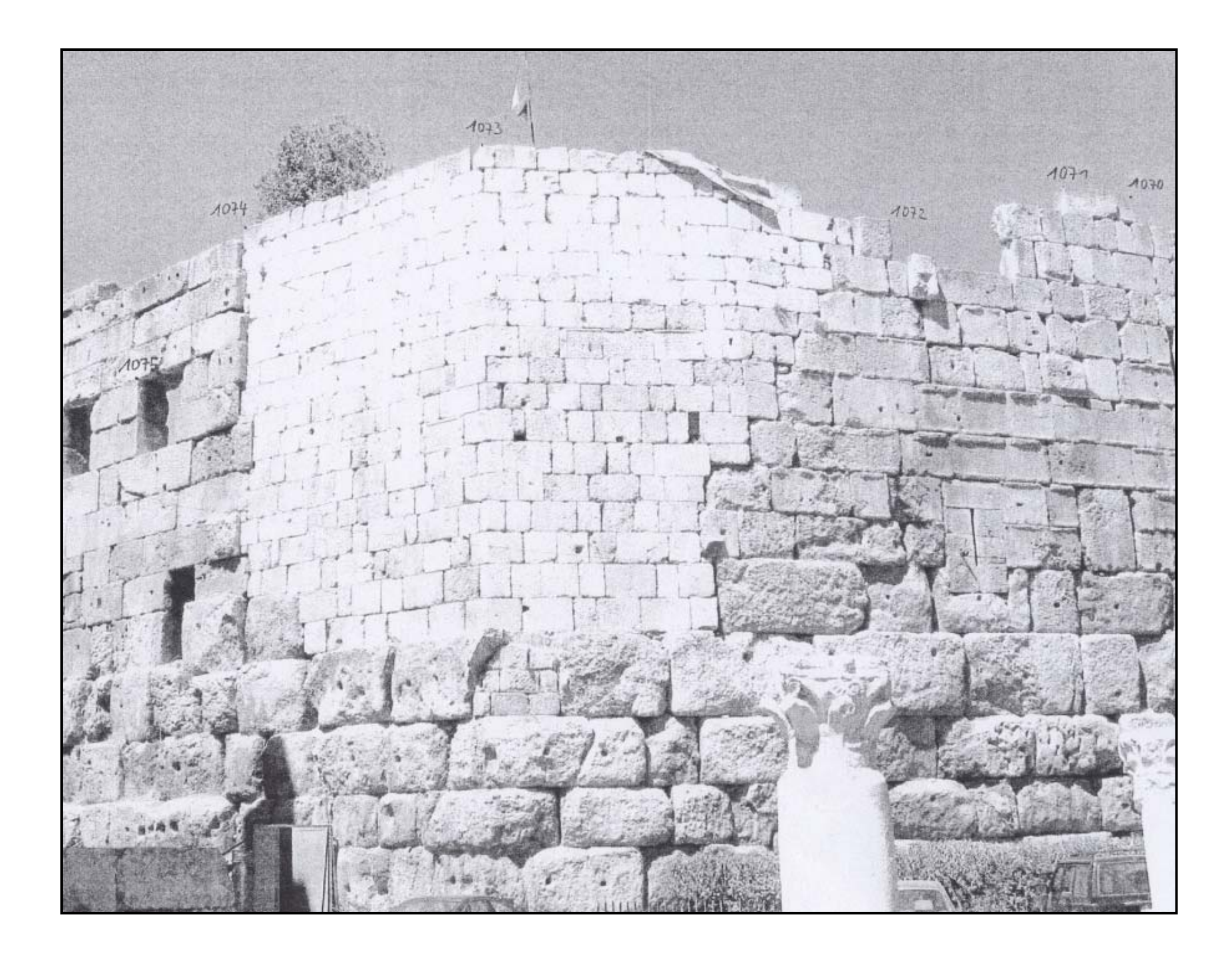

Figure (A.2): Sketch_2 showing control points like: 1070, 1071. 1234 etc. which were measured using Tachymeter in the local coordinate system in Baalbek (source: Department for Surveying BTU-Cottbus)

Appendix B

Fiducial point	Reference coordinates (mm)		Measured coordinates $(pixel)$	
	x	y	x'	y'
1	0.0000	55.0000	3098.0000	367.0000
2	80.0000	0.0000	5895.6250	2396.3750
3	0.0000	-55.0000	3123.2500	4463.2500
4	-80.0000	0.0000	317.7500	2426.4167

Table (B.1): Coordinates of fiducial marks in pixel and ideal system

$\text{Sigma}_0 = 0.78733$

Transformation parameters:

0.028741	-0.000177	-88.998937
-0.000145	-0.026853	65.252615

Appendix C

PROGRAM SYSTEM PICTRAN-B (VERSION4.3 (C) TECHNET (1995-1998)

OUTPUT OF MODULE BUNBIL

BUNDLE ADJUSTMENT

PROJECT: Baalbek's Vertical Images

```
LEGEND OF THE MODULE BUNBIL

V    = RESIDUAL
MFV  = STANDARD DEVIATION OF OBSERVATIONS A PRIORI
EV   = REDUNDANCY NUMBER
GF   = PROBABLE DIMENSION OF A BLUNDER
EK   = DISPLACEMENT IF OBSERVATION DOES NOT TAKE PART OF THE ADJUSTMENT
NV   = NORMALIZED RESIDUAL
GRZW = THRESHOLD VALUE FOR NOT TRACEABLE BLUNDERS
EGK  = EFFECT OF GRZW ON THE RELATIVE POSITION
M    = STANDARD DEVIATION OF UNKNOWNS
STA  = STATE (0=FIX, 1=UNKNOWN, 2=OBSERVED)
**   = BLUNDER IS SUPPOSED
```

IMAGE- AND OBJECT DATA

NU. OF IMAGES	14
NU. OF IMAGE POINTS	153
NU. OF OBJECT POINTS	51
NU. OF CONTROL POINTS	36
NU. OF CAMERAS	1
NU. OF PLANES	0
NU. OF DISTANCES	0
NU. OF DIFFERENCES	0

ITERATIONS

ITERATION	UNKNOWNS	RIGHT SIDE	TIME [s]
1	0.1000E+11	0.1818E+12	0.01
2	0.7506E+01	0.2894E+10	0.03
3	0.6297E-01	0.9368E+07	0.04
4	0.1407E-02	0.1246E+07	0.04
5	0.1306E-03	0.6487E+05	0.06
6	0.8825E-05	0.8434E+04	0.08
7	0.8804E-06	0.4390E+03	0.09
8	0.5963E-07	0.5707E+02	0.11

DATA OF THE ADJUSTMENT

OBSERVATIONS (OB)	549
UNKNOWNS (UN)	305
NU. CONSTR. EQUATIONS (CON)	14
REDUNDANCY (OB-UN+CON)	258
SUM OF REDUNDANCY NUMBERS	258.000
NU. OF DIAGONAL SUBMATRICES	219
NU. OF ALL SUBMATRICES	939
NU. OF ALL SINGLE ELEMENTS	12207

OBJECT COORDINATES

POINT-NU	X / Y / Z	BEOBX / BEOBY / BEOBZ	VX / VY / VZ	MFVX / MFVY / MFVZ	EVX / EVY / EVZ	GFX / GFY / GFZ	EKX / EKY / EKZ	NVX / NVY / NVZ	GRZWX / GRZWY / GRZWZ	EGKX / EGKY / EGKZ	MX / MY / MZ	STAX / STAY / STAZ
5026	10125.234849	10125.054537	0.1803	0.5000	0.313	-0.575	-0.395	0.644	3.689	2.533	0.3424	2
	10711.965651	10712.091391	-0.1257	0.5000	0.319	0.394	0.268	0.445	3.655	2.488	0.3409	2
	1159.213004	1159.162952	0.0501	0.5000	0.024	-2.068	-2.018	0.643	13.273	12.952	0.4082	2
5027	10025.176834	10025.471748	-0.2949	0.5000	0.217	1.356	1.061	1.265	4.428	3.465	0.3655	2
	10467.160067	10467.091392	0.0687	0.5000	0.214	-0.320	-0.251	0.297	4.459	3.502	0.3662	2
	1162.507849	1162.524233	-0.0164	0.5000	0.027	0.600	0.584	0.198	12.496	12.155	0.4075	2
5010	9667.272549	9667.051002	0.2215	0.5000	0.194	-1.145	-0.923	1.007	4.694	3.786	0.3711	2
	10635.163952	10635.295018	-0.1311	0.5000	0.196	0.668	0.537	0.592	4.663	3.748	0.3705	2
	1142.615488	1142.635128	-0.0196	0.5000	0.011	1.755	1.735	0.371	19.519	19.300	0.4109	2
5011	9672.541012	9672.346554	0.1945	0.5000	0.199	-0.980	-0.785	0.873	4.635	3.715	0.3699	2
	10614.115124	10614.233187	-0.1181	0.5000	0.202	0.584	0.466	0.525	4.594	3.665	0.3691	2
	1143.425553	1143.438073	-0.0125	0.5000	0.010	1.240	1.228	0.249	20.552	20.345	0.4111	2
5012	9516.316211	9516.171137	0.1451	0.5000	0.165	-0.877	-0.732	0.713	5.078	4.238	0.3775	2
	10627.226897	10627.612981	-0.3861	0.5000	0.175	2.209	1.823	1.847	4.939	4.076	0.3754	2
	1156.275652	1156.345672	-0.0700	0.5000	0.020	3.532	3.462	0.995	14.667	14.376	0.4091	2
5013	9738.324918	9738.059774	0.2651	0.5000	0.194	-1.364	-1.098	1.203	4.683	3.772	0.3709	2
	10647.396700	10647.411481	-0.0148	0.5000	0.196	0.075	0.061	0.067	4.666	3.752	0.3705	2
	1140.263137	1140.248962	0.0142	0.5000	0.010	-1.396	-1.382	0.281	20.492	20.284	0.4111	2
5014	9686.082138	9686.278919	-0.1968	0.5000	0.280	0.702	0.505	0.743	3.900	2.807	0.3505	2
	10322.382577	10322.447764	-0.0652	0.5000	0.286	0.228	0.162	0.244	3.859	2.753	0.3490	2
	1145.656345	1145.595395	0.0610	0.5000	0.030	-2.029	-1.969	0.703	11.916	11.558	0.4069	2
5015	9736.056904	9736.276893	-0.2200	0.5000	0.285	0.773	0.553	0.825	3.871	2.769	0.3495	2
	10308.649779	10308.590641	0.0591	0.5000	0.291	-0.203	-0.144	0.219	3.830	2.717	0.3480	2
	1153.745552	1153.728275	0.0173	0.5000	0.035	-0.488	-0.471	0.184	10.973	10.585	0.4058	2
5000	9615.097723	9615.173183	-0.0755	0.5000	0.179	0.423	0.347	0.357	4.886	4.014	0.3745	2
	10025.491399	10025.358059	0.1333	0.5000	0.200	-0.665	-0.532	0.596	4.613	3.688	0.3695	2
	1177.546917	1177.603267	-0.0563	0.5000	0.043	1.300	1.244	0.541	9.919	9.489	0.4041	2
5001	9609.789619	9609.860935	-0.0713	0.5000	0.178	0.400	0.329	0.338	4.892	4.021	0.3746	2
	10031.297008	10031.177351	0.1197	0.5000	0.199	-0.601	-0.481	0.536	4.626	3.705	0.3698	2
	1168.194399	1168.244753	-0.0504	0.5000	0.041	1.232	1.182	0.498	10.216	9.799	0.4047	2
5002	9521.355210	9521.473975	-0.1188	0.5000	0.160	0.741	0.622	0.593	5.158	4.331	0.3786	2
	9968.862158	9968.943050	-0.0809	0.5000	0.167	0.485	0.404	0.396	5.058	4.215	0.3772	2
	1076.393487	1076.408245	-0.0148	0.5000	0.023	0.643	0.628	0.195	13.633	13.320	0.4084	2
5003	9524.749304	9524.862488	-0.1132	0.5000	0.162	0.701	0.588	0.563	5.138	4.308	0.3784	2
	9975.511997	9975.585043	-0.0730	0.5000	0.169	0.433	0.360	0.356	5.027	4.179	0.3767	2
	1079.528652	1079.544661	-0.0160	0.5000	0.023	0.691	0.675	0.210	13.564	13.250	0.4084	2
5004	9659.600076	9659.613878	-0.0138	0.5000	0.172	0.080	0.067	0.067	4.982	4.126	0.3760	2
	10088.985845	10088.749159	0.2367	0.5000	0.200	-1.182	-0.946	1.058	4.615	3.692	0.3695	2
	1183.463116	1183.494726	-0.0316	0.5000	0.048	0.664	0.633	0.290	9.466	9.016	0.4032	2
5005	9667.923941	9667.942348	-0.0184	0.5000	0.169	0.109	0.090	0.089	5.019	4.170	0.3766	2
	10082.467510	10082.207060	0.2605	0.5000	0.201	-1.296	-1.036	1.162	4.607	3.681	0.3694	2
	1195.398760	1195.437668	-0.0389	0.5000	0.050	0.772	0.733	0.347	9.200	8.737	0.4027	2

IMAGE COORDINATES

SYSTEM-NU	POINT-NU	X / Y	BEOBX / BEOBY	VX / VY	MFVX / MFVY	EVX / EVY	GFX / GFY	EKX / EKY	NVX / NVY	GRZWX / GRZWY	EGKX / EGKY
1981	1002	-23.108850	-23.246600	0.1377	0.3000	0.823	-0.167	-0.030	0.506	1.366	0.242
		10.800981	10.778000	0.0230	0.3000	0.828	-0.028	-0.005	0.084	1.361	0.234
1981	1003	-23.676760	-23.792300	0.1155	0.3000	0.828	-0.140	-0.024	0.423	1.362	0.235
		9.674592	9.588100	0.0865	0.3000	0.832	-0.104	-0.017	0.316	1.358	0.228
1981	1077	-15.888516	-16.031400	0.1429	0.3000	0.522	-0.274	-0.131	0.659	1.716	0.821
		52.582650	52.886900	-0.3043	0.3000	0.561	0.542	0.238	1.354	1.654	0.726

1981	4027	-67.937640	-67.787200	-0.1504	0.3000	0.704	0.214	0.063	0.598	1.477	0.437
		-47.063267	-47.055100	-0.0082	0.3000	0.746	0.011	0.003	0.032	1.435	0.365
1981	4028	-42.702624	-42.623600	-0.0790	0.3000	0.857	0.092	0.013	0.285	1.338	0.191
		-33.250928	-33.267900	0.0170	0.3000	0.873	-0.019	-0.002	0.061	1.326	0.169
1981	4029	-52.373469	-52.373200	-0.0003	0.3000	0.858	0.000	0.000	0.001	1.338	0.190
		-30.386078	-30.403900	0.0178	0.3000	0.871	-0.020	-0.003	0.064	1.328	0.171
1981	4030	-23.301676	-23.217900	-0.0838	0.3000	0.839	0.100	0.016	0.305	1.353	0.218
		-31.864991	-32.001900	0.1369	0.3000	0.840	-0.163	-0.026	0.498	1.352	0.217
1981	4041	-65.193038	-65.224200	0.0312	0.3000	0.828	-0.038	-0.006	0.114	1.362	0.234
		-29.635624	-29.629100	-0.0065	0.3000	0.835	0.008	0.001	0.024	1.356	0.223
1981	5026	-29.899978	-30.196200	0.2962	0.3000	0.712	-0.416	-0.120	1.170	1.468	0.422
		-46.431864	-46.667700	0.2358	0.3000	0.721	-0.327	-0.091	0.926	1.459	0.407
1981	5027	-75.249607	-74.880300	-0.3693	0.3000	0.631	0.585	0.216	1.550	1.560	0.575
		6.438561	6.627300	-0.1887	0.3000	0.682	0.277	0.088	0.762	1.500	0.477
1982	1002	-21.248375	-21.168400	-0.0800	0.3000	0.757	0.106	0.026	0.306	1.424	0.347
		-37.298755	-37.519400	0.2206	0.3000	0.793	-0.278	-0.058	0.826	1.392	0.288
1982	1003	-21.965410	-21.888200	-0.0772	0.3000	0.752	0.103	0.025	0.297	1.429	0.355
		-38.170716	-38.377500	0.2068	0.3000	0.789	-0.262	-0.055	0.776	1.395	0.295
1982	1077	-6.142177	-5.801300	-0.3409	0.3000	0.865	0.394	0.053	1.222	1.332	0.180
		-3.459086	-3.446100	-0.0130	0.3000	0.851	0.015	0.002	0.047	1.343	0.201
1982	1110	-29.322022	-29.436200	0.1142	0.3000	0.897	-0.127	-0.013	0.402	1.308	0.135
		26.019563	25.823400	0.1962	0.3000	0.900	-0.218	-0.022	0.689	1.306	0.130
1982	1116	-10.344355	-10.242300	-0.1021	0.3000	0.886	0.115	0.013	0.361	1.316	0.150
		18.729507	18.912900	-0.1834	0.3000	0.868	0.211	0.028	0.656	1.330	0.176
1982	1136	-58.473912	-58.718800	0.2449	0.3000	0.818	-0.299	-0.054	0.902	1.370	0.249
		-12.944966	-12.436100	-0.5089	0.3000	0.829	0.613	0.105	1.862	1.360	0.232
1982	1142	-58.364699	-58.524500	0.1598	0.3000	0.817	-0.196	-0.036	0.589	1.371	0.251
		-13.426552	-12.810700	-0.6159	0.3000	0.829	0.743	0.127	2.255	1.361	0.233
1982	1147	-20.646737	-20.704200	0.0575	0.3000	0.773	-0.074	-0.017	0.218	1.409	0.319
		56.006161	56.129200	-0.1230	0.3000	0.779	0.158	0.035	0.465	1.404	0.310
1982	1151	-24.436432	-24.285000	-0.1514	0.3000	0.780	0.194	0.043	0.571	1.403	0.308
		55.221332	55.288100	-0.0668	0.3000	0.788	0.085	0.018	0.251	1.396	0.296
1982	1208	-7.551976	-7.377600	-0.1744	0.3000	0.874	0.199	0.025	0.622	1.325	0.167
		23.544106	23.748400	-0.2043	0.3000	0.854	0.239	0.035	0.737	1.341	0.196
1982	4019	-51.912340	-51.945800	0.0335	0.3000	0.844	-0.040	-0.006	0.121	1.349	0.210
		32.513348	31.812100	0.7012	0.3000	0.850	-0.825	-0.123	2.535**	1.344	0.201
1982	4020	-54.387975	-54.695300	0.3073	0.3000	0.864	-0.356	-0.048	1.102	1.333	0.181
		21.863911	21.487300	0.3766	0.3000	0.861	-0.438	-0.061	1.353	1.335	0.186
1991	1002	22.850551	22.528700	0.3219	0.3000	0.737	-0.437	-0.115	1.249	1.443	0.379
		40.666398	41.054800	-0.3884	0.3000	0.768	0.506	0.118	1.478	1.414	0.328
1991	1110	48.882194	48.850400	0.0318	0.3000	0.879	-0.036	-0.004	0.113	1.321	0.159
		-26.765848	-26.653500	-0.1123	0.3000	0.907	0.124	0.011	0.393	1.301	0.121
1991	1116	26.492811	26.020600	0.4722	0.3000	0.887	-0.532	-0.060	1.671	1.316	0.149
		-23.939877	-24.033900	0.0940	0.3000	0.907	-0.104	-0.010	0.329	1.301	0.121
1991	1136	71.231794	71.314500	-0.0827	0.3000	0.774	0.107	0.024	0.313	1.408	0.318
		22.984883	22.608100	0.3768	0.3000	0.811	-0.465	-0.088	1.395	1.376	0.261
1991	1142	70.989225	70.913000	0.0762	0.3000	0.772	-0.099	-0.022	0.289	1.410	0.321
		23.497064	23.208400	0.2887	0.3000	0.809	-0.357	-0.068	1.070	1.377	0.262
1991	1208	24.787292	24.213700	0.5736	0.3000	0.881	-0.651	-0.077	2.037	1.320	0.157
		-29.712676	-29.873500	0.1608	0.3000	0.899	-0.179	-0.018	0.565	1.306	0.131
1991	4019	75.101300	75.473200	-0.3719	0.3000	0.840	0.443	0.071	1.353	1.352	0.217
		-28.268228	-27.820100	-0.4481	0.3000	0.845	0.530	0.082	1.625	1.348	0.209
1991	4020	75.395221	75.674000	-0.2788	0.3000	0.857	0.325	0.046	1.004	1.338	0.191
		-16.595166	-16.168100	-0.4271	0.3000	0.857	0.498	0.071	1.538	1.338	0.192
1991	5010	-7.495527	-7.241900	-0.2536	0.3000	0.753	0.337	0.083	0.974	1.428	0.352
		-13.964820	-13.930500	-0.0343	0.3000	0.739	0.046	0.012	0.133	1.442	0.377
1991	5011	-2.385208	-2.165400	-0.2198	0.3000	0.764	0.288	0.068	0.838	1.417	0.334
		-15.291844	-15.267600	-0.0242	0.3000	0.751	0.032	0.008	0.093	1.430	0.356
1991	5012	-23.030971	-22.786800	-0.2442	0.3000	0.653	0.374	0.130	1.007	1.533	0.532
		-46.928737	-47.058100	0.1294	0.3000	0.623	-0.208	-0.078	0.546	1.569	0.591
1991	5013	-2.085296	-1.792500	-0.2928	0.3000	0.752	0.389	0.096	1.125	1.429	0.354
		2.598798	2.715200	-0.1164	0.3000	0.741	0.157	0.041	0.451	1.439	0.372
1991	5014	63.871608	63.800200	0.0714	0.3000	0.730	-0.098	-0.026	0.279	1.451	0.392
		-46.719500	-47.003600	0.2841	0.3000	0.731	-0.389	-0.105	1.108	1.449	0.390
1991	5015	73.878637	73.666300	0.2123	0.3000	0.712	-0.298	-0.086	0.839	1.469	0.424
		-38.275314	-38.489700	0.2144	0.3000	0.730	-0.294	-0.079	0.836	1.450	0.391
1993	1002	40.300502	40.351200	-0.0507	0.3000	0.629	0.081	0.030	0.213	1.562	0.579
		34.027430	34.096300	-0.0689	0.3000	0.707	0.097	0.029	0.273	1.474	0.433
1993	1003	40.936144	40.980600	-0.0445	0.3000	0.615	0.072	0.028	0.189	1.580	0.608
		35.347881	35.433500	-0.0856	0.3000	0.697	0.123	0.037	0.342	1.484	0.450
1993	1022	66.465967	66.384300	0.0817	0.3000	0.773	-0.106	-0.024	0.310	1.410	0.321
		5.813792	5.935100	-0.1213	0.3000	0.793	0.153	0.032	0.454	1.392	0.289
1993	1077	33.211928	33.199300	0.0126	0.3000	0.815	-0.015	-0.003	0.047	1.373	0.254
		-12.411126	-12.238700	-0.1724	0.3000	0.807	0.214	0.041	0.640	1.379	0.266

1993	1110	68.174014	68.215200	-0.0412	0.3000	0.663	0.062	0.021	0.169	1.521	0.512
		-37.243354	-37.125300	-0.1181	0.3000	0.702	0.168	0.050	0.470	1.479	0.440
1993	1116	44.585405	44.528000	0.0574	0.3000	0.750	-0.077	-0.019	0.221	1.431	0.358
		-35.518130	-35.842800	0.3247	0.3000	0.788	-0.412	-0.088	1.219	1.396	0.297
1993	1208	42.783849	42.782900	0.0009	0.3000	0.700	-0.001	0.000	0.004	1.481	0.445
		-41.612950	-41.846100	0.2332	0.3000	0.749	-0.311	-0.078	0.898	1.432	0.360
2026	1002	58.112597	58.103400	0.0092	0.3000	0.623	-0.015	-0.006	0.039	1.570	0.593
		-56.540383	-56.600500	0.0601	0.3000	0.539	-0.112	-0.051	0.273	1.688	0.779
2026	1003	59.541416	59.334200	0.2072	0.3000	0.607	-0.342	-0.134	0.887	1.591	0.626
		-57.240118	-57.234800	-0.0053	0.3000	0.519	0.010	0.005	0.025	1.719	0.826
2026	1077	6.219440	6.175600	0.0438	0.3000	0.759	-0.058	-0.014	0.168	1.422	0.343
		-48.541083	-48.453300	-0.0878	0.3000	0.773	0.114	0.026	0.333	1.409	0.320
2026	1116	-21.425316	-21.308800	-0.1165	0.3000	0.683	0.171	0.054	0.470	1.500	0.476
		-59.263729	-59.308200	0.0445	0.3000	0.611	-0.073	-0.028	0.190	1.585	0.617
2026	1208	-28.625702	-28.470500	-0.1552	0.3000	0.628	0.247	0.092	0.653	1.563	0.581
		-57.262398	-57.275700	0.0133	0.3000	0.535	-0.025	-0.012	0.061	1.694	0.788
1984	1003	55.147711	55.031000	0.1167	0.3000	0.365	-0.320	-0.203	0.644	2.051	1.303
		-9.378518	-9.516600	0.1381	0.3000	0.311	-0.445	-0.306	0.826	2.223	1.533
1984	1077	1.126184	0.866500	0.2597	0.3000	0.724	-0.359	-0.099	1.017	1.456	0.402
		-0.790749	-0.649200	-0.1415	0.3000	0.752	0.188	0.047	0.544	1.429	0.355
1984	1116	-27.889422	-27.890000	0.0006	0.3000	0.793	-0.001	0.000	0.002	1.391	0.288
		-13.326691	-13.301100	-0.0256	0.3000	0.823	0.031	0.006	0.094	1.366	0.242
1984	1147	-71.883865	-71.663700	-0.2202	0.3000	0.623	0.353	0.133	0.930	1.570	0.592
		-36.569554	-36.664400	0.0948	0.3000	0.626	-0.152	-0.057	0.400	1.566	0.586
1984	1151	-69.237657	-69.357900	0.1202	0.3000	0.628	-0.191	-0.071	0.506	1.563	0.581
		-40.798913	-40.752800	-0.0461	0.3000	0.628	0.073	0.027	0.194	1.564	0.583
1984	1208	-35.497044	-35.233400	-0.2636	0.3000	0.780	0.338	0.075	0.995	1.403	0.309
		-11.322883	-11.312200	-0.0107	0.3000	0.812	0.013	0.002	0.040	1.375	0.259
2025	1077	-7.670934	-7.577000	-0.0939	0.3000	0.790	0.119	0.025	0.352	1.394	0.293
		30.107697	30.515000	-0.4073	0.3000	0.760	0.536	0.129	1.557	1.421	0.341
2025	1116	-11.658124	-11.733500	0.0754	0.3000	0.717	-0.105	-0.030	0.297	1.463	0.414
		53.498089	53.733200	-0.2351	0.3000	0.729	0.323	0.087	0.918	1.451	0.393
2025	1136	-61.452872	-61.207500	-0.2454	0.3000	0.792	0.310	0.064	0.919	1.392	0.289
		21.789536	21.589100	0.2004	0.3000	0.794	-0.253	-0.052	0.750	1.391	0.287
2025	1142	-61.340914	-61.041500	-0.2994	0.3000	0.794	0.377	0.078	1.120	1.390	0.286
		21.286984	21.144200	0.1428	0.3000	0.795	-0.180	-0.037	0.534	1.390	0.285
2025	1208	-8.679012	-8.789300	0.1103	0.3000	0.677	-0.163	-0.053	0.447	1.506	0.487
		58.540179	58.387700	0.1525	0.3000	0.681	-0.224	-0.072	0.616	1.502	0.480
2025	4028	-49.556076	-49.798700	0.2426	0.3000	0.612	-0.397	-0.154	1.034	1.584	0.615
		-37.394815	-37.599500	0.2047	0.3000	0.683	-0.299	-0.095	0.825	1.499	0.474
2025	4029	-57.088185	-57.318000	0.2298	0.3000	0.634	-0.362	-0.132	0.962	1.556	0.569
		-33.050969	-32.958600	-0.0924	0.3000	0.691	0.134	0.041	0.371	1.491	0.461
2033	1077	27.012881	26.907400	0.1055	0.3000	0.295	-0.357	-0.252	0.647	2.280	1.607
		-15.485675	-15.526800	0.0411	0.3000	0.091	-0.452	-0.411	0.454	4.107	3.733
2033	1116	-12.700165	-12.683900	-0.0163	0.3000	0.606	0.027	0.011	0.070	1.592	0.628
		-37.357014	-37.376500	0.0195	0.3000	0.593	-0.033	-0.013	0.084	1.609	0.655
2033	1208	-23.753082	-23.664900	-0.0882	0.3000	0.522	0.169	0.081	0.407	1.715	0.820
		-35.968180	-35.911700	-0.0565	0.3000	0.408	0.138	0.082	0.295	1.940	1.148
1983	1110	-25.414758	-25.378900	-0.0359	0.3000	0.925	0.039	0.003	0.124	1.288	0.096
		-3.013791	-2.944600	-0.0692	0.3000	0.937	0.074	0.005	0.238	1.280	0.081
1983	1116	-6.817985	-6.210100	-0.6079	0.3000	0.916	0.664	0.056	2.117	1.295	0.109
		-10.316083	-10.213900	-0.1022	0.3000	0.917	0.111	0.009	0.356	1.294	0.108
1983	1136	-54.247410	-54.002900	-0.2445	0.3000	0.822	0.298	0.053	0.899	1.367	0.243
		-40.593598	-40.281700	-0.3119	0.3000	0.830	0.376	0.064	1.141	1.360	0.231
1983	1142	-54.150089	-53.888000	-0.2621	0.3000	0.820	0.320	0.058	0.965	1.368	0.246
		-41.059880	-40.773600	-0.2863	0.3000	0.828	0.346	0.059	1.048	1.361	0.234
1983	1147	-16.306846	-16.009900	-0.2969	0.3000	0.887	0.335	0.038	1.051	1.316	0.149
		26.602654	26.672300	-0.0696	0.3000	0.894	0.078	0.008	0.246	1.310	0.139
1983	1208	-3.968111	-3.338400	-0.6297	0.3000	0.915	0.689	0.059	2.195	1.296	0.111
		-5.596247	-5.404100	-0.1921	0.3000	0.913	0.210	0.018	0.670	1.296	0.112
1983	1239	-64.489791	-64.714400	0.2246	0.3000	0.874	-0.257	-0.032	0.801	1.325	0.167
		-5.861961	-5.738900	-0.1231	0.3000	0.881	0.140	0.017	0.437	1.320	0.158
1983	1240	-64.802843	-65.202600	0.3998	0.3000	0.872	-0.458	-0.059	1.427	1.327	0.170
		0.113016	0.082000	0.0310	0.3000	0.880	-0.035	-0.004	0.110	1.321	0.159
1983	4015	-39.210691	-39.213500	0.0028	0.3000	0.843	-0.003	-0.001	0.010	1.349	0.212
		38.956075	38.642000	0.3141	0.3000	0.851	-0.369	-0.055	1.135	1.343	0.200
1983	4016	-44.750085	-44.842100	0.0920	0.3000	0.838	-0.110	-0.018	0.335	1.353	0.219
		37.537465	37.002300	0.5352	0.3000	0.849	-0.631	-0.095	1.937	1.345	0.204
1983	4019	-47.345911	-47.656300	0.3104	0.3000	0.922	-0.337	-0.026	1.078	1.290	0.101
		3.105357	3.115400	-0.0100	0.3000	0.921	0.011	0.001	0.035	1.291	0.101
1983	4020	-49.965579	-50.248100	0.2825	0.3000	0.918	-0.308	-0.025	0.983	1.293	0.106
		-7.343368	-7.344400	0.0010	0.3000	0.916	-0.001	0.000	0.004	1.294	0.108
1983	5010	20.642246	20.518500	0.1237	0.3000	0.769	-0.161	-0.037	0.471	1.413	0.327
		-25.282869	-25.442500	0.1596	0.3000	0.761	-0.210	-0.050	0.610	1.421	0.340
1983	5011	16.469408	16.354500	0.1149	0.3000	0.782	-0.147	-0.032	0.433	1.401	0.306

		-23.059991	-23.201600	0.1416	0.3000	0.774	-0.183	-0.041	0.537	1.408	0.318
1983	5012	43.258527	42.867700	0.3908	0.3000	0.684	-0.571	-0.180	1.575	1.498	0.473
		-0.172196	-0.116100	-0.0561	0.3000	0.684	0.082	0.026	0.226	1.498	0.473
1983	5013	11.752641	11.788400	-0.0358	0.3000	0.764	0.047	0.011	0.136	1.417	0.334
		-38.178740	-38.450700	0.2720	0.3000	0.757	-0.359	-0.087	1.042	1.424	0.345
1983	5014	-33.816111	-33.843300	0.0272	0.3000	0.827	-0.033	-0.006	0.100	1.362	0.235
		18.647643	18.719800	-0.0722	0.3000	0.836	0.086	0.014	0.263	1.355	0.222
1983	5015	-44.200277	-44.325100	0.1248	0.3000	0.829	-0.151	-0.026	0.457	1.361	0.233
		12.506048	12.652900	-0.1469	0.3000	0.836	0.176	0.029	0.536	1.355	0.223
1985	1110	-22.649303	-22.557200	-0.0921	0.3000	0.899	0.102	0.010	0.324	1.306	0.131
		-51.883125	-51.906600	0.0235	0.3000	0.899	-0.026	-0.003	0.083	1.306	0.131
1985	1116	-4.239285	-3.704700	-0.5346	0.3000	0.854	0.626	0.091	1.928	1.340	0.195
		-59.457418	-59.105900	-0.3515	0.3000	0.835	0.421	0.069	1.282	1.356	0.223
1985	1147	-13.482133	-13.209600	-0.2725	0.3000	0.920	0.296	0.024	0.947	1.292	0.104
		-22.487301	-22.401700	-0.0856	0.3000	0.904	0.095	0.009	0.300	1.303	0.125
1985	1208	-1.386513	-0.872500	-0.5140	0.3000	0.859	0.598	0.084	1.848	1.336	0.188
		-54.864052	-54.736800	-0.1273	0.3000	0.846	0.150	0.023	0.461	1.347	0.207
1985	1239	-60.818014	-61.206300	0.3883	0.3000	0.810	-0.479	-0.091	1.438	1.376	0.261
		-54.643712	-54.544500	-0.0992	0.3000	0.826	0.120	0.021	0.364	1.363	0.237
1985	1240	-61.134633	-61.492400	0.3578	0.3000	0.848	-0.422	-0.064	1.295	1.345	0.204
		-49.006942	-48.801500	-0.2054	0.3000	0.861	0.239	0.033	0.738	1.335	0.185
1985	4008	-52.360544	-52.252100	-0.1084	0.3000	0.763	0.142	0.034	0.414	1.419	0.337
		42.772056	42.426500	0.3456	0.3000	0.780	-0.443	-0.097	1.304	1.403	0.308
1985	4009	-53.822385	-53.682500	-0.1399	0.3000	0.764	0.183	0.043	0.533	1.417	0.334
		41.356308	40.942700	0.4136	0.3000	0.786	-0.526	-0.113	1.555	1.398	0.299
1985	4010	-43.392492	-43.498100	0.1056	0.3000	0.882	-0.120	-0.014	0.375	1.319	0.156
		18.722898	18.712700	0.0102	0.3000	0.894	-0.011	-0.001	0.036	1.310	0.139
1985	4012	-39.806010	-39.922100	0.1161	0.3000	0.909	-0.128	-0.012	0.406	1.299	0.118
		6.223508	6.375000	-0.1515	0.3000	0.914	0.166	0.014	0.528	1.296	0.112
1985	4013	-41.281672	-41.495500	0.2138	0.3000	0.911	-0.235	-0.021	0.747	1.298	0.116
		4.783569	4.891100	-0.1075	0.3000	0.914	0.118	0.010	0.375	1.296	0.111
1985	4015	-35.991240	-36.203100	0.2119	0.3000	0.929	-0.228	-0.016	0.733	1.286	0.091
		-10.360879	-10.304400	-0.0565	0.3000	0.929	0.061	0.004	0.195	1.285	0.091
1985	4016	-41.465288	-41.695800	0.2305	0.3000	0.930	-0.248	-0.017	0.797	1.285	0.090
		-12.051221	-12.145400	0.0942	0.3000	0.930	-0.101	-0.007	0.326	1.285	0.090
1985	4017	39.641814	39.950700	-0.3089	0.3000	0.652	0.473	0.165	1.275	1.534	0.533
		17.856503	17.641100	0.2154	0.3000	0.653	-0.330	-0.114	0.888	1.533	0.532
1985	4019	-44.191145	-44.499400	0.3083	0.3000	0.906	-0.340	-0.032	1.079	1.301	0.122
		-46.015217	-45.943800	-0.0714	0.3000	0.911	0.078	0.007	0.249	1.298	0.115
1985	4020	-46.826887	-46.988200	0.1613	0.3000	0.878	-0.184	-0.022	0.574	1.322	0.161
		-56.408483	-56.330600	-0.0779	0.3000	0.876	0.089	0.011	0.277	1.324	0.164
1985	5014	-30.724647	-30.710400	-0.0142	0.3000	0.845	0.017	0.003	0.052	1.348	0.209
		-30.037944	-30.088800	0.0509	0.3000	0.845	-0.060	-0.009	0.184	1.348	0.209
1985	5015	-40.973650	-40.837600	-0.1360	0.3000	0.835	0.163	0.027	0.496	1.356	0.223
		-36.334927	-36.463700	0.1288	0.3000	0.841	-0.153	-0.024	0.468	1.351	0.215
1980	1147	7.770013	7.695700	0.0743	0.3000	0.801	-0.093	-0.018	0.277	1.384	0.276
		53.874455	53.783700	0.0908	0.3000	0.791	-0.115	-0.024	0.340	1.393	0.292
1980	4008	47.896824	47.550700	0.3461	0.3000	0.868	-0.399	-0.053	1.238	1.330	0.176
		-9.504546	-9.244900	-0.2596	0.3000	0.893	0.291	0.031	0.916	1.311	0.141
1980	4009	49.307127	49.000000	0.3071	0.3000	0.874	-0.352	-0.044	1.095	1.325	0.167
		-7.866749	-7.586300	-0.2804	0.3000	0.894	0.314	0.033	0.988	1.310	0.138
1980	4010	38.237732	38.304300	-0.0666	0.3000	0.916	0.073	0.006	0.232	1.295	0.109
		13.985797	14.057700	-0.0719	0.3000	0.925	0.078	0.006	0.249	1.288	0.097
1980	4012	34.337819	34.275400	0.0624	0.3000	0.914	-0.068	-0.006	0.218	1.296	0.112
		26.263049	26.130500	0.1325	0.3000	0.921	-0.144	-0.011	0.460	1.291	0.102
1980	4013	35.757220	35.724600	0.0326	0.3000	0.914	-0.036	-0.003	0.114	1.296	0.112
		27.846064	27.626000	0.2201	0.3000	0.921	-0.239	-0.019	0.764	1.291	0.102
1980	4015	30.041662	30.391300	-0.3496	0.3000	0.880	0.397	0.048	1.243	1.321	0.159
		42.013749	42.118800	-0.1051	0.3000	0.889	0.118	0.013	0.371	1.314	0.146
1980	4016	35.321494	35.927500	-0.6060	0.3000	0.873	0.694	0.088	2.162	1.326	0.169
		43.852054	44.158100	-0.3060	0.3000	0.882	0.347	0.041	1.086	1.319	0.156
1980	4017	-45.520270	-45.434800	-0.0855	0.3000	0.579	0.148	0.062	0.374	1.629	0.686
		14.326278	13.921800	0.4045	0.3000	0.492	-0.822	-0.417	1.922	1.766	0.896
1980	5000	66.887519	66.826100	0.0614	0.3000	0.776	-0.079	-0.018	0.232	1.406	0.315
		7.315396	7.287200	0.0282	0.3000	0.789	-0.036	-0.008	0.106	1.394	0.294
1980	5001	64.198001	64.159400	0.0386	0.3000	0.788	-0.049	-0.010	0.145	1.396	0.296
		6.932419	6.960900	-0.0285	0.3000	0.800	0.036	0.007	0.106	1.386	0.278
1980	5002	54.312890	54.275400	0.0375	0.3000	0.748	-0.050	-0.013	0.144	1.432	0.361
		-18.849732	-19.196800	0.3471	0.3000	0.772	-0.449	-0.102	1.316	1.410	0.321
1980	5003	53.957913	53.927500	0.0304	0.3000	0.755	-0.040	-0.010	0.117	1.426	0.349
		-17.336176	-17.646900	0.3107	0.3000	0.778	-0.399	-0.088	1.174	1.404	0.311
1980	5004	62.690685	62.630400	0.0603	0.3000	0.780	-0.077	-0.017	0.228	1.403	0.309
		24.643014	24.859300	-0.2163	0.3000	0.794	0.272	0.056	0.809	1.391	0.287
1980	5005	66.193497	66.130400	0.0631	0.3000	0.759	-0.083	-0.020	0.241	1.423	0.344
		25.740337	25.967400	-0.2271	0.3000	0.776	0.292	0.065	0.859	1.406	0.315

1989	4005	-36.945705	-36.696900	-0.2488	0.3000	0.765	0.325	0.076	0.948	1.416	0.332
		40.305070	40.249200	0.0559	0.3000	0.798	-0.070	-0.014	0.208	1.387	0.280
1989	4006	-40.835993	-40.597500	-0.2385	0.3000	0.765	0.312	0.073	0.909	1.417	0.333
		40.410357	40.713800	-0.3034	0.3000	0.795	0.382	0.078	1.134	1.390	0.285
1989	4007	-61.134277	-61.735200	0.6009	0.3000	0.736	-0.816	-0.215	2.334	1.444	0.381
		35.269358	35.657100	-0.3877	0.3000	0.769	0.504	0.116	1.474	1.413	0.326
1989	4008	-34.861356	-34.890100	0.0287	0.3000	0.919	-0.031	-0.003	0.100	1.292	0.104
		-20.383654	-20.459400	0.0757	0.3000	0.916	-0.083	-0.007	0.264	1.294	0.108
1989	4009	-36.251385	-36.438800	0.1874	0.3000	0.920	-0.204	-0.016	0.651	1.292	0.103
		-21.956191	-22.263500	0.3073	0.3000	0.917	-0.335	-0.028	1.070	1.294	0.107
1989	4010	-26.514200	-26.630000	0.1158	0.3000	0.904	-0.128	-0.012	0.406	1.303	0.125
		-43.508438	-43.665900	0.1575	0.3000	0.910	-0.173	-0.016	0.550	1.299	0.117
1989	4012	-23.154010	-23.188300	0.0343	0.3000	0.876	-0.039	-0.005	0.122	1.323	0.164
		-55.860433	-55.747500	-0.1129	0.3000	0.881	0.128	0.015	0.401	1.320	0.157
1989	4013	-24.578677	-24.679700	0.1010	0.3000	0.873	-0.116	-0.015	0.360	1.326	0.169
		-57.443324	-57.278200	-0.1651	0.3000	0.877	0.188	0.023	0.588	1.323	0.163
1989	4017	55.385560	55.138600	0.2470	0.3000	0.549	-0.450	-0.203	1.111	1.672	0.755
		-45.428420	-45.551900	0.1235	0.3000	0.534	-0.231	-0.108	0.563	1.696	0.791
1989	5000	-53.858812	-53.675900	-0.1829	0.3000	0.802	0.228	0.045	0.681	1.384	0.275
		-36.506309	-36.586400	0.0801	0.3000	0.809	-0.099	-0.019	0.297	1.378	0.263
1989	5001	-51.340000	-51.152000	-0.1880	0.3000	0.808	0.233	0.045	0.697	1.378	0.264
		-36.134665	-36.149100	0.0144	0.3000	0.816	-0.018	-0.003	0.053	1.372	0.253
1989	5002	-41.509538	-41.515300	0.0058	0.3000	0.819	-0.007	-0.001	0.021	1.369	0.248
		-10.894671	-11.001900	0.1072	0.3000	0.830	-0.129	-0.022	0.392	1.360	0.231
1989	5003	-41.205740	-41.199800	-0.0059	0.3000	0.821	0.007	0.001	0.022	1.368	0.245
		-12.364039	-12.450600	0.0866	0.3000	0.831	-0.104	-0.018	0.316	1.359	0.229
1989	5004	-50.699737	-50.463700	-0.2360	0.3000	0.772	0.306	0.070	0.896	1.410	0.322
		-53.811901	-53.834100	0.0222	0.3000	0.776	-0.029	-0.006	0.084	1.406	0.315
1989	5005	-54.053806	-53.790600	-0.2632	0.3000	0.753	0.350	0.086	1.011	1.428	0.353
		-54.898939	-54.927500	0.0286	0.3000	0.759	-0.038	-0.009	0.109	1.422	0.343
1986	4027	50.080001	50.141600	-0.0616	0.3000	0.878	0.070	0.009	0.219	1.322	0.161
		5.617846	5.996900	-0.3791	0.3000	0.895	0.424	0.045	1.336	1.310	0.138
1986	4028	25.888689	26.023200	-0.1345	0.3000	0.903	0.149	0.014	0.472	1.304	0.127
		-6.987902	-6.812800	-0.1751	0.3000	0.904	0.194	0.019	0.614	1.303	0.126
1986	4029	35.121768	35.189400	-0.0676	0.3000	0.903	0.075	0.007	0.237	1.304	0.126
		-9.739997	-9.532400	-0.2076	0.3000	0.909	0.228	0.021	0.726	1.300	0.119
1986	4030	7.333364	6.974900	0.3585	0.3000	0.873	-0.411	-0.052	1.279	1.326	0.169
		-7.455575	-7.275100	-0.1805	0.3000	0.855	0.211	0.031	0.651	1.340	0.195
1986	4032	-0.321378	-0.300800	-0.0206	0.3000	0.741	0.028	0.007	0.080	1.440	0.373
		45.661067	45.921500	-0.2604	0.3000	0.748	0.348	0.088	1.004	1.433	0.361
1986	4037	36.090637	35.934100	0.1565	0.3000	0.881	-0.178	-0.021	0.556	1.320	0.158
		22.230418	22.042900	0.1875	0.3000	0.895	-0.210	-0.022	0.661	1.310	0.138
1986	4038	41.854062	41.720200	0.1339	0.3000	0.819	-0.164	-0.030	0.493	1.369	0.248
		33.321469	32.622400	0.6991	0.3000	0.851	-0.821	-0.122	2.525**	1.343	0.200
1986	4041	47.332738	47.620900	-0.2882	0.3000	0.882	0.327	0.038	1.023	1.319	0.155
		-10.319877	-10.239500	-0.0804	0.3000	0.899	0.089	0.009	0.283	1.306	0.131
1986	4042	32.666181	32.468200	0.1980	0.3000	0.843	-0.235	-0.037	0.719	1.349	0.211
		-30.292058	-30.555400	0.2633	0.3000	0.857	-0.307	-0.044	0.948	1.338	0.191
1986	4045	81.235689	81.363800	-0.1281	0.3000	0.390	0.329	0.201	0.684	1.985	1.211
		-44.546924	-44.480100	-0.0668	0.3000	0.575	0.116	0.049	0.294	1.634	0.694
1986	5025	0.560453	0.587200	-0.0267	0.3000	0.644	0.042	0.015	0.111	1.544	0.550
		50.922248	51.007300	-0.0851	0.3000	0.643	0.132	0.047	0.354	1.545	0.552
1986	5026	13.596022	13.584500	0.0115	0.3000	0.797	-0.014	-0.003	0.043	1.388	0.282
		6.172683	6.058100	0.1146	0.3000	0.791	-0.145	-0.030	0.429	1.393	0.291
1986	5027	56.070155	56.185600	-0.1154	0.3000	0.651	0.177	0.062	0.477	1.536	0.537
		-44.073304	-44.208200	0.1349	0.3000	0.681	-0.198	-0.063	0.545	1.502	0.480
2032	4027	60.937456	60.734200	0.2033	0.3000	0.825	-0.246	-0.043	0.746	1.364	0.238
		-31.861258	-31.495800	-0.3655	0.3000	0.807	0.453	0.088	1.356	1.379	0.267
2032	4028	36.396214	36.348400	0.0478	0.3000	0.845	-0.057	-0.009	0.173	1.348	0.210
		-43.658074	-43.545900	-0.1122	0.3000	0.863	0.130	0.018	0.403	1.334	0.183
2032	4029	45.629450	45.791700	-0.1623	0.3000	0.822	0.197	0.035	0.596	1.366	0.243
		-46.291203	-46.422800	0.1316	0.3000	0.840	-0.157	-0.025	0.478	1.351	0.216
2032	4030	17.659864	17.461600	0.1983	0.3000	0.812	-0.244	-0.046	0.733	1.375	0.258
		-43.524674	-43.681600	0.1569	0.3000	0.794	-0.198	-0.041	0.587	1.391	0.287
2032	4032	10.258020	10.436700	-0.1787	0.3000	0.699	0.256	0.077	0.712	1.482	0.446
		7.547873	7.558500	-0.0106	0.3000	0.720	0.015	0.004	0.042	1.460	0.408
2032	4037	46.947316	46.713100	0.2342	0.3000	0.869	-0.270	-0.035	0.838	1.329	0.175
		-15.311964	-15.157600	-0.1544	0.3000	0.874	0.177	0.022	0.550	1.325	0.167
2032	4038	52.915347	52.845500	0.0698	0.3000	0.793	-0.088	-0.018	0.261	1.392	0.288
		-4.485768	-4.654500	0.1687	0.3000	0.826	-0.204	-0.036	0.619	1.363	0.237
2032	4041	57.844594	58.200600	-0.3560	0.3000	0.777	0.458	0.102	1.346	1.405	0.313
		-46.712183	-47.019800	0.3076	0.3000	0.780	-0.395	-0.087	1.161	1.403	0.309
2032	5025	11.196676	11.271600	-0.0749	0.3000	0.602	0.124	0.050	0.322	1.597	0.636
		12.605981	12.742200	-0.1362	0.3000	0.633	0.215	0.079	0.571	1.557	0.571

```
        2032           5026       24.078963       24.054700     0.0243     0.3000  0.780 -0.031 -0.007  0.092     1.403  0.308
                                 -30.666890      -30.654500    -0.0124     0.3000  0.767  0.016  0.004  0.047     1.414  0.329


------------------------------------------------ PRINCIPAL POINT AND FOCAL LENGTH ------------------------------------------------
     CAMERANAME              X0           BEOBX0         VX0      MFVX0   EVX0   GFX0   EKX0   NVX0    GRZWX0  EGKX0        MX0  STAX0
                             Y0           BEOBY0         VY0      MFVY0   EVY0   GFY0   EKY0   NVY0    GRZWY0  EGKY0        MY0  STAY0
                              C            BEOBC          VC       MFVC    EVC    GFC    EKC    NVC     GRZWC   EGKC         MC   STAC
------------------------------------------------------------------------------------------------------------------------------------

     baalbek-G1       -0.069894         0.000000     -0.0699     0.5000  0.039  1.781  1.711  0.706    10.424 10.015     0.4050      2
                      -0.049059         0.000000     -0.0491     0.5000  0.036  1.359  1.310  0.516    10.869 10.477     0.4057      2
                     200.253031       200.000000      0.2530     0.5000  0.418 -0.605 -0.352  0.782     3.193  1.857     0.3151      2

---------------------------------------------------- CONTROL OF THE ADJUSTMENT ----------------------------------------------------
                   TOTAL  IMAGE COORD    PROJ.CENT OBJECT COORD          DIS          DIF     PLANE PO  PLANE PARAM   PRINC PO+C
------------------------------------------------------------------------------------------------------------------------------------

REDUNDANCY    258.000000   240.996959    9.788426    6.720941    0.000000    0.000000    0.000000    0.000000    0.493674
     SIGMA      0.826395     0.830752    0.794084    0.712721    1.000000    1.000000    1.000000    1.000000    0.760162
      VTPV    176.195421   166.323820    6.172284    3.414050    0.000000    0.000000    0.000000    0.000000    0.285268

+----------------------------------------------------------------------------------------------------------------------------------+
| DATE :  07/03/20 10:05:31                                                                                    PAGE:      23  |
|                                                      BUNBIL-OUTPUT                                                              |
| PROJECT: GRUPPE                                                                                                                  |
+----------------------------------------------------------------------------------------------------------------------------------+


======================================================= Final observations =======================================================

TERMINATION LIMIT REACHED AFTER    8. ITERATIONS
TOTAL TIME OF CALCULATION [MIN]    0.0

MAXIMUM NORMALIZED RESIDUAL AT:    IMAGE COORDINATES
SYSTEM NU.:                                     1982
POINT NU .:                                     4019
NORMALIZED RESIDUAL (NV):                       2.53
```

Appendix D

Image	Point	X_i (m)	Y_i (m)	Z_i (m)	D_i (m)	d'_i (cm)	m_{bq}
20878	1110	9730.840	10414.949	1156.706	287.803	5.39	5341
	1003	9922.737	10629.434	1158.164			
20886	1003	9922.737	10629.434	1158.164	171.425	5.20	3299
	1077	9759.969	10575.893	1163.317			
20891	1077	9759.969	10575.893	1163.317	163.692	5.31	3082
	1110	9730.840	10414.949	1156.706			
20892	1110	9730.840	10414.949	1156.706	87.519	2.54	3448
	1116	9699.321	10496.582	1158.154			
20893	1110	9730.840	10414.949	1156.706	106.296	3.13	3400
	4020	9814.598	10350.906	1170.192			
20899	1110	9730.840	10414.949	1156.706	87.519	1.89	4627
	1116	9699.321	10496.582	1158.154			
Average							**3866**

Table (D.1): Determination of the oblique image scale numbers

Appendix E

PROGRAM SYSTEM PICTRAN-B (VERSION4.3 (C) TECHNET 1995-1998)

OUTPUT OF MODULE BUNBIL

BUNDLE ADJUSTMENT

PROJECT: Baalbek's oblique images

```
LEGEND OF THE MODULE BUNBIL

V    = RESIDUAL
MFV  = STANDARD DEVIATION OF OBSERVATIONS A PRIORI
EV   = REDUNDANCY NUMBER
GF   = PROBABLE DIMENSION OF A BLUNDER
EK   = DISPLACEMENT IF OBSERVATION DOES NOT TAKE PART OF THE ADJUSTMENT
NV   = NORMALIZED RESIDUAL
GRZW = THRESHOLD VALUE FOR NOT TRACEABLE BLUNDERS
EGK  = EFFECT OF GRZW ON THE RELATIVE POSITION
M    = STANDARD DEVIATION OF UNKNOWNS
STA  = STATE (0=FIX, 1=UNKNOWN, 2=OBSERVED)
**   = BLUNDER IS SUPPOSED
***  = BLUNDER IS PROBABLE
```

```
===================================================== IMAGE- AND OBJECT DATA ======================================================

    NU. OF IMAGES                          8
    NU. OF IMAGE POINTS                   70
    NU. OF OBJECT POINTS                  19
    NU. OF CONTROL POINTS                 19
    NU. OF CAMERAS                         1
    NU. OF PLANES                          0
    NU. OF DISTANCES                       0
    NU. OF DIFFERENCES                     0
```

```
===================================================== DATA OF THE ADJUSTMENT ======================================================

    OBSERVATIONS (OB)                    237
    UNKNOWNS (UN)                        135
    NU. CONSTR. EQUATIONS (CON)            8
    REDUNDANCY (OB-UN+CON)               110
    SUM OF REDUNDANCY NUMBERS        110.000
    NU. OF DIAGONAL SUBMATRICES           98
    NU. OF ALL SUBMATRICES               433
    NU. OF ALL SINGLE ELEMENTS          6423
    FILLING OF ATPA [%]           0.3196E+02
```

IMAGE COORDINATES

SYSTEM-NU	POINT-NU	X Y	BEOBX BEOBY	VX VY	MFVX MFVY	EVX EVY	GFX GFY	EKX EKY	NVX NVY	GRZWX GRZWY	EGKX EGKY
20886	1002	50.267484	50.213500	0.0540	0.0800	0.679	-0.079	-0.025	0.819	0.401	0.129
		-13.862180	-13.855600	-0.0066	0.0800	0.624	0.011	0.004	0.104	0.418	0.157
20886	1003	51.684257	51.567800	0.1165	0.0800	0.661	-0.176	-0.060	1.791	0.406	0.138
		-14.220538	-14.393800	0.1733	0.0800	0.609	-0.284	-0.111	2.775**	0.423	0.165
20886	1022	-11.133199	-11.093100	-0.0401	0.0800	0.858	0.047	0.007	0.541	0.357	0.051
		-15.652374	-15.689800	0.0374	0.0800	0.870	-0.043	-0.006	0.502	0.354	0.046
20886	1077	-1.189401	-1.057000	-0.1324	0.0800	0.851	0.156	0.023	1.794	0.358	0.053
		-0.352972	-0.307500	-0.0455	0.0800	0.863	0.053	0.007	0.612	0.356	0.049
20886	1110	-63.561715	-63.668300	0.1066	0.0800	0.778	-0.137	-0.030	1.510	0.374	0.083
		-6.845573	-6.947000	0.1014	0.0800	0.790	-0.128	-0.027	1.426	0.372	0.078
20886	1116	-36.401845	-36.367800	-0.0340	0.0800	0.858	0.040	0.006	0.459	0.357	0.050
		-0.762562	-0.757900	-0.0047	0.0800	0.863	0.005	0.001	0.063	0.356	0.049
20886	1136	-27.676003	-27.614400	-0.0616	0.0800	0.750	0.082	0.020	0.889	0.381	0.095
		-26.804675	-26.711700	-0.0930	0.0800	0.774	0.120	0.027	1.321	0.375	0.085
20886	1142	-26.556055	-26.513300	-0.0428	0.0800	0.749	0.057	0.014	0.617	0.382	0.096
		-26.872911	-26.711700	-0.1612	0.0800	0.774	0.208	0.047	2.290	0.375	0.085
20886	1162	-28.463375	-28.462200	-0.0012	0.0800	0.781	0.002	0.000	0.017	0.374	0.082
		8.044093	8.138700	-0.0946	0.0800	0.788	0.120	0.025	1.332	0.372	0.079
20886	1164	-27.722180	-27.691500	-0.0307	0.0800	0.784	0.039	0.008	0.433	0.373	0.081
		7.876565	7.941000	-0.0644	0.0800	0.791	0.081	0.017	0.906	0.372	0.078
20886	4020	-85.345121	-85.397600	0.0525	0.0800	0.654	-0.080	-0.028	0.811	0.408	0.141
		-12.227314	-12.389300	0.1620	0.0800	0.586	-0.276	-0.114	2.645**	0.432	0.179
20878	1003	-3.827697	-3.771100	-0.0566	0.0800	0.807	0.070	0.014	0.788	0.368	0.071
		-11.975342	-12.065300	0.0900	0.0800	0.700	-0.129	-0.039	1.344	0.395	0.119

20878	1022	-46.593950	-46.469900	-0.1240	0.0800	0.862	0.144	0.020	1.671	0.356	0.049
		-0.539058	-0.433800	-0.1053	0.0800	0.877	0.120	0.015	1.405	0.353	0.044
20878	1077	-6.503548	-6.650400	0.1469	0.0800	0.792	-0.185	-0.039	2.063	0.371	0.077
		12.460206	12.565100	-0.1049	0.0800	0.683	0.154	0.049	1.587	0.400	0.127
20878	1110	-52.869819	-52.756900	-0.1129	0.0800	0.811	0.139	0.026	1.567	0.367	0.069
		15.911920	15.810700	0.1012	0.0800	0.848	-0.119	-0.018	1.374	0.359	0.055
20878	1116	-25.029943	-25.175600	0.1457	0.0800	0.799	-0.182	-0.037	2.037	0.370	0.074
		17.861710	17.765700	0.0960	0.0800	0.765	-0.125	-0.029	1.372	0.378	0.089
20878	1136	-83.211324	-83.289100	0.0778	0.0800	0.833	-0.093	-0.016	1.065	0.362	0.060
		-7.161808	-7.089800	-0.0720	0.0800	0.795	0.091	0.019	1.010	0.371	0.076
20878	1142	-82.871096	-82.859700	-0.0114	0.0800	0.834	0.014	0.002	0.156	0.362	0.060
		-7.412782	-7.298500	-0.1143	0.0800	0.796	0.144	0.029	1.601	0.370	0.076
20878	4019	-85.017223	-85.012200	-0.0050	0.0800	0.766	0.007	0.002	0.072	0.378	0.089
		15.759377	15.717300	0.0421	0.0800	0.739	-0.057	-0.015	0.612	0.384	0.101
20878	4020	-85.954019	-85.937100	-0.0169	0.0800	0.772	0.022	0.005	0.241	0.376	0.086
		13.227429	13.191100	0.0363	0.0800	0.755	-0.048	-0.012	0.523	0.380	0.093
20878	4028	-24.252958	-24.135100	-0.1179	0.0800	0.616	0.191	0.073	1.876	0.421	0.161
		-51.553933	-51.534300	-0.0196	0.0800	0.621	0.032	0.012	0.312	0.419	0.159
20878	4029	-46.912413	-46.992900	0.0805	0.0800	0.610	-0.132	-0.051	1.288	0.423	0.165
		-51.882216	-51.929700	0.0475	0.0800	0.635	-0.075	-0.027	0.745	0.415	0.152
20893	1022	73.213817	73.257400	-0.0436	0.0800	0.196	0.222	0.179	1.230	0.746	0.600
		-13.288671	-13.384400	0.0957	0.0800	0.267	-0.359	-0.263	2.318	0.640	0.469
20893	1077	21.283102	21.481500	-0.1984	0.0800	0.569	0.349	0.150	3.287**	0.438	0.189
		14.461843	14.597000	-0.1352	0.0800	0.652	0.207	0.072	2.093	0.409	0.142
20893	1110	-56.401568	-56.458300	0.0567	0.0800	0.735	-0.077	-0.020	0.827	0.385	0.102
		-14.768942	-14.904500	0.1356	0.0800	0.770	-0.176	-0.041	1.932	0.377	0.087
20893	1116	-35.954284	-36.037400	0.0831	0.0800	0.738	-0.113	-0.030	1.210	0.385	0.101
		5.448573	5.436800	0.0118	0.0800	0.729	-0.016	-0.004	0.172	0.387	0.105
20893	1208	-49.987637	-50.108900	0.1213	0.0800	0.690	-0.176	-0.054	1.824	0.398	0.123
		6.762117	6.754800	0.0073	0.0800	0.662	-0.011	-0.004	0.112	0.406	0.137
20893	4019	-86.813614	-86.729900	-0.0837	0.0800	0.244	0.342	0.259	2.116	0.668	0.505
		-44.488026	-44.493900	0.0059	0.0800	0.384	-0.015	-0.009	0.118	0.533	0.329
20893	4020	-34.892367	-34.958400	0.0660	0.0800	0.374	-0.177	-0.111	1.351	0.541	0.339
		-39.382307	-39.265800	-0.1165	0.0800	0.493	0.236	0.120	2.074	0.470	0.238
20891	1077	22.657191	22.626600	0.0306	0.0800	0.576	-0.053	-0.023	0.504	0.435	0.184
		3.074937	3.108300	-0.0334	0.0800	0.238	0.140	0.107	0.855	0.678	0.517
20891	1110	-25.618924	-25.621500	0.0026	0.0800	0.524	-0.005	-0.002	0.044	0.456	0.217
		-24.306877	-24.313700	0.0068	0.0800	0.546	-0.013	-0.006	0.115	0.447	0.203
20891	1116	-24.157080	-24.267200	0.1101	0.0800	0.802	-0.137	-0.027	1.537	0.369	0.073
		-7.276466	-7.293000	0.0165	0.0800	0.807	-0.020	-0.004	0.230	0.368	0.071
20891	1160	-75.711668	-75.668000	-0.0437	0.0800	0.743	0.059	0.015	0.633	0.383	0.099
		3.396373	3.430500	-0.0341	0.0800	0.690	0.049	0.015	0.514	0.398	0.123
20891	1162	-73.595819	-73.590700	-0.0051	0.0800	0.751	0.007	0.002	0.074	0.381	0.095
		3.360487	3.364600	-0.0041	0.0800	0.708	0.006	0.002	0.061	0.393	0.115
20891	1164	-71.365392	-71.351800	-0.0136	0.0800	0.758	0.018	0.004	0.195	0.379	0.092
		3.383597	3.379200	0.0044	0.0800	0.724	-0.006	-0.002	0.065	0.388	0.107
20891	1208	-38.948718	-38.872600	-0.0761	0.0800	0.815	0.093	0.017	1.054	0.366	0.068
		-7.046195	-7.089800	0.0436	0.0800	0.834	-0.052	-0.009	0.597	0.362	0.060
20891	1228	3.526031	2.660900	0.8651	8.0000	1.000	-0.865	0.000	0.108	33.046	0.013
		-57.126053	-55.931300	-1.1948	8.0000	1.000	1.195	0.001	0.149	33.047	0.014
20905	1077	-39.454733	-39.417700	-0.0370	0.0800	0.598	0.062	0.025	0.598	0.427	0.172
		-7.369618	-7.367300	-0.0023	0.0800	0.649	0.004	0.001	0.036	0.410	0.144
20905	1110	-34.872841	-34.895100	0.0223	0.0800	0.846	-0.026	-0.004	0.302	0.359	0.055
		14.868698	14.875600	-0.0069	0.0800	0.838	0.008	0.001	0.094	0.361	0.059
20905	1116	-16.522531	-16.499300	-0.0232	0.0800	0.798	0.029	0.006	0.325	0.370	0.075
		6.097964	6.067500	0.0305	0.0800	0.714	-0.043	-0.012	0.451	0.391	0.112
20905	1208	-6.839727	-6.920100	0.0804	0.0800	0.784	-0.103	-0.022	1.135	0.373	0.081
		7.735052	7.771000	-0.0359	0.0800	0.581	0.062	0.026	0.590	0.433	0.182
20905	1228	-66.142739	-66.096200	-0.0465	0.0800	0.782	0.060	0.013	0.658	0.374	0.082
		29.477901	29.435800	0.0421	0.0800	0.768	-0.055	-0.013	0.600	0.377	0.087
20905	1240	-76.270806	-76.313900	0.0431	0.0800	0.718	-0.060	-0.017	0.636	0.390	0.110
		30.138499	30.210200	-0.0717	0.0800	0.662	0.108	0.037	1.102	0.406	0.137
20905	4019	-54.525802	-54.447000	-0.0788	0.0800	0.831	0.095	0.016	1.081	0.362	0.061
		25.494951	25.475700	0.0193	0.0800	0.839	-0.023	-0.004	0.263	0.361	0.058
20905	4020	-69.556371	-69.597500	0.0411	0.0800	0.809	-0.051	-0.010	0.572	0.367	0.070
		24.150727	24.126100	0.0246	0.0800	0.762	-0.032	-0.008	0.353	0.378	0.090
20892	1110	-31.823763	-31.956200	0.1324	0.0800	0.847	-0.156	-0.024	1.799	0.359	0.055
		-21.667345	-21.897300	0.2300	0.0800	0.833	-0.276	-0.046	3.149**	0.362	0.060
20892	1116	-16.502582	-16.383700	-0.1189	0.0800	0.831	0.143	0.024	1.630	0.362	0.061
		-0.210459	-0.307500	0.0970	0.0800	0.680	-0.143	-0.046	1.471	0.401	0.128
20892	1158	-58.158063	-58.168600	0.0105	0.0800	0.795	-0.013	-0.003	0.148	0.371	0.076
		16.458309	16.508100	-0.0498	0.0800	0.772	0.065	0.015	0.709	0.376	0.086
20892	1160	-55.978260	-56.010500	0.0322	0.0800	0.803	-0.040	-0.008	0.450	0.369	0.073
		16.312935	16.354300	-0.0414	0.0800	0.788	0.053	0.011	0.583	0.372	0.079

```
      20892          1162     -53.991652     -54.006600     0.0149     0.0800  0.809 -0.018 -0.004  0.208     0.367  0.070
                               16.170265      16.244500    -0.0742     0.0800  0.799  0.093  0.019  1.038     0.370  0.074

      20892          1164     -51.911635     -51.870600    -0.0410     0.0800  0.813  0.050  0.009  0.569     0.366  0.068
                               16.076270      16.112700    -0.0364     0.0800  0.809  0.045  0.009  0.506     0.367  0.070

      20892          1208     -31.107239     -31.093700    -0.0135     0.0800  0.855  0.016  0.002  0.183     0.357  0.052
                                1.036272       1.010500     0.0258     0.0800  0.833 -0.031 -0.005  0.353     0.362  0.060

      20892          4019     -52.550579     -52.498200    -0.0524     0.0800  0.390  0.134  0.082  1.048     0.529  0.323
                              -54.393453     -54.433900     0.0404     0.0800  0.305 -0.133 -0.092  0.916     0.599  0.416

      20892          4020       1.789751       1.761700     0.0281     0.0800  0.433 -0.065 -0.037  0.533     0.502  0.284
                              -48.381544     -48.195300    -0.1862     0.0800  0.395  0.471  0.285  3.702**   0.525  0.318

      20899          1110       6.366392       6.380600    -0.0142     0.0800  0.768  0.019  0.004  0.203     0.377  0.088
                              -28.540026     -28.578500     0.0385     0.0800  0.763 -0.050 -0.012  0.551     0.378  0.090

      20899          1116       8.420109       8.500100    -0.0800     0.0800  0.821  0.097  0.017  1.103     0.365  0.065
                               -8.620313      -8.650400     0.0301     0.0800  0.750 -0.040 -0.010  0.434     0.382  0.096

      20899          1160     -26.625507     -26.645500     0.0200     0.0800  0.746 -0.027 -0.007  0.289     0.382  0.097
                               10.124412      10.154900    -0.0305     0.0800  0.729  0.042  0.011  0.446     0.387  0.105

      20899          1162     -25.152273     -25.192100     0.0398     0.0800  0.751 -0.053 -0.013  0.575     0.381  0.095
                               10.018146      10.022100    -0.0040     0.0800  0.743  0.005  0.001  0.057     0.383  0.099

      20899          1164     -23.598096     -23.606600     0.0085     0.0800  0.755 -0.011 -0.003  0.122     0.380  0.093
                                9.927284       9.845100     0.0822     0.0800  0.756 -0.109 -0.026  1.181     0.380  0.093

      20899          1208      -1.251930      -1.233200    -0.0187     0.0800  0.850  0.022  0.003  0.254     0.358  0.054
                               -7.741128      -7.632700    -0.1084     0.0800  0.832  0.130  0.022  1.486     0.362  0.061

      20899          4019       8.158918       8.114800     0.0441     0.0800  0.400 -0.110 -0.066  0.872     0.522  0.313
                              -54.133796     -54.126100    -0.0077     0.0800  0.506  0.015  0.008  0.135     0.464  0.229

      20899          4020      33.744969      34.738200    -0.9932     8.0000  1.000  0.993  0.000  0.124    33.041  0.002
                              -50.059542     -50.143800     0.0843     8.0000  1.000 -0.084  0.000  0.011    33.041  0.003

      20907          1110       3.305058       3.226100     0.0790     0.0800  0.786 -0.100 -0.021  1.113     0.373  0.080
                              -23.863915     -23.816400    -0.0475     0.0800  0.760  0.063  0.015  0.681     0.379  0.091

      20907          1116      -1.538913      -1.618500     0.0796     0.0800  0.835 -0.095 -0.016  1.089     0.362  0.060
                               -4.478474      -4.502200     0.0237     0.0800  0.777 -0.031 -0.007  0.337     0.375  0.084

      20907          1158     -49.007707     -48.963800    -0.0439     0.0800  0.800  0.055  0.011  0.613     0.369  0.074
                               11.303949      11.301600     0.0023     0.0800  0.769 -0.003 -0.001  0.033     0.377  0.087

      20907          1160     -47.100760     -47.055300    -0.0455     0.0800  0.806  0.056  0.011  0.633     0.368  0.072
                               11.255857      11.264700    -0.0088     0.0800  0.782  0.011  0.002  0.125     0.374  0.081

      20907          1162     -45.414980     -45.389000    -0.0260     0.0800  0.809  0.032  0.006  0.361     0.367  0.070
                               11.221392      11.220500     0.0009     0.0800  0.793 -0.001  0.000  0.013     0.371  0.077

      20907          1164     -43.628425     -43.605300    -0.0231     0.0800  0.813  0.028  0.005  0.321     0.367  0.069
                               11.214750      11.198400     0.0164     0.0800  0.803 -0.020 -0.004  0.228     0.369  0.073

      20907          1208     -12.311873     -12.342800     0.0309     0.0800  0.856 -0.036 -0.005  0.418     0.357  0.051
                               -4.214591      -4.236700     0.0221     0.0800  0.843 -0.026 -0.004  0.301     0.360  0.057

      20907          1228      33.030002      33.075600    -0.0456     0.0800  0.326  0.140  0.094  0.998     0.579  0.390
                              -58.793509     -58.783200    -0.0103     0.0800  0.305  0.034  0.023  0.233     0.598  0.415



------------------------------------------------ PRINCIPAL POINT AND FOCAL LENGTH ------------------------------------------------
     CAMERANAME             X0         BEOBX0        VX0     MFVX0   EVX0   GFX0   EKX0   NVX0    GRZWX0  EGKX0         MX0  STAX0
                            Y0         BEOBY0        VY0     MFVY0   EVY0   GFY0   EKY0   NVY0    GRZWY0  EGKY0         MY0  STAY0
                             C          BEOBC         VC      MFVC    EVC    GFC    EKC    NVC     GRZWC   EGKC          MC   STAC
-----------------------------------------------------------------------------------------------------------------------------------

   Schrägkamera       0.096526       0.000000     0.0965    0.5000  0.025 -3.795 -3.699  1.211    12.948 12.619     0.5201      2
                     -0.353679       0.000000    -0.3537    0.5000  0.078  4.523  4.169  2.530**   7.385  6.807     0.5059      2
                    259.707205     260.000000    -0.2928    0.5000  0.781  0.375  0.082  0.663     2.337  0.513     0.2468      2

---------------------------------------------------- CONTROL OF THE ADJUSTMENT ----------------------------------------------------
                   TOTAL  IMAGE COORD    PROJ.CENT OBJECT COORD          DIS          DIF      PLANE PO  PLANE PARAM   PRINC PO+C
-----------------------------------------------------------------------------------------------------------------------------------

REDUNDANCY   110.000000  101.265491    7.850212    0.000000    0.000000    0.000000    0.000000    0.000000    0.884298
     SIGMA     1.053778    1.075683    0.722255    1.000000    1.000000    1.000000    1.000000    1.000000    0.997873
      VTPV   122.149335  117.173714    4.095082    0.000000    0.000000    0.000000    0.000000    0.000000    0.880539

======================================================= Final observations =======================================================

TERMINATION LIMIT REACHED AFTER    6. ITERATIONS
TOTAL TIME OF CALCULATION [MIN]    0.0

MAXIMUM NORMALIZED RESIDUAL AT:    IMAGE COORDINATES
SYSTEM NU.:                                    20892
POINT NU .:                                     4020
NORMALIZED RESIDUAL (NV):                       3.70
```

Appendix F

<table>
<tr><th>Image</th><th>Point</th><th>X_i (m)</th><th>Y_i (m)</th><th>Z_i (m)</th><th>D_i (m)</th><th>d'_i (cm)</th><th>m_{bq}</th></tr>
<tr><td rowspan="2">2083-23</td><td>1228</td><td>9804.655</td><td>10299.092</td><td>1171.202</td><td rowspan="2">32.714</td><td rowspan="2">2.07</td><td rowspan="2">1583</td></tr>
<tr><td>1240</td><td>9833.117</td><td>10282.963</td><td>1171.291</td></tr>
<tr><td rowspan="2">2083-25</td><td>1208</td><td>9675.400</td><td>10491.349</td><td>1158.152</td><td rowspan="2">94.407</td><td rowspan="2">2.71</td><td rowspan="2">3484</td></tr>
<tr><td>1110</td><td>9730.840</td><td>10414.949</td><td>1156.706</td></tr>
<tr><td rowspan="2">637 126</td><td>1208</td><td>9675.400</td><td>10491.349</td><td>1158.152</td><td rowspan="2">94.407</td><td rowspan="2">3.49</td><td rowspan="2">2704</td></tr>
<tr><td>1110</td><td>9730.840</td><td>10414.949</td><td>1156.706</td></tr>
<tr><td>$\bar{m}_b$</td><td colspan="6"></td><td>2590</td></tr>
</table>

Table (F.1): Determination of the terrestrial image scale numbers

Appendix G

PROGRAM SYSTEM PICTRAN-B (VERSION4.3 (C) TECHNET 1995-1998)

OUTPUT OF MODULE BUNBIL

BUNDLE ADJUSTMENT

PROJECT: Baalbek's terrestrial images

```
V    = RESIDUAL
MFV  = STANDARD DEVIATION OF OBSERVATIONS A PRIORI
EV   = REDUNDANCY NUMBER
GF   = PROBABLE DIMENSION OF A BLUNDER
EK   = DISPLACEMENT IF OBSERVATION DOES NOT TAKE PART OF THE ADJUSTMENT
NV   = NORMALIZED RESIDUAL
GRZW = THRESHOLD VALUE FOR NOT TRACEABLE BLUNDERS
EGK  = EFFECT OF GRZW ON THE RELATIVE POSITION
M    = STANDARD DEVIATION OF UNKNOWNS
STA  = STATE (0=FIX, 1=UNKNOWN, 2=OBSERVED)
**   = BLUNDER IS SUPPOSED
***  = BLUNDER IS PROBABLE


===================================================== IMAGE- AND OBJECT DATA =======================================================

    NU. OF IMAGES                         3
    NU. OF IMAGE POINTS                  26
    NU. OF OBJECT POINTS                 11
    NU. OF CONTROL POINTS                11
    NU. OF CAMERAS                        1
    NU. OF PLANES                         0
    NU. OF DISTANCES                      0
    NU. OF DIFFERENCES                    0

=========================================================== ITERATIONS =============================================================

    ITERATION         UNKNOWNS        RIGHT SIDE       TIME [s]

            1       0.1000E+11       0.3936E+10          0.00
            2       0.3555E+01       0.1066E+07          0.01
            3       0.1409E+00       0.1090E+04          0.03
            4       0.8298E-03       0.5393E-01          0.03
            5       0.1029E-04       0.1384E-04          0.05

===================================================== DATA OF THE ADJUSTMENT =======================================================

    OBSERVATIONS (OB)                    88
    UNKNOWNS (UN)                        48
    NU. CONSTR. EQUATIONS (CON)           3
    REDUNDANCY (OB-UN+CON)               43
    SUM OF REDUNDANCY NUMBERS        43.000
    NU. OF DIAGONAL SUBMATRICES          41
    NU. OF ALL SUBMATRICES              162
    NU. OF ALL SINGLE ELEMENTS         2094
    FILLING OF ATPA [%]          0.4895E+02

------------------------------------------------------- IMAGE COORDINATES ----------------------------------------------------------
      SYSTEM-NU        POINT-NU                X           BEOBX          VX        MFVX    EVX    GFX    EKX    NVX      GRZWX   EGKX
                                               Y           BEOBY          VY        MFVY    EVY    GFY    EKY    NVY      GRZWY   EGKY
------------------------------------------------------------------------------------------------------------------------------------

         208323           1160      -17.615565      -17.162000     -0.4536      0.7000  0.797  0.569  0.116  0.726      3.238  0.658
                                      9.450442        9.484900     -0.0345      0.7000  0.730  0.047  0.013  0.058      3.384  0.914
```

```
     208323          1162    -16.188906     -16.006700    -0.1822    0.7000  0.800  0.228  0.046  0.291     3.232  0.646
                               9.341065       9.384400    -0.0433    0.7000  0.739  0.059  0.015  0.072     3.362  0.876

     208323          1164    -14.631639     -14.750900     0.1193    0.7000  0.803 -0.148 -0.029  0.190     3.225  0.634
                               9.274965       9.409500    -0.1345    0.7000  0.748  0.180  0.045  0.222     3.342  0.841

     208323          1199     -7.697375      -8.618700     0.9213    0.7000  0.831 -1.108 -0.187  1.443     3.170  0.534
                               6.952130       6.827900     0.1242    0.7000  0.791 -0.157 -0.033  0.200     3.250  0.679

     208323          1228     46.014397      45.613200     0.4012    0.7000  0.800 -0.501 -0.100  0.641     3.232  0.645
                               0.045324      -0.044000     0.0893    0.7000  0.748 -0.119 -0.030  0.148     3.343  0.843

     208323          1239     69.609259      69.451700     0.1576    0.7000  0.729 -0.216 -0.058  0.264     3.385  0.917
                              -3.187156      -2.876900    -0.3103    0.7000  0.535  0.580  0.269  0.606     3.951  1.836

     208323          1240     58.472842      59.422400    -0.9496    0.7000  0.758  1.253  0.303  1.558     3.320  0.803
                              -1.915364      -2.223600     0.3082    0.7000  0.667 -0.462 -0.154  0.539     3.540  1.179

     208325          1110     -1.490263      -3.141300     1.6510    0.7000  0.897 -1.841 -0.190  2.491     3.053  0.315
                             -31.490993     -31.897000     0.4060    0.7000  0.889 -0.457 -0.051  0.615     3.066  0.340

     208325          1116    -13.153649     -14.813900     1.6603    0.7000  0.902 -1.842 -0.181  2.498     3.045  0.300
                             -29.277527     -28.731200    -0.5463    0.7000  0.891  0.613  0.067  0.827     3.062  0.333

     208325          1158    -55.377890     -54.632000    -0.7459    0.7000  0.840  0.888  0.142  1.163     3.154  0.505
                             -26.746660     -26.972400     0.2257    0.7000  0.778 -0.290 -0.064  0.366     3.278  0.728

     208325          1160    -53.922626     -53.234000    -0.6886    0.7000  0.844  0.816  0.127  1.071     3.147  0.491
                             -26.820280     -26.871900     0.0516    0.7000  0.787 -0.066 -0.014  0.083     3.259  0.695

     208325          1162    -52.762254     -52.088600    -0.6737    0.7000  0.847  0.795  0.122  1.046     3.141  0.480
                             -26.904070     -26.897000    -0.0071    0.7000  0.794  0.009  0.002  0.011     3.245  0.670

     208325          1164    -51.473497     -50.842200    -0.6313    0.7000  0.850  0.742  0.111  0.978     3.135  0.469
                             -26.949573     -26.947200    -0.0024    0.7000  0.801  0.003  0.001  0.004     3.231  0.644

     208325          1208    -19.907859     -21.298600     1.3907    0.7000  0.900 -1.545 -0.154  2.094     3.047  0.304
                             -28.871828     -28.781400    -0.0904    0.7000  0.895  0.101  0.011  0.137     3.056  0.320

     208325          1228     28.315737      28.659300    -0.3436    0.7000  0.837  0.410  0.067  0.536     3.159  0.514
                             -30.247983     -30.263800     0.0158    0.7000  0.773 -0.020 -0.005  0.026     3.288  0.747

     208325          1239     43.726196      44.155300    -0.4291    0.7000  0.787  0.545  0.116  0.691     3.259  0.694
                             -32.096705     -31.997500    -0.0992    0.7000  0.669  0.148  0.049  0.173     3.535  1.171

     208325          1240     38.867676      39.978100    -1.1104    0.7000  0.803  1.383  0.273  1.771     3.227  0.637
                             -31.145894     -31.193500     0.0476    0.7000  0.706 -0.067 -0.020  0.081     3.442  1.013

     637126          1110     41.220062      39.848600     1.3715    0.7000  0.848 -1.618 -0.246  2.128     3.140  0.478
                              31.225695      30.496100     0.7296    0.7000  0.786 -0.928 -0.198  1.175     3.260  0.696

     637126          1116     26.722033      24.801300     1.9207    0.7000  0.878 -2.187 -0.266  2.928**   3.085  0.375
                              34.361863      34.448200    -0.0863    0.7000  0.829  0.104  0.018  0.135     3.174  0.541

     637126          1158    -25.494378     -24.581400    -0.9130    0.7000  0.848  1.076  0.163  1.416     3.139  0.476
                              34.797561      34.874100    -0.0765    0.7000  0.786  0.097  0.021  0.123     3.262  0.699

     637126          1160    -23.678256     -22.890200    -0.7881    0.7000  0.852  0.924  0.136  1.219     3.131  0.462
                              34.843896      34.974300    -0.1304    0.7000  0.798  0.164  0.033  0.209     3.237  0.656

     637126          1162    -22.219383     -21.486600    -0.7328    0.7000  0.856  0.857  0.124  1.132     3.126  0.451
                              34.853609      34.974300    -0.1207    0.7000  0.806  0.150  0.029  0.192     3.220  0.624

     637126          1164    -20.609180     -19.981400    -0.6278    0.7000  0.859  0.731  0.103  0.968     3.120  0.441
                              34.920308      35.099600    -0.1793    0.7000  0.815  0.220  0.041  0.284     3.202  0.592


     637126          1199     -4.847217      -5.365300     0.5181    0.7000  0.885 -0.586 -0.068  0.787     3.074  0.355
                              33.629150      33.452300     0.1768    0.7000  0.870 -0.203 -0.026  0.271     3.099  0.402

     637126          1208     17.894373      16.379200     1.5152    0.7000  0.888 -1.707 -0.192  2.297     3.069  0.345
                              34.204624      33.997200     0.2074    0.7000  0.873 -0.238 -0.030  0.317     3.095  0.394

     637126          1228     81.439093      83.603900    -2.1648    0.7000  0.659  3.287  1.122  3.811**   3.562  1.216
                              33.394741      33.922100    -0.5274    0.7000  0.381  1.383  0.855  1.220     4.681  2.896


------------------------------------------------ PRINCIPAL POINT AND FOCAL LENGTH ---------------------------------------------------
     CAMERANAME              X0         BEOBX0         VX0     MFVX0   EVX0   GFX0   EKX0   NVX0    GRZWX0  EGKX0        MX0  STAX0
                             Y0         BEOBY0         VY0     MFVY0   EVY0   GFY0   EKY0   NVY0    GRZWY0  EGKY0        MY0  STAY0
                              C          BEOBC          VC      MFVC    EVC    GFC    EKC    NVC     GRZWC   EGKC         MC   STAC
-------------------------------------------------------------------------------------------------------------------------------------

Messbild_Kamera        0.000000              0           -         -      -      -      -      -         -      -          -      0
                       0.000000              0           -         -      -      -      -      -         -      -          -      0
                     346.629555     350.000000     -3.3704    5.0000  0.921  3.659  0.289  0.702    21.517  1.698     1.6838      2



---------------------------------------------------- CONTROL OF THE ADJUSTMENT ------------------------------------------------------
                   TOTAL  IMAGE COORD    PROJ.CENT OBJECT COORD         DIS          DIF      PLANE PO  PLANE PARAM   PRINC PO+C
-------------------------------------------------------------------------------------------------------------------------------------

REDUNDANCY    43.000000    41.484400     0.594531     0.000000     0.000000     0.000000     0.000000     0.000000     0.921070
     SIGMA     1.198635     1.214145     0.535758     1.000000     1.000000     1.000000     1.000000     1.000000     0.702378
      VTPV    61.779212    61.154164     0.170652     0.000000     0.000000     0.000000     0.000000     0.000000     0.454396

===================================================== Final observations ============================================================

TERMINATION LIMIT REACHED AFTER     5. ITERATIONS
TOTAL TIME OF CALCULATION [MIN]     0.0

MAXIMUM NORMALIZED RESIDUAL AT:     IMAGE COORDINATES
SYSTEM NU.:                                    637126
POINT NU .:                                      1228
NORMALIZED RESIDUAL (NV):                        3.81
```

Appendix H

Camera name	Distortion parameter	Status
Baalbek-G1	A1	Status A1
	A2	Status A2
	A3	Status A3
	A4	Status A4
	A5	Status A5
	A6	Status A6
	-0.208866D-06	1
	0.106185D-10	1
	0.722547D-02	1
	0.804372D-03	1
	0.558588D-06	1
	-0.980329D-05	1

Table (H.1): Distortion parameters referred to vertical images of Baalbek, where A1 & A2 are parameters available for radial distortion, A3 & A4 are scale and shear parameters, respectively. In addition, A5 and A6 are parameters for decentring distortion

Appendix I

Camera name	Distortion parameter	Status
Schrägkamera	A1	Status A1
	A2	Status A2
	A3	Status A3
	A4	Status A4
	A5	Status A5
	A6	Status A6
	0.108700D-05	1
	-0.175551D-09	1
	0.850927D-04	1
	-0.190090D-03	1
	-0.985190D-05	1
	-0.731519D-05	1

Table (I.1): Distortion parameters referred to oblique images of Baalbek, where A1 & A2 are parameters available for radial distortion, A3 & A4 are scale and shear parameters, respectively. In addition, A5 and A6 are parameters for decentring distortion

Appendix J

PROGRAM SYSTEM PICTRAN-B (VERSION4.3 (C) TECHNET 1995-1998)

OUTPUT OF MODULE BUNBIL

BUNDLE ADJUSTMENT

PROJECT: TWO_TYPES (vertical and oblique)

```
LEGEND OF THE MODULE BUNBIL

V    = RESIDUAL
MFV  = STANDARD DEVIATION OF OBSERVATIONS A PRIORI
EV   = REDUNDANCY NUMBER
GF   = PROBABLE DIMENSION OF A BLUNDER
EK   = DISPLACEMENT IF OBSERVATION DOES NOT TAKE PART OF THE ADJUSTMENT
NV   = NORMALIZED RESIDUAL
GRZW = THRESHOLD VALUE FOR NOT TRACEABLE BLUNDERS
EGK  = EFFECT OF GRZW ON THE RELATIVE POSITION
M    = STANDARD DEVIATION OF UNKNOWNS
STA  = STATE (0=FIX, 1=UNKNOWN, 2=OBSERVED)
**   = BLUNDER IS SUPPOSED
***  = BLUNDER IS PROBABLE

===================================================== IMAGE- AND OBJECT DATA =======================================================

    NU. OF IMAGES                          12
    NU. OF IMAGE POINTS                   124
    NU. OF OBJECT POINTS                   35
    NU. OF CONTROL POINTS                   6
```

```
    NU. OF CAMERAS                           2
    NU. OF PLANES                            0
    NU. OF DISTANCES                         0
    NU. OF DIFFERENCES                       0

=========================================================== ITERATIONS ============================================================

    ITERATION         UNKNOWNS        RIGHT SIDE       TIME [s]

            1       0.1000E+11       0.9541E+08           0.00
            2       0.2527E+01       0.1375E+07           0.01
            3       0.2121E-01       0.2489E+03           0.03
            4       0.1613E-03       0.2606E-02           0.03
            5       0.3235E-05       0.7690E-03           0.05
            6       0.3378E-07       0.4698E-03           0.05

===================================================== DATA OF THE ADJUSTMENT ======================================================

    OBSERVATIONS (OB)                      489
    UNKNOWNS (UN)                          295
    NU. CONSTR. EQUATIONS (CON)             12
    REDUNDANCY (OB-UN+CON)                 206
    SUM OF REDUNDANCY NUMBERS          206.000
    NU. OF DIAGONAL SUBMATRICES            173
    NU. OF ALL SUBMATRICES                 785
    NU. OF ALL SINGLE ELEMENTS           11464
    FILLING OF ATPA [%]             0.1943E+02


+---------------------------------------------------------------------------------------------------------------------------------+
| DATE :  07/20/20 12:21:06                                                                                       PAGE:        4  |
|                                                   BUNNAE-OUTPUT                                                                 |
| PROJECT: TWO_TYPES                                                                                                              |
+---------------------------------------------------------------------------------------------------------------------------------+


>>>>>>>>>>>>>>>>>>>>>>>>>>>>>>>>>>>>>>>>>>>>>>>>>>>>>>>>>>>>>>>>>>>>>>>>>>>>>>>>>>>>>>>>>>>>>>>>>>>>>>>>>>>>>>>>>>>>>>>>>>>>>>>
<<<<<<<<<<<<<<<<<<<<<<<<<<<<<<<<<<<<<<<<<<<<<<<<<<<<<  RESULTS OF ADJUSTMENT  <<<<<<<<<<<<<<<<<<<<<<<<<<<<<<<<<<<<<<<<<<<<<<<<<<<<<
>>>>>>>>>>>>>>>>>>>>>>>>>>>>>>>>>>>>>>>>>>>>>>>>>>>>>>>>>>>>>>>>>>>>>>>>>>>>>>>>>>>>>>>>>>>>>>>>>>>>>>>>>>>>>>>>>>>>>>>>>>>>>>>

------------------------------------------------- ELEMENTS OF ROTATION MATRICES   -------------------------------------------------
      SYSTEM-NU            A11             A12             A13           OMEGA
    CAMMERANAME            A21             A22             A23             PHI
                           A31             A32             A33           KAPPA
-----------------------------------------------------------------------------------------------------------------------------------

           1981      -0.470976       -0.879025        0.074134        4.531503
     baalbek-G1       0.876729       -0.475727       -0.070925        4.723843
                      0.097612        0.031591        0.994723      131.313483

           1982      -0.670204       -0.742017        0.015417        8.348914
     baalbek-G1       0.734381       -0.666024       -0.130753        0.981525
                      0.107289       -0.076309        0.991295      146.765510

           2025      -0.687534       -0.724747       -0.045144        9.619294
     baalbek-G1       0.721897       -0.675465       -0.150372       -2.874932
                      0.078488       -0.135975        0.987598      148.322941

          20886       0.432106       -0.189275        0.881737       70.334748
   Schrägkamera       0.901812        0.095493       -0.421445       68.725096
                     -0.004431        0.977270        0.211953       26.283109

          20878      -0.256793       -0.338635        0.905198      -39.981949
   Schrägkamera       0.966128       -0.065149        0.249705       72.055536
                     -0.025586        0.938660        0.343895      141.304050

          20893       0.862714       -0.150543        0.482764       78.048073
   Schrägkamera       0.505691        0.254893       -0.824201       32.073423
                      0.001024        0.955179        0.296028       10.998217

          20891       0.955115       -0.058220        0.290457       85.971887
   Schrägkamera       0.296208        0.200924       -0.933751       18.761469
                     -0.003997        0.977875        0.209151        3.875808

           1983      -0.681866       -0.730360       -0.040404        4.103334
     baalbek-G1       0.731215       -0.679104       -0.064358       -2.572921
                      0.019566       -0.073428        0.997109      147.814799

           1985      -0.679044       -0.729407       -0.082856        0.596787
     baalbek-G1       0.732420       -0.680789       -0.009342       -5.280830
                     -0.049593       -0.067029        0.996518      147.724578

          20892       0.866274       -0.136472        0.480567       78.870589
   Schrägkamera       0.499512        0.251166       -0.829098       31.913799
                     -0.007553        0.958275        0.285748        9.947497

          20899       0.901486       -0.171344        0.397447       67.593067
   Schrägkamera       0.431950        0.413970       -0.801279       26.020750
                     -0.027237        0.894019        0.447200       11.957479

           1980       0.658914        0.726752       -0.194072        0.826624
     baalbek-G1      -0.742468        0.669761       -0.012737      -12.433890
                      0.120725        0.152485        0.980905      -53.114241

------------------------------------------------------- OBJECT COORDINATES --------------------------------------------------------
       POINT-NU              X           BEOBX          VX       MFVX    EVX    GFX    EKX    NVX     GRZWX  EGKX        MX  STAX
                             Y           BEOBY          VY       MFVY    EVY    GFY    EKY    NVY     GRZWY  EGKY        MY  STAY
                             Z           BEOBZ          VZ       MFVZ    EVZ    GFZ    EKZ    NVZ     GRZWZ  EGKZ        MZ  STAZ
-----------------------------------------------------------------------------------------------------------------------------------

           1002    9917.775688     9917.785000     -0.0093     0.1000  0.031  0.296  0.287  0.525     2.328  2.255    0.1141     2
                  10629.227858    10629.229000     -0.0011     0.1000  0.038  0.030  0.029  0.059     2.131  2.051    0.1137     2
                   1157.800514     1157.803000     -0.0025     0.1000  0.019  0.130  0.128  0.180     2.990  2.932    0.1148     2


------------------------------------------------------- OBJECT COORDINATES --------------------------------------------------------
       POINT-NU              X           BEOBX          VX       MFVX    EVX    GFX    EKX    NVX     GRZWX  EGKX        MX  STAX
```

	Y Z	BEOBY BEOBZ	VY VZ	MFVY MFVZ	EVY EVZ	GFY GFZ	EKY EKZ	NVY NVZ	GRZWY GRZWZ	EGKY EGKZ	MY MZ	STAY STAZ
1003	9922.726682	9922.737000	-0.0103	0.1000	0.036	0.283	0.273	0.541	2.164	2.085	0.1138	2
	10629.435616	10629.434000	0.0016	0.1000	0.060	-0.027	-0.025	0.066	1.690	1.589	0.1124	2
	1158.146295	1158.164000	-0.0177	0.1000	0.037	0.475	0.457	0.917	2.139	2.060	0.1137	2
1077	9759.961983	9759.969000	-0.0070	0.1000	0.083	0.085	0.078	0.244	1.438	1.319	0.1110	2
	10575.913814	10575.893000	0.0208	0.1000	0.057	-0.363	-0.343	0.870	1.726	1.627	0.1125	2
	1163.343845	1163.317000	0.0268	0.1000	0.070	-0.383	-0.356	1.014	1.560	1.451	0.1118	2
4027	10189.251000	-	-	-	-	-	-	-	-	-	-	0
	10588.229000	-	-	-	-	-	-	-	-	-	-	0
	1165.729000	-	-	-	-	-	-	-	-	-	-	0
4028	10101.942177	10101.945000	-0.0028	0.1000	0.029	0.096	0.094	0.165	2.413	2.343	0.1142	2
	10645.263469	10645.258000	0.0055	0.1000	0.047	-0.116	-0.111	0.252	1.903	1.813	0.1131	2
	1163.371271	1163.374000	-0.0027	0.1000	0.029	0.093	0.090	0.159	2.409	2.338	0.1142	2
4029	10109.018814	10109.009000	0.0098	0.1000	0.032	-0.303	-0.293	0.546	2.296	2.222	0.1140	2
	10608.162538	10608.189000	-0.0265	0.1000	0.046	0.579	0.553	1.238	1.933	1.844	0.1132	2
	1162.071857	1162.079000	-0.0071	0.1000	0.031	0.234	0.227	0.409	2.365	2.293	0.1141	2
4030	10064.847000	-	-	-	-	-	-	-	-	-	-	0
	10707.655100	-	-	-	-	-	-	-	-	-	-	0
	1155.805600	-	-	-	-	-	-	-	-	-	-	0
4041	10128.910600	-	-	-	-	-	-	-	-	-	-	0
	10564.572600	-	-	-	-	-	-	-	-	-	-	0
	1158.126900	-	-	-	-	-	-	-	-	-	-	0
1110	9730.836907	9730.840000	-0.0031	0.1000	0.177	0.017	0.014	0.073	0.980	0.806	0.1051	2
	10414.910436	10414.949000	-0.0386	0.1000	0.135	0.285	0.246	1.048	1.122	0.970	0.1078	2
	1156.636396	1156.706000	-0.0696	0.1000	0.207	0.336	0.266	1.529	0.907	0.719	0.1032	2
1116	9699.273921	9699.321000	-0.0471	0.1000	0.141	0.333	0.286	1.252	1.098	0.943	0.1074	2
	10496.604513	10496.582000	0.0225	0.1000	0.100	-0.225	-0.203	0.712	1.306	1.175	0.1100	2
	1158.126605	1158.154000	-0.0274	0.1000	0.148	0.185	0.157	0.712	1.073	0.914	0.1070	2
1136	9940.013361	9940.020000	-0.0066	0.1000	0.037	0.178	0.171	0.344	2.138	2.058	0.1137	2
	10436.240947	10436.271000	-0.0301	0.1000	0.068	0.439	0.409	1.149	1.579	1.471	0.1119	2
	1161.901379	1161.894000	0.0074	0.1000	0.052	-0.142	-0.135	0.324	1.814	1.720	0.1129	2
1142	9941.289674	9941.310000	-0.0203	0.1000	0.037	0.543	0.522	1.050	2.134	2.054	0.1137	2
	10437.974682	10438.000000	-0.0253	0.1000	0.068	0.370	0.345	0.968	1.579	1.471	0.1119	2
	1161.897801	1161.885000	0.0128	0.1000	0.052	-0.246	-0.233	0.561	1.810	1.716	0.1129	2
1147	9607.906000	-	-	-	-	-	-	-	-	-	-	0
	10354.673000	-	-	-	-	-	-	-	-	-	-	0
	1147.167000	-	-	-	-	-	-	-	-	-	-	0
1151	9621.660000	-	-	-	-	-	-	-	-	-	-	0
	10345.144000	-	-	-	-	-	-	-	-	-	-	0
	1147.307000	-	-	-	-	-	-	-	-	-	-	0
1208	9675.348362	9675.400000	-0.0516	0.1000	0.129	0.399	0.347	1.435	1.148	0.999	0.1081	2
	10491.391558	10491.349000	0.0426	0.1000	0.081	-0.526	-0.483	1.496	1.451	1.334	0.1111	2
	1158.137992	1158.152000	-0.0140	0.1000	0.131	0.107	0.093	0.387	1.141	0.991	0.1080	2
4019	9774.173719	9774.114000	0.0597	0.1000	0.191	-0.312	-0.252	1.365	0.944	0.764	0.1042	2
	10327.873285	10327.852000	0.0213	0.1000	0.156	-0.137	-0.115	0.539	1.046	0.883	0.1065	2
	1164.711853	1164.719000	-0.0071	0.1000	0.201	0.036	0.028	0.159	0.921	0.736	0.1036	2
4020	9814.656185	9814.598000	0.0582	0.1000	0.162	-0.359	-0.300	1.445	1.025	0.859	0.1061	2
	10350.882610	10350.906000	-0.0234	0.1000	0.133	0.175	0.152	0.640	1.131	0.980	0.1079	2
	1170.204990	1170.192000	0.0130	0.1000	0.170	-0.076	-0.063	0.315	1.000	0.830	0.1056	2
1022	9869.809594	9869.807000	0.0026	0.1000	0.055	-0.047	-0.045	0.111	1.761	1.665	0.1127	2
	10499.630090	10499.626000	0.0041	0.1000	0.046	-0.088	-0.084	0.190	1.918	1.829	0.1132	2
	1157.724136	1157.727000	-0.0029	0.1000	0.065	0.044	0.041	0.112	1.617	1.511	0.1121	2
1162	9560.563375	9560.576000	-0.0126	0.1000	0.050	0.254	0.242	0.567	1.854	1.762	0.1130	2
	10568.724880	10568.729000	-0.0041	0.1000	0.038	0.109	0.104	0.212	2.120	2.040	0.1137	2
	1154.125295	1154.110000	0.0153	0.1000	0.072	-0.214	-0.199	0.572	1.544	1.434	0.1117	2
1164	9565.208799	9565.215000	-0.0062	0.1000	0.050	0.123	0.117	0.276	1.840	1.747	0.1130	2
	10569.703548	10569.705000	-0.0015	0.1000	0.038	0.038	0.037	0.075	2.124	2.044	0.1137	2
	1154.227523	1154.221000	0.0065	0.1000	0.073	-0.090	-0.083	0.242	1.531	1.420	0.1116	2
1160	9556.284468	9556.294000	-0.0095	0.1000	0.048	0.199	0.190	0.436	1.889	1.798	0.1131	2
	10567.608696	10567.612000	-0.0033	0.1000	0.029	0.114	0.111	0.194	2.430	2.360	0.1142	2
	1154.182112	1154.170000	0.0121	0.1000	0.061	-0.198	-0.186	0.490	1.669	1.567	0.1123	2
1228	9804.606165	9804.655000	-0.0488	0.1000	0.088	0.555	0.506	1.646	1.392	1.269	0.1107	2
	10299.096810	10299.092000	0.0048	0.1000	0.023	-0.211	-0.206	0.318	2.734	2.671	0.1146	2
	1171.243273	1171.202000	0.0413	0.1000	0.081	-0.511	-0.470	1.453	1.454	1.336	0.1111	2
1239	9852.354262	9852.336000	0.0183	0.1000	0.014	-1.334	-1.316	1.561	3.530	3.482	0.1151	2
	10300.757282	10300.924000	-0.1667	0.2000	0.055	3.015	2.848	3.545**	3.512	3.318	0.2253	2
	1168.969936	1168.877000	0.0929	0.3000	0.022	-4.265	-4.172	2.099	8.393	8.210	0.3439	2
1240	9833.141427	9833.117000	0.0244	0.1000	0.014	-1.761	-1.737	2.074	3.507	3.458	0.1151	2
	10282.794318	10282.963000	-0.1687	0.2000	0.057	2.983	2.814	3.547**	3.473	3.277	0.2252	2
	1171.396410	1171.291000	0.1054	0.3000	0.021	-5.086	-4.981	2.441	8.606	8.428	0.3441	2
4015	9635.986333	9635.959000	0.0273	0.1000	0.020	-1.386	-1.358	1.946	2.941	2.882	0.1148	2
	10245.582236	10245.583000	-0.0008	0.1000	0.021	0.036	0.036	0.053	2.848	2.788	0.1147	2
	1148.030062	1148.014000	0.0161	0.3000	0.019	-0.838	-0.822	0.387	8.952	8.780	0.3444	2
4016	9656.767146	9656.573000	0.1941	0.2000	0.074	-2.611	-2.417	3.560**	3.029	2.804	0.2230	2
	10233.627554	10233.629000	-0.0014	0.1000	0.021	0.068	0.067	0.099	2.834	2.774	0.1147	2
	1154.190893	1154.118000	0.0729	0.3000	0.021	-3.409	-3.336	1.662	8.473	8.292	0.3440	2
4008	9511.737102	9511.719000	0.0181	0.1000	0.012	-1.485	-1.467	1.640	3.741	3.695	0.1152	2
	10034.792113	10034.752000	0.0401	0.1000	0.014	-2.924	-2.884	3.425**	3.526	3.478	0.1151	2
	1145.932462	1146.003000	-0.0705	0.3000	0.014	4.904	4.833	1.960	10.331	10.182	0.3452	2
4009	9520.182731	9520.162000	0.0207	0.1000	0.012	-1.694	-1.674	1.874	3.734	3.688	0.1152	2
	10035.583837	10035.543000	0.0408	0.1000	0.014	-2.940	-2.899	3.465**	3.504	3.455	0.1151	2
	1150.194975	1150.262000	-0.0670	0.3000	0.015	4.445	4.378	1.820	10.090	9.938	0.3451	2

4010	9563.078971	9563.068000	0.0110	0.1000	0.013	-0.831	-0.820	0.955	3.593	3.546	0.1151	2
	10134.448091	10134.444000	0.0041	0.1000	0.014	-0.284	-0.280	0.341	3.440	3.391	0.1151	2
	1146.127457	1146.110000	0.0175	0.3000	0.013	-1.297	-1.280	0.502	10.681	10.537	0.3454	2
4012	9592.490068	9592.494000	-0.0039	0.1000	0.013	0.294	0.290	0.340	3.574	3.526	0.1151	2
	10183.816832	10183.822000	-0.0052	0.1000	0.015	0.355	0.350	0.429	3.424	3.375	0.1151	2
	1149.819317	1149.834000	-0.0147	0.3000	0.014	1.022	1.008	0.408	10.339	10.191	0.3452	2
4013	9600.831147	9600.833000	-0.0019	0.1000	0.013	0.139	0.137	0.160	3.571	3.523	0.1151	2
	10183.976076	10183.987000	-0.0109	0.1000	0.015	0.747	0.736	0.903	3.416	3.366	0.1151	2
	1153.769389	1153.780000	-0.0106	0.3000	0.015	0.696	0.686	0.287	10.038	9.885	0.3451	2
1158	9551.290876	9551.294000	-0.0031	0.1000	0.017	0.181	0.178	0.238	3.142	3.088	0.1149	2
	10566.675026	10566.677000	-0.0020	0.1000	0.015	0.133	0.131	0.162	3.386	3.335	0.1150	2
	1154.150641	1154.123000	0.0276	0.3000	0.202	-0.137	-0.109	0.205	2.755	2.197	0.3106	2
4017	9319.114000	-	-	-	-	-	-	-	-	-	-	0
	10402.003000	-	-	-	-	-	-	-	-	-	-	0
	1127.981000	-	-	-	-	-	-	-	-	-	-	0

IMAGE COORDINATES

SYSTEM-NU	POINT-NU	X Y	BEOBX BEOBY	VX VY	MFVX MFVY	EVX EVY	GFX GFY	EKX EKY	NVX NVY	GRZWX GRZWY	EGKX EGKY
1981	1002	-23.226796	-23.246600	0.0198	0.2500	0.807	-0.025	-0.005	0.088	1.149	0.221
		10.884899	10.778000	0.1069	0.2500	0.825	-0.130	-0.023	0.471	1.137	0.199
1981	1003	-23.791153	-23.792300	0.0011	0.2500	0.813	-0.001	0.000	0.005	1.145	0.214
		9.753990	9.588100	0.1659	0.2500	0.829	-0.200	-0.034	0.729	1.134	0.194
1981	1077	-15.958417	-16.031400	0.0730	0.2500	0.456	-0.160	-0.087	0.432	1.529	0.832
		52.883178	52.886900	-0.0037	0.2500	0.588	0.006	0.003	0.019	1.347	0.556
1981	4027	-67.761182	-67.787200	0.0260	0.2500	0.706	-0.037	-0.011	0.124	1.229	0.361
		-47.167428	-47.055100	-0.1123	0.2500	0.731	0.154	0.041	0.526	1.208	0.325
1981	4028	-42.732392	-42.623600	-0.1088	0.2500	0.827	0.132	0.023	0.479	1.135	0.196
		-33.353178	-33.267900	-0.0853	0.2500	0.844	0.101	0.016	0.371	1.124	0.175
1981	4029	-52.316612	-52.373200	0.0566	0.2500	0.827	-0.068	-0.012	0.249	1.135	0.196
		-30.435248	-30.403900	-0.0313	0.2500	0.835	0.038	0.006	0.137	1.130	0.187
1981	4030	-23.508347	-23.217900	-0.2904	0.2500	0.832	0.349	0.058	1.273	1.132	0.190
		-32.028477	-32.001900	-0.0266	0.2500	0.835	0.032	0.005	0.116	1.130	0.187
1981	4041	-65.007352	-65.224200	0.2168	0.2500	0.803	-0.270	-0.053	0.968	1.152	0.227
		-29.636656	-29.629100	-0.0076	0.2500	0.797	0.009	0.002	0.034	1.156	0.235
1982	1002	-21.340739	-21.168400	-0.1723	0.2500	0.765	0.225	0.053	0.788	1.181	0.278
		-37.603885	-37.519400	-0.0845	0.2500	0.863	0.098	0.013	0.364	1.111	0.152
1982	1003	-22.050608	-21.888200	-0.1624	0.2500	0.759	0.214	0.051	0.745	1.185	0.285
		-38.479860	-38.377500	-0.1024	0.2500	0.862	0.119	0.016	0.441	1.112	0.154
1982	1077	-6.370013	-5.801300	-0.5687	0.2500	0.892	0.637	0.069	2.408	1.093	0.118
		-3.583090	-3.446100	-0.1370	0.2500	0.877	0.156	0.019	0.585	1.102	0.135
1982	1110	-29.341454	-29.436200	0.0947	0.2500	0.895	-0.106	-0.011	0.401	1.091	0.114
		26.109238	25.823400	0.2858	0.2500	0.908	-0.315	-0.029	1.200	1.083	0.100
1982	1116	-10.524488	-10.242300	-0.2822	0.2500	0.903	0.312	0.030	1.188	1.086	0.105
		18.746931	18.912900	-0.1660	0.2500	0.889	0.187	0.021	0.704	1.095	0.121
1982	1136	-58.229405	-58.718800	0.4894	0.2500	0.850	-0.576	-0.087	2.124	1.120	0.169
		-13.031826	-12.436100	-0.5957	0.2500	0.851	0.700	0.104	2.583**	1.119	0.167
1982	1142	-58.118604	-58.524500	0.4059	0.2500	0.848	-0.479	-0.073	1.763	1.121	0.170
		-13.515006	-12.810700	-0.7043	0.2500	0.851	0.828	0.123	3.054**	1.119	0.167
1982	1147	-20.719661	-20.704200	-0.0155	0.2500	0.783	0.020	0.004	0.070	1.167	0.253
		56.260528	56.129200	0.1313	0.2500	0.866	-0.152	-0.020	0.564	1.109	0.148
1982	1151	-24.475858	-24.285000	-0.1909	0.2500	0.787	0.242	0.052	0.860	1.164	0.247
		55.475457	55.288100	0.1874	0.2500	0.872	-0.215	-0.028	0.803	1.106	0.142
1982	1208	-7.750642	-7.377600	-0.3730	0.2500	0.895	0.417	0.044	1.577	1.091	0.115
		23.583092	23.748400	-0.1653	0.2500	0.880	0.188	0.023	0.705	1.101	0.132
1982	4019	-51.714873	-51.945800	0.2309	0.2500	0.865	-0.267	-0.036	0.993	1.110	0.150
		32.657019	31.812100	0.8449	0.2500	0.871	-0.970	-0.125	3.622**	1.106	0.143
1982	4020	-54.180545	-54.695300	0.5148	0.2500	0.886	-0.581	-0.066	2.188	1.097	0.125
		21.958261	21.487300	0.4710	0.2500	0.869	-0.542	-0.071	2.021	1.108	0.145
2025	1002	-23.758175	-23.712300	-0.0459	0.2500	0.868	0.053	0.007	0.197	1.108	0.146
		-4.746265	-4.586100	-0.1602	0.2500	0.878	0.182	0.022	0.684	1.102	0.134
2025	1003	-24.496713	-24.376200	-0.1205	0.2500	0.866	0.139	0.019	0.518	1.109	0.148
		-5.608106	-5.434900	-0.1732	0.2500	0.879	0.197	0.024	0.739	1.101	0.134
2025	1077	-7.872136	-7.577000	-0.2951	0.2500	0.851	0.347	0.052	1.280	1.119	0.167
		30.095823	30.515000	-0.4192	0.2500	0.834	0.503	0.084	1.836	1.131	0.188
2025	1116	-11.725663	-11.733500	0.0078	0.2500	0.751	-0.010	-0.003	0.036	1.192	0.297
		53.647698	53.733200	-0.0855	0.2500	0.811	0.105	0.020	0.380	1.147	0.217
2025	1136	-61.191622	-61.207500	0.0159	0.2500	0.845	-0.019	-0.003	0.069	1.123	0.174
		21.991166	21.589100	0.4021	0.2500	0.824	-0.488	-0.086	1.771	1.137	0.200
2025	1142	-61.079842	-61.041500	-0.0383	0.2500	0.846	0.045	0.007	0.167	1.123	0.173
		21.486782	21.144200	0.3426	0.2500	0.825	-0.415	-0.073	1.509	1.137	0.199
2025	1208	-8.747797	-8.789300	0.0415	0.2500	0.717	-0.058	-0.016	0.196	1.220	0.345
		58.705581	58.387700	0.3179	0.2500	0.788	-0.403	-0.085	1.432	1.163	0.246
2025	4028	-49.606966	-49.798700	0.1917	0.2500	0.698	-0.275	-0.083	0.918	1.236	0.373
		-37.614063	-37.599500	-0.0146	0.2500	0.819	0.018	0.003	0.064	1.141	0.206
2025	4029	-57.064280	-57.318000	0.2537	0.2500	0.718	-0.353	-0.100	1.198	1.219	0.344
		-33.203810	-32.958600	-0.2452	0.2500	0.809	0.303	0.058	1.091	1.148	0.219

20886	1002	50.256138	50.213500	0.0426	0.2500	0.762	-0.056	-0.013	0.195	1.182	0.281
		-13.852240	-13.855600	0.0034	0.2500	0.622	-0.005	-0.002	0.017	1.309	0.495
20886	1003	51.674249	51.567800	0.1064	0.2500	0.755	-0.141	-0.035	0.490	1.188	0.291
		-14.215547	-14.393800	0.1783	0.2500	0.611	-0.292	-0.114	0.912	1.321	0.514
20886	1022	-11.148538	-11.093100	-0.0554	0.2500	0.869	0.064	0.008	0.238	1.108	0.145
		-15.681078	-15.689800	0.0087	0.2500	0.870	-0.010	-0.001	0.037	1.107	0.144
20886	1077	-1.205544	-1.057000	-0.1485	0.2500	0.877	0.169	0.021	0.634	1.102	0.135
		-0.357702	-0.307500	-0.0502	0.2500	0.855	0.059	0.009	0.217	1.117	0.162
20886	1110	-63.460660	-63.668300	0.2076	0.2500	0.837	-0.248	-0.040	0.908	1.128	0.183
		-6.850915	-6.947000	0.0961	0.2500	0.779	-0.123	-0.027	0.436	1.170	0.259
20886	1116	-36.382802	-36.367800	-0.0150	0.2500	0.867	0.017	0.002	0.064	1.109	0.148
		-0.774334	-0.757900	-0.0164	0.2500	0.853	0.019	0.003	0.071	1.118	0.165
20886	1136	-27.665239	-27.614400	-0.0508	0.2500	0.750	0.068	0.017	0.235	1.192	0.298
		-26.799566	-26.711700	-0.0879	0.2500	0.762	0.115	0.027	0.403	1.183	0.281
20886	1142	-26.548479	-26.513300	-0.0352	0.2500	0.750	0.047	0.012	0.163	1.193	0.299
		-26.864271	-26.711700	-0.1526	0.2500	0.763	0.200	0.047	0.699	1.182	0.280
20886	1162	-28.478008	-28.462200	-0.0158	0.2500	0.795	0.020	0.004	0.071	1.158	0.237
		8.046283	8.138700	-0.0924	0.2500	0.781	0.118	0.026	0.418	1.168	0.256
20886	1164	-27.736975	-27.691500	-0.0455	0.2500	0.798	0.057	0.011	0.204	1.156	0.233
		7.875843	7.941000	-0.0652	0.2500	0.784	0.083	0.018	0.294	1.166	0.252
20886	4020	-85.402986	-85.397600	-0.0054	0.2500	0.741	0.007	0.002	0.025	1.199	0.310
		-12.208178	-12.389300	0.1811	0.2500	0.618	-0.293	-0.112	0.921	1.313	0.501
20878	1003	-3.844385	-3.771100	-0.0733	0.2500	0.831	0.088	0.015	0.322	1.132	0.191
		-12.031803	-12.065300	0.0335	0.2500	0.726	-0.046	-0.013	0.157	1.212	0.333
20878	1022	-46.527711	-46.469900	-0.0578	0.2500	0.889	0.065	0.007	0.245	1.095	0.122
		-0.570540	-0.433800	-0.1367	0.2500	0.886	0.154	0.018	0.581	1.097	0.125
20878	1077	-6.504052	-6.650400	0.1463	0.2500	0.841	-0.174	-0.028	0.638	1.126	0.178
		12.450790	12.565100	-0.1143	0.2500	0.700	0.163	0.049	0.546	1.234	0.370
20878	1110	-52.787605	-52.756900	-0.0307	0.2500	0.849	0.036	0.005	0.133	1.120	0.169
		15.857021	15.810700	0.0463	0.2500	0.847	-0.055	-0.008	0.201	1.122	0.172
20878	1116	-25.009580	-25.175600	0.1660	0.2500	0.842	-0.197	-0.031	0.724	1.125	0.178
		17.832633	17.765700	0.0669	0.2500	0.777	-0.086	-0.019	0.304	1.171	0.261
20878	1136	-83.227297	-83.289100	0.0618	0.2500	0.844	-0.073	-0.011	0.269	1.124	0.175
		-7.159552	-7.089800	-0.0698	0.2500	0.794	0.088	0.018	0.313	1.159	0.239
20878	1142	-82.877054	-82.859700	-0.0174	0.2500	0.844	0.021	0.003	0.076	1.124	0.175
		-7.406672	-7.298500	-0.1082	0.2500	0.795	0.136	0.028	0.485	1.158	0.237
20878	4019	-85.102570	-85.012200	-0.0904	0.2500	0.815	0.111	0.020	0.400	1.143	0.211
		15.795824	15.717300	0.0785	0.2500	0.764	-0.103	-0.024	0.359	1.181	0.278
20878	4020	-86.064625	-85.937100	-0.1275	0.2500	0.827	0.154	0.027	0.561	1.135	0.196
		13.266086	13.191100	0.0750	0.2500	0.771	-0.097	-0.022	0.342	1.176	0.269
20878	4028	-24.226067	-24.135100	-0.0910	0.2500	0.613	0.148	0.057	0.465	1.318	0.510
		-51.508492	-51.534300	0.0258	0.2500	0.617	-0.042	-0.016	0.131	1.315	0.504
20878	4029	-46.860398	-46.992900	0.1325	0.2500	0.625	-0.212	-0.080	0.670	1.306	0.490
		-51.838529	-51.929700	0.0912	0.2500	0.649	-0.141	-0.049	0.453	1.282	0.451
20893	1022	73.231042	73.257400	-0.0264	0.2500	0.418	0.063	0.037	0.163	1.597	0.930
		-13.299868	-13.384400	0.0845	0.2500	0.266	-0.318	-0.234	0.656	2.004	1.472
20893	1077	21.244572	21.481500	-0.2369	0.2500	0.692	0.343	0.106	1.140	1.241	0.383
		14.465164	14.597000	-0.1318	0.2500	0.624	0.211	0.080	0.668	1.308	0.492
20893	1110	-56.306360	-56.458300	0.1519	0.2500	0.757	-0.201	-0.049	0.698	1.187	0.288
		-14.767033	-14.904500	0.1375	0.2500	0.729	-0.189	-0.051	0.644	1.209	0.328
20893	1116	-35.967375	-36.037400	0.0700	0.2500	0.737	-0.095	-0.025	0.326	1.203	0.317
		5.439949	5.436800	0.0031	0.2500	0.697	-0.005	-0.001	0.015	1.236	0.374
20893	1208	-49.933948	-50.108900	0.1750	0.2500	0.686	-0.255	-0.080	0.845	1.247	0.391
		6.776943	6.754800	0.0221	0.2500	0.629	-0.035	-0.013	0.112	1.302	0.483
20893	4019	-87.026817	-86.729900	-0.2969	0.2500	0.433	0.685	0.388	1.804	1.568	0.889
		-44.574792	-44.493900	-0.0809	0.2500	0.444	0.182	0.101	0.485	1.549	0.860
20893	4020	-34.771174	-34.958400	0.1872	0.2500	0.449	-0.417	-0.230	1.118	1.541	0.849
		-39.284665	-39.265800	-0.0189	0.2500	0.502	0.038	0.019	0.107	1.457	0.726
20891	1077	22.553482	22.626600	-0.0731	0.2500	0.660	0.111	0.038	0.360	1.271	0.432
		3.070154	3.108300	-0.0381	0.2500	0.257	0.149	0.110	0.301	2.038	1.515
20891	1110	-25.828533	-25.621500	-0.2070	0.2500	0.814	0.254	0.047	0.918	1.145	0.213
		-24.106537	-24.313700	0.2072	0.2500	0.815	-0.254	-0.047	0.918	1.143	0.211
20891	1116	-24.297816	-24.267200	-0.0306	0.2500	0.840	0.036	0.006	0.134	1.126	0.180
		-7.231337	-7.293000	0.0617	0.2500	0.807	-0.076	-0.015	0.275	1.149	0.222
20891	1160	-75.606776	-75.668000	0.0612	0.2500	0.753	-0.081	-0.020	0.282	1.190	0.293
		3.362721	3.430500	-0.0678	0.2500	0.684	0.099	0.031	0.328	1.248	0.394
20891	1162	-73.481576	-73.590700	0.1091	0.2500	0.759	-0.144	-0.035	0.501	1.185	0.285
		3.324741	3.364600	-0.0399	0.2500	0.700	0.057	0.017	0.191	1.235	0.371
20891	1164	-71.240246	-71.351800	0.1116	0.2500	0.765	-0.146	-0.034	0.510	1.181	0.278
		3.340336	3.379200	-0.0389	0.2500	0.714	0.054	0.016	0.184	1.222	0.349
20891	1208	-39.021547	-38.872600	-0.1489	0.2500	0.838	0.178	0.029	0.651	1.128	0.182
		-6.979154	-7.089800	0.1106	0.2500	0.833	-0.133	-0.022	0.485	1.131	0.189
20891	1228	2.887296	2.660900	0.2264	0.2500	0.376	-0.602	-0.376	1.477	1.684	1.050
		-56.151642	-55.931300	-0.2203	0.2500	0.369	0.596	0.376	1.450	1.699	1.071
20891	4019	-19.358727	-19.290400	-0.0683	0.2500	0.580	0.118	0.050	0.359	1.356	0.570

		-46.400159	-46.438000	0.0378	0.2500	0.590	-0.064	-0.026	0.197	1.345	0.552
1983	1110	-25.487880	-25.378900	-0.1090	0.2500	0.915	0.119	0.010	0.456	1.080	0.092
		-2.995196	-2.944600	-0.0506	0.2500	0.902	0.056	0.006	0.213	1.087	0.107
1983	1116	-7.027357	-6.210100	-0.8173	0.2500	0.895	0.913	0.096	3.456**	1.091	0.115
		-10.346940	-10.213900	-0.1330	0.2500	0.838	0.159	0.026	0.581	1.128	0.183
1983	1136	-54.002863	-54.002900	0.0000	0.2500	0.764	0.000	0.000	0.000	1.181	0.279
		-40.815433	-40.281700	-0.5337	0.2500	0.861	0.620	0.086	2.300	1.113	0.154
1983	1142	-53.903037	-53.888000	-0.0150	0.2500	0.761	0.020	0.005	0.069	1.184	0.283
		-41.283707	-40.773600	-0.5101	0.2500	0.861	0.593	0.083	2.199	1.113	0.155
1983	1147	-16.495204	-16.009900	-0.4853	0.2500	0.861	0.564	0.078	2.092	1.113	0.155
		26.792816	26.672300	0.1205	0.2500	0.866	-0.139	-0.019	0.518	1.109	0.148
1983	1208	-4.205322	-3.338400	-0.8669	0.2500	0.898	0.966	0.099	3.660**	1.090	0.111
		-5.601612	-5.404100	-0.1975	0.2500	0.825	0.239	0.042	0.870	1.137	0.199
1983	1239	-64.240011	-64.714400	0.4744	0.2500	0.877	-0.541	-0.066	2.026	1.102	0.135
		-5.845868	-5.738900	-0.1070	0.2500	0.849	0.126	0.019	0.464	1.121	0.170
1983	1240	-64.561055	-65.202600	0.6415	0.2500	0.880	-0.729	-0.088	2.736**	1.101	0.133
		0.165738	0.082000	0.0837	0.2500	0.848	-0.099	-0.015	0.364	1.122	0.171
1983	4015	-39.215984	-39.213500	-0.0025	0.2500	0.790	0.003	0.001	0.011	1.162	0.244
		39.224187	38.642000	0.5822	0.2500	0.877	-0.664	-0.082	2.487	1.103	0.136
1983	4016	-44.732846	-44.842100	0.1093	0.2500	0.789	-0.138	-0.029	0.492	1.162	0.245
		37.770198	37.002300	0.7679	0.2500	0.867	-0.886	-0.118	3.299**	1.109	0.147
1983	4019	-47.231303	-47.656300	0.4250	0.2500	0.912	-0.466	-0.041	1.780	1.081	0.095
		3.141286	3.115400	0.0259	0.2500	0.906	-0.029	-0.003	0.109	1.085	0.102
1983	4020	-49.820567	-50.248100	0.4275	0.2500	0.906	-0.472	-0.044	1.797	1.085	0.102
		-7.364082	-7.344400	-0.0197	0.2500	0.900	0.022	0.002	0.083	1.088	0.108
1983	5014	-33.813910	-33.843300	0.0294	0.2500	0.428	-0.069	-0.039	0.180	1.578	0.902
		18.712950	18.719800	-0.0068	0.2500	0.023	0.294	0.288	0.180	6.769	6.612
1983	5015	-44.192265	-44.325100	0.1328	0.2500	0.427	-0.311	-0.178	0.813	1.580	0.905
		12.621887	12.652900	-0.0310	0.2500	0.023	1.332	1.301	0.813	6.767	6.610
1985	1110	-22.692569	-22.557200	-0.1354	0.2500	0.888	0.152	0.017	0.575	1.096	0.123
		-51.979095	-51.906600	-0.0725	0.2500	0.903	0.080	0.008	0.305	1.086	0.105
1985	1116	-4.408116	-3.704700	-0.7034	0.2500	0.857	0.821	0.117	3.039**	1.115	0.159
		-59.572404	-59.105900	-0.4665	0.2500	0.854	0.546	0.080	2.019	1.117	0.163
1985	1147	-13.736055	-13.209600	-0.5265	0.2500	0.932	0.565	0.039	2.182	1.070	0.073
		-22.414746	-22.401700	-0.0130	0.2500	0.915	0.014	0.001	0.055	1.080	0.092
1985	1208	-1.599983	-0.872500	-0.7275	0.2500	0.868	0.838	0.110	3.123**	1.108	0.146
		-54.948159	-54.736800	-0.2114	0.2500	0.854	0.248	0.036	0.915	1.117	0.163
1985	1239	-60.499144	-61.206300	0.7072	0.2500	0.850	-0.832	-0.125	3.068**	1.120	0.168
		-54.830352	-54.544500	-0.2859	0.2500	0.867	0.330	0.044	1.228	1.109	0.148
1985	1240	-60.838787	-61.492400	0.6536	0.2500	0.865	-0.756	-0.102	2.812**	1.110	0.150
		-49.162286	-48.801500	-0.3608	0.2500	0.873	0.413	0.052	1.544	1.105	0.140
1985	4008	-52.443611	-52.252100	-0.1915	0.2500	0.745	0.257	0.066	0.888	1.196	0.305
		43.069753	42.426500	0.6433	0.2500	0.853	-0.754	-0.111	2.785**	1.118	0.164
1985	4009	-53.886180	-53.682500	-0.2037	0.2500	0.751	0.271	0.068	0.940	1.192	0.297
		41.643751	40.942700	0.7011	0.2500	0.855	-0.820	-0.119	3.033**	1.117	0.162
1985	4010	-43.496047	-43.498100	0.0021	0.2500	0.859	-0.002	0.000	0.009	1.114	0.157
		18.926689	18.712700	0.2140	0.2500	0.906	-0.236	-0.022	0.899	1.085	0.102
1985	4012	-39.899295	-39.922100	0.0228	0.2500	0.896	-0.025	-0.003	0.096	1.091	0.114
		6.379903	6.375000	0.0049	0.2500	0.919	-0.005	0.000	0.020	1.077	0.087
1985	4013	-41.356222	-41.495500	0.1393	0.2500	0.898	-0.155	-0.016	0.588	1.089	0.111
		4.931318	4.891100	0.0402	0.2500	0.919	-0.044	-0.004	0.168	1.077	0.087
1985	4015	-36.068051	-36.203100	0.1350	0.2500	0.923	-0.146	-0.011	0.562	1.075	0.082
		-10.281291	-10.304400	0.0231	0.2500	0.927	-0.025	-0.002	0.096	1.072	0.078
1985	4016	-41.508333	-41.695800	0.1875	0.2500	0.914	-0.205	-0.018	0.784	1.080	0.092
		-12.019521	-12.145400	0.1259	0.2500	0.915	-0.138	-0.012	0.526	1.079	0.091
1985	4019	-44.046270	-44.499400	0.4531	0.2500	0.900	-0.504	-0.050	1.911	1.088	0.109
		-46.144227	-45.943800	-0.2004	0.2500	0.915	0.219	0.019	0.838	1.080	0.092
1985	4020	-46.620610	-46.988200	0.3676	0.2500	0.871	-0.422	-0.054	1.575	1.106	0.143
		-56.597278	-56.330600	-0.2667	0.2500	0.900	0.296	0.029	1.124	1.088	0.108
1985	5014	-30.740390	-30.710400	-0.0300	0.2500	0.446	0.067	0.037	0.180	1.546	0.857
		-30.081793	-30.088800	0.0070	0.2500	0.024	-0.288	-0.281	0.180	6.617	6.456
1985	5015	-40.974021	-40.837600	-0.1364	0.2500	0.450	0.303	0.166	0.813	1.538	0.845
		-36.431831	-36.463700	0.0319	0.2500	0.025	-1.296	-1.265	0.813	6.585	6.424
20892	1110	-31.869999	-31.956200	0.0862	0.2500	0.791	-0.109	-0.023	0.388	1.161	0.243
		-21.724907	-21.897300	0.1724	0.2500	0.796	-0.217	-0.044	0.773	1.157	0.236
20892	1116	-16.582334	-16.383700	-0.1986	0.2500	0.819	0.243	0.044	0.878	1.141	0.207
		-0.220201	-0.307500	0.0873	0.2500	0.641	-0.136	-0.049	0.436	1.290	0.464
20892	1158	-58.121167	-58.168600	0.0474	0.2500	0.772	-0.061	-0.014	0.216	1.175	0.268
		16.471412	16.508100	-0.0367	0.2500	0.612	0.060	0.023	0.188	1.320	0.513
20892	1160	-55.947420	-56.010500	0.0631	0.2500	0.778	-0.081	-0.018	0.286	1.170	0.259
		16.317577	16.354300	-0.0367	0.2500	0.751	0.049	0.012	0.170	1.192	0.297
20892	1162	-53.966775	-54.006600	0.0398	0.2500	0.782	-0.051	-0.011	0.180	1.168	0.255
		16.175803	16.244500	-0.0687	0.2500	0.762	0.090	0.021	0.315	1.182	0.281
20892	1164	-51.888674	-51.870600	-0.0181	0.2500	0.785	0.023	0.005	0.082	1.166	0.251
		16.077123	16.112700	-0.0356	0.2500	0.772	0.046	0.011	0.162	1.175	0.268

20892	1208	-31.161062	-31.093700	-0.0674	0.2500	0.836	0.081	0.013	0.295	1.129	0.186
		1.037261	1.010500	0.0268	0.2500	0.794	-0.034	-0.007	0.120	1.158	0.238
20892	4019	-52.482050	-52.498200	0.0161	0.2500	0.378	-0.043	-0.027	0.105	1.680	1.045
		-54.373773	-54.433900	0.0601	0.2500	0.293	-0.205	-0.145	0.444	1.906	1.347
20892	4020	1.779767	1.761700	0.0181	0.2500	0.405	-0.045	-0.027	0.114	1.623	0.966
		-48.361338	-48.195300	-0.1660	0.2500	0.370	0.449	0.283	1.092	1.698	1.071
20899	1110	6.544825	6.380600	0.1642	0.2500	0.826	-0.199	-0.035	0.723	1.136	0.198
		-28.597211	-28.578500	-0.0187	0.2500	0.835	0.022	0.004	0.082	1.130	0.187
20899	1116	8.519422	8.500100	0.0193	0.2500	0.850	-0.023	-0.003	0.084	1.120	0.168
		-8.607783	-8.650400	0.0426	0.2500	0.820	-0.052	-0.009	0.188	1.140	0.205
20899	1160	-26.636736	-26.645500	0.0088	0.2500	0.755	-0.012	-0.003	0.040	1.188	0.291
		10.086705	10.154900	-0.0682	0.2500	0.743	0.092	0.024	0.316	1.198	0.308
20899	1162	-25.165256	-25.192100	0.0268	0.2500	0.758	-0.035	-0.009	0.123	1.186	0.287
		9.986007	10.022100	-0.0361	0.2500	0.753	0.048	0.012	0.166	1.190	0.294
20899	1164	-23.608795	-23.606600	-0.0022	0.2500	0.760	0.003	0.001	0.010	1.184	0.284
		9.897167	9.845100	0.0521	0.2500	0.763	-0.068	-0.016	0.238	1.182	0.281
20899	1208	-1.175324	-1.233200	0.0579	0.2500	0.851	-0.068	-0.010	0.251	1.119	0.167
		-7.747997	-7.632700	-0.1153	0.2500	0.850	0.136	0.020	0.500	1.120	0.168
20899	4019	8.497494	8.114800	0.3827	0.2500	0.618	-0.619	-0.236	1.947	1.313	0.501
		-54.139142	-54.126100	-0.0130	0.2500	0.698	0.019	0.006	0.062	1.236	0.374
20899	4020	34.094096	34.738200	-0.6441	0.2500	0.625	1.030	0.386	3.259**	1.306	0.489
		-50.004418	-50.143800	0.1394	0.2500	0.587	-0.238	-0.098	0.728	1.348	0.557
1980	1147	7.830233	7.695700	0.1345	0.2500	0.795	-0.169	-0.035	0.604	1.158	0.238
		54.066657	53.783700	0.2830	0.2500	0.825	-0.343	-0.060	1.246	1.137	0.199
1980	4008	47.849210	47.550700	0.2985	0.2500	0.765	-0.390	-0.091	1.365	1.180	0.277
		-9.684113	-9.244900	-0.4392	0.2500	0.823	0.533	0.094	1.936	1.138	0.201
1980	4009	49.249007	49.000000	0.2490	0.2500	0.773	-0.322	-0.073	1.133	1.175	0.267
		-8.032237	-7.586300	-0.4459	0.2500	0.819	0.544	0.098	1.971	1.141	0.206
1980	4010	38.178939	38.304300	-0.1254	0.2500	0.868	0.144	0.019	0.538	1.108	0.147
		13.965687	14.057700	-0.0920	0.2500	0.866	0.106	0.014	0.395	1.109	0.148
1980	4012	34.269462	34.275400	-0.0059	0.2500	0.876	0.007	0.001	0.025	1.103	0.137
		26.318189	26.130500	0.1877	0.2500	0.871	-0.215	-0.028	0.804	1.106	0.142
1980	4013	35.679465	35.724600	-0.0451	0.2500	0.873	0.052	0.007	0.193	1.105	0.141
		27.914943	27.626000	0.2889	0.2500	0.868	-0.333	-0.044	1.241	1.108	0.147
1980	4015	29.974034	30.391300	-0.4173	0.2500	0.843	0.495	0.078	1.818	1.125	0.177
		42.180988	42.118800	0.0622	0.2500	0.863	-0.072	-0.010	0.268	1.112	0.153
1980	4016	35.248272	35.927500	-0.6792	0.2500	0.826	0.822	0.143	2.989**	1.136	0.197
		44.075714	44.158100	-0.0824	0.2500	0.846	0.097	0.015	0.358	1.122	0.172
1980	4017	-44.884599	-45.434800	0.5502	0.2500	0.789	-0.697	-0.147	2.477	1.162	0.245
		14.187863	13.921800	0.2661	0.2500	0.438	-0.608	-0.342	1.609	1.561	0.878

PRINCIPAL POINT AND FOCAL LENGTH

CAMERANAME	X0 Y0 C	BEOBX0 BEOBY0 BEOBC	VX0 VY0 VC	MFVX0 MFVY0 MFVC	EVX0 EVY0 EVC	GFX0 GFY0 GFC	EKX0 EKY0 EKC	NVX0 NVY0 NVC	GRZWX0 GRZWY0 GRZWC	EGKX0 EGKY0 EGKC	MX0 MY0 MC	STAX0 STAY0 STAC
baalbek-G1	0.000000	-	-	-	-	-	-	-	-	-	-	0
	0.000000	-	-	-	-	-	-	-	-	-	-	0
	200.000000	-	-	-	-	-	-	-	-	-	-	0
Schräg-kamera	0.000000	-	-	-	-	-	-	-	-	-	-	0
	0.000000	-	-	-	-	-	-	-	-	-	-	0
	260.000000	-	-	-	-	-	-	-	-	-	-	0

CONTROL OF THE ADJUSTMENT

	TOTAL	IMAGE COORD	PROJ.CENT	OBJECT COORD	DIS	DIF	PLANE PO	PLANE PARAM	PRINC PO+C
REDUNDANCY	206.000000	189.771219	11.384357	4.844423	0.000000	0.000000	0.000000	0.000000	0.000000
SIGMA	1.159089	1.183233	0.627299	1.166456	1.000000	1.000000	1.000000	1.000000	1.000000
VTPV	276.758475	265.687264	4.479794	6.591417	0.000000	0.000000	0.000000	0.000000	0.000000

Final observations

TERMINATION LIMIT REACHED AFTER 6. ITERATIONS
TOTAL TIME OF CALCULATION [MIN] 0.0

MAXIMUM NORMALIZED RESIDUAL AT: IMAGE COORDINATES
SYSTEM NU.: 1983
POINT NU .: 1208
NORMALIZED RESIDUAL (NV): 3.66

Appendix K

➢ **Orientation result protocols – comparison of combination of vertical and oblique images to the 1st orientation step (orientation of each image type separately)**

- Protocol (i) – vertical image 1981

Figure (K.1): The aerial vertical image 1981 (source: IFPO-Damascus)

<table>
<tr><td>OS</td><td colspan="7">Image ID: 1981, Camera: Baalbek-G1</td></tr>
<tr><td rowspan="4">Step 1</td><td rowspan="2">IP</td><td colspan="2">$x'_o\ (mm)$</td><td colspan="2">$y'_o\ (mm)$</td><td colspan="2">$c_k\ (mm)$</td></tr>
<tr><td colspan="2">-0.069894</td><td colspan="2">-0.049059</td><td colspan="2">200.25303</td></tr>
<tr><td rowspan="2">EP</td><td>$X_0\ (m)$</td><td>$Y_0\ (m)$</td><td>$Z_0\ (m)$</td><td>$\omega\ (gon)$</td><td>$\varphi\ (gon)$</td><td>$\kappa\ (gon)$</td></tr>
<tr><td>9970.141</td><td>10673.541</td><td>1940.080</td><td>4.425129</td><td>4.625882</td><td>131.135824</td></tr>
<tr><td rowspan="4">Step 2</td><td rowspan="2">IP</td><td colspan="2">$x'_o\ (mm)$</td><td colspan="2">$y'_o\ (mm)$</td><td colspan="2">$c_k\ (mm)$</td></tr>
<tr><td colspan="2">0.00</td><td colspan="2">0.00</td><td colspan="2">200.00</td></tr>
<tr><td rowspan="2">EP</td><td>$X_0\ (m)$</td><td>$Y_0\ (m)$</td><td>$Z_0\ (m)$</td><td>$\omega\ (gon)$</td><td>$\varphi\ (gon)$</td><td>$\kappa\ (gon)$</td></tr>
<tr><td>9970.199</td><td>10673.474</td><td>1940.379</td><td>4.531503</td><td>4.723843</td><td>131.313483</td></tr>
</table>

Table (K.1): Orientation results associated with the vertical image 1981; where OS: Orientation Step, IP: Interior orientation parameters and EP: Exterior orientation parameters

- Protocol (ii) – vertical image 2025

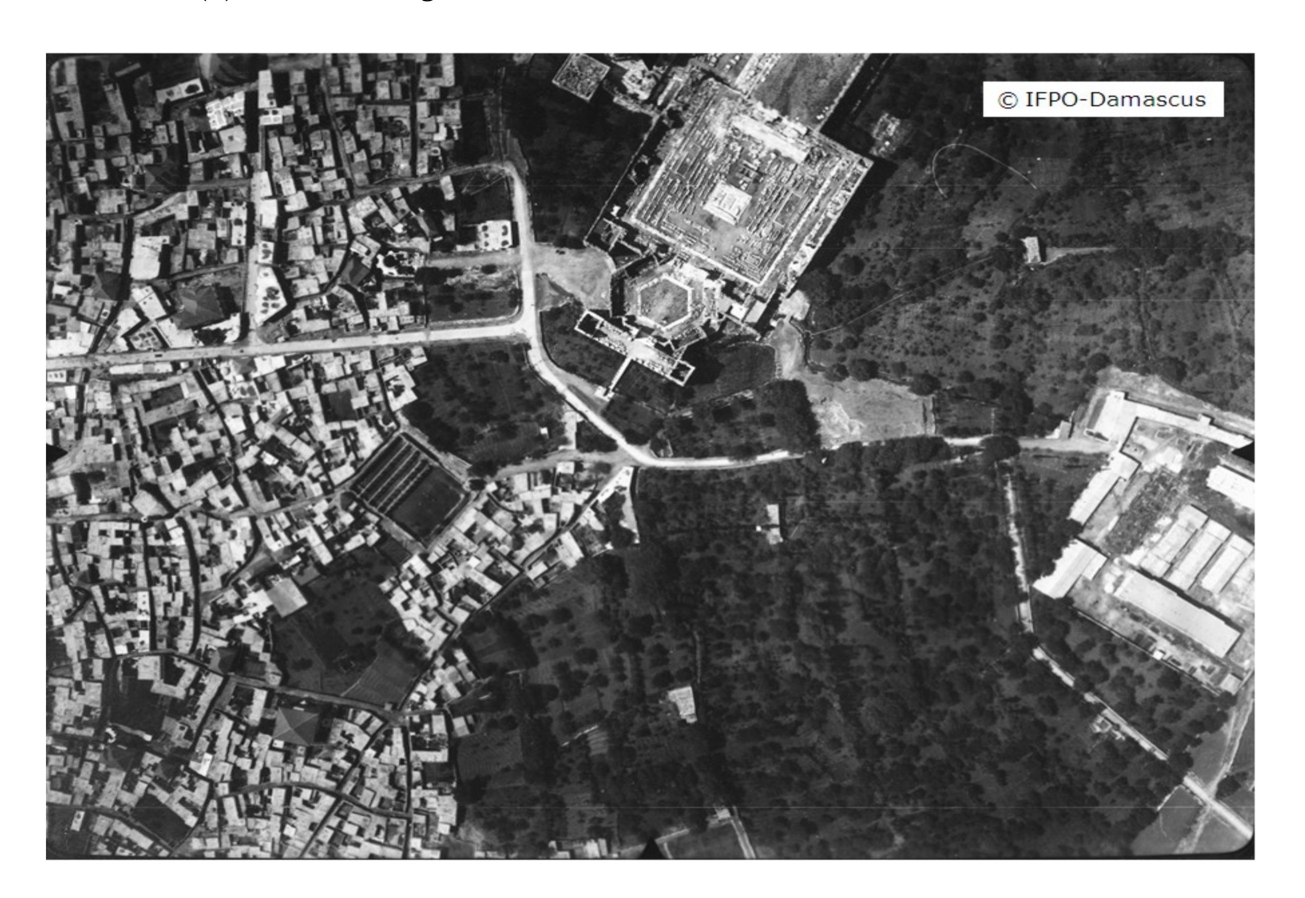

Figure (K.2): The aerial vertical image 2025 (source: IFPO-Damascus)

OS	Image ID: 2025, Camera: Baalbek-G1						
Step 1	IP	x'_o (mm)		y'_o (mm)		c_k (mm)	
		-0.069894		-0.049059		200.25303	
	EP	X_0 (m)	Y_0 (m)	Z_0 (m)	ω (gon)	φ (gon)	κ (gon)
		9791.510	10558.579	2028.774	9.571998	-3.034766	148.071746
Step 2	IP	x'_o (mm)		y'_o (mm)		c_k (mm)	
		0.00		0.00		200.00	
	EP	X_0 (m)	Y_0 (m)	Z_0 (m)	ω (gon)	φ (gon)	κ (gon)
		9791.513	10558.523	2029.001	9.619294	-2.874932	148.322941

Table (K.2): Orientation results associated with the vertical image 2025; where OS: Orientation Step, IP: Interior orientation parameters and EP: Exterior orientation parameters

- Protocol (iii) – oblique image 20878

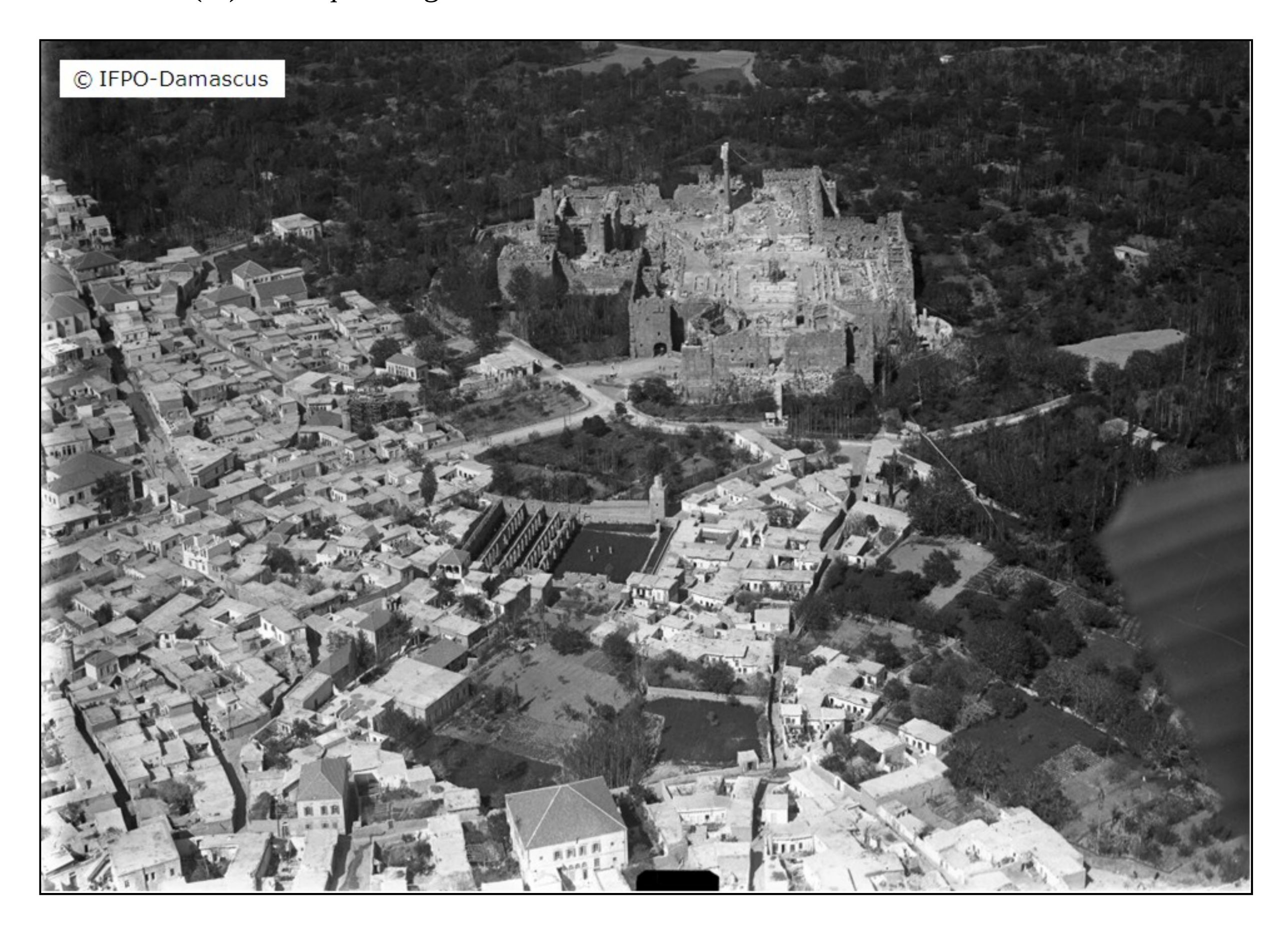

Figure (K.3): The oblique image 20878 (source: IFPO-Damascus)

<table>
<tr><td>OS</td><td colspan="7">Image ID: 20878, Camera: Schrägkamera</td></tr>
<tr><td rowspan="4">Step 1</td><td rowspan="2">IP</td><td colspan="2">$x'_o\ (mm)$</td><td colspan="2">$y'_o\ (mm)$</td><td colspan="2">$c_k\ (mm)$</td></tr>
<tr><td colspan="2">0.09653</td><td colspan="2">- 0.35368</td><td colspan="2">259.7072</td></tr>
<tr><td rowspan="2">EP</td><td>$X_0\ (m)$</td><td>$Y_0\ (m)$</td><td>$Z_0\ (m)$</td><td>$\omega\ (gon)$</td><td>$\varphi\ (gon)$</td><td>$\kappa\ (gon)$</td></tr>
<tr><td>10448.362</td><td>10784.164</td><td>1387.663</td><td>-39.795513</td><td>72.007589</td><td>141.144015</td></tr>
<tr><td rowspan="4">Step 2</td><td rowspan="2">IP</td><td colspan="2">$x'_o\ (mm)$</td><td colspan="2">$y'_o\ (mm)$</td><td colspan="2">$c_k\ (mm)$</td></tr>
<tr><td colspan="2">0.00</td><td colspan="2">0.00</td><td colspan="2">260.00</td></tr>
<tr><td rowspan="2">EP</td><td>$X_0\ (m)$</td><td>$Y_0\ (m)$</td><td>$Z_0\ (m)$</td><td>$\omega\ (gon)$</td><td>$\varphi\ (gon)$</td><td>$\kappa\ (gon)$</td></tr>
<tr><td>10448.289</td><td>10784.290</td><td>1387.752</td><td>-39.981949</td><td>72.055536</td><td>141.304050</td></tr>
</table>

Table (K.3): Orientation results associated with the oblique image 20878; where OS: Orientation Step, IP: Interior orientation parameters and EP: Exterior orientation parameters

- Protocol (iv) – oblique image 20886

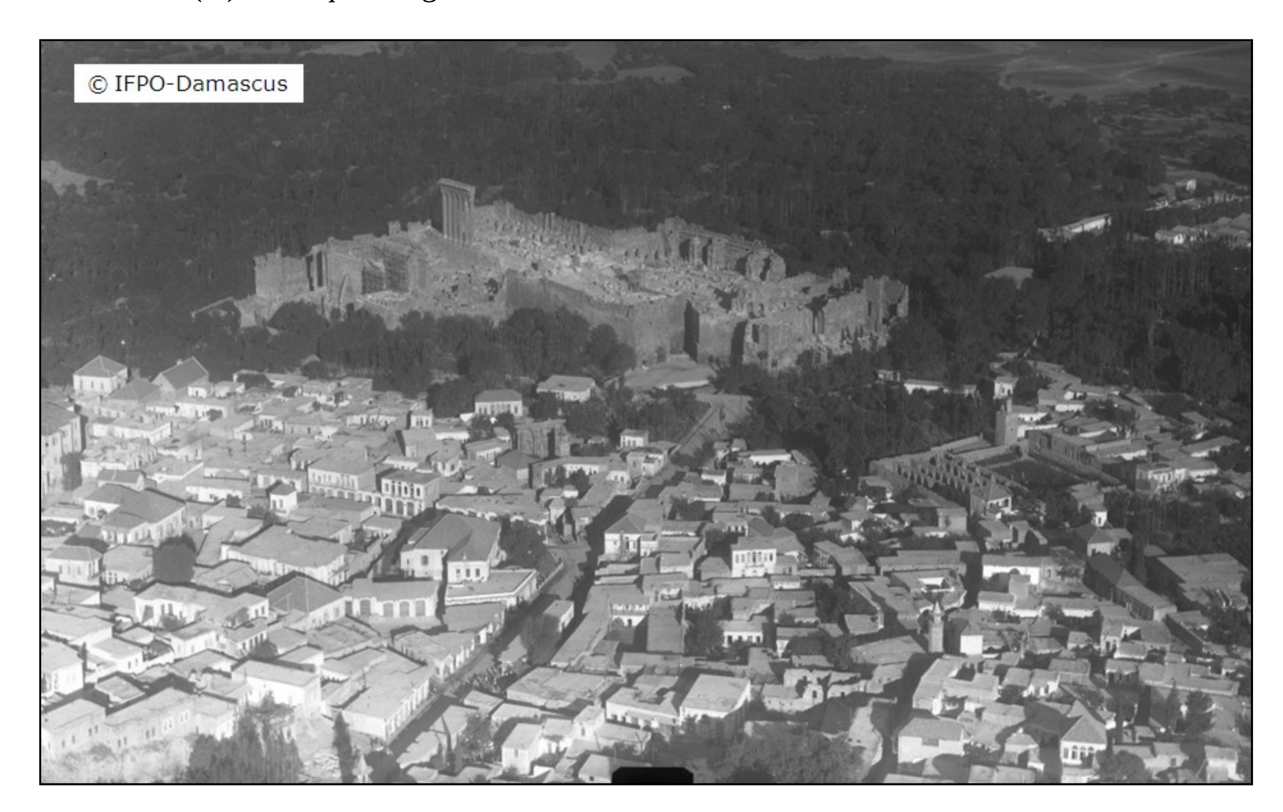

Figure (K.4): The oblique image 20886 (source: IFPO-Damascus)

OS		Image ID: 20886, Camera: Schrägkamera					
Step 1	IP	x'_o (mm)		y'_o (mm)		c_k (mm)	
		0.09653		- 0.35368		259.7072	
	EP	X_0 (m)	Y_0 (m)	Z_0 (m)	ω (gon)	φ (gon)	κ (gon)
		10378.696	10283.857	1312.589	70.189405	68.681595	26.408128
Step 2	IP	x'_o (mm)		y'_o (mm)		c_k (mm)	
		0.00		0.00		260.00	
	EP	X_0 (m)	Y_0 (m)	Z_0 (m)	ω (gon)	φ (gon)	κ (gon)
		10378.719	10283.770	1312.715	70.334748	68.725096	26.283109

Table (K.4): Orientation results associated with the oblique image 20886; where OS: Orientation Step, IP: Interior orientation parameters and EP: Exterior orientation parameters

- **Orientation result protocols – comparison of combined evaluation of three image types to the 1st and 2nd orientation steps**

- Protocol (v) – vertical image 2025

Figure (K.5): The aerial vertical image 2025 (source: IFPO-Damascus)

OS	Image ID: 2025, Camera: Baalbek-G1						
Step 1	IP	$x'_o\ (mm)$		$y'_o\ (mm)$		$c_k\ (mm)$	
		-0.069894		-0.049059		200.25303	
	EP	$X_0\ (m)$	$Y_0\ (m)$	$Z_0\ (m)$	$\omega\ (gon)$	$\varphi\ (gon)$	$\kappa\ (gon)$
		9791.510	10558.579	2028.774	9.571998	-3.034766	148.071746
Step 2	IP	$x'_o\ (mm)$		$y'_o\ (mm)$		$c_k\ (mm)$	
		0.00		0.00		200.00	
	EP	$X_0\ (m)$	$Y_0\ (m)$	$Z_0\ (m)$	$\omega\ (gon)$	$\varphi\ (gon)$	$\kappa\ (gon)$
		9791.513	10558.523	2029.001	9.619294	-2.874932	148.322941
Step 3	IP	$x'_o\ (mm)$		$y'_o\ (mm)$		$c_k\ (mm)$	
		0.173740		0.138436		200.354646	
	EP	$X_0\ (m)$	$Y_0\ (m)$	$Z_0\ (m)$	$\omega\ (gon)$	$\varphi\ (gon)$	$\kappa\ (gon)$
		9791.504	10558.522	2029.064	9.609923	-2.814618	148.325941

Table (K.5): Orientation results associated with the vertical image 2025; where OS: Orientation Step, IP: Interior orientation parameters and EP: Exterior orientation parameters

- Protocol (vi) – oblique image 20892

Figure (K.6): The oblique image 20892 (source: IFPO-Damascus)

OS	Image ID: 20892, Camera: Schrägkamera						
Step 1	IP	$x'_o\ (mm)$		$y'_o\ (mm)$		$c_k\ (mm)$	
		0.09653		- 0.35368		259.707205	
	EP	$X_0\ (m)$	$Y_0\ (m)$	$Z_0\ (m)$	$\omega\ (gon)$	$\varphi\ (gon)$	$\kappa\ (gon)$
		9913.973	10177.051	1272.780	78.784011	31.881270	10.013510
Step 2	IP	$x'_o\ (mm)$		$y'_o\ (mm)$		$c_k\ (mm)$	
		0.000		0.000		206.000	
	EP	$X_0\ (m)$	$Y_0\ (m)$	$Z_0\ (m)$	$\omega\ (gon)$	$\varphi\ (gon)$	$\kappa\ (gon)$
		9913.952	10177.201	1272.770	78.870589	31.913799	9.947497
Step 3	IP	$x'_o\ (mm)$		$y'_o\ (mm)$		$c_k\ (mm)$	
		0.199348		-0.566046		260.484178	
	EP	$X_0\ (m)$	$Y_0\ (m)$	$Z_0\ (m)$	$\omega\ (gon)$	$\varphi\ (gon)$	$\kappa\ (gon)$
		9913.893	10177.268	1272.665	78.742428	31.879360	10.039255

Table (K.6): Orientation results associated with the vertical image 20892; where OS: Orientation Step, IP: Interior orientation parameters and EP: Exterior orientation parameters

- Protocol (vii) – terrestrial image 208323

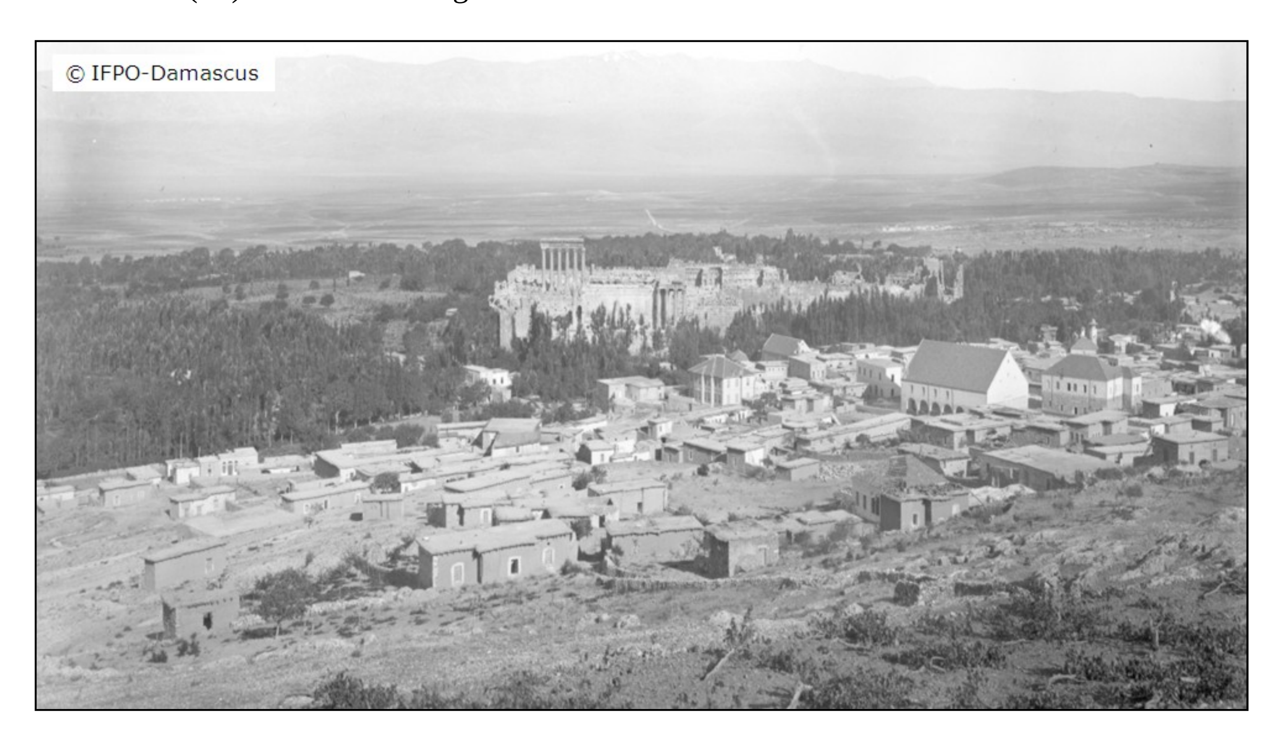

Figure (K.7): The terrestrial image 208323 (source: Meydenbauer's archive - Germany)

OS		Image ID: 208323, Camera: Messbild_Kamera					
Step 1	IP	$x'_o\ (mm)$		$y'_o\ (mm)$		$c_k\ (mm)$	
		0.000		0.000		346.629555	
	EP	$X_0\ (m)$	$Y_0\ (m)$	$Z_0\ (m)$	$\omega\ (gon)$	$\varphi\ (gon)$	$\kappa\ (gon)$
		9945.214	9609.729	1242.932	92.586885	21.070925	6.023199
Step 2	IP	$x'_o\ (mm)$		$y'_o\ (mm)$		$c_k\ (mm)$	
		-		-		-	
	EP	$X_0\ (m)$	$Y_0\ (m)$	$Z_0\ (m)$	$\omega\ (gon)$	$\varphi\ (gon)$	$\kappa\ (gon)$
		-	-	-	-	-	-
Step 3	IP	$x'_o\ (mm)$		$y'_o\ (mm)$		$c_k\ (mm)$	
		-0.089678		0.607910		345.845772	
	EP	$X_0\ (m)$	$Y_0\ (m)$	$Z_0\ (m)$	$\omega\ (gon)$	$\varphi\ (gon)$	$\kappa\ (gon)$
		9945.255	9609.743	1242.905	92.523778	22.599575	6.174791

Table (K.7): Orientation results associated with the terrestrial image 208323; where OS: Orientation Step, IP: Interior orientation parameters and EP: Exterior orientation parameters

Appendix L

PROGRAM SYSTEM PICTRAN-B (VERSION4.3 (C) TECHNET 1995-1998)

OUTPUT OF MODULE BUNBIL

BUNDLE ADJUSTMENT

PROJECT: THREE-TYPES (vertical, oblique and terrestrial)

LEGEND OF THE MODULE BUNBIL

```
V    = RESIDUAL
MFV  = STANDARD DEVIATION OF OBSERVATIONS A PRIORI
EV   = REDUNDANCY NUMBER
GF   = PROBABLE DIMENSION OF A BLUNDER
EK   = DISPLACEMENT IF OBSERVATION DOES NOT TAKE PART OF THE ADJUSTMENT
NV   = NORMALIZED RESIDUAL
GRZW = THRESHOLD VALUE FOR NOT TRACEABLE BLUNDERS
EGK  = EFFECT OF GRZW ON THE RELATIVE POSITION
M    = STANDARD DEVIATION OF UNKNOWNS
STA  = STATE (0=FIX, 1=UNKNOWN, 2=OBSERVED)
**   = BLUNDER IS SUPPOSED
***  = BLUNDER IS PROBABLE
```

=== IMAGE- AND OBJECT DATA ===

NU. OF IMAGES	10
NU. OF IMAGE POINTS	121
NU. OF OBJECT POINTS	32
NU. OF CONTROL POINTS	23
NU. OF CAMERAS	3
NU. OF PLANES	0
NU. OF DISTANCES	0
NU. OF DIFFERENCES	0

=== ITERATIONS ===

ITERATION	UNKNOWNS	RIGHT SIDE	TIME [s]
1	0.1000E+11	0.1823E+11	0.00
2	0.1587E+03	0.6484E+09	0.03
3	0.6789E+02	0.7664E+08	0.03
4	0.5044E+01	0.2429E+06	0.04
5	0.1963E-01	0.8660E+01	0.06
6	0.3292E-03	0.1481E-02	0.08
7	0.1201E-05	0.9220E-04	0.09

=== DATA OF THE ADJUSTMENT ===

OBSERVATIONS (OB)	402
UNKNOWNS (UN)	227
NU. CONSTR. EQUATIONS (CON)	10
REDUNDANCY (OB-UN+CON)	185
SUM OF REDUNDANCY NUMBERS	185.000
NU. OF DIAGONAL SUBMATRICES	166
NU. OF ALL SUBMATRICES	763
NU. OF ALL SINGLE ELEMENTS	11568
FILLING OF ATPA [%]	0.2197E+02

--- IMAGE COORDINATES ---

SYSTEM-NU	POINT-NU	X Y	BEOBX BEOBY	VX VY	MFVX MFVY	EVX EVY	GFX GFY	EKX EKY	NVX NVY	GRZWX GRZWY	EGKX EGKY
1981	1002	-23.217709	-23.246600	0.0289	0.8000	0.789	-0.037	-0.008	0.041	3.720	0.785
		10.879573	10.778000	0.1016	0.8000	0.798	-0.127	-0.026	0.142	3.698	0.746
1981	1003	-23.783499	-23.792300	0.0088	0.8000	0.792	-0.011	-0.002	0.012	3.712	0.771
		9.746889	9.588100	0.1588	0.8000	0.800	-0.198	-0.040	0.222	3.694	0.739
1981	1077	-15.958366	-16.031400	0.0730	0.8000	0.364	-0.201	-0.128	0.151	5.477	3.484
		52.946812	52.886900	0.0599	0.8000	0.674	-0.089	-0.029	0.091	4.025	1.313
1981	4028	-42.746934	-42.623600	-0.1233	0.8000	0.585	0.211	0.088	0.202	4.320	1.793
		-33.450645	-33.267900	-0.1827	0.8000	0.746	0.245	0.062	0.265	3.826	0.973
1981	4029	-52.343408	-52.373200	0.0298	0.8000	0.600	-0.050	-0.020	0.048	4.267	1.709
		-30.533070	-30.403900	-0.1292	0.8000	0.701	0.184	0.055	0.193	3.947	1.182
2025	1002	-23.739999	-23.734000	-0.0060	0.8000	0.874	0.007	0.001	0.008	3.534	0.445
		-4.774517	-4.565600	-0.2089	0.8000	0.881	0.237	0.028	0.278	3.519	0.417
2025	1003	-24.480808	-24.397900	-0.0829	0.8000	0.872	0.095	0.012	0.111	3.538	0.452
		-5.638203	-5.496500	-0.1417	0.8000	0.882	0.161	0.019	0.189	3.519	0.417
2025	1077	-7.825952	-7.577000	-0.2490	0.8000	0.854	0.292	0.043	0.337	3.576	0.524
		30.127407	30.515000	-0.3876	0.8000	0.840	0.462	0.074	0.529	3.606	0.578
2025	1116	-11.689908	-11.733500	0.0436	0.8000	0.754	-0.058	-0.014	0.063	3.805	0.936
		53.707124	53.733200	-0.0261	0.8000	0.803	0.032	0.006	0.036	3.688	0.728
2025	1136	-61.232510	-61.207500	-0.0250	0.8000	0.852	0.029	0.004	0.034	3.580	0.530
		22.008341	21.589100	0.4192	0.8000	0.832	-0.504	-0.085	0.575	3.623	0.610

2025	1142	-61.123428	-61.041500	-0.0819	0.8000	0.853	0.096	0.014	0.111	3.577	0.526
		21.501547	21.144200	0.3573	0.8000	0.832	-0.429	-0.072	0.490	3.622	0.607
2025	1208	-8.711239	-8.789300	0.0781	0.8000	0.719	-0.109	-0.031	0.115	3.897	1.096
		58.773178	58.387700	0.3855	0.8000	0.776	-0.497	-0.112	0.547	3.752	0.842
2025	4028	-49.646895	-49.798700	0.1518	0.8000	0.703	-0.216	-0.064	0.226	3.940	1.170
		-37.705261	-37.599500	-0.1058	0.8000	0.812	0.130	0.024	0.147	3.666	0.689
2025	4029	-57.111672	-57.318000	0.2063	0.8000	0.721	-0.286	-0.080	0.304	3.892	1.087
		-33.288885	-32.958600	-0.3303	0.8000	0.803	0.411	0.081	0.461	3.687	0.727
20891	1077	22.729126	22.626600	0.1025	0.8000	0.772	-0.133	-0.030	0.146	3.762	0.859
		3.202791	3.108300	0.0945	0.8000	0.684	-0.138	-0.044	0.143	3.994	1.260
20891	1110	-25.669945	-25.621500	-0.0484	0.8000	0.877	0.055	0.007	0.065	3.528	0.433
		-23.997992	-24.313700	0.3157	0.8000	0.891	-0.354	-0.039	0.418	3.501	0.383
20891	1116	-24.159195	-24.267200	0.1080	0.8000	0.897	-0.120	-0.012	0.143	3.488	0.358
		-7.158390	-7.293000	0.1346	0.8000	0.899	-0.150	-0.015	0.177	3.485	0.353
20891	1158	-77.969448	-78.048100	0.0787	0.8000	0.833	-0.094	-0.016	0.108	3.620	0.604
		3.364084	3.476300	-0.1122	0.8000	0.788	0.142	0.030	0.158	3.721	0.787
20891	1160	-75.591048	-75.668000	0.0770	0.8000	0.839	-0.092	-0.015	0.105	3.607	0.581
		3.343775	3.430500	-0.0867	0.8000	0.799	0.109	0.022	0.121	3.696	0.742
20891	1162	-73.460406	-73.590700	0.1303	0.8000	0.844	-0.154	-0.024	0.177	3.597	0.561
		3.307666	3.364600	-0.0569	0.8000	0.808	0.070	0.013	0.079	3.675	0.704
20891	1164	-71.218938	-71.351800	0.1329	0.8000	0.849	-0.157	-0.024	0.180	3.586	0.543
		3.331071	3.379200	-0.0481	0.8000	0.817	0.059	0.011	0.067	3.654	0.667
20891	1208	-38.909905	-38.872600	-0.0373	0.8000	0.901	0.041	0.004	0.049	3.481	0.345
		-6.940993	-7.089800	0.1488	0.8000	0.902	-0.165	-0.016	0.196	3.479	0.341
20891	1228	3.169545	2.660900	0.5086	0.8000	0.526	-0.966	-0.458	0.876	4.554	2.157
		-56.091233	-55.931300	-0.1599	0.8000	0.554	0.289	0.129	0.269	4.439	1.980
20891	6001	-19.763437	-18.486700	-1.2767	0.8000	0.600	2.127	0.851	2.060	4.265	1.706
		-28.898558	-28.743700	-0.1549	0.8000	0.663	0.233	0.079	0.238	4.057	1.366
20891	6002	44.740893	44.647700	0.0932	0.8000	0.121	-0.769	-0.675	0.335	9.489	8.339
		-14.686769	-14.640900	-0.0459	0.8000	0.471	0.097	0.052	0.084	4.814	2.547
20891	6003	47.626245	47.532400	0.0938	0.8000	0.121	-0.777	-0.683	0.338	9.508	8.360
		-13.417626	-13.410800	-0.0068	0.8000	0.456	0.015	0.008	0.013	4.892	2.661
20893	1077	21.082659	21.481500	-0.3988	0.8000	0.748	0.533	0.134	0.576	3.820	0.962
		14.646916	14.597000	0.0499	0.8000	0.617	-0.081	-0.031	0.079	4.205	1.610
20893	1110	-56.486816	-56.458300	-0.0285	0.8000	0.892	0.032	0.003	0.038	3.499	0.380
		-14.674639	-14.904500	0.2299	0.8000	0.896	-0.257	-0.027	0.304	3.491	0.364
20893	1116	-36.189462	-36.037400	-0.1521	0.8000	0.904	0.168	0.016	0.200	3.475	0.334
		5.559148	5.436800	0.1223	0.8000	0.903	-0.136	-0.013	0.161	3.477	0.338
20893	1158	-72.241022	-72.366700	0.1257	0.8000	0.847	-0.148	-0.023	0.171	3.590	0.550
		21.801742	21.895500	-0.0938	0.8000	0.831	0.113	0.019	0.129	3.625	0.614
20893	1160	-70.134871	-70.263600	0.1287	0.8000	0.851	-0.151	-0.023	0.174	3.582	0.534
		21.642756	21.763700	-0.1209	0.8000	0.838	0.144	0.023	0.165	3.610	0.586
20893	1162	-68.206010	-68.336800	0.1308	0.8000	0.854	-0.153	-0.022	0.177	3.574	0.520
		21.486969	21.598900	-0.1119	0.8000	0.843	0.133	0.021	0.152	3.598	0.563
20893	1164	-66.195319	-66.321900	0.1266	0.8000	0.858	-0.148	-0.021	0.171	3.567	0.507
		21.380071	21.478100	-0.0980	0.8000	0.849	0.115	0.017	0.133	3.586	0.541
20893	1208	-50.200552	-50.108900	-0.0917	0.8000	0.907	0.101	0.009	0.120	3.470	0.323
		6.871636	6.754800	0.1168	0.8000	0.908	-0.129	-0.012	0.153	3.468	0.321
20893	4019	-87.202059	-86.729900	-0.4722	0.8000	0.655	0.721	0.248	0.729	4.082	1.407
		-44.643393	-44.493900	-0.1495	0.8000	0.653	0.229	0.079	0.231	4.088	1.417
20893	4020	-34.833458	-34.958400	0.1249	0.8000	0.711	-0.176	-0.051	0.185	3.917	1.131
		-39.269357	-39.265800	-0.0036	0.8000	0.732	0.005	0.001	0.005	3.861	1.034
20893	6001	-54.544757	-54.777300	0.2325	0.8000	0.461	-0.505	-0.272	0.428	4.867	2.624
		-20.891901	-21.011300	0.1194	0.8000	0.637	-0.188	-0.068	0.187	4.141	1.505
20893	6002	29.644006	29.519200	0.1248	0.8000	0.263	-0.475	-0.350	0.304	6.442	4.748
		-8.907475	-8.885600	-0.0219	0.8000	0.459	0.048	0.026	0.040	4.878	2.641
20893	6003	34.386209	34.231700	0.1545	0.8000	0.259	-0.596	-0.441	0.379	6.488	4.805
		-7.522478	-7.523700	0.0012	0.8000	0.440	-0.003	-0.002	0.002	4.981	2.790
1983	1110	-25.519554	-25.378900	-0.1407	0.8000	0.925	0.152	0.011	0.183	3.435	0.256
		-2.998476	-2.944600	-0.0539	0.8000	0.910	0.059	0.005	0.071	3.463	0.311
1983	1116	-7.036327	-6.210100	-0.8262	0.8000	0.898	0.920	0.093	1.090	3.486	0.354
		-10.352829	-10.213900	-0.1389	0.8000	0.843	0.165	0.026	0.189	3.599	0.567
1983	1136	-54.083902	-54.002900	-0.0810	0.8000	0.779	0.104	0.023	0.115	3.744	0.829
		-40.908235	-40.281700	-0.6265	0.8000	0.868	0.722	0.095	0.841	3.547	0.468
1983	1142	-53.986293	-53.888000	-0.0983	0.8000	0.776	0.127	0.028	0.140	3.752	0.842
		-41.378664	-40.773600	-0.6051	0.8000	0.867	0.698	0.093	0.812	3.548	0.472
1983	1147	-16.524967	-16.009900	-0.5151	0.8000	0.866	0.595	0.080	0.692	3.551	0.477
		26.853765	26.672300	0.1815	0.8000	0.864	-0.210	-0.029	0.244	3.555	0.485
1983	1208	-4.215030	-3.338400	-0.8766	0.8000	0.900	0.974	0.097	1.155	3.483	0.348
		-5.594753	-5.404100	-0.1907	0.8000	0.831	0.230	0.039	0.261	3.625	0.614
1983	1228	-57.392938	-58.023300	0.6304	0.8000	0.918	-0.687	-0.057	0.823	3.449	0.284
		2.428153	2.404900	0.0233	0.8000	0.901	-0.026	-0.003	0.031	3.481	0.345
1983	1239	-64.319819	-64.714400	0.3946	0.8000	0.905	-0.436	-0.041	0.518	3.472	0.328
		-5.884934	-5.738900	-0.1460	0.8000	0.878	0.166	0.020	0.195	3.526	0.430
1983	1240	-64.640627	-65.202600	0.5620	0.8000	0.908	-0.619	-0.057	0.737	3.467	0.318

		0.138916	0.082000	0.0569	0.8000	0.877	-0.065	-0.008	0.076	3.527	0.432
1983	4015	-39.288063	-39.213500	-0.0746	0.8000	0.807	0.092	0.018	0.104	3.678	0.709
		39.303499	38.642000	0.6615	0.8000	0.882	-0.750	-0.088	0.880	3.518	0.415
1983	4016	-44.786702	-44.842100	0.0554	0.8000	0.813	-0.068	-0.013	0.077	3.665	0.686
		37.872340	37.002300	0.8700	0.8000	0.884	-0.984	-0.114	1.157	3.514	0.407
1983	4019	-47.308766	-47.656300	0.3475	0.8000	0.926	-0.375	-0.028	0.451	3.434	0.255
		3.161607	3.115400	0.0462	0.8000	0.920	-0.050	-0.004	0.060	3.444	0.275
1983	4020	-49.892113	-50.248100	0.3560	0.8000	0.920	-0.387	-0.031	0.464	3.445	0.276
		-7.372428	-7.344400	-0.0280	0.8000	0.916	0.031	0.003	0.037	3.453	0.291
1983	5014	-33.787861	-33.843300	0.0554	0.8000	0.423	-0.131	-0.076	0.107	5.079	2.929
		18.706902	18.719800	-0.0129	0.8000	0.023	0.563	0.550	0.107	21.828	21.328
1983	5015	-44.161814	-44.325100	0.1633	0.8000	0.426	-0.383	-0.220	0.313	5.060	2.902
		12.614834	12.652900	-0.0381	0.8000	0.023	1.643	1.604	0.313	21.704	21.201
1985	1110	-22.765795	-22.557200	-0.2086	0.8000	0.901	0.232	0.023	0.275	3.481	0.346
		-51.851079	-51.906600	0.0555	0.8000	0.886	-0.063	-0.007	0.074	3.510	0.400
1985	1116	-4.465933	-3.783400	-0.6825	0.8000	0.858	0.796	0.113	0.921	3.568	0.508
		-59.459847	-59.154000	-0.3058	0.8000	0.771	0.397	0.091	0.435	3.763	0.861
1985	1147	-13.776303	-13.209600	-0.5667	0.8000	0.871	0.651	0.084	0.759	3.540	0.456
		-22.225373	-22.401700	0.1763	0.8000	0.855	-0.206	-0.030	0.238	3.573	0.518
1985	1208	-1.653466	-0.872500	-0.7810	0.8000	0.872	0.896	0.115	1.045	3.539	0.453
		-54.825430	-54.736800	-0.0886	0.8000	0.757	0.117	0.028	0.127	3.798	0.923
1985	1228	-53.990099	-54.426300	0.4362	0.8000	0.900	-0.485	-0.048	0.575	3.483	0.348
		-46.903660	-46.823100	-0.0806	0.8000	0.861	0.094	0.013	0.108	3.560	0.493
1985	1239	-60.621620	-61.206300	0.5847	0.8000	0.873	-0.670	-0.085	0.782	3.536	0.449
		-54.695889	-54.544500	-0.1514	0.8000	0.818	0.185	0.034	0.209	3.653	0.666
1985	1240	-60.956521	-61.492400	0.5359	0.8000	0.887	-0.604	-0.068	0.711	3.508	0.397
		-49.015614	-48.801500	-0.2141	0.8000	0.820	0.261	0.047	0.296	3.649	0.657
1985	4015	-36.142573	-36.203100	0.0605	0.8000	0.800	-0.076	-0.015	0.085	3.694	0.739
		-10.050377	-10.304400	0.2540	0.8000	0.892	-0.285	-0.031	0.336	3.498	0.378
1985	4016	-41.567341	-41.695800	0.1285	0.8000	0.808	-0.159	-0.031	0.179	3.676	0.707
		-11.759767	-12.145400	0.3856	0.8000	0.888	-0.434	-0.048	0.511	3.505	0.391
1985	4019	-44.159349	-44.499400	0.3401	0.8000	0.910	-0.374	-0.034	0.446	3.463	0.311
		-45.972057	-45.943800	-0.0283	0.8000	0.898	0.031	0.003	0.037	3.487	0.356
1985	4020	-46.736841	-46.988200	0.2514	0.8000	0.882	-0.285	-0.034	0.335	3.518	0.415
		-56.449565	-56.330600	-0.1190	0.8000	0.883	0.135	0.016	0.158	3.516	0.411
1985	5014	-30.766948	-30.710400	-0.0565	0.8000	0.440	0.128	0.072	0.107	4.979	2.786
		-30.075555	-30.088800	0.0132	0.8000	0.024	-0.548	-0.535	0.107	21.257	20.744
1985	5015	-41.005228	-40.837600	-0.1676	0.8000	0.449	0.373	0.205	0.313	4.929	2.714
		-36.424440	-36.463700	0.0393	0.8000	0.025	-1.593	-1.553	0.313	21.044	20.525
20892	1110	-31.781908	-31.956200	0.1743	0.8000	0.892	-0.195	-0.021	0.231	3.499	0.379
		-21.719727	-21.897300	0.1776	0.8000	0.894	-0.199	-0.021	0.235	3.493	0.369
20892	1116	-16.457503	-16.383700	-0.0738	0.8000	0.893	0.083	0.009	0.098	3.495	0.372
		-0.243641	-0.307500	0.0639	0.8000	0.880	-0.073	-0.009	0.085	3.521	0.421
20892	1158	-58.100574	-58.168600	0.0680	0.8000	0.839	-0.081	-0.013	0.093	3.608	0.583
		16.470758	16.508100	-0.0373	0.8000	0.819	0.046	0.008	0.052	3.652	0.663
20892	1160	-55.919532	-56.010500	0.0910	0.8000	0.842	-0.108	-0.017	0.124	3.600	0.567
		16.322833	16.354300	-0.0315	0.8000	0.826	0.038	0.007	0.043	3.635	0.632
20892	1162	-53.932793	-54.006600	0.0738	0.8000	0.846	-0.087	-0.013	0.100	3.593	0.555
		16.178209	16.244500	-0.0663	0.8000	0.833	0.080	0.013	0.091	3.621	0.606
20892	1164	-51.853524	-51.870600	0.0171	0.8000	0.848	-0.020	-0.003	0.023	3.587	0.543
		16.082678	16.112700	-0.0300	0.8000	0.839	0.036	0.006	0.041	3.608	0.583
20892	1208	-31.074982	-31.093700	0.0187	0.8000	0.901	-0.021	-0.002	0.025	3.481	0.345
		1.010849	1.010500	0.0003	0.8000	0.898	0.000	0.000	0.000	3.486	0.354
20892	4019	-52.533036	-52.498200	-0.0348	0.8000	0.663	0.053	0.018	0.053	4.057	1.366
		-54.447089	-54.433900	-0.0132	0.8000	0.662	0.020	0.007	0.020	4.060	1.371
20892	4020	1.867708	1.761700	0.1060	0.8000	0.691	-0.153	-0.047	0.159	3.976	1.230
		-48.447709	-48.195300	-0.2524	0.8000	0.688	0.367	0.115	0.380	3.984	1.244
20892	6001	-28.583232	-28.572300	-0.0109	0.8000	0.569	0.019	0.008	0.018	4.382	1.890
		-28.230000	-28.348300	0.1183	0.8000	0.618	-0.192	-0.073	0.188	4.204	1.607
20892	6002	53.830979	54.028600	-0.1976	0.8000	0.534	0.370	0.173	0.338	4.523	2.109
		-14.771696	-14.838600	0.0669	0.8000	0.418	-0.160	-0.093	0.129	5.111	2.975
20892	6003	58.248099	58.476900	-0.2288	0.8000	0.530	0.432	0.203	0.393	4.538	2.132
		-13.269463	-13.279000	0.0095	0.8000	0.398	-0.024	-0.014	0.019	5.237	3.152
208323	1110	24.458866	21.414800	3.0441	0.8000	0.886	-3.435	-0.391	4.042***	3.510	0.399
		0.985193	1.042700	-0.0575	0.8000	0.900	0.064	0.006	0.076	3.483	0.348
208323	1160	-18.418865	-17.162000	-1.2569	0.8000	0.854	1.471	0.214	1.700	3.575	0.521
		9.594003	9.484900	0.1091	0.8000	0.775	-0.141	-0.032	0.155	3.753	0.844
208323	1162	-16.958242	-16.006700	-0.9515	0.8000	0.856	1.111	0.160	1.285	3.570	0.513
		9.479228	9.384400	0.0948	0.8000	0.785	-0.121	-0.026	0.134	3.728	0.800
208323	1164	-15.400355	-14.750900	-0.6495	0.8000	0.858	0.757	0.107	0.876	3.566	0.505
		9.408596	9.409500	-0.0009	0.8000	0.796	0.001	0.000	0.001	3.703	0.755
208323	1199	-8.472317	-8.618700	0.1464	0.8000	0.872	-0.168	-0.021	0.196	3.538	0.452
		7.087575	6.827900	0.2597	0.8000	0.839	-0.310	-0.050	0.354	3.608	0.582
208323	1228	45.092478	45.613200	-0.5207	0.8000	0.862	0.604	0.083	0.701	3.559	0.491
		0.090527	-0.044000	0.1345	0.8000	0.825	-0.163	-0.028	0.185	3.637	0.635

208323	1239	69.010626	69.451700	-0.4411	0.8000	0.809	0.545	0.104	0.613	3.674	0.703
		-3.198984	-2.876900	-0.3221	0.8000	0.627	0.513	0.191	0.508	4.172	1.555
208323	1240	57.795583	59.422400	-1.6268	0.8000	0.836	1.946	0.319	2.224	3.614	0.593
		-1.898658	-2.223600	0.3249	0.8000	0.735	-0.442	-0.117	0.474	3.853	1.019
208323	6001	28.268518	26.186700	2.0818	0.8000	0.766	-2.717	-0.635	2.973**	3.774	0.882
		-0.764297	-0.138200	-0.6261	0.8000	0.799	0.784	0.158	0.876	3.696	0.743
208323	7001	13.378598	13.327800	0.0508	0.8000	0.000	----------- UNCONTROLED -----------				
		-7.565801	-7.500000	-0.0658	0.8000	0.543	0.121	0.055	0.112	4.486	2.052
208323	7002	13.717421	13.662600	0.0548	0.8000	0.000	----------- UNCONTROLED -----------				
		-3.578326	-3.630700	0.0524	0.8000	0.545	-0.096	-0.044	0.089	4.476	2.037
208323	7003	12.091952	12.038500	0.0535	0.8000	0.000	----------- UNCONTROLED -----------				
		-3.422213	-3.505000	0.0828	0.8000	0.547	-0.151	-0.069	0.140	4.468	2.025
208323	7004	10.322361	10.263700	0.0587	0.8000	0.000	----------- UNCONTROLED -----------				
		-5.354779	-5.364300	0.0095	0.8000	0.547	-0.017	-0.008	0.016	4.468	2.024
208325	1110	-1.723168	-3.141300	1.4181	0.8000	0.918	-1.545	-0.126	1.850	3.448	0.282
		-31.658803	-31.897000	0.2382	0.8000	0.922	-0.258	-0.020	0.310	3.440	0.267
208325	1116	-13.357942	-14.813900	1.4560	0.8000	0.922	-1.580	-0.124	1.896	3.442	0.270
		-29.422515	-28.731200	-0.6913	0.8000	0.925	0.747	0.056	0.898	3.435	0.257
208325	1158	-55.310795	-54.632000	-0.6788	0.8000	0.883	0.769	0.090	0.903	3.516	0.411
		-26.814878	-26.972400	0.1575	0.8000	0.788	-0.200	-0.043	0.222	3.723	0.791
208325	1160	-53.925748	-53.234000	-0.6917	0.8000	0.886	0.781	0.089	0.919	3.510	0.400
		-26.889988	-26.871900	-0.0181	0.8000	0.796	0.023	0.005	0.025	3.704	0.756
208325	1162	-52.741580	-52.088600	-0.6530	0.8000	0.888	0.735	0.082	0.866	3.505	0.391
		-26.978341	-26.897000	-0.0813	0.8000	0.803	0.101	0.020	0.113	3.688	0.728
208325	1164	-51.459707	-50.842200	-0.6175	0.8000	0.891	0.693	0.076	0.818	3.501	0.382
		-27.028205	-26.947200	-0.0810	0.8000	0.810	0.100	0.019	0.113	3.671	0.698
208325	1208	-20.086451	-21.298600	1.2121	0.8000	0.921	-1.315	-0.103	1.578	3.442	0.270
		-29.003703	-28.781400	-0.2223	0.8000	0.919	0.242	0.020	0.290	3.447	0.279
208325	1228	27.970442	28.659300	-0.6889	0.8000	0.884	0.779	0.090	0.916	3.513	0.406
		-30.490312	-30.263800	-0.2265	0.8000	0.833	0.272	0.045	0.310	3.620	0.605
208325	1239	43.573606	44.155300	-0.5817	0.8000	0.852	0.683	0.101	0.788	3.580	0.531
		-32.372302	-31.997500	-0.3748	0.8000	0.738	0.508	0.133	0.545	3.845	1.005
208325	1240	38.691521	39.978100	-1.2866	0.8000	0.863	1.491	0.204	1.731	3.557	0.488
		-31.409103	-31.193500	-0.2156	0.8000	0.772	0.279	0.064	0.307	3.761	0.858
208325	6001	2.397672	2.261200	0.1365	0.8000	0.734	-0.186	-0.050	0.199	3.857	1.028
		-32.765215	-32.556500	-0.2087	0.8000	0.856	0.244	0.035	0.282	3.571	0.514
208325	7001	4.621598	4.391900	0.2297	0.8000	0.583	-0.394	-0.164	0.376	4.328	1.805
		-36.587577	-37.028900	0.4413	0.8000	0.718	-0.615	-0.174	0.651	3.900	1.101
208325	7002	3.480712	3.208700	0.2720	0.8000	0.582	-0.467	-0.195	0.446	4.330	1.809
		-33.852195	-34.283900	0.4317	0.8000	0.720	-0.599	-0.168	0.636	3.893	1.088
208325	7003	1.803866	1.524300	0.2796	0.8000	0.580	-0.482	-0.203	0.459	4.340	1.825
		-33.820390	-34.208500	0.3881	0.8000	0.721	-0.538	-0.150	0.571	3.890	1.083
208325	7004	0.959210	0.682200	0.2770	0.8000	0.578	-0.479	-0.202	0.456	4.347	1.835
		-35.209669	-35.665800	0.4561	0.8000	0.721	-0.633	-0.177	0.671	3.891	1.086
637126	1110	41.362882	39.848600	1.5143	0.8000	0.889	-1.703	-0.189	2.008	3.504	0.389
		31.468484	30.496100	0.9724	0.8000	0.874	-1.112	-0.140	1.300	3.533	0.444
637126	1116	26.801285	24.801300	2.0000	0.8000	0.902	-2.217	-0.217	2.632**	3.478	0.340
		34.546090	34.448200	0.0979	0.8000	0.907	-0.108	-0.010	0.128	3.469	0.322
637126	1158	-25.341237	-24.581400	-0.7598	0.8000	0.879	0.865	0.105	1.013	3.525	0.428
		34.770105	34.874100	-0.1040	0.8000	0.789	0.132	0.028	0.146	3.720	0.785
637126	1160	-23.605785	-22.890200	-0.7156	0.8000	0.881	0.812	0.097	0.953	3.520	0.418
		34.818634	34.974300	-0.1557	0.8000	0.799	0.195	0.039	0.218	3.696	0.743
637126	1162	-22.111332	-21.486600	-0.6247	0.8000	0.883	0.707	0.083	0.831	3.516	0.411
		34.834006	34.974300	-0.1403	0.8000	0.807	0.174	0.033	0.195	3.677	0.708
637126	1164	-20.502747	-19.981400	-0.5213	0.8000	0.885	0.589	0.068	0.693	3.512	0.403
		34.904813	35.099600	-0.1948	0.8000	0.816	0.239	0.044	0.270	3.657	0.673
637126	1199	-4.769035	-5.365300	0.5963	0.8000	0.901	-0.661	-0.065	0.785	3.480	0.343
		33.689780	33.452300	0.2375	0.8000	0.882	-0.269	-0.032	0.316	3.518	0.416
637126	1208	17.958397	16.379200	1.5792	0.8000	0.906	-1.743	-0.164	2.074	3.471	0.326
		34.354121	33.997200	0.3569	0.8000	0.915	-0.390	-0.033	0.466	3.454	0.294
637126	1228	81.718382	83.603900	-1.8855	0.8000	0.780	2.418	0.532	2.669**	3.741	0.823
		33.787080	33.922100	-0.1350	0.8000	0.624	0.216	0.081	0.214	4.182	1.572
637126	6001	46.878677	47.095400	-0.2167	0.8000	0.595	0.364	0.148	0.351	4.285	1.737
		30.222138	29.769500	0.4526	0.8000	0.762	-0.594	-0.142	0.648	3.785	0.902
637126	7001	49.130256	49.327800	-0.1975	0.8000	0.342	0.578	0.381	0.422	5.653	3.722
		23.162606	23.431000	-0.2684	0.8000	0.546	0.492	0.224	0.454	4.473	2.033
637126	7002	47.458616	47.678800	-0.2202	0.8000	0.345	0.639	0.419	0.469	5.629	3.690
		26.993955	27.376900	-0.3829	0.8000	0.548	0.699	0.316	0.647	4.464	2.019
637126	7003	45.171774	45.395700	-0.2239	0.8000	0.347	0.644	0.420	0.475	5.605	3.657
		26.944112	27.326800	-0.3827	0.8000	0.550	0.695	0.313	0.645	4.454	2.003
637126	7004	44.065516	44.296500	-0.2310	0.8000	0.348	0.663	0.432	0.489	5.598	3.647
		24.900443	25.259900	-0.3595	0.8000	0.551	0.652	0.293	0.605	4.450	1.996

-- PRINCIPAL POINT AND FOCAL LENGTH --

CAMERANAME	X0	BEOBX0	VX0	MFVX0	EVX0	GFX0	EKX0	NVX0	GRZWX0	EGKX0	MX0	STAX0

```
                              Y0          BEOBY0        VY0      MFVY0   EVY0   GFY0   EKY0   NVY0    GRZWY0  EGKY0         MY0  STAY0
                               C           BEOBC         VC       MFVC    EVC    GFC    EKC    NVC     GRZWC   EGKC          MC   STAC
-------------------------------------------------------------------------------------------------------------------------------------

     baalbek-G1         0.173740       -0.016135     0.1899     1.0000  0.033 -5.671 -5.481  1.038    22.570 21.814      0.7116      2
                        0.138436       -0.009015     0.1475     1.0000  0.049 -2.981 -2.834  0.663    18.571 17.653      0.7057      2
                      200.354646      200.253031     0.1016     2.0000  0.837 -0.121 -0.020  0.056     9.028  1.470      0.5842      2

   Schrägkamera         0.199348        0.153628     0.0457     1.0000  0.022 -2.118 -2.073  0.311    28.112 27.505      0.7160      2
                       -0.566046       -0.459920    -0.1061     1.0000  0.011  9.879  9.773  1.024    39.847 39.419      0.7200      2
                      260.484178      259.707205     0.7770     2.0000  0.685 -1.134 -0.357  0.469     9.979  3.142      0.8123      2

Messbild_Kamera        -0.089678       -0.051000    -3.0897     3.0000  0.068 45.388 42.298  3.947**  47.488 44.255      2.0964      2
                        0.607910        0.500000     0.1079     2.0000  0.011 -9.506 -9.398  0.506    77.525 76.645      1.4395      2
                      345.845772      346.629555    -0.7838     2.0000  0.625  1.254  0.470  0.496    10.446  3.915      0.8863      2


--------------------------------------- CORRELATION BETWEEN INTERIOR ORIENTATION PARAMETERS ---------------------------------------
     CAMERANAME     PARAMETER1     PARAMETER2    CORRELATION
-------------------------------------------------------------------------------------------------------------------------------------


     baalbek-G1             X0             Y0        -0.0125
                            X0              C        -0.2341
                            Y0              C        -0.0383

   Schrägkamera             X0             Y0         0.0002
                            X0              C        -0.1276
                            Y0              C        -0.0166

Messbild_Kamera             X0             Y0        -0.0153
                            X0              C         0.1642
                            Y0              C        -0.0072

---------------------------------------------------- CONTROL OF THE ADJUSTMENT ----------------------------------------------------
                   TOTAL  IMAGE COORD    PROJ.CENT OBJECT COORD          DIS          DIF     PLANE PO  PLANE PARAM   PRINC PO+C
-------------------------------------------------------------------------------------------------------------------------------------

REDUNDANCY    185.000000  179.715417     2.942319     0.000000     0.000000     0.000000     0.000000     0.000000     2.342264
     SIGMA      0.723867    0.728131     0.270100     1.000000     1.000000     1.000000     1.000000     1.000000     0.784580
      VTPV     96.937008   95.280536     0.214654     0.000000     0.000000     0.000000     0.000000     0.000000     1.441819

======================================================= Final observations =======================================================

TERMINATION LIMIT REACHED AFTER    7. ITERATIONS
TOTAL TIME OF CALCULATION [MIN]    0.0

MAXIMUM NORMALIZED RESIDUAL AT:    IMAGE COORDINATES
SYSTEM NU.:                                   208323
POINT NU .:                                     1110
NORMALIZED RESIDUAL (NV):                       4.04
```

Appendix M

LPS-system control parameters

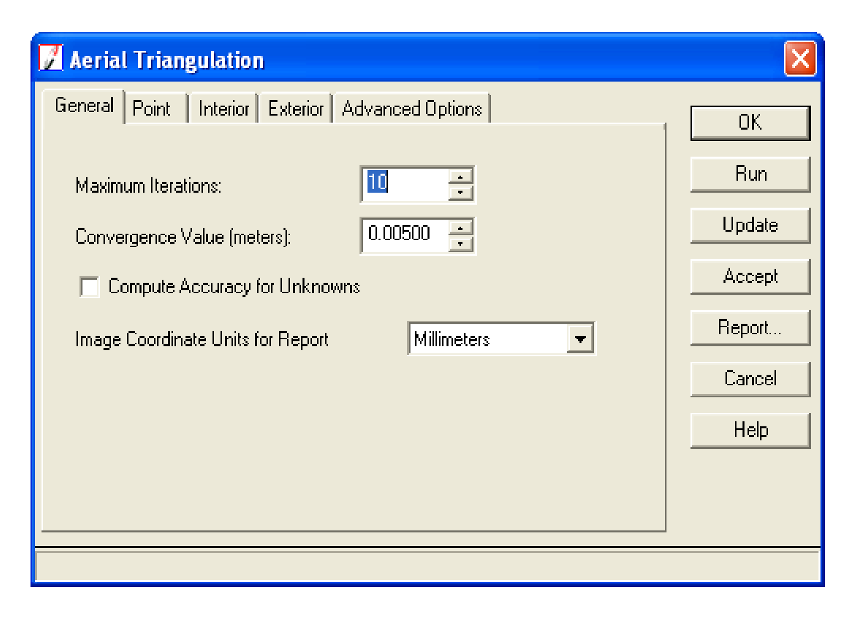

Figure (M.1): The convergence value applied into the triangulation process of Baalbek's vertical images achieved using LPS - System control parameters

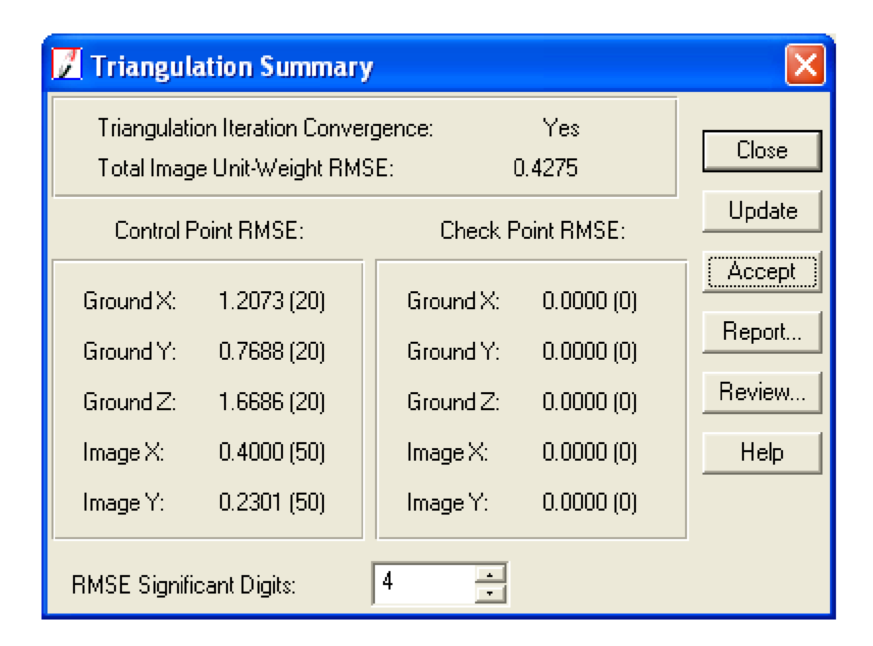

Figure (M.2): The total RMSE resulted after the triangulation process - vertical images

Appendix N

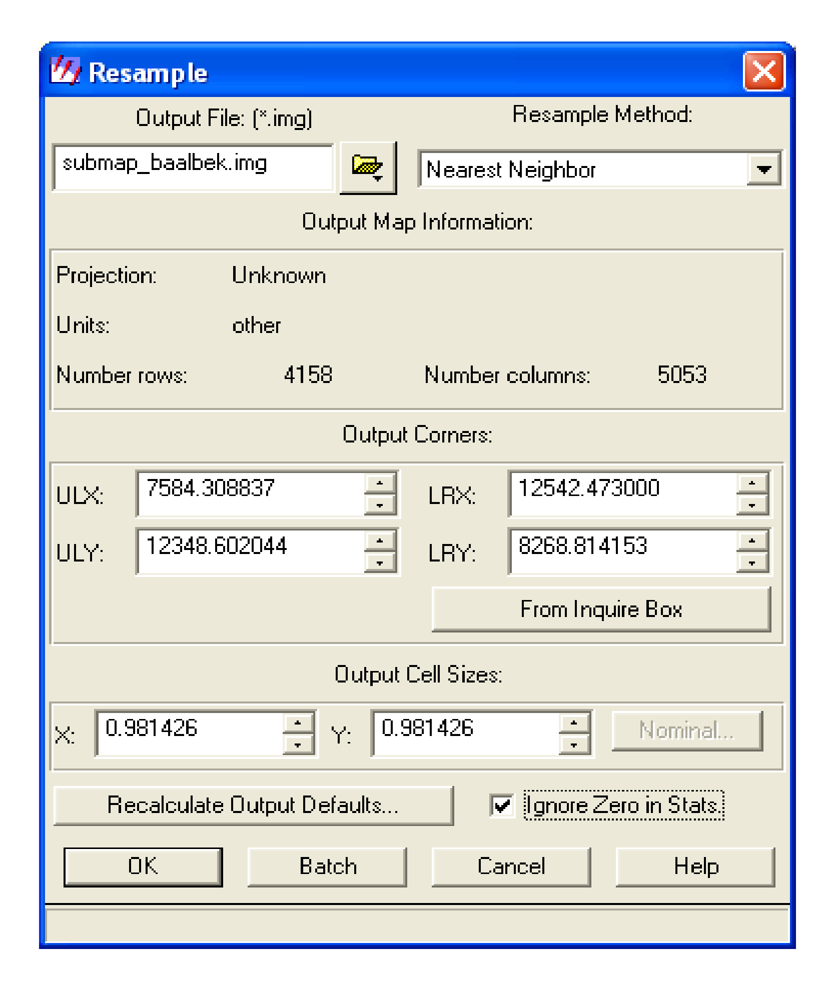

Figure (N.1): The interpolation method used in the georeferencing process of Baalbek' map as well as the output cell size is ca. 10 × 10

Appendix O

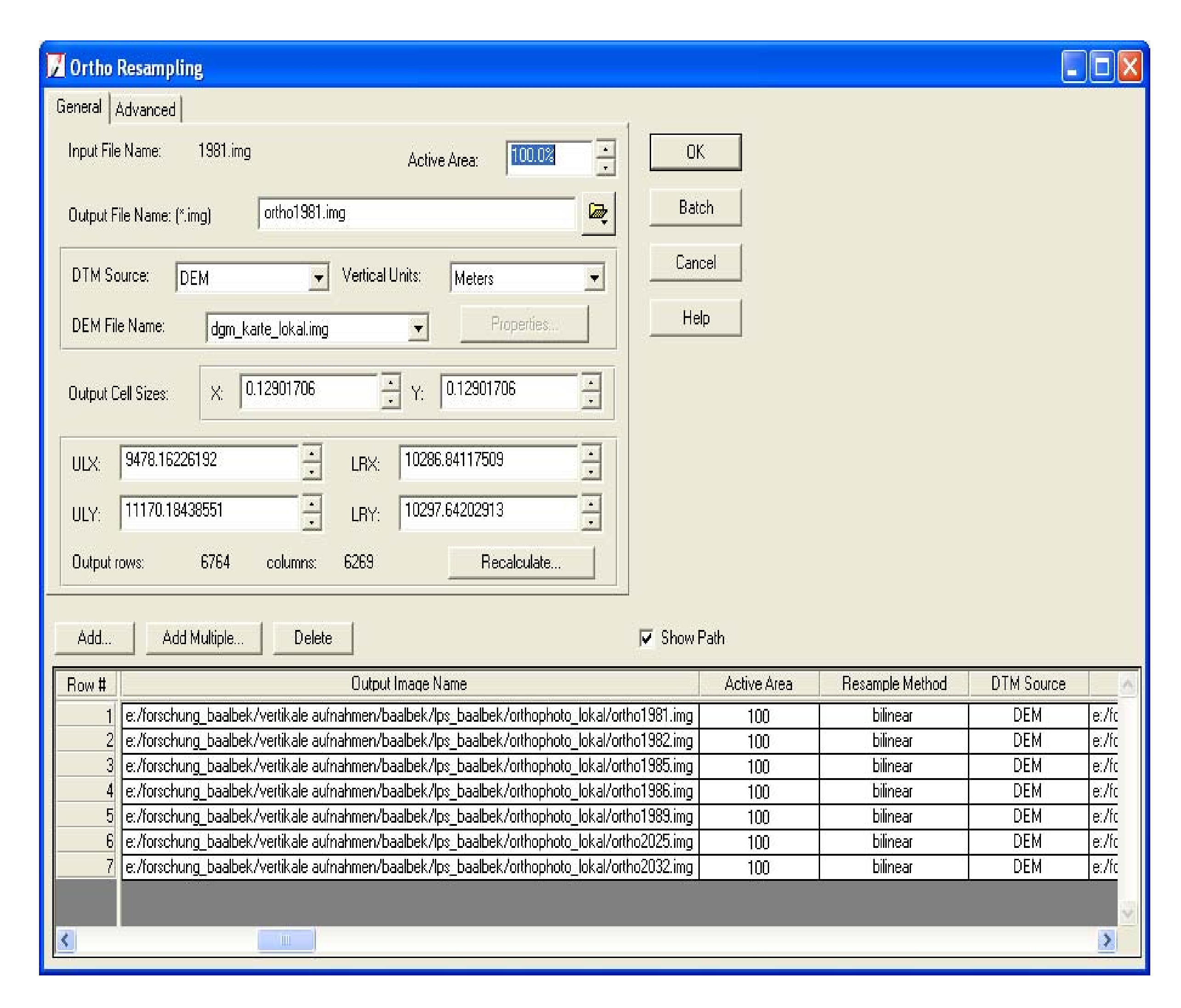

Figure (O.1): Baalbek’s orthophoto parameters

Appendix P

```
<?xml version="1.0" encoding="UTF-8"?>

<CityModel
xmlns="http://www.citygml.org/citygml/1/0/0"
           xmlns:gml="http://www.opengis.net/gml">
      <cityObjectMember>
       <GenericCityObject gml:id="…">
        .
        <!-- Four Attributes: AREA, PERIMETER, ID, Z
      -->
        .
        <lod4Geometry>
         <gml:Polygon>
          <gml:exterior>
           <gml:LinearRing>
            <gml:posList>
             .
             <!—List of Coordinates -->
             .
            </gml:posList>
           </gml:LinearRing>
          </gml:exterior>
         </gml:Polygon>
        </lod4Geometry>
       </GenericCityObject>
      </cityObjectMember>
      <cityObjectMember>
       <GenericCityObject gml:id="…">
        .
        <!-- Four Attributes: AREA, PERIMETER, ID, Z
      -->
        .
        <lod4Geometry>
         <gml:Solid srsName="" srsDimension="3">
          <gml:exterior>
           <gml:CompositeSurface>
            <gml:surfaceMember>
             <gml:Polygon>
              <gml:exterior>
               <gml:LinearRing>
                <gml:posList>
                 .
                 <!-- List of Coordinates -->
                 .
                </gml:posList>
               </gml:LinearRing>
              </gml:exterior>
             </gml:Polygon>
            </gml:surfaceMember>
            .
            <!-- At least 3 Further Surface Members -
      ->
            .
           </gml:CompositeSurface>
          </gml:exterior>
         </gml:Solid>
        </lod4Geometry>
       </GenericCityObject>
      </cityObjectMember>
      .
      <!-- 64 Further City Object Members -->
      .
</CityModel>
```

Figure (P.1): CityGML Schema referred to the original CityGML file representing the photogrammetric reconstruction of the temple Jupiter

Appendix Q

```
<?xml version="1.0" encoding="UTF-8"?>

<CityModel xmlns="http://www.citygml.org/citygml/1/0/0"
     xmlns:gml="http://www.opengis.net/gml">
  <core:cityObjectMember>
    <bldg:Building>
     .
     <!-- Five Attributes: NAME, EPOCH, RESTORATION,
        function, yearOfConstruction -->
     .
      <bldg:lod2MultiSurface>
        <gml:MultiSurface>
          <gml:surfaceMember>
            <gml:Polygon gml:id="…">
              <gml:exterior>
                <gml:LinearRing>
                  <gml:posList>
                   .
                   <!-- List of Coordinates -->
                   .
                  </gml:posList>
                </gml:LinearRing>
              </gml:exterior>
            </gml:Polygon>
          </gml:surfaceMember>
         .
           <!-- 419 Further Surface Members -->
           .
         </gml:MultiSurface>
      </bldg:lod2MultiSurface>
    </bldg:Building>
  </core:cityObjectMember>
</core:CityModel>
```

Figure (Q.1): CityGML Schema referred to the new CityGML file representing the photogrammetric reconstruction of the temple Jupiter

Appendix LST (Extension - Chapter 2)

2.4. Least Squares Theory (LST)

Basically, “the BBA can be defined as the process of evaluating coordinates of targets and exterior orientation parameters of cameras using the least squares theory based on the collinearity equations” (Cooper & Robson, 2001, pp. 35-38). To develop the principle of LST, suppose that there are *n* independent weighted measurements: $x_1, x_2 \ldots x_n$ and their most probable value is *M*. By definition:

$$\begin{Bmatrix} M - x_1 = v_1 \\ M - x_2 = v_2 \\ \vdots \\ M - x_n = v_n \end{Bmatrix} \tag{2.11}$$

where v_1 to v_n are the residual errors (in practice, they are also called: residuals). They can be used in the normal distribution function because they behave in manner similar to errors. This can be mathematically formed as following (Ghilani & Wolf, 2006, pp. 173-176):

$$y = f(v) = Ke^{-h^2v^2} \tag{2.12}$$

where: $h = 1/\sigma\sqrt{2}$ and $K = h/\sqrt{\pi}$

The probability for the residuals occurrence is the product of the individual probabilities due to stochastic independencies; with respect to the infinitesimal small increment (Δv) of v that means:

$$P = K^n(\Delta v)^n e^{-h^2(v_1^2+v_2^2+\cdots+v_n^2)} \tag{2.13}$$

The relationship (2.13) reveals that to maximize the probability, the sum of the squares of the residuals must be minimized. Therefore, the fundamental principle of the least squares theory can be presented by the following equation:

$$\Sigma v^2 = v_1^2 + v_2^2 + \cdots + v_n^2 = \text{minimum} \tag{2.14}$$

Consequently, the least squares adjustment enables to compute the most probable value for a quantity which has been observed. The computation flow in the least squares method depends on the mathematical model presenting the adjustment problem. This mathematical model can

be structured into: *functional model* and *stochastic model*. They will be described in details in the next section.

2.4.1. The mathematical model

“It is defined as a theoretical system or an abstract concept which used to describe a physical situation or a set of events. This description is not necessarily meant to be complete, but to relate only to those aspects or properties that are under consideration” (see: Mikhail & Ackermann 1976, pp. 3-6). The mathematical model consists of the two parts: the *functional model* and the *stochastic model*.

2.4.1.1. The functional model

“The functional model in the adjustment computation is an equation or set of equations that represents or defines an adjustment condition” (Ghilani & Wolf, 2006). Basically, the functional models can be classified into three types: the conditional, parametric and mixed adjustments. In the first one, the geometric conditions are based on the observations and their residuals. In contrast, the parametric adjustment describes the observation based on unknown parameters that were never observed directly. In some cases the conditional and parametric adjustments should be used together in order to define the functional model optimally. In our research we focus on the parametric adjustment due to the large systems of the equations, moreover, it is easier in its development and solution.

To express the parametric adjustment, suppose that there are (n) observations $\tilde{L}_i$ measured based on (u) unknown parameters $\tilde{X}_j$. Thus, the main task in the bundle block adjustment is the formulation of the functional relationship between the observations $\tilde{L}_i$ and the unknown parameters $\tilde{X}_j$ associated with a certain adjustment problem.

The mentioned relationship could be expressed as following (according to Luhmann, 2003, pp. 50-52, Niemeier, 2008, pp. 120-124):

$$\tilde{L}_i = f\left(\tilde{X}_1, \tilde{X}_2, \dots, \tilde{X}_u\right) = f(\tilde{X}_j) \tag{2.15}$$

where: *i=1…n* (*n* the number of the observations)

j=1… u (*u* the number of the unknowns)

The functional model presented by the equation (2.15) describes the relationship between the true values of the observations and the true values of the unknowns. Due to that the true values are not known, the observations vector $\tilde{L}_i$ will be substituted by the actual observations vector L_i (measured values) with the consideration of the residual vector (v_i). Similarly, the vector $\tilde{X}_j$ should be estimated by the vector of the adjusted unknowns ($\hat{X}_j$). That means that the formula (2.15) can be re-formed:

$$\hat{L}_i = L_i + v_i = f\left(\hat{X}_1, \hat{X}_2, \dots, \hat{X}_u\right) \tag{2.16}$$

In general, the constraint equations involved in an adjustment problem can be non-linear. However, the adjustment method is generally performed with linear functions, since it is rather difficult and often impractical to seek a least squares solution of non-linear equations. Therefore, a linearization of the formula (2.16) has to be enforced to get linear form (Mikhail & Ackermann, 1976, pp. 108-110).

2.4.1.2. Linearization process of non-linear functions

Series expansions and Taylor's series are used to obtain linear equations with respect that only the zero and first order terms are used and all other higher order terms are neglected. To demonstrate how the linearization process is achieved, let any set of non-linear equations (e.g. the equations presented in the formula 2.16) be regarded. The value of the function f can be determined in the position ($X^0 + \Delta x$) through the Taylor's series if the value of the function f^0 in the position X^0 is known; with respect that the value Δx is small. Hence, the requested value $f(X^0 + \Delta x)$ is given (Niemeier, 2008):

$$f(X^0 + \Delta x) = f(X^0) + \left(\frac{\partial f}{\partial X}\right)_{X=X^0} . \Delta x \tag{2.17}$$

In analogue manner the equations (2.16) can be linearized as following:

$$L_i + v_i = f_i(X_1^0, X_2^0, \dots, X_u^0) + \left(\frac{\partial f_i}{\partial X_1}\right)_{X^0} . \hat{x}_1 + \left(\frac{\partial f_i}{\partial X_2}\right)_{X^0} . \hat{x}_2 + \cdots + \left(\frac{\partial f_i}{\partial X_u}\right)_{X^0} . \hat{x}_u \tag{2.18}$$

where:

$\hat{x}_j = \hat{X}_j - X_j^0$; X_j^0 approximations of unknowns

$i = 1, \dots, n$ and $j = 1, \dots, u$

The partial derivations of the functions could be expressed through:

$$a_{ij} = \left(\frac{\partial f_i}{\partial X_j}\right)_{X^0} \tag{2.19}$$

The design matrix $A_{(u,u)}$ is built based on the partial derivations:

$$A_{(n,u)} = \begin{bmatrix} a_{11} & a_{12} & \cdots & a_{1u} \\ a_{21} & a_{22} & \cdots & a_{2u} \\ \vdots & \vdots & \ddots & \vdots \\ a_{n1} & a_{n2} & \cdots & a_{nu} \end{bmatrix} \tag{2.20}$$

On one hand the vector $\hat{X}_j$ is computed based on the non-stochastic approximate values X_j^0 of the unknowns and the stochastic vector $\hat{x}_j$:

$$\hat{X}_j = X_j^0 + \hat{x}_j \tag{2.21}$$

On the other hand and based on the equation (2.16), the approximate values of observations can be calculated as following:

$$L_i^0 = f_i(X_1^0, X_2^0, \dots, X_u^0) \tag{2.22}$$

The differences between the actual measured observations and the calculated one are given:

$$l_i = L_i - L_i^0 \tag{2.23}$$

According to the equation (2.19) and (2.22), the equation (2.18) is expressed:

$$L_i + v_i = L_i^0 + a_{ij}.\hat{x}_j \tag{2.24}$$

With respect to (2.23) we find:

$$l_i + v_i = a_{ij}.\hat{x}_j \tag{2.25}$$

The linear form presented in the equation (2.25) can be formulated in matrix form:

$$\mathrm{l}_{(n,1)} + \mathrm{v}_{(n,1)} = \mathrm{A}_{(n,u)}.\hat{\mathrm{x}}_{(u,1)} \tag{2.26}$$

2.4.1.3. Stochastic model

It describes the non-deterministic or stochastic (probabilistic) properties of the variables involved. When the measurements of some variables are achieved, all relevant physical and environmental circumstances should be recorded during the measuring period to model the stochastic properties correctly (Mikhail & Ackermann, 1976, pp. 5-8). On other words, the

variances and subsequently the weights of the measurements should be determined. This determination is known as stochastic model in the least squares adjustment.

In order to explain the meaning of the stochastic model and what it reveals, let any set of measurements (observations) be considered, which could be expressed in the vector of the observations:

$$L_{(n,1)} = \begin{bmatrix} L_1 \\ L_2 \\ \vdots \\ L_n \end{bmatrix} \tag{2.27}$$

The stochastic properties of the vector $L_{(n,1)}$ are presented in the covariance matrix (Luhmann 2003, pp. 52-54 & Niemeier, 2008, pp. 124-126):

$$C_{ll} = \begin{bmatrix} {\sigma^2}_1 & \rho_{12}\sigma_1\sigma_2 & \cdots & \rho_{1n}\sigma_1\sigma_n \\ \rho_{21}\sigma_2\sigma_1 & {\sigma^2}_2 & \cdots & \rho_{2n}\sigma_2\sigma_n \\ \vdots & \vdots & \ddots & \vdots \\ \rho_{n1}\sigma_n\sigma_1 & \rho_{n2}\sigma_n\sigma_2 & \cdots & {\sigma^2}_n \end{bmatrix} \tag{2.28}$$

where: σ_i: standard deviation of the observation L_i, $i = 1 \ldots n$

ρ_{ij}: the correlation coefficient between L_i and L_j $(i \neq j)$

If the observations are independent and homogeneous, the covariance matrix can be given:

$$C_{ll} = \begin{bmatrix} {\sigma^2}_1 & 0 & \cdots & 0 \\ 0 & {\sigma^2}_2 & \cdots & 0 \\ \vdots & \vdots & \ddots & \vdots \\ 0 & 0 & \cdots & {\sigma^2}_n \end{bmatrix} = \sigma^2 \cdot \mathrm{I}_{(n,n)} \tag{2.29}$$

It is essential to compute the cofactor matrix Q_{ll} of the observations because it includes information about the accuracy of observations. This matrix for stochastical independent observations can be determined starting from the equation (2.29):

$$C_{ll} = \sigma_0^2 \cdot Q_{ll} = \sigma_0^2 \begin{bmatrix} {\sigma^2}_1/\sigma_0^2 & 0 & \cdots & 0 \\ 0 & {\sigma^2}_2/\sigma_0^2 & \cdots & 0 \\ \vdots & \vdots & \ddots & \vdots \\ 0 & 0 & \cdots & {\sigma^2}_n/\sigma_0^2 \end{bmatrix} = \sigma_0^2 \cdot W^{-1} \tag{2.30.a}$$

Consequently, the matrix Q_{ll} is calculated as following:

$$Q_{ll} = W^{-1} \quad (2.30.b)$$

where: W the weight matrix

Particularly, the value σ_0 is applied into the computation as a prior standard deviation of the unit weight s_0 (in general, $s_0 = 1$); that means the weight value of an observation should be:

$$W_i = \frac{1}{\sigma_i^2} \quad (2.31)$$

The equation (2.31) shows that the observation, with the largest standard deviation, will take the smallest weight in the adjustment. Due to the observations have weights, moreover, the residuals are related to the observations; the equation (2.14) should be rewritten as:

$$\Sigma wv^2 = w_1v_1^2 + w_2v_2^2 + \cdots + w_nv_n^2 = \text{minimum} \quad (2.32)$$

2.4.2. Estimation of the unknown parameters

To estimate the unknown parameters, the parametric adjustment can be used. Based on the Equation (2.26) the residuals are:

$$\mathrm{v} = \mathrm{A}\hat{\mathrm{x}} - \mathrm{l} \quad (2.33)$$

With the assumption that the observations have the same weight and with respect to the LST principle (Equation 2.14) we find:

$$\mathrm{v}^{\mathrm{T}} \cdot \mathrm{v} \rightarrow \min$$

This leads to:

$$\mathrm{v}^{\mathrm{T}} \cdot \mathrm{v} = (\mathrm{A}\hat{\mathrm{x}} - \mathrm{l})^{\mathrm{T}}(\mathrm{A}\hat{\mathrm{x}} - \mathrm{l})$$

$$\mathrm{v}^{\mathrm{T}} \cdot \mathrm{v} = \hat{\mathrm{x}}^{\mathrm{T}}\mathrm{A}^{\mathrm{T}}\mathrm{A}\hat{\mathrm{x}} - 2\hat{\mathrm{x}}^{\mathrm{T}}\mathrm{A}^{\mathrm{T}}\mathrm{l} + \mathrm{l}^{\mathrm{T}}\mathrm{l} \quad (2.34)$$

The 1st derivation of the relation (2.34), in according to $\hat{\mathrm{x}}$, gives:

$$\mathrm{d}(\mathrm{v}^{\mathrm{T}} \cdot \mathrm{v}) = 2\mathrm{d}\hat{\mathrm{x}}^{\mathrm{T}}(\mathrm{A}^{\mathrm{T}}\mathrm{A}\hat{\mathrm{x}} - \mathrm{A}^{\mathrm{T}}\mathrm{l}) \quad (2.35)$$

The 1st derivation will be zero, if the:

$$\mathrm{A}^{\mathrm{T}}\mathrm{A}\hat{\mathrm{x}} - \mathrm{A}^{\mathrm{T}}\mathrm{l} = 0 \quad (2.36)$$

Thus, the unknown parameters could be given:

$$\hat{x} = (A^T A)^{-1}(A^T l) \quad (2.37)$$

For simplification of the last equation we assume:

$N = A^T A$: the normal equation, and $n = A^T l$: the right part of the normal equation; this means the formula (2.37) can be expressed as following:

$$\hat{x} = N^{-1} n \quad (2.38)$$

In the weighted case, the equation (2.38) should be formed with respect to the weight values associated with measurements:

$$\left\{ \begin{array}{c} N = A^T W A \\ n = A^T W l \\ \hat{x} = N^{-1} n \end{array} \right\} \quad (2.39)$$

2.4.3. Quality assessment of the estimated parameters

On one hand to ensure that the parameters estimated are relative qualitative, it will be important to calculate the cofactormatrix of the adjusted unknown parameters. This matrix can be derived based on the normal equation:

$$Q_{\hat{x}\hat{x}} = N^{-1} \quad (2.40)$$

It follows to the cofactormatrix of the adjusted observations

$$Q_{\hat{l}\hat{l}} = A Q_{\hat{x}\hat{x}} A^T \quad (2.41)$$

On the other hand to check the global accuracy of the adjustment calculation, the estimated standard deviation of the unit weight $\hat{s}_0$ (a posterior standard deviation of the unit weight) should be taken into the account. Particularly, if $\hat{s}_0$ is in the range [0.7-1.3] that could mean there is no large errors shown in the adjustment calculations and the primary standard deviation of the unit weight (before the adjustment) is confirmed by $\hat{s}_0$ and therefore a balance stochastical model is guaranteed. In contrast, if the value of $\hat{s}_0$ is not in the above mentioned range, this can be interpreted as following (Gründig, 2003a & 2003b):

- The stochastic model is applied into the computations faultily; that means the stochastic properties of the observations should be controlled (note that the value s_0 doesn't affect the numerical values of the adjusted parameters).
- The functional model is insufficient (e.g. large failures in the observations will affect the parameters calculation).

However, the estimated standard deviation of the unit weight is given (after the adjustment):

$$\hat{s}_0 = \sqrt{\frac{\mathrm{v}^{\mathrm{T}} \cdot \mathrm{W} \cdot \mathrm{v}}{n-u}} \tag{2.42}$$

Based on the equation (2.42) the estimated standard deviations of the unknown parameters $\hat{x}_j$ could be denoted:

$$\hat{s}_j = \hat{s}_0 \sqrt{q_{jj}} \tag{2.43}$$

where: q_{jj} the elements of the main diagonal of the matrix $Q_{\hat{x}\hat{x}}$

PUBLICATIONS OF THE DISSERTATION

- **Alamouri, A.** and Gründig, L.: *Generation of 3d city model of Baalbek to analyse the historical development of the city using non-calibrated historical photos*. Proceeding of the 36th Annual Conference on Computer Applications and Quantitative Methods in Archaeology. Budapest, 2008.

- **Alamouri, A.**, Gründig, L. and Kolbe, T. H.: *A new approach for relative orientation of non calibrated historical photos of Baalbek/Libanon*. The proceeding of the XXI Congress of ISPRS. Vol. XXXVII, Band 5-1, Commission V. Beijing, 2008.

- **Alamouri, A.** and Gründig, L.: *3D reconstruction of historic Baalbek based on historical vertical, oblique and terrestrial images*. The proceeding of the 22nd CIPA symposium, Oct. 2009, Kyoto, Japan.

- **Alamouri,** A., Kolbe, T. H.: *Quality assessment of historical Baalbek's 3D city model*. In: Proceedings for ISPRS WG II/2+3+4 and Cost Workshop on Quality, Scale & Analysis Aspects of Urban City Models, Lund, Sweden, 3-4 December, 2009. ISPRS XXXVIII-2/W11.

- Alfraheed, M., **Alamouri, A.**, Jeschke, S.: *A MDV- Based approach for appearance enhancement of historical images*. In: Publikationen der Deutschen Gesellschaft für Photogrammetrie, Fernerkundung und Geoinformation e. V. Band 19. Voträge dreiländertagung, 30 wissenschaftlich-Technische Jahrestagung der DGPF. Juli, 2010 Wien.

- **Alamouri, A.** and Pecchioli, L.: *Retrieving Information through Navigation in Historical Baalbek*. ISPRS Conference: International Conference on 3D Geoinformation, Vol. XXXVIII-4, Part W15. Berlin, Germany, Nov. 2010.

CURRICULUM VITAE

Personal profile

Last name: Alamouri

Name: Ahmed

Jan. 06, 1977……….born in Edlib, Syria

Academic Study

1983-1988………….Primary School, Edlib, Syria

1989-1994………….Secondary School

1995-2000………….B.Sc. in Civil Engineering, Aleppo University, Syria

2001-2002………….Diploma in Topographic Engineering, Aleppo University, Syria

2004-2005………….Preparation for the PhD

Since April 2005….PhD-Student at the Institute for Geodesy and Geoinformation Sciences, Technical University of Berlin, Germany

Career Progression

2002-2003………….Working at Engineering Company for the Water Management (ECWM)

2003-2004………….Scientific Assistant at the Department for Topographic Engineering, Aleppo University, Syria

March 2010………...Chair of SGFG (Special Group For Geoinformation)

Contact

a.amouri@hotmail.de